The chiral cyclobutane motif in advanced materials and catalysis: organogelators, surfactants, hybrid silicas and metal ligands.

Marta Sans Valls
PhD Thesis 2014

Facultat de Ciències
Departament de Química
Programa de Doctorat en Química

Supervised by Prof. Rosa M. Ortuño and Dr. Ona Illa

Universitat Autònoma de Barcelona

The chiral cyclobutane motif in advanced materials and catalysis: organogelators, surfactants, hybrid silicas and metal ligands.

Marta Sans Valls

Tesi doctoral

Programa de Doctorat en Química

Supervisors: Prof. Rosa M. Ortuño Mingarro
Dr. Ona Illa Soler

Departament de Química
Facultat de Ciències

2014

Memòria presentada per aspirer al grau de Doctor per **Marta Sans Valls**

Vist i Plau,

Prof. Rosa María Ortuño Mingarro **Dr. Ona Illa Soler**

Bellaterra, 22 de Setembre 2014

ACKNOWLEDGEMENTS

The present PhD Thesis has been carried out in the Chemistry Department at the Universitat Autònoma de Barcelona (UAB) under the direction of Professor Rosa Maria Ortuño and Doctor Ona Illa. I really would like to thank Rosa the chance she gave me to work in her group and participate in several projects that resulted in this Thesis, as well as the financial support to carry out my PhD. I want to thank both of them, Rosa and Ona, for the huge support, confidence placed in me and the excellent supervision they have done within this work. It has been a pleasure to become part of this team!

I am very grateful to Prof. Montserrat Gómez from the Université Paul Sabatier in Toulouse for giving me the opportunity to stay in her laboratory to learn about the synthesis of nanoparticles. Also Dr. Isabelle Favier, who helped me in everything I needed.

I would like to thank Prof. Ramon Pons from the Consejo Superior de Investigaciones Cientificas de Barcelona (CSIC) for the opportunity to carry out the surface tension measurements in his laboratory as well as Dr. Alessandro Sorrenti for his collaboration in this project of Chapter 5 and his very nice advices.

I would also mention Prof. J.C. Estévez from the Universidad de Santiago de Compostela for providing several molecules included in this work to be studied as organogels.

Don't forget about the help received from Dr. Pau Nolis from the SeRMN at UAB on carrying out structural studies as well as the training in the equipment manipulation. I would also like to mention Dr. Judith Oró, from the Instituto de Ciencia de Materiales de Barcelona (ICMAB), for her huge help in SEM analysis. Also thank to all the members of Servei d'Anàlisi Química (SAQ) and Servei de Ressonància Magnètica (RMN) of the UAB for their valuable help during all my Thesis.

Special mention for all the lab mates who helped me with everything and the really nice moments we all had together, inside and out of the laboratory, making it all more than a professional project. All the best for you!

To my friends from Barcelona and from Alcanar, thank you for your true support and for sharing with me good and bad times. Also to show me that we can be together although the distance. I love you all!

Finally, I can not finish my acknowledgments without giving very special thanks to my family, especially to my parents and my sister, for their motivation and incessant support in all. This wouldn't be possible without your help!

Moltes gràcies a tots!

To my family

ABBREVIATIONS

AFM	Atomic force microscopy
Boc	*tert*-butyl carbamate
Cbz	Benzyl carbamate
CD	Circular dichroism
CMC	Critical micellar concentration
CPPs	Cell penetrating peptides
CP MAS	Cross polarization magic-angle spinning
DAGK	Diacylglycerol kinase
DCE	Dichloroethane
DCM	Dichloromethane
DMAP	Dimethylaminopyridine
DIAD	Diisopropyl azodicarboxylate
DIBAL	Diisobuylaluminium hydride
DIPEA	*N*,*N'*-diisopropylethylenediamine
DMF	Dimethylformamide
DMSO	Dimethylsulfoxide
EDAC	1-ethyl-3-(3-dimethylaminopropyl)carbodiimide
FDPP	Pentafluorophenyl diphenyl phosphinate
GABA	Y-amino butyric acid
HOPG	Highly oriented pyrolytic graphite
ICP-MAS	Inductively coupled plasma mass spectrometry
IR	Infrared spectroscopy
LMWG	Low molecular weight gelator

Lys	Lysine
mgc	Minimum gelation concentration
MPs	Membrane proteines
MMFF	Merck Molecular Force Field
NMR	Nuclear magnetic resonance
NOE	Nuclear Overhauser Effect
PDC	Pyridinium dichromate
Phe	Phenylalanine
PLE	Pig liver esterase
PPTS	Pyridinium *p*-toluenesulfonate
PyBOP	(Benzotriazol-1-yloxy)tripyrrolidinophosphonium hexafluorophosphate
SEM	Scanning electron microscopy
TEM	Transmission electron microscopy
TEOS	Tetraethyl orthosilicate
TFA	Trifluoroacetic acid
THF	Tetrathiafulvalene
Val	Valine

NUMBERING AND STRUCTURAL DESCRIPTION

1. The numbering of the molecules is established according to their order of appearance.

2. The numbering of atoms in the molecules is established according to the following criteria:

   i) In β-aminoacids, cyclobutane-1,2-diamines and cyclobutane-1,2-dicarboxylic acids used as intermediates only the cyclobutane ring is numbered starting with the preferential functional group.

   ii) Cyclobutane derivatives substituted with different alkyl chains or thioureas are numbered from one *C*-terminus to the other *C*-terminus arbitrarily (from top to bottom side).

   iii) Other molecules are numbered according to SI nomenclature.

3. Structural description of ^{1}H and ^{13}C NMR spectra for amino acids, peptides and pseudopeptides is assigned with the corresponding number given to the molecules. For SI-named compounds, the assignment of signals is done by functional or characteristic R groups, highlighting with italics the specific parts of these groups when confusion is possible.

NOMENCLATURE

1) In order to facilitate the writing of this work, the diastereomers *cis*- and *trans*- of each final compound which is going to be studied in different chapters (bolaamphiphiles, triethoxysilane derivatives and C_{16}-*C*-centered-amides) will be described with the same number although they are different molecules. An exemple is shown:

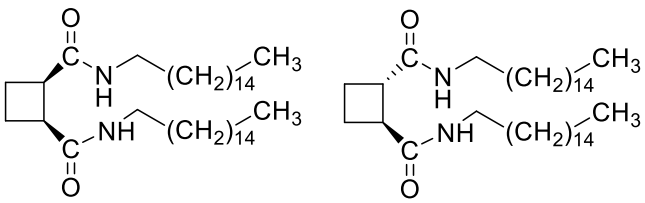

cis-**190** *trans*-**190**

2) All the precursors of this Thesis are going to be described using the absolute configuration of chiral centres (*S*,*R*)-, (*R*,*S*)-, (*S*,*S*)- or (*R*,*R*)-. However, to remark the stereochemistry of the compounds studied and to facilitate the task of understanding the Thesis, the final compounds and materials will be described using *cis*- or *trans*- instead of using the absolute configuration. Some illustrative examples:

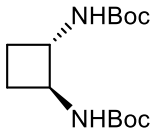

(*S*,*S*)-**174**

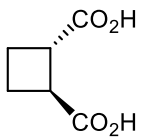

(*S*,*S*)-**155**

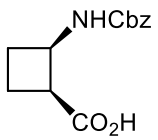

(*S*,*R*)-**16**

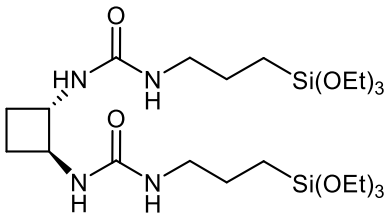

trans-**189**

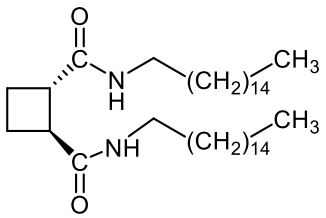

trans-**190**

3) 1,3-disubstituted compounds in Chapter 7 of this Thesis are going to be described according to SI nomenclature without remarking the absolute configuration of chiral centres.

TABLE OF CONTENTS

1. General introduction and general objectives 27

2. Precedents in the research group 34

2.1 Synthesis of compounds containing the 1,2-disusbstituted cyclobutane moiety 34

2.1.1 Synthesis of amino acids and peptides 35

2.1.2 Synthesis of ureas and thioureas 40

2.2 Applications of 1,2-disubstituted cyclobutane in materials 46

2.2.1 Conductive materials 46

2.2.2 Low molecular weight gelators 47

2.3 Applications as metallocarboxypeptidase inhibitors 51

2.4 Applications in organocatalysis 53

2.5 Synthesis of compounds containing the 1,3-disubstituted cyclobutane moiety 54

2.6 Applications of 1,3-disubstituted cyclobutane in materials 56

2.6.1 Dendrimers 56

2.6.2 Surfactants 57

2.7 Biological applications: CPPs (Cell penetrating peptides) 60

3. Synthesis of the cyclobutane derivatives used as precursors 67

3.1 Introduction 67

3.1.1 The chemistry of the vicinal diamines 67

3.1.2 Cyclohexane-1,2-diamines 68

3.1.3 Cyclopentane-1,2-diamines 69

3.1.4 Cyclobutane-1,2-diamines 70

3.2 Objectives 72

3.3 Results and discussion 74

3.3.1 Stereoselective synthesis of cyclobutane-1,2-diamines 74

3.3.1.1 Synthesis of chiral precursor (*S*,*R*)-**9** 75
3.3.1.2 Enantiocontrolled synthesis of amino acids (*R*,*S*)- and (*S*,*R*)-**156** 76
3.3.1.3 Enantio- and diastereocontrolled synthesis of intermediates **157** and **158** 78
3.3.1.4 Synthesis of diamines **152** and **153** 81
3.3.2 Selective deprotection of cyclobutane-1,2-diamines **152** and **153** 82
3.3.3 Stereoselective synthesis of cyclobutane-1,2-dicarboxylic acids **154** and **155** 84
3.3.4 Synthesis of bolaamphiphiles 85
3.3.4.1 Synthesis of *cis*- and *trans*- bolaamphiphiles derived from cyclobutane-1,2-diamines 86
3.3.4.2 Synthesis of *cis*- and *trans*- bolaamphiphiles derived from cyclobutane-1,2-dicarboxylic acid 92
3.3.5 Synthesis of *cis*- and *trans*- triethoxysilane derivatives from cyclobutane-1,2-diamines 93
3.3.6 Synthesis of cis- and trans-C_{16}-(*C*-centered) amides based on cyclobutane-1,2-dicarboxylic acids 95
3.4 Summary and conclusions 97

4. Supramolecular study of C_{16}-amido derivatives as organogels 100

4.1 Introduction 100
4.1.1 Gels: definition and general classification 100
4.1.2 Low molecular weitght gelators 101
4.1.3 Amide-based LMWGs 103
4.1.4 Cyclobutane-containing LMWGs 106
4.2 Objectives 108

4.3 Results and discussion 109
4.3.1 Preparation of the gels 110
4.3.2 Supramolecular study of the gels formed 114

4.3.2.1 High-resolution NMR spectroscopy 115
4.3.2.2 SEM (Scanning Electron Microscopy) 121
4.3.2.3 IR spectroscopy 124
4.4 Summary and conclusions 126

5. Physicochemical behavior of novel bolaamphiphiles 130
5.1 Introduction 130
5.1.1 Surfactants: definition, classification and some properties 130
5.1.2 Self-assembly of surfactants 134
5.1.3 Bolaamphiphiles 136
5.1.3.1 Applications of bolaamphiphiles 141
5.2 Objectives 146
5.3 Results and discussion 147
5.3.1 Surface tension measurements of bolaamphiphiles *cis*-**177** and *trans*-**177** derived from cyclobutane-1,2-diamine 149
5.3.2 TEM studies on *cis*-**177** 154
5.3.3 TEM studies on *trans*-**177** 156
5.3.4 Organogelator behavior of *trans*-**193** 157
5.3.5 Surface tension mesurements of bolaamphiphiles *cis*-**187** and *trans*-**187** derived from cyclobutane-1,2-dicarboxylic acid 160
5.3.6 Aggregation properties of **187** 161
5.4 Summary and conclusions 163

6. Hybrid materials based on cyclobutane-1,2-diamines 166
6.1 Introduction 166
6.1.1 Definition of hybrid material 166
6.1.2 Class II hybrid silica 167

6.1.3 Structural Engineering 168
6.1.4 Mechanism of the formation of hybrid silicas 170
6.1.5 NMR as a powerful technique to study the structure of hybrid materials 172
6.1.6 Applications of hybrid silicas 173
6.1.6.1 Diureido derivatives as chiral hybrid silica 174
6.1.6.2 Applications in metal and non-metal catalysis 175
6.1.6.3 Materials containing the 1,2-diamine moiety in catalysis 178
6.2 Objectives 181
6.3 Results and discussion 182
6.3.1 Synthesis of organo bridged silsesquioxanes based on cyclobutane-1,2-diamine 182
6.3.1.1 Acid catalyzed hydrolysis and condensation of *trans*-**189** 183
6.3.1.2 Base catalyzed hydrolysis and condensation of *trans*-**189** 187
6.3.1.3 CP MAS NMR of *trans*-**229** 188
6.3.1.4 SEM studies on *trans*-**229** 188
6.3.1.5 Hydrolysis and condensation of *cis*-**189** 190
6.3.1.6 CP MAS NMR of *cis*-**229** 190
6.3.1.7 SEM studies on *cis*-**229** 191
6.3.2 Synthesis and complexation of new hybrid material with rhodium, *trans*-**230-Rh** 193
6.3.2.1 Spectroscopic data of *trans*-**230-Rh** 195
6.3.2.2 SEM/EDX analyses 196
6.3.2.3 ICP-MAS spectrum 199
6.3.3 Catalytic activity of *trans*-**230-Rh** in the enantioselective reduction of acetophenone 200

6.4 Summary and conclusions 204

7. Synthesis of cyclobutane ligands and applications in the stabilization of ruthenium nanocatalysts 208

7.1 Introduction 208

7.1.1 Background 208

7.1.2 Nanoparticles in catalysis 210

7.1.3 Synthesis of metal nanoparticles 210

7.1.4 Stabilization of metal nanoparticles 212

7.1.4.1 Electrostatic stabilization 213

7.1.4.2 Steric stabilization 213

7.1.4.3 Ligand stabilization 214

7.2 Objectives 217

7.3 Results and discussion 218

7.3.1 Synthesis of pyrrolidines **237** and **238** from intermediate nitro ester **236** 218

7.3.2 Synthesis of pyrrolidine **239** 229

7.3.3 Synthesis of ruthenium nanoparticles stabilized by **237**, **238** and **239** 221

7.3.4 Characterisation of ruthenium nanoparticles 223

7.3.5 Ruthenium nanoparticles in heterogeneous catalysis 225

7.3.6.1 Influence of the nanoparticles nature: preformed, formed in situ or under one pot conditions 228

7.4 Summary and conclusions 231

8. General conclusions 235

9. Experimental section 239

9.1 General methodology 239

9.2 Experimental procedures 243

- 3-Oxabicyclo [3.2.0] heptane-2,4-dione, **3**
- Dimethyl (1R,2S)-cyclobutane-1,2-dicarboxylate, **8**

- (1*S*,2*R*)-2-methoxycarbonylcyclobutane-1-carboxylic acid, **9**
- Methyl (1*R*,2*S*)-2-azidocarbonylcyclobutane-1-carboxylate, **47**
- Methyl (1*R*,2*S*)-2-(tert-butoxycarbonylamino)cyclobutane-1-carboxylate, **156**
- Methyl (1*R*,2*S*)-2-(benzyloxycarbonylamino)cyclobutane-1-carboxylate, **10**
- (1*S*,2*R*)-1-*tert*-butyl-3-methyl cyclobutane-1,2-dicarboxylate, **43**
- (1*R*,2*S*)-2-(*tert*-butoxycarbonyl)cyclobutane-1-carboxylic acid, **160**
- tert-Butyl(1S,2R)-2-(benzyloxycarbonylamino)cyclobutane-1-carboxylate, **162**
- (1S,2R)-2-(Benzyloxycarbonylamino)cyclobutane-1-carboxylic acid, **16**
- Diazomethane distillation from Diazald®
- Methyl-(1S,2R)-2-(benzyloxycarbonylamino)cyclobutane-1-carboxylate, **10**
- Methyl-(1S,2R)-2-(tert-butoxycarbonylamino)cyclobutane-1-carboxylate, **156**
- (1S,2R)-methyl 2-(bis(tert-butoxycarbonyl)amino)cyclobutanecarboxylate, **165**
- (1S,2R)-2-bis(tert-butoxycarbonylamino)cyclobutane-1-carboxylic acid, **157**
- *tert*-Butyl ((1*R*,2*S*)-2-(benzyloxycarbonylamino)cyclobutane)(*tert*-butoxycarbonyl)carbamate, **152**
- (1*R*,2*S*)-2-(*tert*-butoxycarbonylamino)cyclobutane-1-carboxylic acid, **51**
- *tert*-Butyl (1*S,*2*R*)-2-carbamoylcyclobutanecarbamate, **163**
- (1*S*,2*S*)-2-(*tert*-butoxycarbonylamino)cyclobutane-1-carboxylic acid, **158**
- Benzyl *tert*-butyl ((1*S*,2*S*)-cyclobutane-1,2-diyl)dicarbamate, **153**
- Methyl 2-bis(*tert*-butoxycarbonylamino)-*(*1R*,*2S*)*-cyclobutan-1-carboxylate, **165**
- *(*1*R,*2*S)*-2-bis(*tert*-butoxicarbonylamino)cyclobutane-1-carboxylic acid, **157**
- *tert*-butyl ((1*S*,2*R*)-2-(benzyloxycarbonylamino)cyclobutane)(*tert*-butoxycarbonyl)carbamate, **152**
- (1*R*,2*R*)-2-(*tert*-butoxycarbonylamino)cyclobutane-1-carboxylic acid, **158**
- Benzyl *tert*-butyl ((1*R*,2*R*)-cyclobutane-1,2-diyl)dicarbamate, **153**
- (1*S*,2*S*)-2-(benzyloxycarbonylamino)cyclobutanaminium chloride, **170**
- (1*R*,2*R*)-2-(benzyloxycarbonylamino)cyclobutane-1-aminium chloride, **170**
- (1*S*,2*R*)-2-(benzyloxycarbonylamino)cyclobutane-1-aminium chloride, **168**
- *Tert*-butyl ((1*S*,2*S*)-2-aminocyclobutane)carbamate, **172**
- Benzyl ((1*S*,2*S*)-2-(3'-(3'',5''-bis(trifluoromethyl)phenyl)thioureido)cyclobutane)carbamate, **171**

- Benzyl ((1*R*,2*S*)-2-(3'-(3'',5''-bis(trifluoromethyl)phenyl)thioureido)cyclobutane) carbamate, **169**
- Benzyl (1*R*,2*R*)-2-(isobutylamino)cyclobutane carbamate, **173**
- (22*R*,19*S*)-*N*22,*N*19-dihexadecylcyclobutane-22,19-dicarboxamide, *cis*-**190**
- (19*S*,22*S*)-*N*19,*N*22-dihexadecylcyclobutane-19,22-dicarboxamide, *trans*-**190**
- *tert*-butyl (1*S*,2*S*)-cyclobutane-1,2-diyldicarbamate, **174**
- C_{12}-NH-centered-bromoalkyl, **176**
- Bolaamphiphile *trans*-**177**
- *tert*-butyl(*tert*-butoxycarbonyl)((1*S*,2*R*)-2-(*tert*-butoxycarbonylamino)cyclobutane) carbamate, **183**
- ((14*R,*17*S*)-cyclobutane-14,1-diyl)bis(1,1'-bromododecanamide), **188**
- Bolaamphiphile *cis*-**177**
- Benzyl ((1*R*,2*S*)-2-(13'-bromododecanamido)cyclobutane)carbamate, **181**
- (1*R*,2*S*)-cyclobutane-1,2-dicarboxylic acid, **154**
- 12-bromododecan-1-aminium bromide, **185**
- 12-bromodo (15*R*,18*S*)-*N*1,*N*2-bis(1-bromododecyl)cyclobutane-15,18-dicarboxamide, **188**
- Bolaamphiphile, *cis*-**187**
- (1*S*,2*S*)-cyclobutane-1,2-dicarboxylic acid, **155**
- (15*S*,18*S*)-*N*1,*N*2-bis(1-bromododecyl)cyclobutane-15,18-dicarboxamide, **186**
- Bolaamphiphile, *trans*-**187**
- Triethoxysilane derivative *trans*-**189**
- Hybrid silica *trans*-**229**
- Silanol *trans*-**231**
- Hybrid silica *cis*-**229**
- (7*S*,10*S*)-*N*6-(3-triethoxysilylpropyl)cyclobutane-7,10-diamine, *trans*-**230**
- Hybrid base catalyzed complex of Rhodium, *trans*-**230-Rh**
- (4*S*,1'*R*,3'*R*)-4-[2',2'-dimethyl-3'-(2''-methyl-[1'',3'']-dioxolan-2''-yl)cyclobutane]-*N*-isopropylpyrrolidin-2-one, **240**
- (4S,1'*R*,3'*R*)-3'-acetyl-[2',2'-dimethylcyclobutane]-*N*-isopropylpyrrolidin-2-one, **241**

- (1’*R*,3’*R,*3’’*S*)-3’-[2’,2’-dimetil-3’-(1’’-isopropylpyrrolidin-3’’-yl)cyclobutane] methanol, **242**
- (1’*R*,3’*R*,3’’*S*)-4-Benzyl-1-[3’-(1’’-isopropylpyrrolidin-3’’-yl)-2’,2’-dimethyl-cyclobutane)metyl]-piperidine, **237**
- (3*S*,1’*R*,3’*R*)-3-[2’,2’-dimethyl-3’-(2’’-methyl-[1’’,3’’]-dioxolan-2’’-yl)cyclobutane]-4-nitrobutan-1-ol, **238**
- (3*S*,1’*R*,3’*R*)-4-amino-3-[2’,2’-dimethyl-3’-(2’’-methyl-[1’’,3’’]-dioxolan-2’’-yl) cyclobutane]-butan-1-ol, **243**
- (3*S*,1’*R*,3’*R*)-4-tosylamino-3-[2’,2’-dimethyl-3’-(2’’-methyl[1’’,3’’]dioxolan-2’’-yl)cyclobutane]-butan-1-ol, **245**
- (3*S*,1’*R*,3’*R*)-3-[2’,2’-dimethyl-3’-(2’’-methyl[1’’,3’’]dioxolan-2’’-yl)cyclobutane]-*N*-tosylpyrrolidine, **246**
- (1’*R*,3’*R,*3’’*S*)-1-[2’,2’-dimethyl-3’-(*N*-tosylpyrrolidin-3’’-yl)-cyclobutane]ethan-one, **247**
- (1*S*,1’*R*,3’*R,*3’’*S*)-1-[2’’,2’-dimethyl-3’-[N-tosylpyrrolidin-3’’-yl)cyclobutane] ethanol, **239**
- Synthesis of ruthenium nanoparticles, **Ru237, Ru238 and Ru239**
- Catalytic hydrogenation reactions

CHAPTER I

General introduction and general objectives

1. GENERAL INTRODUCION AND GENERAL OBJECTIVES

The present doctoral Thesis has been developed in the context of the Synthesis, Structure and Chemical Reactivity research group. Taking advantage of the broad experience held by this group in the synthesis of the highly constrained cyclobutane motif and several useful derivatives, a series of new materials with potential very interesting applications have been prepared. Thus, first of all on this PhD Thesis several cyclobutane derivatives based on 1,2-diamine or 1,2-dicarboxylic acid have been synthesized in order to functionalize them with different groups including long alkyl chains, ureas, amphiphilic or silylated chains.

Furthermore, the inherent rigidity of the cyclobutane moiety together with the flexibility of alkyl chains, demonstrates their determinant structural effect, yielding molecules with a wide range of properties, from low molecular weight organogelators to surfactants.

In addition, the presence of two chiral centers in the four-membered ring when the cyclobutane is substituted in the 1,2- or 1,3- positions provides the molecule with a chiral environment which is interesting to explore in several fields as for instance asymmetric catalysis.

In the first part of this Thesis, the enantio- and diastereocontrolled synthesis of the four stereoisomers of orthogonally protected cyclobutane-1,2-diamine was carried out in view of opening a new access for a wide range of useful enantiopure molecules containing this moiety. As will be seen in the introduction of this Thesis, only three synthesis of *trans*-cyclobutane-1,2-diamine had been reported previously, but in most cases with low yields and without stereoselectivity. Then, some of these enantiopure molecules were functionalized in order to obtain compounds with some interesting properties as for example, organogelators, bolaamphiphiles, hybrid materials or metal ligands for catalysis. Those compounds were studied by different techniques in order to compare the effect on stereo- and regiochemistry and also their morphology.

1 General introduction and general objectives

Scheme **1** shows schematically the precursors and the scaffolds used in the preparation of different materials. Thus, the molecular precursors had to be prepared employing cyclobutane-1,2-diamines and cyclobutane-1,2-dicarboxylic acids as key intermediate scaffolds.

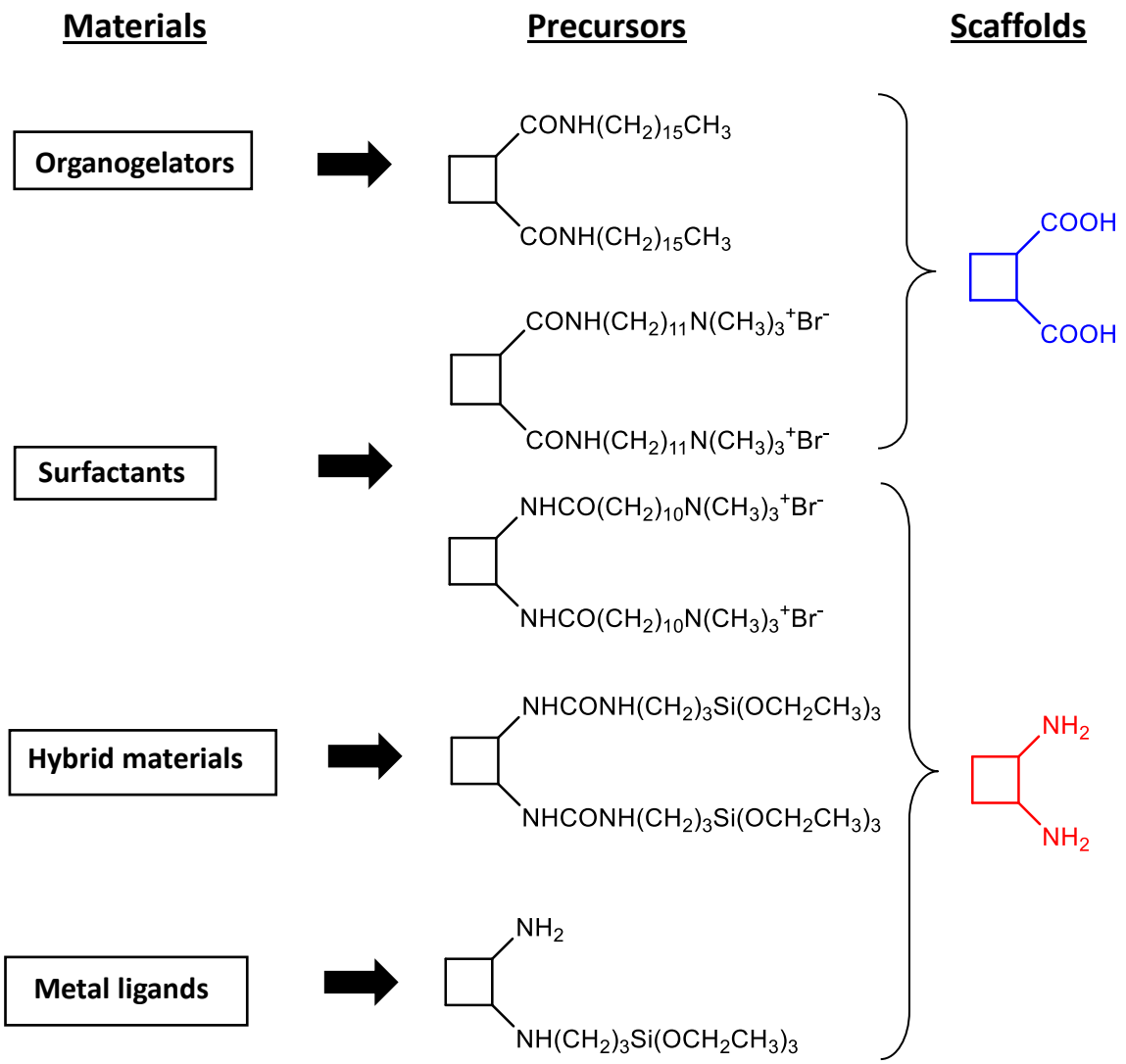

Scheme 1. General Scheme for the preparation of organogelators, surfactants, hybrid materials and metal ligands.

Finally, in the last part of this Thesis, the cyclobutane moiety disubstituted in positions 1,3 was used to prepare chiral ligands to stabilize ruthenium nanoparticles and first assays in asymmetric catalysis were performed in order to test their activity.

CHAPTER II

Precedents in the research group

2. PRECEDENTS IN THE RESEARCH GROUP

2.1 Synthesis of compounds containing the 1,2-disubstituted cyclobutane moiety.

In the last decade, our research group has been interested in the use of cyclobutane as a conformational restriction element in a wide variety of works.[1,2,3] The presence of the highly constricted four-membered ring in the molecules provides rigidity and two chiral centres of known configuration. Moreover, our research group is pioneer in the synthesis of optically active cyclobutane amino acids. Some of these compounds have been incorporated in peptides which could be used both in the medicinal[2] and materials field.[3] The presence of the cyclobutane induces the formation of defined secondary structures that have been deeply studied.[4,5,6]

The synthesis of one of the most versatile amino acid and some derivatives was achieved by using a chemoenzymatic approach to induce asymmetry in achiral precursors. Then, selective manipulation of the functional groups allowed the free amino acid to be obtained, as well as the fully and the partially protected amino acids shown in Scheme **2**. On the other side, the commercially available diacid **7** can be used as the achiral precursor, which after methylation can allow the preparation of the meso diester **8**. The selective enzymatic saponification of that compound, allowed the achievement of an enantiopure half-ester as the chiral precursor in the synthetic route, (-)-**9**. Finally, having the Curtius rearrangement as key step for the preparation of the target molecule, the synthesis of the enantiomer (1*R*,2*S*)-2-aminocyclobutane-1-carboxylic acid was achieved. During the last decade, some steps of the presented

---

[1] Fernández, D.; Torres, E.; Avilés, F. X.; Ortuño, R. M.; Vendrell *J. Bioorg. Med. Chem.* **2009**, *17*, 3824.
[2] Berlicki, L.; Kaske, M.; Gutiérrez-Abad, R.; Bernhardt, G.; Illa, O.; Ortuño, R. M.; Cabrele, C.; Buschauer, A.; Reiser, O. *J. Med. Chem.* **2013,** *56,* 8422.
[3] Torres, E.; Puigmarti-Luis, J.; Perez del Pino, A.; Ortuño, R. M.; Amabilino, D. B. *Org. Biomol. Chem.* **2010,** *8*, 1661.
[4] Torres, E.; Gorrea, E.; Burusco, K. K.; Da Silva, E.; Nolis, P.; Rua, F.; Boussert, S.; Diez-Perez, I.; Dannenberg, S.; Izquierdo, S.; Giralt, E.; Jaime, C.; Branchadell, V.; Ortuño, R. M., *Org. Biomol. Chem.* **2010**, 8, 564.
[5] Torres, E.; Gorrea, E.; Silva, E. D.; Nolis, P.; Branchadell, V.; Ortuño, R. M. *Org. Lett.* **2009,** 11, 2301.
[6] Gorrea, E.; Nolis, P.; Torres, E.; Da Silva, E.; Amabilino, D. B.; Branchadell, V.; Ortuño, R. M. *Chem. Eur. J.* **2011,** 17, 4588.

synthetic route have been improved by introducing different methodologies.[7] Recently, a new key step has been introduced to the preparation of the cyclobutane amino acids, this being the formation of the cyclobutane moiety from maleic anhydride and ethylene in a [2+2] photochemical reaction.

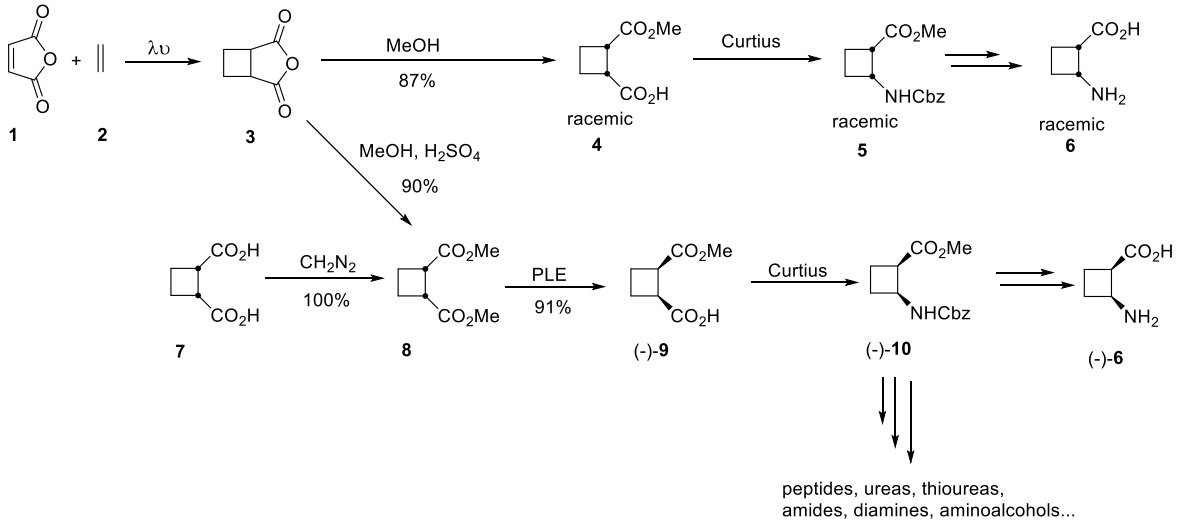

Scheme 2. Stereoselective synthesis of cyclobutane derivatives.

2.1.1 Synthesis of amino acids and peptides

The biological properties shown as antiviral and antitumoral agents by cyclobutane-containing amino acids and peptides,[8,9] and on the other hand, the constriction offered by the four-membered ring, have awakened the interest of chemists in this kind of compounds. Moreover, in recent years, the conformational restriction in small molecules with potential biological activity is crucial in many cases to guarantee unique interactions with the target receptor and to increase their metabolic stability and activity. Owing to that, there are many examples in the literature on the synthesis of restricted amino acids by action of a tensioned ring. Nevertheless, there are few examples of amino acids and peptides containing a four-membered ring.

[7] Izquierdo, S.; Martin-Vila, M.; Moglioni, A. G.; Branchadell, V.; Ortuno, R. M. *Tetrahedron Asymmetry,* **2002**, *13*, 2403.
[8] Miles, D. H.; Tunsuwan, K.; Chittawong, V.; Kokpol, U.; Choudhary, M. I.; Clardy, J., *Phytochemistry* **1993,** *34*, 1277.
[9] Stevens, C. V.; Smagghe, G.; Rammeloo, T.; De Kimpe, N., *J. Agric. Food Chem.* **2005**, *53*, 1945.

In 2005,[10] a family of β-peptides derived from different stereoisomers of 2-aminocyclobutane-1-carboxylic acid, **6**, shown in Figure **1**, were synthesized and studied. The formation of a six-membered hydrogen-bonded ring in diastereomeric bis(cyclobutane) β-dipeptides **12a** and **13** in $CDCl_3$ solution was reported. Dimer **13** was used in the convergent synthesis of tetramer **15b** through selective deprotection of the amine and the carboxylic acid, respectively. Peptide coupling of the resultant intermediates in the presence of pentafluorophenyl diphenyl phosphinate (FDPP) as a coupling reagent produced octamer **15d**.

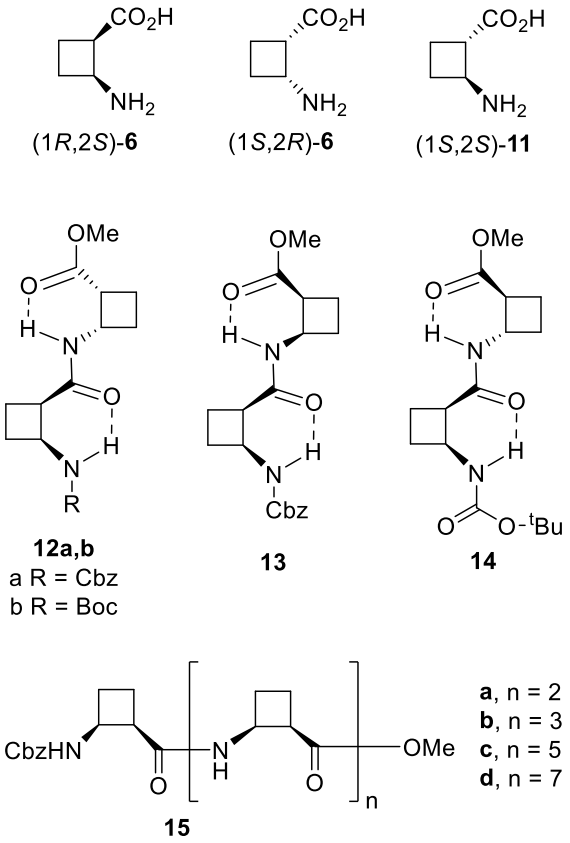

Figure 1. Structure of some cyclobutane β-amino acids and related β-peptides.

The aggregation of this peptide **15b** was also studied. Comparison of the CD spectra in MeOH for the oligomers of this series account for the same preferential conformation in these β-peptides. Figure **2** shows the superposition of CD spectra of 0.5 mM solutions of dimer, tetramer, hexamer and octamer. TEM micrographs (Figure

[10] Izquierdo, S.; Rúa, F.; Sbai, A.; Parella, T.; Álvarez-Larena, A.; Branchadell, V.; Ortuño, R. M. *J. Org. Chem.* **2005**, *70*, 7963.

2a, 2b and **2c**) of all β-peptides in this series show strong tendency to self-assemble from methanol solutions giving nanosized fibres whose morphology remained unaltered after one week incubation. High-resolution NMR experiments, CD spectra and computational studies reveal that β-peptides constituted by residues derived from (1*R*,2*S*)-2-aminocyclobutane-1-carboxylic acid to adopt a strand-type conformation in solution, independently of their size and the terminal amine protecting group. The presence of the small cyclobutane ring imposes this conformational bias, which results from the formation of intra-residue hydrogen bonded six-membered rings giving rise to *cis*-fused [4.2.0]octane structural units that confer high rigidity on these β-peptides. As an example, in Figure **3** a strand-type conformation for hexamer **15c** in $CDCl_3$ solution can be observed.

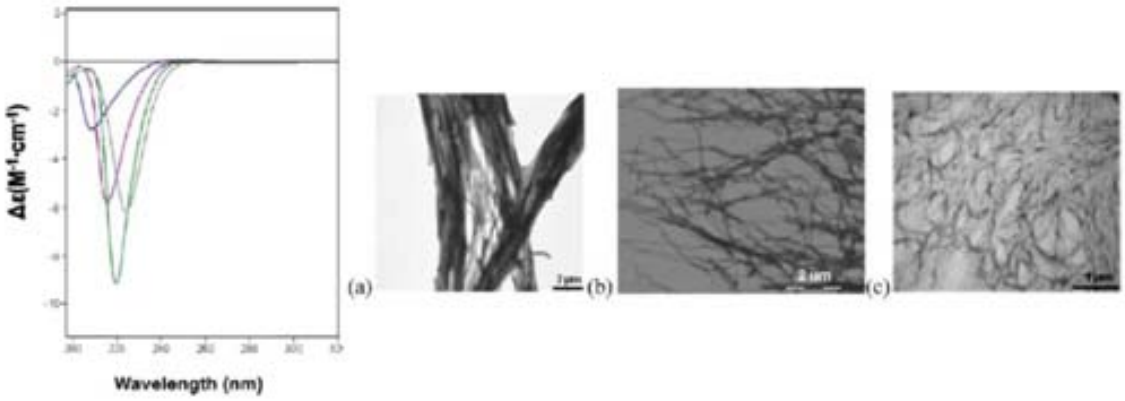

Figure 2. CD spectra of 0.5 mM methanol solutions of dimer, tetramer, hexamer and octamer for the series with Cbz protected amino acid and TEM images of the nanosized fibres formed by (a) **15a** from a 5 mM, (b) **15b** from a 1 mM, (c) **15d** from a 0.5 mM solution in MeOH (1 d incubation) placed onto a carbon film-coated copper grid and stained with 2% uranyl acetate.

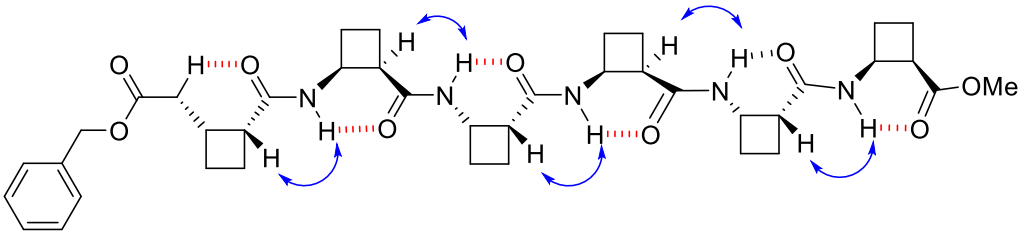

Figure 3. Strand-type conformation for hexamer **15c** in $CDCl_3$ solution. Arrows show inter-residue Hα and N*H* NOE contacts.

More recently, several oligomers constructed with (1*R*,2*S*)-2-aminocyclobutane-1-carboxylic acid and glycine, β-alanine, and ϒ-amino butyric acid (GABA), respectively, joined in alternation have been synthesized.[11] Combination of different types of cyclic or linear amino acids in heterogeneous backbones to afford hybrid peptides offers unique possibilities of folding.[12]

Convergent synthetic routes allowed the easy and efficient preparation of the desired oligomers. The general strategy is illustrated in Scheme **3.** *N*-Cbz-(1*R*,2S)-2-aminocyclobutane-1-carboxylic acid **16**,[13] was reacted with O-Me protected glycine, β-alanine, and GABA ammonium salts, **17-19**, respectively, in the presence of DIPEA and using PyBOP as coupling agent. In this way, hybrid dipeptides **20-22** were obtained in 80–90% yield under mild conditions. The ammonium triflates **23-25** were quantitatively prepared by submitting **20-22** to hydrogenation of N-Cbz protection in the presence of TFA, at room temperature. Protonation of the amino function prevented the cyclobutane ring opening which was previously observed in similar compounds.[14]

[11] Celis, S.; Gorrea, E.; Nolis, P.; Illa, O.; Ortuño, R.M. *Org. Biomol. Chem.* **2012**, *10*, 861.
[12] Horne, W. S.; Gellman, S. H. *Acc. Chem. Res.* **2008**, *41*, 1399.
[13] Izquierdo, S.; Kogan, M. J.; Parella, T.; Moglioni, A. G.; Branchadell, V.; Giralt, E.; Ortuño, R. M. *J. Org. Chem.* **2004**, *69*, 5093.
[14] Aitken, D. J.; Gauzy, C.; Pereira, E. *Tetrahedron Lett.* **2004**, *45*, 2359.

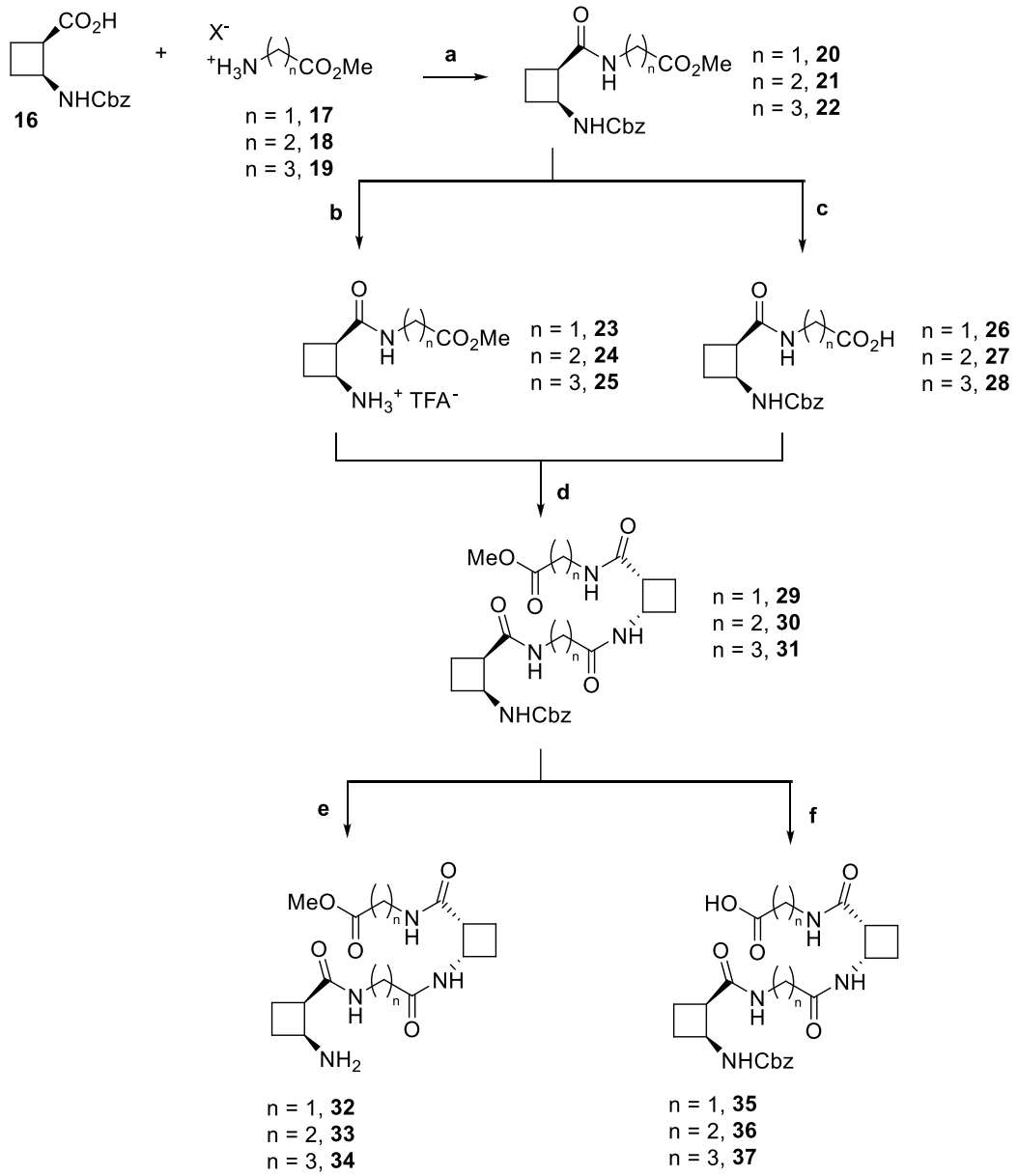

Scheme 3. Synthetic route of some hybrid peptides prepared in our laboratory. Reagents and conditions: (a) DIPEA, PyBOP, CH_2Cl_2, rt, 1.5 h (80–90%); (b) H_2 (6–7 atm), 10% $Pd(OH)_2/C$, TFA, rt (quantitative); (c) 0.25 M NaOH, 1 : 1 THF-H_2O, 0 °C, 3 h (93–96%); (d) DIPEA, FDPP, 20 : 1 CH_2Cl_2-DMF, rt, overnight (55–60%); (e) H_2 (7–8 atm), 10% $Pd(OH)_2/C$, MeOH, rt (quantitative); (f) 0.25 M NaOH, 1 : 1 THF-H_2O, 0 °C to rt, (80–94%).

Following an alternative route, mild saponification of the ester function in **20-22** afforded free acids **26-28** in nearly quantitative yields. Subsequent coupling of the amines with the corresponding carboxylic acids afforded hybrid tetrapeptides **29-31**, respectively, in 55–60% yield. These compounds were selectively deprotected to

provide amines **32-34** and carboxylic acids **35-37**, respectively, which were used in the synthesis of hexamers **38-39** and octamers **40-42** (Figure **4**).

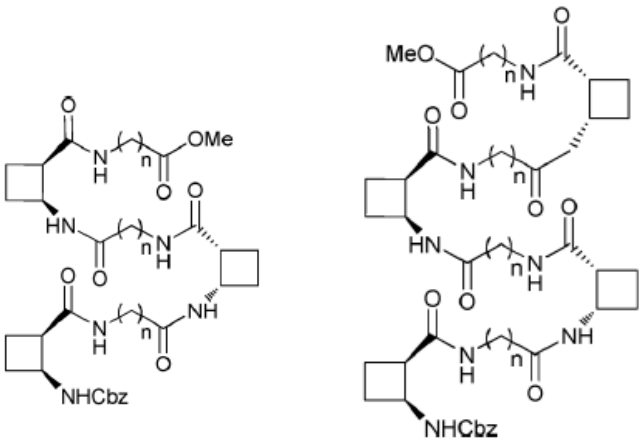

n = 1, **38**
n = 3, **39**

n = 1, **40**
n = 2, **41**
n = 3, **42**

Figure 4. Structures of hexamers and octamers synthesized and studied in this work.

CD spectra of all hybrid peptides exhibited negative peaks. Peaks at 190 nm were found for tetramer **30** and octamer **41** in the β-alanine series. This excellent concordance allowed the assumption of a helical conformational preference for octamer **41** in view of previous results. For tetramer **30**, a 14-helical folding stabilized by hydrogen bonding interaction between NH and CO was found, on the basis of NMR experiments and theoretical calculations.[11] For tetra-, hexa- and octamers in glycine and GABA series, a β-sheet-like structure was observed.

2.1.2 Synthesis of ureas and thioureas.

Other interesting cyclobutane derivatives prepared in the group are ureas and thioureas which were used in this Thesis for the preparation of hybrid materials as described in Chapter 6. Our research group has a broad experience in their synthesis. The ones synthesized in the group contain two cyclobutane rings and they were

achieved by an enantioselective strategy, starting from the recurring common chiral precursor (*S*,*R*)-**9** (Scheme **4**).

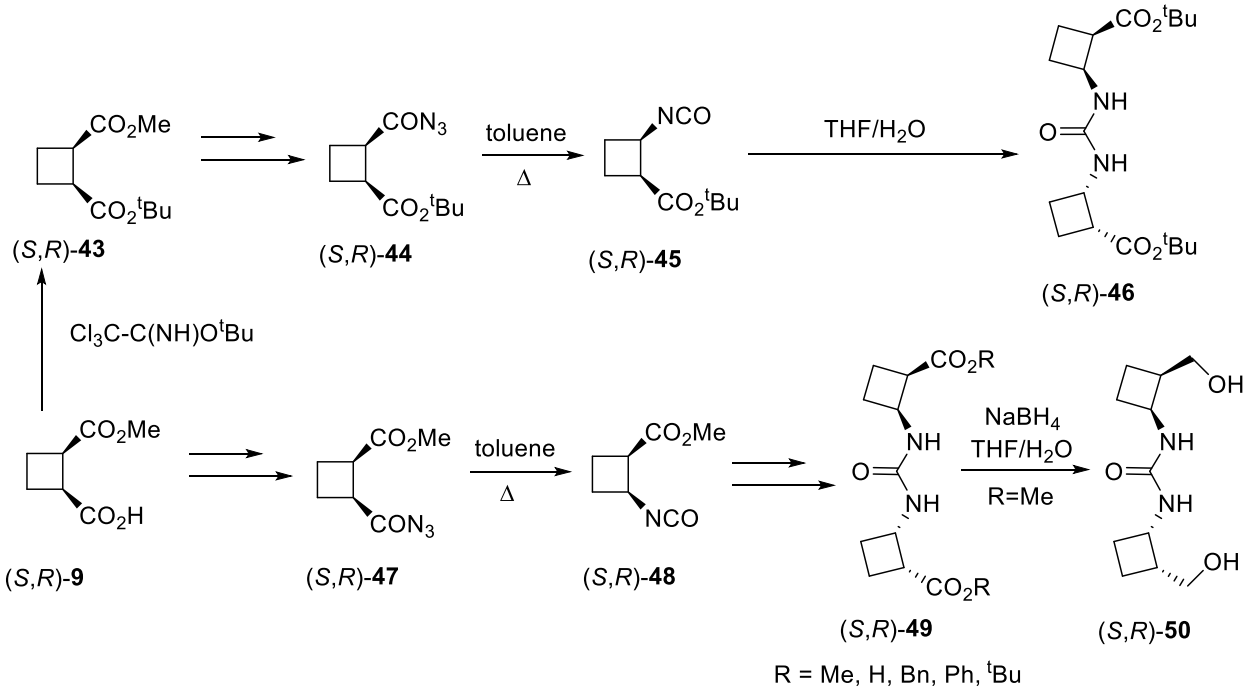

Scheme 4. Synthesis of bis-cyclobutane ureas via an enantioselective strategy.

Structural studies of such ureas were carried out by X-ray crystallography, since some of them formed crystals easily in common solvents. The X-ray analysis showed that the R substituent was critical for the adoption of the tertiary structure (Figure **5**).

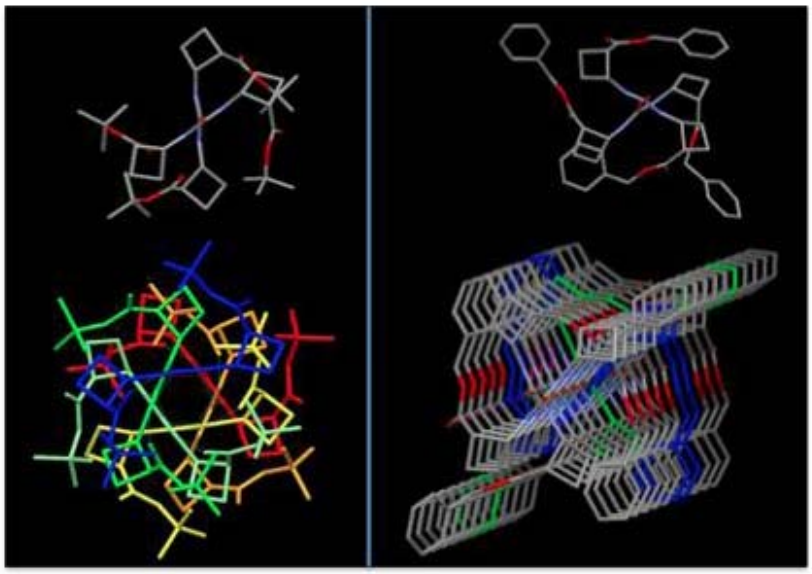

Figure 5. Crystal packing of urea **49** (R=^{t}Bu) (left) and urea **49** (R=Bn) (right).

Other ureas were obtained by serendipity when cyclobutane β-peptides were being synthesized. Nevertheless, later on, a stereoselective and efficient synthetic route was developed to afford chiral *cis*-fused *N*-monoprotected bicyclic ureas (*S*,*R*)-**52**, (*S*,*R*)-**53** and (*R*,*S*)-**54**. Proper chemical transformations on both functional groups of the chiral precursor (*S*,*R*)-**9** were necessary to direct the synthesis to three key stereoisomers, which underwent an intramolecular Curtius rearrangement, in the presence of diphenylphosphoryl azide (DPPA) and Et_3N, giving the corresponding ureas in one-pot reactions in 70-80% yield (Scheme **5**).[15]

[15] Gorrea, E.; Nolis, P.; Álvarez-Larena, A.; Da Silva, E.; Branchadell, V.; Ortuño, R. M. *Tetrahedron: Asymmetry* **2010**, *21*, 339.

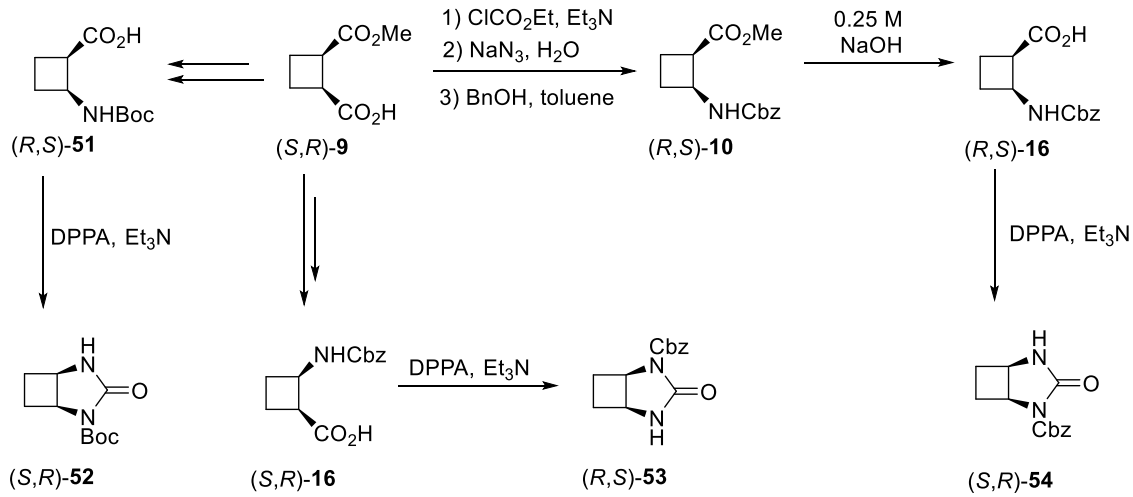

Scheme 5. Synthesis of chiral *cis*-fused-*N*-monoprotected cyclobutane bicyclic ureas via a stereoselective strategy.

Both structural studies in solution and in the solid state revealed a great tendency of these ureas to form ordered aggregates. NMR, IR and TEM techniques showed that ureas interacted through hydrogen bonds to form fibrillar assemblies in solution, while X-ray analysis presented two urea molecules interacting via only one hydrogen bond, which yielded infinite chains (Figure **6**). Moreover, the coplanarity of both carbamate and urea groups led the crystal packing to a parallel molecular arrangement. Theoretical calculations supported this last result, reproducing well the geometry and predicting favourable energies for the formation of tetramers and higher aggregates.

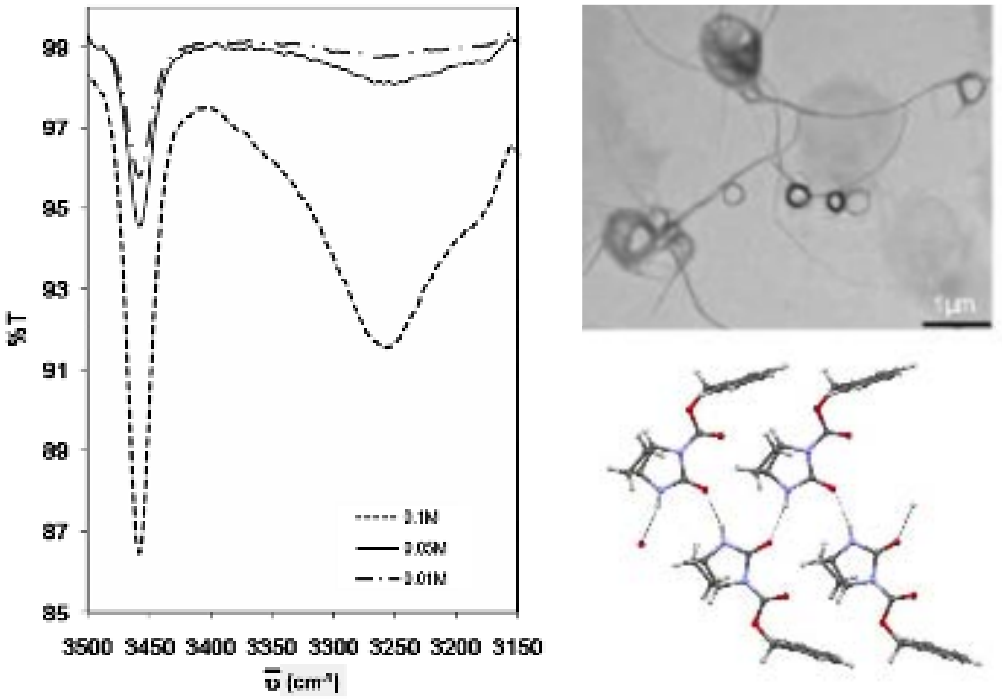

Figure 6. Urea (*R*,*S*)-**53**: IR spectra at the NH stretching region in $CDCl_3$ (left); TEM image of fibres formed from 5 mM solutions in MeOH (right-top); view of infinite chains parallel to the crystallographic a axis (right-bottom). Dashed lines represent hydrogen bonds.

Cyclobutane-containing thioureas, alternatively, have been reported as organocatalysts. Starting from the same hemiester (*S*,*R*)-**9**, *cis*- and *trans*- cyclobutane containing 1,3-diamines and 1,3-amino alcohols were synthesized in a stereocontrolled manner.[16] Afterwards, efficient functionalization via substitution with 3,5-bis(trifluoromethyl)phenyl isothiocyanate afforded the desired thioureas **59**, **60**, **61** and **62** (Scheme **6**).

[16] Mayans, E.; Gargallo, A.; Álvarez-Larena, Á.; Illa, O.; Ortuño R. M. *Eur. J. Org. Chem.* **2013**, *8*, 1425.

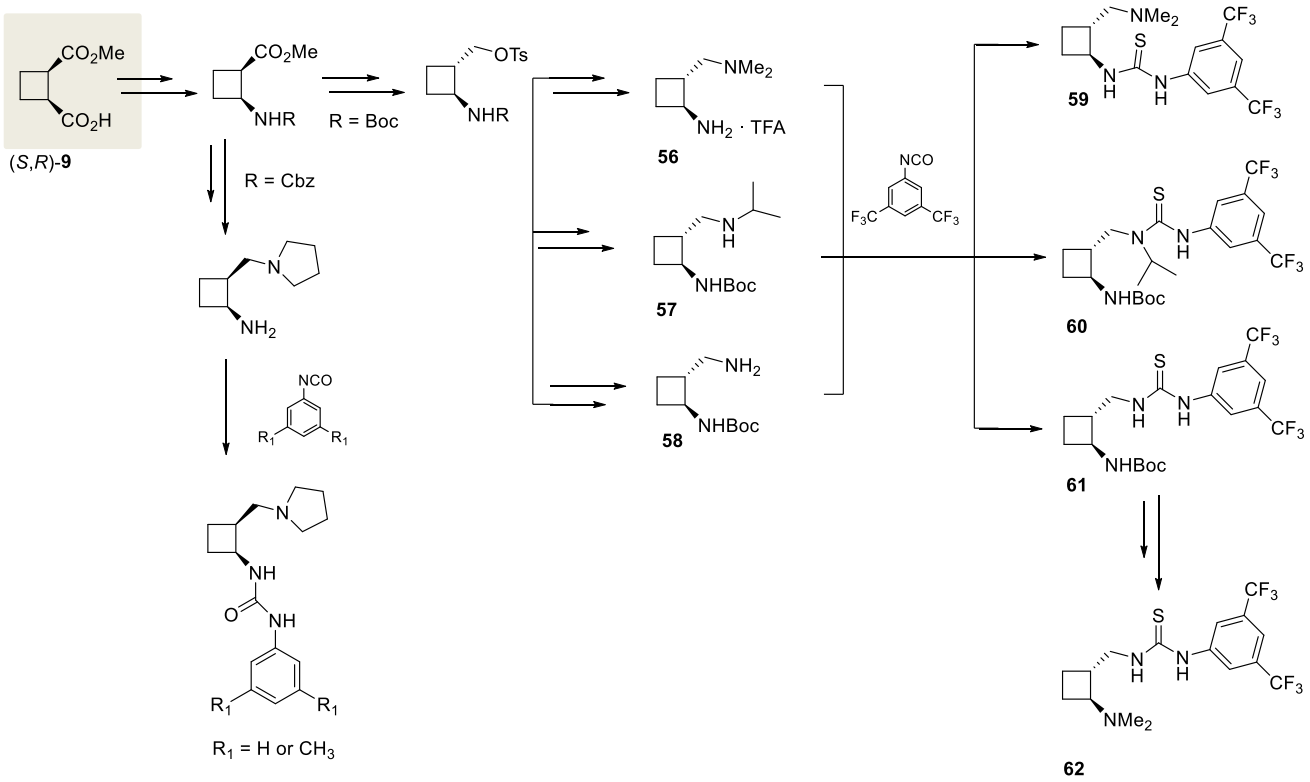

Scheme 6. Diastereodivergent synthesis of chiral vic-disubstituted-cyclobutane scaffolds: 1,3-diamines and 1,3-amino alcohols. Further functionalization into thioureas **59**, **60**, **61** and **62**.

2.2 Applications of 1,2-disubstituted cyclobutane in materials

2.2.1 Conductive materials

The use of unnatural peptides in molecular-based systems presents enormous possibilities for the preparation of new chiral materials with novel properties, because these products can adopt well defined secondary and, in some cases, tertiary and quaternary structures.[17] Among them, β-peptides are prominent. Their propensity to fold, forming sheets, helices and reversed turns, has been well established in our group.[12]

However, the use of these peptide derivatives to generate chiral conducting materials was an unexplored area of great interest,[18] and for that reason, compound (*R*,*S*,*R*,*S*)-**65** was prepared in our research group (Scheme **7**).[19] The interest of such a material lies on the gaining of a fibrous system capable of conducting electricity, once doped (oxidized) to produce a conduction pathway. The product was obtained by simple reaction of the amide derivative from the dipeptide and the acid derivative from TTF, using EDAC/HOBt coupling agents.

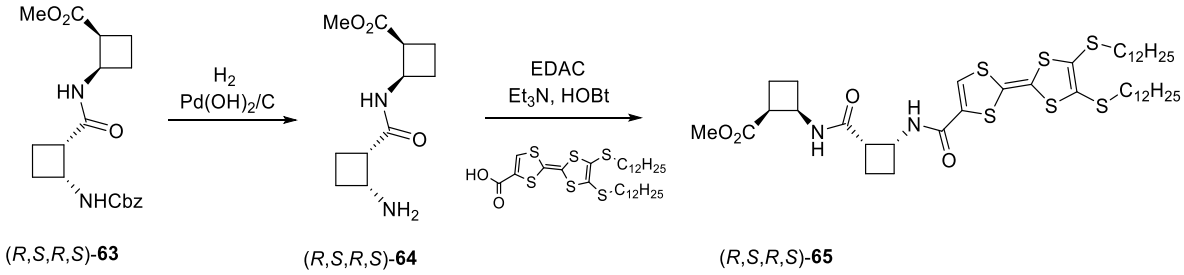

Scheme 7. Synthesis of (*R*,*S*,*R*,*S*)-**65**.

Afterwards, characterization of compound (*R*,*S*,*R*,*S*)-**65** was carried out and supramolecular fibres were observed to be formed by the compound using TEM (Figure **7**).

[17] Gellman, S. H. *Acc. Chem. Res.* **1998**, *31*, 173.
[18] Avarvari, N.; Wallis, J. D. *J. Mater. Chem.* **2009**, *19*, 4061.
[19] Torres, E.; Puigmartí-Luis, J.; Pérez del Pino, A.; Ortuño, R.M.; Amabilino, D. B. *Org. Biomol. Chem.*, **2010**, *8*, 1661.

Figure 7. TEM micrograph of the TTF-cyclobutane compound **65**.

Conductivity could be probed when charge carriers were introduced by doping the films of (*R*,*S*,*R*,*S*)-**65** with iodine vapour. Current-sensing atomic force microscopy (CS-AFM) was used to explore the films on HOPG and the conductivity was appreciated from the current-potential curve performed with the tip of the microscope. Such conductivity was uniform over hundreds of square nanometres, an important aspect of these materials for further applications (Figure **8**).

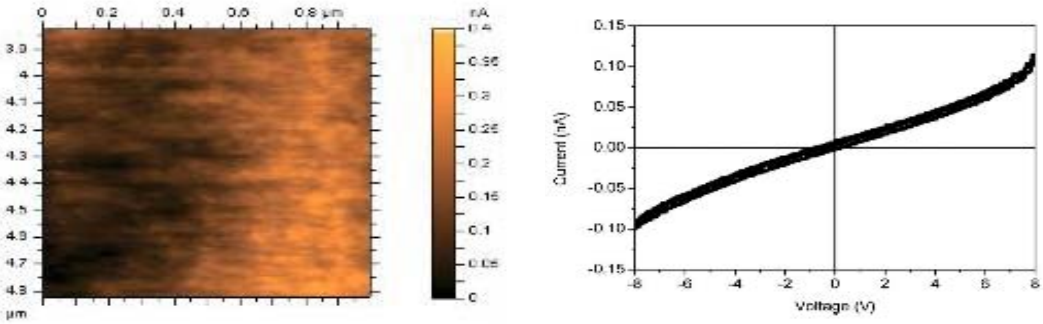

Figure 8. CS-AFM image (at 5 V applied potential) of a doped film of **65** on HOPG (left) and a representative spectroscopy curve (right).

2.2.2 Low molecular weight gelators (LMWGs)

In the last few years there has been a growing interest in the design of molecules that are able to self-assemble in a predictable manner. Particular examples are gels, which will be widely discussed in Chapter 3 and which are materials that nowadays have multiple applications in the fields of cosmetics, lubricants, and the

food industry, among many others.[20] Apart from that, our group has a broad experience in the synthesis and structural studies of designed peptides based on optically active 2-aminocyclobutane-1-carboxylic acid derivatives.[10,11]

Low molecular weight peptides, often incorporating hydrophobic amino acids, have been widely employed as organogelators.[21] Peptides aggregate through hydrogen bonding whereas the apolar groups maintain the solubility in the organic solvent and avoid the precipitation.

For instance, in a study of 2011 from our research group, two chiral synthetic β-dipeptides were constructed, one with two *trans*-cyclobutane residues and the other with one *trans* and one *cis* fragment, **66** and **67**, respectively (Figure **9**). They were investigated in order to get insight into the non-covalent interactions responsible for their self-assembly to form ordered aggregates, as well into parameters such as their morphology and size.[10]

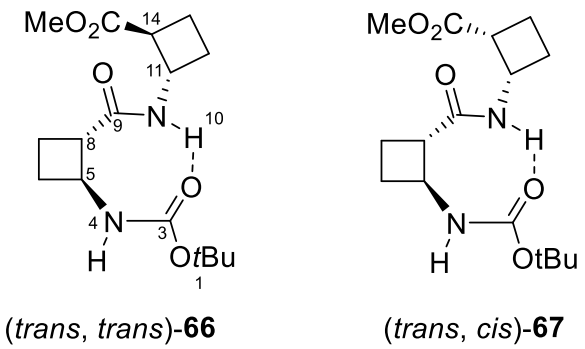

Figure 9. Compounds **66** and **67** synthesized and studied in this work.[10]

In solution, the structural effect due to the introduction of *trans* residues in β-dipeptides was demonstrated. Using different techniques such as NMR, SEM, TEM, AFM, IR, CD and computational calculations, (*trans*,*trans*)-**66** and (*trans*,*cis*)-**67** dipeptides were investigated, exhibiting some key differences with respect to the all-*cis*-polycyclobutane β-oligomers. Both dipeptides formed gels in toluene, so this solvent was employed to perform the main experiments.

[20] Hirst, A. R.; Escuder, B.; Miravet J. F.; Smith, D. K. *Angew. Chem. Int. Ed.* **2008**, *47*, 8002.
[21] Iqbal, S.; Miravet, J. F.; Escuder, B. *Eur. J. Org. Chem.* **2008**, 4580.

TEM and SEM images showed well-defined fibrillar aggregates for both samples, besides the evident differences of the resulting images concerning each technique and their different preparation procedures. TEM images presented more dispersed fibrils, while images of the surface of xerogels obtained by SEM consisted of intertwined fibres and bundles of variable width. In addition, AFM images afforded the heights of aggregates, which could also pile themselves (Figure **10**).

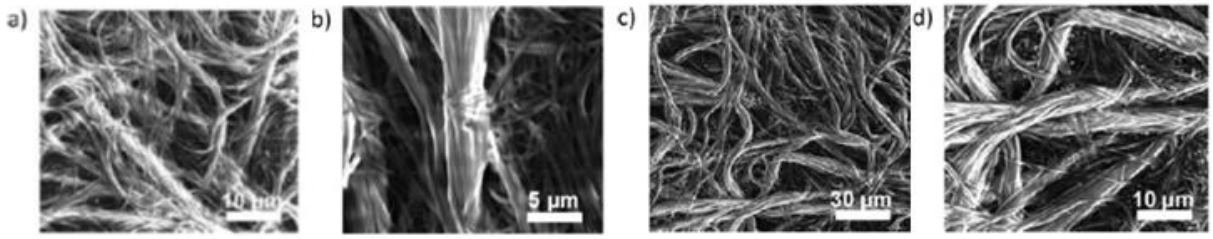

Figure 10. SEM images of samples **66** (**a** and **b**) and **67** (**c** and **d**) as xerogels (from toluene) on graphite at 60 Pa.

In addition, NMR experiments on 40 mM solutions of (*S*,*S*,*S*,*R*)-**66** and (*S*,*S*,*S*,*S*)-**67** in toluene-d_8 allowed to determine their temperature of gelation at three different concentrations. Gelation processes were monitored by variable-temperature ^{1}H-NMR experiments; the representation of normalized integrals vs. temperature showed a hydrogen-bond fixing and a sample gelation subprocesses, which converged at the gelation temperatures (T_{gel}) (Figure **11**).

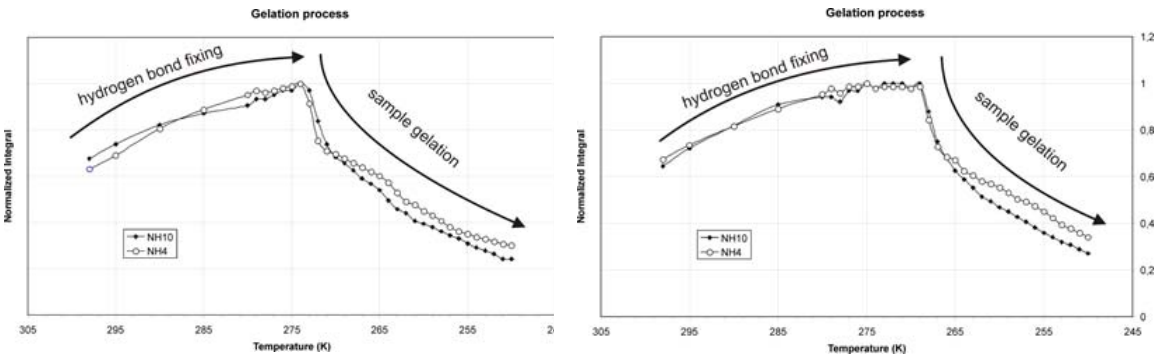

Figure 11. Graphical representation of the normalized NH proton integrals NH^4 and NH^{10} during the gelation process for 40 mM solutions of a) **66** and b) **67** in toluene-d_8.

Another recent work has been published in our research group by Dr. Sergi Celis. In his PhD thesis, cyclobutane-base hybrid peptides **35-37** were prepared (Figure **12**). They were fully characterized[11] and they were evaluated as low-molecular weight

gelators yielding very nice gels in toluene in a 7-12 mM (mgc) range. Furthermore, the lowest values of concentration were generally obtained for the molecules with the shortest linear spacer.[22]

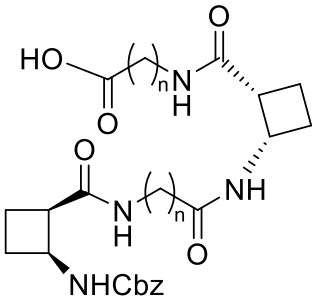

n = 1, **35**
n = 2, **36**
n = 3, **37**

Figure 12. Study of cyclobutane-based hybrid peptides subjected to this study.

Their physical properties such as morphology, size and type of supramolecular arrangement were analyzed by using several techniques, including scanning electron microscopy (SEM), circular dichroism (CD) and IR spectroscopy. For some selected gels produced from β,α-tetrapeptide **35** in toluene, the self-assembly of the molecules was modelled to investigate their tridimensional arrangement. High-resolution NMR experiments were also carried out, with the aim of studying the dynamics of the sol-gel process. Computational calculations for **35** allowed them to model the self-assembly of the molecules and a head-to-head arrangement to give helical structures corresponding to hydrogen bonded single chains was suggested. These features were corroborated by a high-resolution NMR spectroscopy study of the dynamics of the gelation process in toluene-d_8 which evidenced that molecules self-assemble to afford ordered aggregates with a supramolecular chirality (Figure **13**).

[22] Celis, S.; Nolis, P.; Illa, O.; Branchadell, V.; Ortuño, R. M. *Org. Biomol. Chem.* **2013**, *11*, 2839.

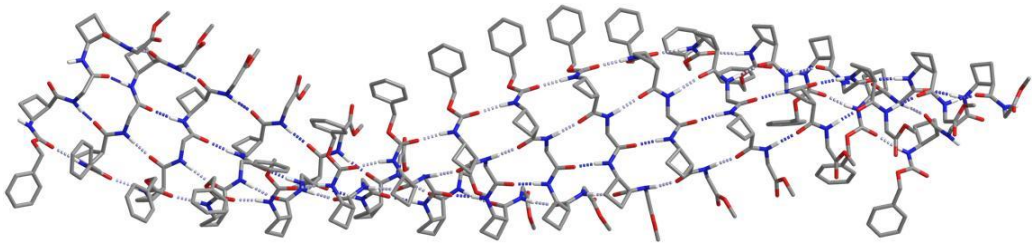

Side view

Top view

Figure 13. Structure of the hexadecameric aggregate of peptide **35** optimized at the MMFF level of calculation in chloroform.

2.3 Applications as metallocarboxypeptidase inhibitors

Since their discovery, carboxypeptidase CPA and CPB are considered to be good biomarkers for the early detection of acute pancreatitis and cancer.[23] Nevertheless, CPA and CPB are currently underway to discern potential ways to overcome the problem of poor oral absorption of peptide and protein drugs.[24] Peptidomimetics containing non hydrolyzable bonds have been widely exploited in the design of extremely potent protease inhibitors.[25] Compound BX528 (a phosphinate-containing mimic of the tripeptide Phe-Val-Lys), an inhibitor to human plasma CPB, appears as a recent example of application of this strategy.[26] An alternative approach may involve the use of β- and ϒ-peptides. Such compounds proved to be resistant to hydrolytic cleavage by benchmark proteases, including CPA. β- and ϒ-peptides share some

[23] Matsugi, S.; Hamada, T.; Shioi, N.; Tanaka, T.; Kumada, T.; Satomura, S. *Clin. Chim. Acta* **2007**, *378*, 147.
[24] Bernkop-Schnurch, A.; Schmitz, T. *Curr. Drug Metab.* **2007**, *8*, 509.
[25] Bartlett, P. A.; Marlowe, C. K.; Giannousis, P. P.; Hanson, J. E. *Cold Spring Harb. Symp. Quant. Biol.* **1987**, *52*, 83.
[26] Vovchuk, I. L.; Petrov, S. *A. Biomed. Khim.* **2008**, *54*, 167.

common properties such as natural origin, stability, and propensity to form folding structures.[27]

Thus, compounds **68-74** were synthesized, following standard procedures previously applied in our research group (Figure **14**), and their properties as possible ligands of MPCs were assayed. As results of the search for novel molecules, they showed that CBPs exert an inhibitory action against two prototypical M14 family proteases, carboxypeptidase A (CPA) and carboxypeptidase B (CPB), in the micromolar range. Compound **70** was the most potent compound and behaved better as a CPB inhibitor, while compound **71** provided with a longer alkyl chain with a blocked carboxylate, showed a preference to inhibit CPA (Figure **15**).[28]

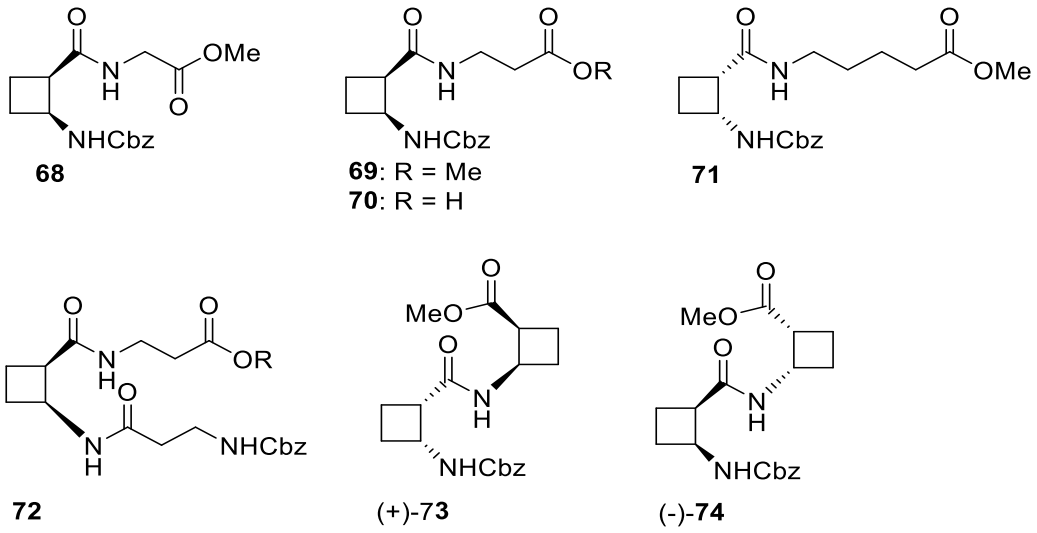

Figure 14. Structures of the CBPs that were analyzed.

[27] Seebach, D.; Beck, A. K.; Bierbaum, D. *J. Chem. Biodivers.* **2004**, *1*, 1111.
[28] Fernández, D.; Torres, E.; Avilés, F. X.; Ortuño, R.M.; Vendrell, *J. Bioorg. Med. Chem.* **2009**, *17*, 3824.

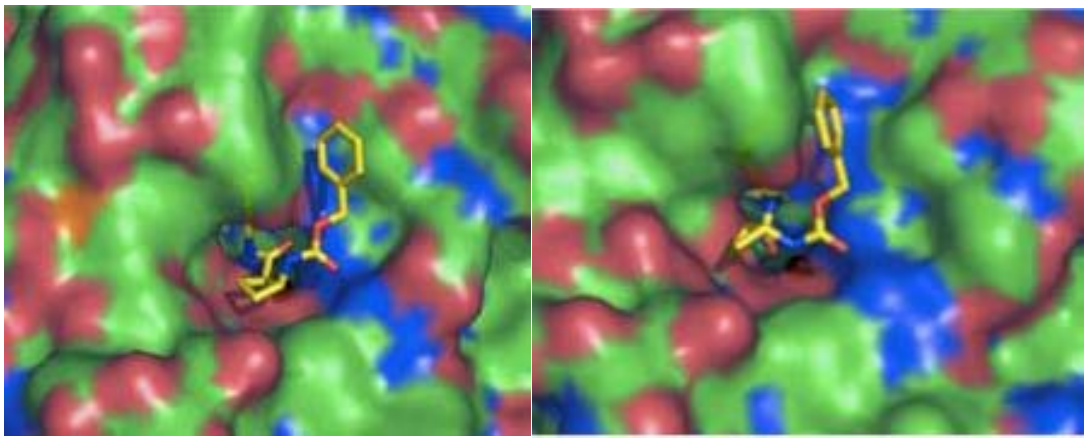

Figure 15. Docking images of the interactions between **70** and CPB (left) and between **71** and CPA (right).

2.4 Applications in organocatalysis.

In our research group there are also some examples in catalysis. Inspired in Takemoto's work,[29] thioureas which have (*R*,*R*)-1,2-cyclohexanediamine as a chiral scaffold were prepared. For instance, some of the thioureas before mentioned were used as bifunctional organocatalysts to assist a Michael reaction, resulting in good yields and moderated enantioselectivities (Figure **16**).[16]

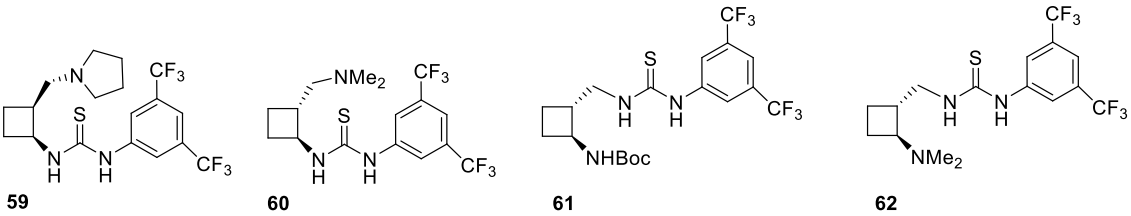

Figure 16. Thioureas employed as bifunctional organocatalysts for the Michael addition reaction.[16]

Thus, information about the influence of stereochemical features on the reaction acceleration and the asymmetric induction was gained in order to complete the studies. The best result in terms of conversion and enantioselectivity was obtained for thiourea **59** (85% yield, 48% ee) using toluene at room temperature for 24 h.

[29] Okino, T.; Hoashi, Y.; Takemoto, Y. *J. Am. Chem. Soc.* **2003**, *125*, 12672.

Otherwise, it appeared that the *cis* stereochemistry of the cyclobutane moiety induced better enantioselectivity for such reactions than did the *trans* configuration.

2.5 Synthesis of compounds containing the 1,3-disubstituted cyclobutane moiety.

Our group also works with the 1,3-disubstituted cyclobutane moiety. Interesting γ-amino acids and γ-peptides have been derived from (-)-verbenone resulting in hybrid peptides, dendrimers and polyfunctional platforms, for instance. Starting from this bicyclic monoterpenic product, efficient and stereodivergent synthetic approaches were optimized to achieve enantiomerically pure γ-amino acids, lactams and pyrrolidines, where the cyclobutane ring plays a central role (Scheme **8**).[30,31]

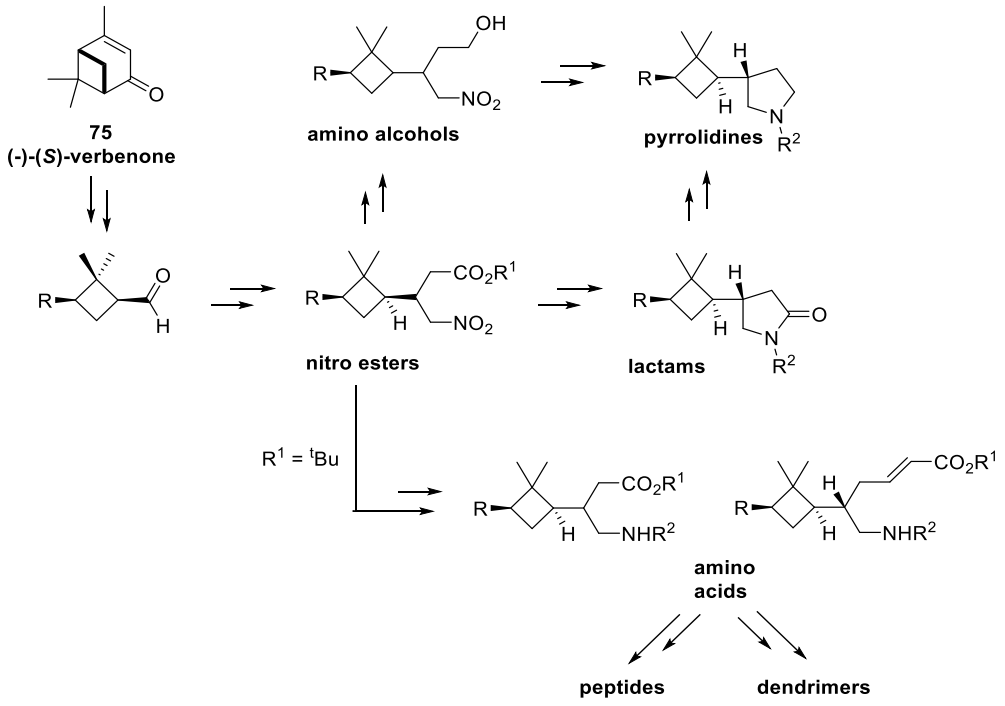

Scheme 8. Diastereoselective synthetic approaches to prepare 1,3-cyclobutane derivatives.

[30] Rouge, P. D.; Moglioni, A. G.; Moltrasio, G.; Ortuño, R. M. *Tetrahedron: Asymmetry* **2003**, *14*, 193.
[31] Aguilera, J.; Gutiérrez-Abad, R.; Mor, À.; Moglioni, A. G.; Moltrasio, G. Y.; Ortuño, R M. *Tetrahedron:Asymmetry* **2008**, *19*, 2864.

2 Precedents in the research group

The synthesis of optically pure cyclobutane γ-amino acids and their incorporation into γ-peptides with modulable conformational restriction has also been achieved in our group (**Scheme 9**).[32] Their secondary structure was investigated and, as a result of the preliminary structural studies, these cyclobutane γ-peptides showed to adopt an extended conformation probably due to the rigidity introduced by the cyclobutane ring and the gem-dimethyl substitution. This tendency contrasts with the natural trend of γ-peptides to fold by the action of hydrogen bonds between the nearest neighbour amides.[33,34]

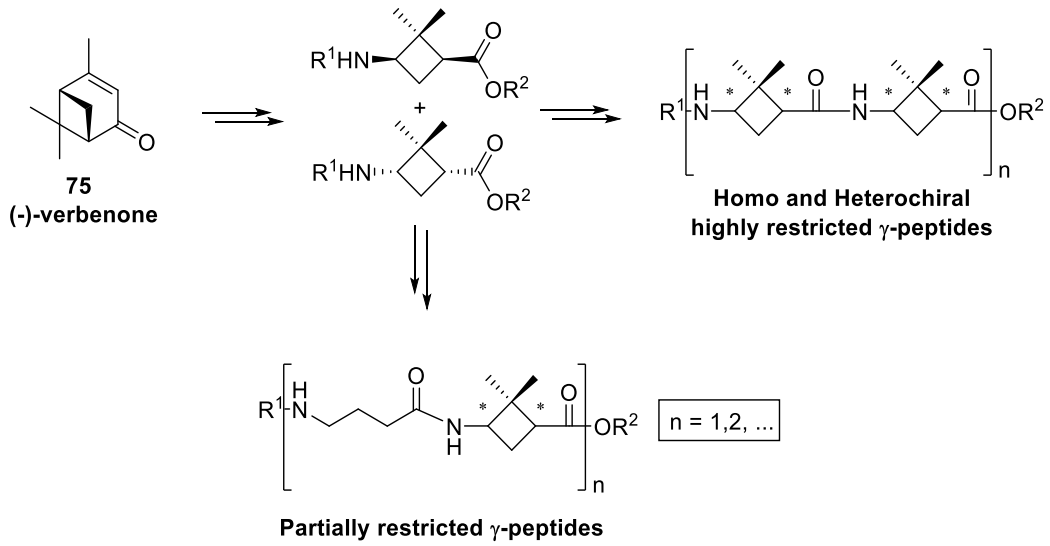

Scheme 9. Synthesis of differently restricted hybrid γ-peptides.

[32] Aguilera, J.; Moglioni, A. G.; Moltrasio, G. Y.; Ortuño, R. M., *Tetrahedron: Asymmetry* **2008**, *19*, 302.
[33] Dado, G. P.; Gellman, S. H. *J. Am. Chem. Soc.* **1994**, *116*, 1054.
[34] Aguilera, J.; Cobos, J. A.; Gutiérrez-Abad, R.; Acosta, C.; Nolis, P.; Illa, O.; Ortuño, R. M. *Eur. J. Org. Chem.* **2013**, *17*, 3494

2.6 Applications of 1,3-disubstituted-cyclobutane in materials

2.6.1 Dendrimers

Dendrimers[35,36] are a class of polymeric materials. Their structures are based on repetitively branched molecules typically symmetric around the core which often adopt a spherical three-dimensional morphology. They usually contain a single chemically addressable group called the focal point. Of special interest are those linked to the core through a urea, *C*-amide, or *N*-amide group. They have been described as good nucleation agents for polymers,[37] new materials,[38] and especially as organogelators,[39] some of them with interesting conducting properties.[40] Nevertheless, there are very scarce examples of benzene-cored dendrimers containing a peptide nature in their dendron structure.

In our research group, Dr. Raquel Gutierrez-Abad described in her PhD thesis the preparation of new branched polyfunctional benzene-cored C_3-symmetric dendrimers through a convergent approach.[41] This synthetic strategy, which consisted on the attachment of presynthesized dendrons to the core, led to dendrimers of monodisperse molecular weight which are easy to purify. Those dendrimers were highly functionalized and orthogonally protected, which could allow the elongation of their structures selectively. The different possible combinations of deprotected monomers and functionalized benzene cores led to urea (**78**, **79**), *N*-centered amide (**80**), and *C*-centered amide derivatives (**83**, **84**) (Scheme **10**).

---

[35] Astruc, D.; Boisselier, E.; Ornelas C. *Chem. Rev.* **2010**, *4*, 1857.
[36] Vögtle, F.; Richardt, G.; Werner, N. *Dendrimer Chemistry Concepts, Synthesis, Properties, Applications,* Wiley, New York, 2009.
[37] Mohmeyer, N.; Behrendt, N.; Zhang, X.; Smith, P.; Altsta¨dt, V.; Sessler, G. M.; Schmidt, H.-W. *Polymer* **2007**, *48*, 1612.
[38] Kreger, K.; Wolfer, P.; Audorff, H.; Kador, L.; Stingelin-Stutzmann, N.; Smith, P.; Schmidt, H.W. *J. Am. Chem. Soc.* **2010**, *132*, 509.
[39] Zhou, Y.; Xu, M.; Li, T.; Guo, Y.; Yi, T.; Xiao, S.; Li, F.; Huang, C. *J. Colloid Interface Sci.* **2008**, *321*, 205.
[40] Danila, I.; Riobé, F.; Puigmartí-Luis, J.; Pérez del Pino, A.; Wallis, J. D.; Amabilino, D. B.; Avarvari, N. *J. Mater. Chem.* **2009**, *19*, 4495.
[41] Gutiérrez-Abad, R.; Illa, O.; Ortuño, R.M. *Org. Lett.* **2010**, *12*, 3148.

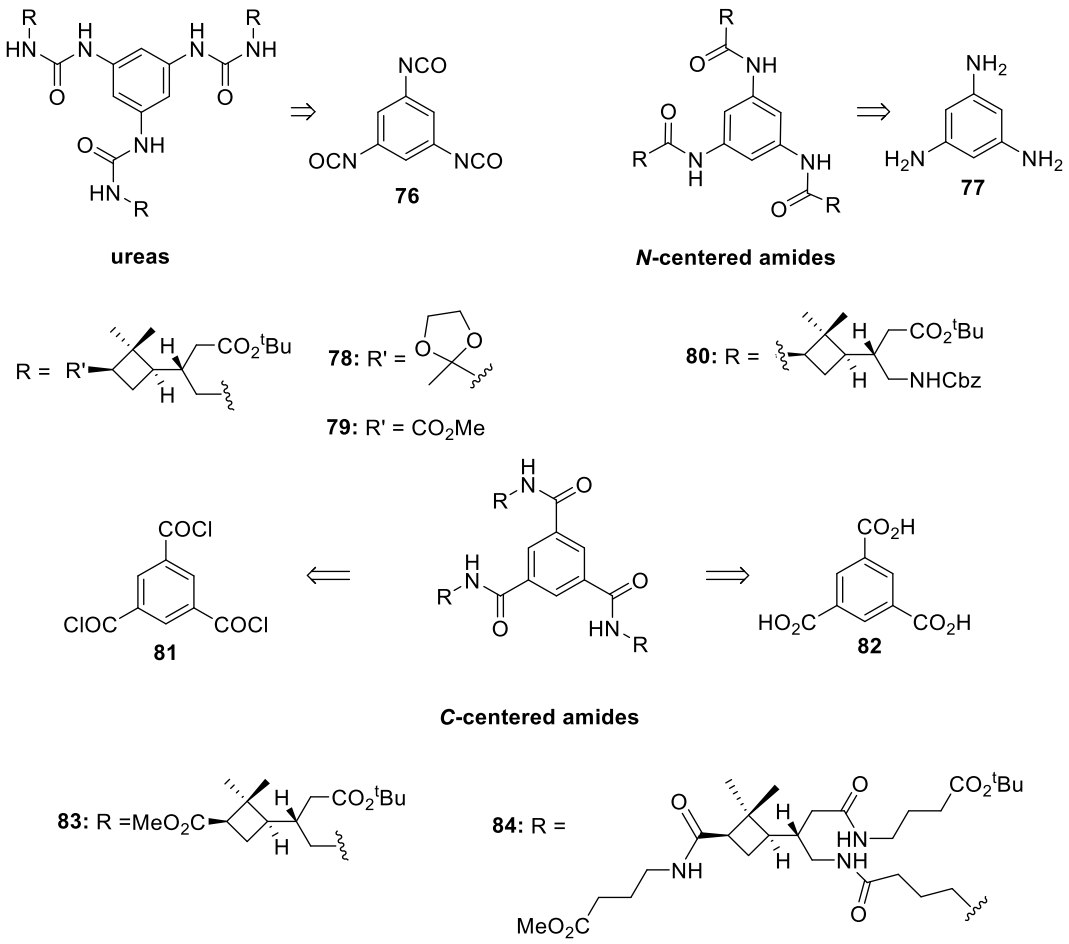

Scheme 10. Types of dendrimers and retrosynthetic analysis.

2.6.2 Surfactants

Jimena Ospina in her Master's work, presented the synthesis of new enantiopure cyclobutane derivatives from a chiral precursor derived from (-)-verbenone and their behavior as surfactants was studied.[42]

Surfactants are 'surface active agents'. This term is used to describe those molecules that tend to diminish the superficial tension of an interface, namely water-

[42] Ospina, J.; Sorrenti, A.; Illa, O.; Pons, R.; Ortuño, R. *Tetrahedron: Asymmetry* **2013**, *24*, 713.

air or fat-water. On the other hand, amino acid based surfactants are relevant[43] due to their good levels of biodegradability and biocompatibility.[44]

Thus, the stereoselective synthesis of two types of chiral cyclobutane containing ϒ-amino acids (**85**, **86**) was described. These include a C_{16}-alkyl chain that, jointly with the gem-dimethyl group of the cyclobutane, confers hydrophobicity to the molecule. Both amino acids differ in that the chain is linked to the cyclobutane moiety by means of an amine or an amide function (Figure **17**).

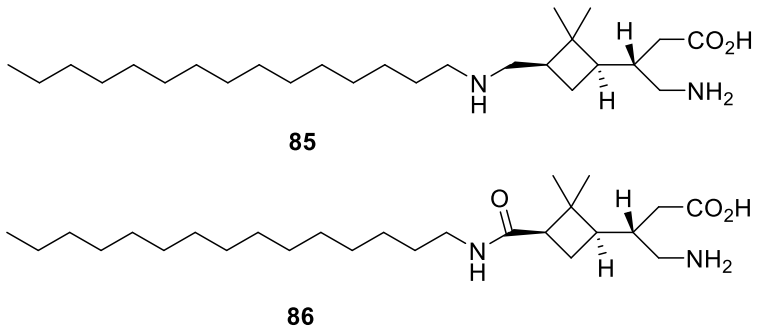

Figure 17. Types of surfactants synthesized in our laboratory.

The synthesis of these compounds started with **75** as chiral precursor to provide aminoacid **87**.[33] Then, several steps took place in order to afford intermediate **88**. Next, hydrogenolysis of the benzyl carbamate led to the formation of what was expected to be exclusively the free ϒ-amino acid **86**. Nevertheless, high resolution mass spectrometry in positive and negative mode and elemental analysis of this sample revealed the presence of not only **86** but also salt **89** (Scheme **11**), which would come from some of the TFA left in the hydrogenation step of **88**. The ratio of 10:11 was calculated to be 0.35:0.65. Attempts to eliminate residual acid after this step by lyophilization were unsuccessful. They attempted to convert the mixture into **86** by stirring it in dichloromethane in the presence of trifluoroacetic acid, but the amount of **89** was never increased suggesting that the mixture composition corresponds to the acid–base equilibrium ratio.

[43] Infante, M. R.; Pérez, L.; Morán, M. C.; Pons, R.; Mitjans, M.; Vinardell, M. P.; Garcia, M. T.; Pinazo, A. *Eur. J. Lipid Sci. Technol.* **2010**, *112*, 110.
[44] Foley, P.; Kermanshahi pour, A.; Beach, E. S.; Zimmerman, J. B. *Chem. Soc. Rev.* **2012**, *41*, 1499.

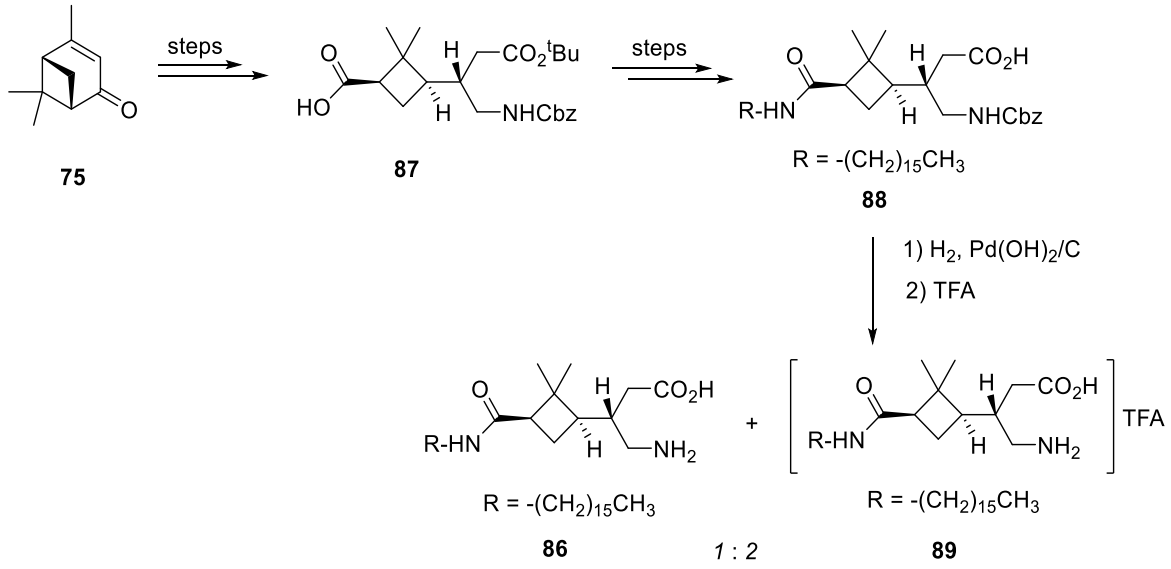

Scheme 11. Schematic representation to achieve **86.**

The surface tension (ϒ) of small volumes of the surfactant mixture (**86** + **89**) was measured using a home-made pendant drop tensiometer. Surface tension was followed as a function of time until equilibrium was reached. The surface tension of the mixture decreased progressively upon increasing concentration (Figure **18**). The break occurred at a concentration of 2.4 x 10^{-4} mol kg^{-1}, as determined from the intersection of the two fitting straight lines in the plot of ϒ versus logC, which corresponds to the critical micellar concentration (CMC), which is defined as the concentration of surfactants above which micelles form and all additional surfactants added to the system go to micelles of the mixture. This value of critical micellar concentration was in good agreement with the value obtained in the preliminary foaming experiment, where the maximum foaming was observed just above the value of CMC.[45]

[45] Rossen, M. J. *Surfactants and Interfacial Phenomena*, Wiley-Interscience, New Jersey, **2004**.

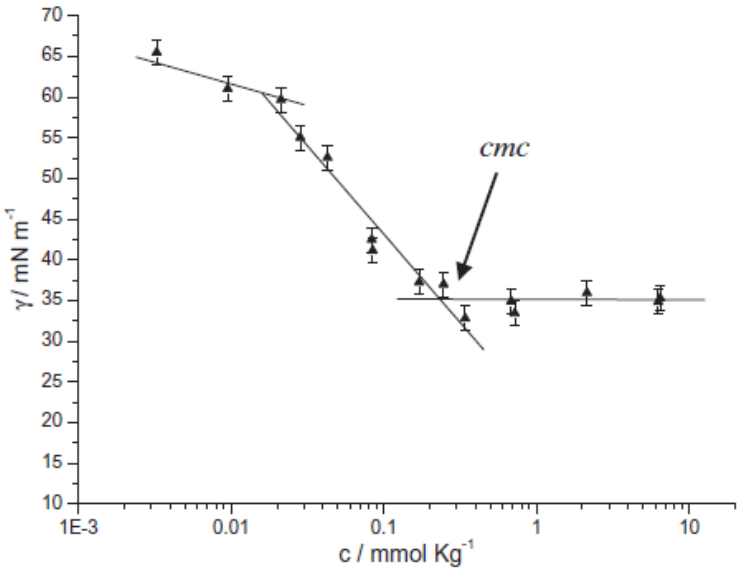

Figure 18. Plot of surface tension as a function of surfactant concentration for the **86** + **89** mixture in water at 25 °C.

2.7 Biological applications: CPPs (Cell penetrating peptides)

Our research group has also used these cyclobutane derivatives in biological applications. In recent years, the use of peptides as drug carriers has been one of the most explored applications. Since the discovery of peptide sequences capable of translocating cell membrane in the late 80s, cell-penetrating peptides (CPPs)[46] have been demonstrated to be a good alternative to other drug transporter systems such as viral delivery agents, liposomes, encapsulation in polymers, or electroporation, which often have not shown sufficiently good efficiency, in addition to causing high cellular toxicities in some cases (Figure **19**). Moreover, some of these methods are restricted to *in vitro* applications. Most CPPs described in the literature are natural peptides derived from peptide sequences responsible for cellular internalization of membrane proteins or proteins that cross the cell membrane. TAT peptide[47] has been used as a

[46] Lindgren, M.; Hällbrink, M.; Prochiantz, A.; Langel, U. *TiPS*, **2000**, *21*, 99.
[47] Vivès, E.; Brodin, P.; Lebleu, B. *J. Biol. Chem.* **1997**, *272*, 16010.

reference when preparing, studying and analysing the properties of different new peptides as possible cell-penetrating agents.

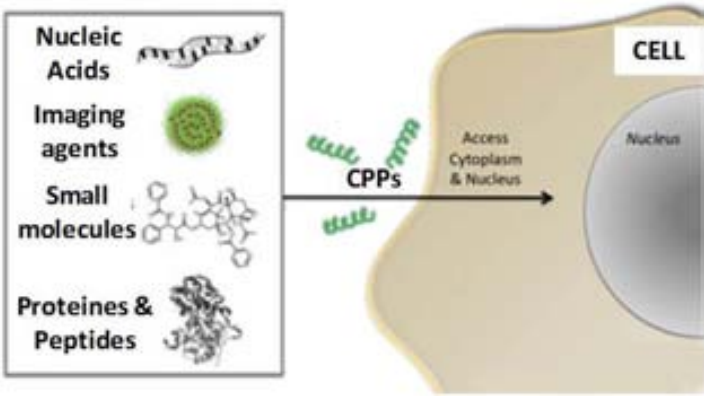

Figure 19. Molecules that can be carried by CPPs into cytoplasm and/or nucleus.

In a work from Dr. Raquel Gutierrez and Dr. Esther Gorrea,[48] two generations of hybrid γ,γ-peptides containing cyclobutane amino acids and *cis*-γ-amino-L-proline joined in alternation were synthesized and their capacity to cross the eukaryotic cell membrane was evaluated. The first generation consisted of di-, tetra- and hexapeptides (Figure **20**) and their properties were analyzed as well as the influence of peptide length and chirality of the cyclobutane residues. Results showed that the absolute configuration of the cyclobutane amino acid does not have a relevant influence.

[48] Gorrea, E.; Carbajo, D.; Gutiérrez-Abad, R.; Illa, O.; Branchadell, V.; Royo, M.; Ortuño, R.M. *Org. Biomol. Chem.* **2012**, *10*, 4050.

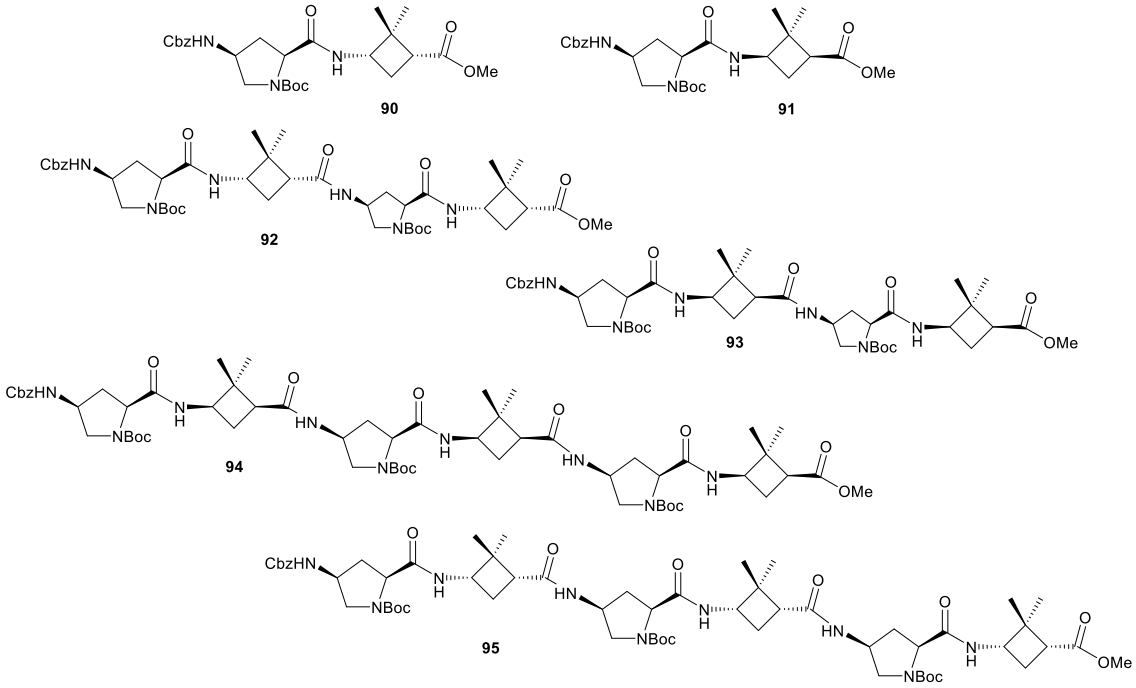

Figure 20. Structures of the first generation of hybrid cyclobutane–proline γ,γ-peptides.

The second generation consisted of hybrid γ,γ-hexapeptides with a common backbone and distinct side chains introduced with different linkage types through the α-amino group (Nα) of the proline monomers (Figure **21**). These peptides showed to be non-toxic towards HeLa cells and to internalize them effectively, the best results being obtained for the peptides with a spacer of five carbons between the Nα atom and the guanidinium group. The introduction of cyclobutane residues inside the sequence afforded a good balance between charge and hydrophobicity, reducing the number of positive charges. This resulted in lower toxicity and similar cell-uptake properties when compared to previously described peptide agents.[49]

[49] Farrera-Sinfreu, J.; Royo, M.; Albericio, F. *Tetrahedron Lett.* **2002**, *43*, 7813.

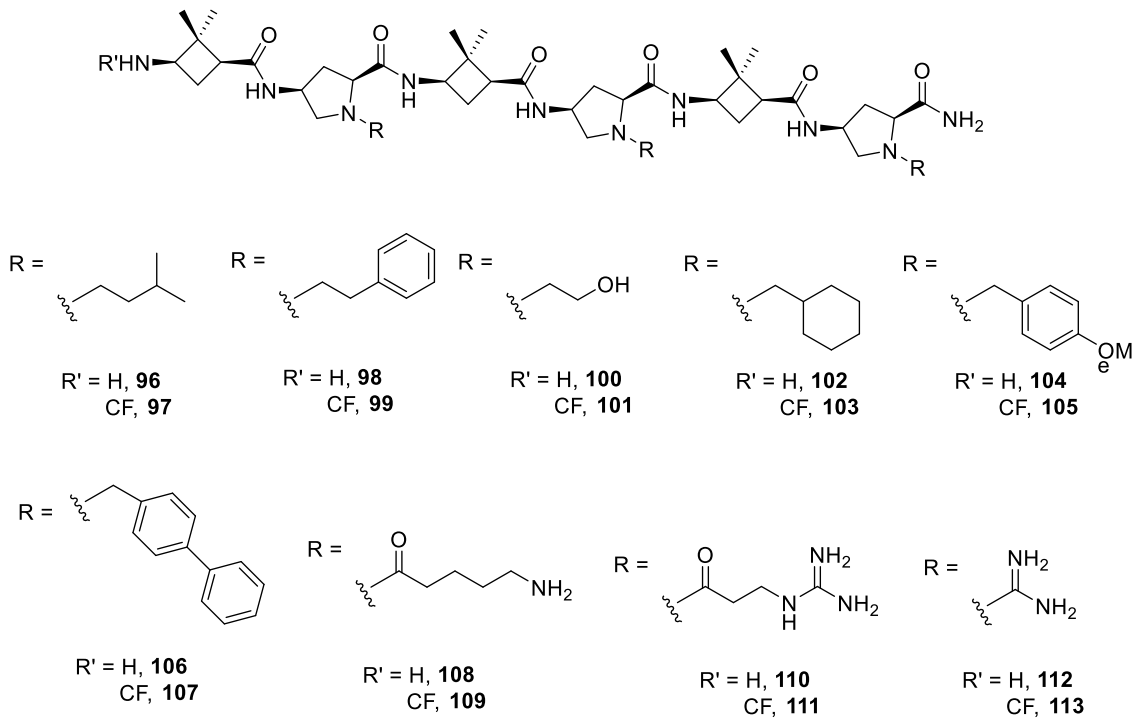

Figure 21. Chemical structure of the second generation of hybrid γ-γ-proline–cyclobutane hexapeptides synthesized.

The N-terminal proline γ-amino group of di-, tetra-, and hexapeptides of the first generation in Figure **20** were labeled with 5(6)-carboxyfluorescein. All the compounds were shown to be non-toxic in the presence of the cells being some of them less toxic than TAT peptide. Once their toxicity was tested, their ability to penetrate HeLa cells was studied at 37 °C by flow cytometry. The cell-uptake results showed that the different peptides do not behave in the same way, indicating that the ability to cross the cell membrane depends on the structure and charge changes introduced by the Nα-side chains.

CHAPTER III

Synthesis of the cyclobutane derivatives used as precursors.

3.1 INTRODUCTION

3.1.1 The chemistry of vicinal diamines

In recent years, compounds that incorporate a 1,2-diamine functionality have been described due to their numerous applications. Some of them have important biological activities and many are medicinal agents. Among them are antidepressant and antianxiety agents, antiarrythmics and specially chemotherapy drugs. For instance, there are well known complexes 1,2-diamine with platinium due to their uses in chemotherapy (Figure **22**).

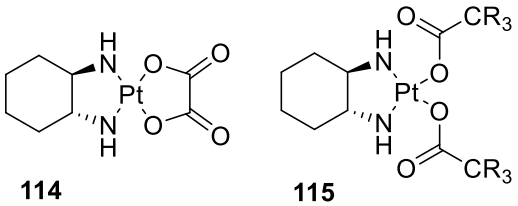

Figure 22. Platinium complexes containing the 1,2-diamine moiety as a ligand.

These vicinal diamines **114** and **115** have found also application as building blocks to afford macrocycles containing nitrogen. These molecules have also been described as chiral auxiliaries or ligands for organocatalysts, with interesting applications in stereoselective synthesis.[50,51,52]

When the vicinal amine functionalities are linked to a carbocyclic ring the most studied ones are cyclohexyl-1,2-diamines,[53] whose *trans* stereoisomer has been used, for instance, in the preparation of nanostructured hybrid materials which will be shown in Chapter 6.[54]

[50] Bhadury, P. S.; Song, B.A.; Yang, S.; Hu, D.-Y.; Xue, W. *Curr. Org. Synth.* **2009**, *6*, 380.
[51] Kotti, S. R. S. S.; Timmons, C.; Li, G. *Chem Biol Drug Des* **2006,** *67*, 101.
[52] Le Gall, T.; Mioskowski, C.; Lucet, D. *Angew. Chem. Int. Ed*. **1998**, *37*, 2580.
[53] Bennani, Y. L.; Hanessian, S. *Chem. Rev.* **1997**, *97*, 3161.
[54] Arrachart, G.; Creff, G.; Wadespohl, H.; Blanc, C.; Bonhomme, C. ; Babonneau, F. ; Alonso, B. ; Bantignies, J.L.. ; Carcel, C. ; Moreau, J. J. E. ; Dieudonn, P. ; Sauvajol, J.L.; Massiot, D. ; Wong Chi Man, M. *Chem. Eur. J.*, **2009**, *15*, 5002.

3.1.2 Cyclohexane-1,2-diamines

The first cyclohexane-1,2-diamine was described in 1926 by Wireland, Schlichtung and Langsdorf.[55] They prepared it starting from hexahydrophtalic acid. Nevertheless, the product was a mixture between *cis* and *trans* isomers. In 1936, Jaeger and Van Dijk described *trans*-cyclohexane-1,2-diamine as the only product of the reduction of 1,2-hydroxylamine using sodium in ethanol (Scheme **12**).[56] The resolution of the product in the dextrorotatory and levorotatory forms was achieved using D-(-)-tartaric acid.

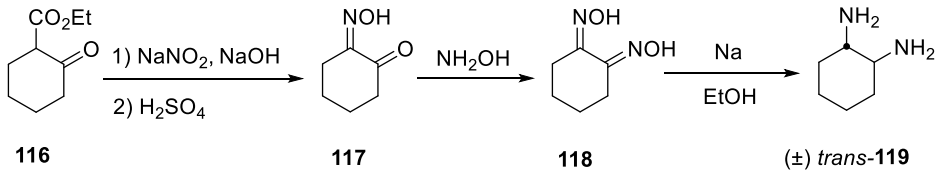

Scheme 12. Synthethic route described for Jaeger and Van Dijk.

Research was also focused in the synthesis of *cis*-cyclohexane-1,2-diamine, which was synthesized in 1958 by Yashunkii.[57] Since then, numerous synthesis for the preparation of this compound have been described.[58,59] Finally, the first stereoselective synthesis was achieved in 1967 by Swift and Swern (Scheme **13**).[60]

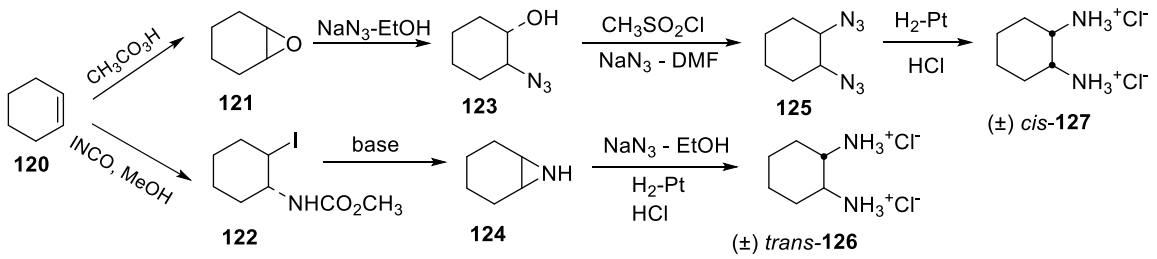

Scheme 13. First stereoselective synthesis of *cis*- and *trans*- cyclohexane-1,2-diamine.

[55] Wireland, H.; Schlichtung, O.; Langsdorf, W. B. *Z. Physiol. Chem.* **1926**, *74*, 161.
[56] Jaeger, F. M.; J. A. Van Dijk, J. A. *Proc. Akad. Sci. Amsterdam* **1936**, *40*, 12.
[57] Yashunkii, V. G.; Zh. Obshch. Khim. **1958**, *28*, 1361.
[58] Simons, C. U. S. Patent 2, 850, 532 (1958).
[59] Winternitz, F.; Moussereon, M.; Dennilauler, R. *Bull. Soc. Chim. France* **1956**, 382.
[60] Swift, G.; Swern, D. *J. Org. Chem.* **1967**, *32*, 511.

3.1.3 Cyclopentane-1,2-diamines

trans-Cylopentane-1,2-diamines have been used in several fields, for instance in medicine or biochemistry. However, because of the fact that they are not commercially available and their intrinsic instability they have produced less interest among the scientific community than their homologous *trans*-cyclohexane-1,2-diamine.

Jaeger et al. synthesized *trans*-cyclopentane-1,2-diamine for the first time in 1928.[61] They carried out a complex synthesis with low yields in all cases. The first applications of these compounds were as ligands in complexes with Co (III), Cr (III), Rh (III) and Pt (II).[62] It was not until 2002 when Gotor et al. performed the first racemic resolution of the two enantiomers of *trans*-cyclopentane-1,2-diamine.[63]

In 2000, Husson et al. developed a short synthesis to afford the *trans*-cyclopentane-1,2-diamine.[64] As starting product they used the commercially available enantiomerically pure *trans*-cyclopentane-1,2-dicarboxylic acid (Scheme **14**).

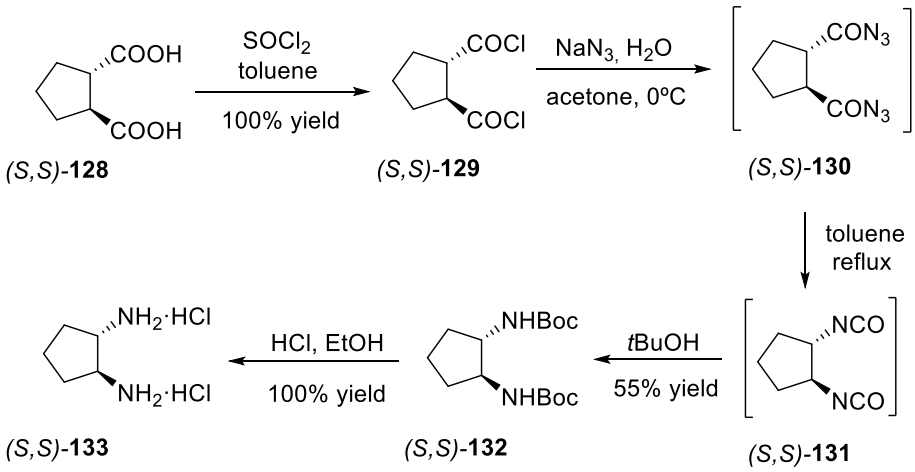

Scheme 14. Synthesis of *trans*-cyclopentane-1,2-diamine by Husson and co-workers.

[61] Jaeger, F. M.; Blumendal, H. B. Z. *Anorg. Chem.* **1928**, *175*, 161.
[62] Toflund, A.; Pedersen, E.; *Acta Chemica Scandinavica* **1972**, *26*, 4019.
[63] Luna, A.; Alfonso, I.; Gotor, V. *Org. Lett.* **2002**, *4*, 3627.
[64] Ongeri, A. S.; Aitken, D. J.; Husson, P. *Synth. Commun.* **2000**, *30*, 2593.

3.1.4 Cyclobutane-1,2-diamines

These molecules were first described by Schlatter et al. in 1942.[65] They achieved the synthesis of *cis* and *trans* through the degradation of acid *cis*- and *trans*-cyclobutane-1,2-dicarboxylic acid to the corresponding diamines. In this procedure, one of the key steps is a Schmidt rearrangement in the presence of hydrazoic acid which takes place without changing the absolute configuration of the stereogenic centres of the molecule (Scheme **15**).

SCHMIDT TRANSPOSITION

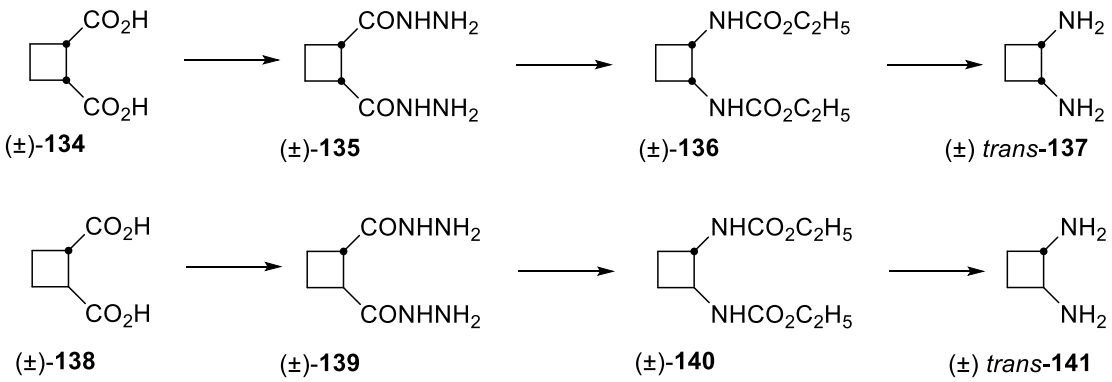

Scheme 15. Schmidt transposition to cyclobutane-1,2-diamines.

In 1996, Husson et al. reported a synthesis for the racemic *trans*-cyclobutane compound based on the reduction of the compound 1-(difenilmetil)amino-1-cyclopropanecarbonyl with borane.[66] Surprisingly, in addition to the product of the cyclopropane reduction, they got also the *trans*-cyclobutane-1,2-diamine in a racemic form as a by-product in 30% yield (Scheme **16**).

[65] Edwin, R.; Reims, O. A.; Skei, T.; Schlatter, J. M. *J. Am. Chem. Soc.*, **1942**, *64*, 2696.
[66] Vergne, F.; Partogyan, K.; Aitken, D. J.; Husson, H. P.; *Tetrahedron*, **1996**, *52*, 2421.

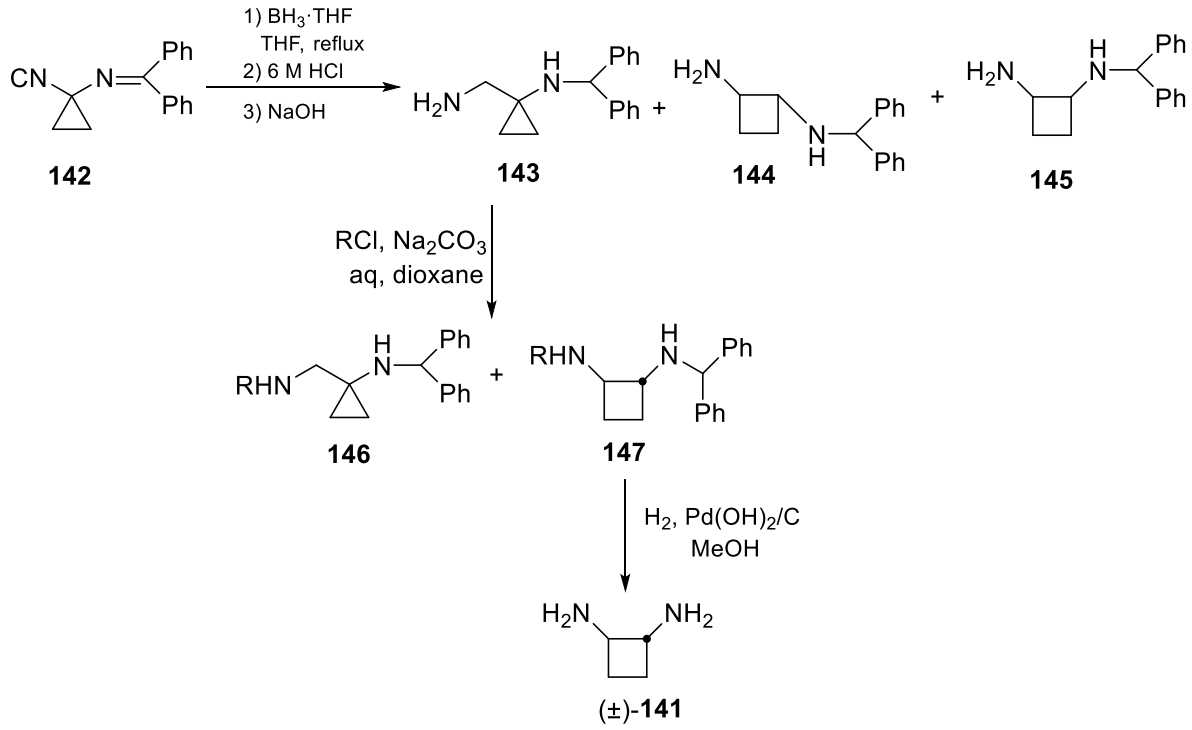

Scheme 16. Synthesis of racemic *trans*-cyclobutane-1,2-diamine.

In 2003, Daly and Gilheany carried out the synthesis of the compounds *trans*-cyclobutane-1,2-diamine and *trans*-cyclopentane-1,2-diamine, in both cases in a racemic form (Scheme **17**).[67]

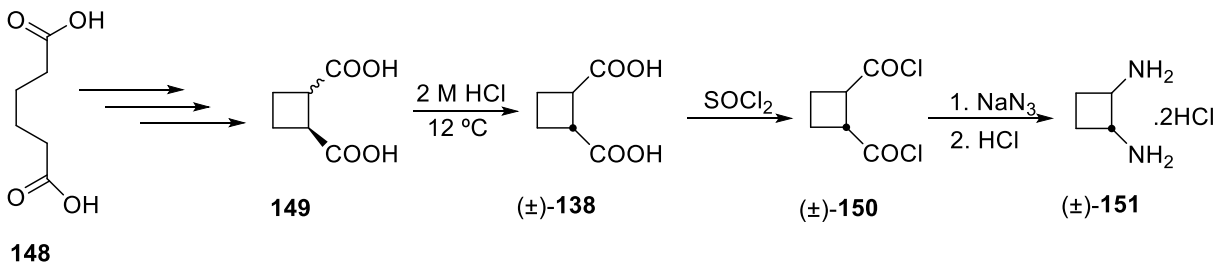

Scheme 17. Synthesis of *trans*-cyclobutane-1,2-diamine by Daly and Gilheany.

[67] Daly, A. M.; Gilheany, D. G.; *Tetrahedron: Asymmetry*, **2003**, *14*, 127.

3.2 OBJECTIVES

As a part of our research program on the synthesis and use of chiral cyclobutane scaffolds in the preparation of foldamers, organogelators, enzyme inhibitors and organoconducting materials among other products of interest, the first objective of this part of the Thesis was the enantio- and diastereocontrolled synthesis of the four stereoisomers of orthogonally protected cyclobutane-1,2-diamines from a common chiral intermediate (*S*,*R*)-**9** in view of opening a new route for a wide range of useful enantiopure molecules containing this moiety (Scheme **18**).

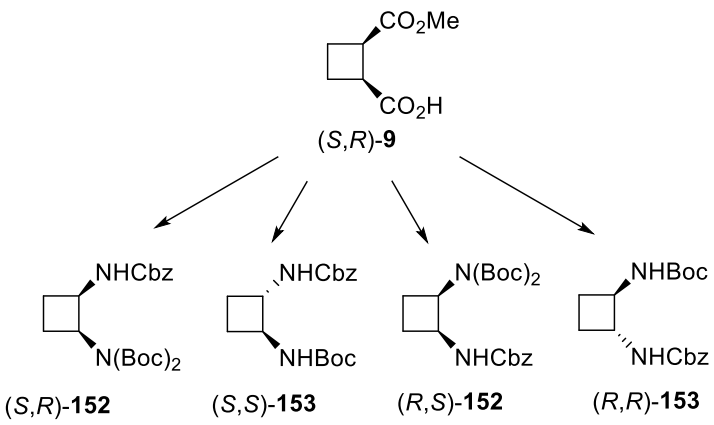

Scheme 18. Cyclobutane-1,2-diamines synthesized in this Thesis.

In addition, *cis*- and *trans*- cyclobutane-1,2-dicarboxylic acid, (*R*,*S*)-**154** and (*S*,*S*)-**155** were also prepared in our group in order to functionalize them into enantiopure derivatives to be used in the preparation of interesting materials (Figure **23**).

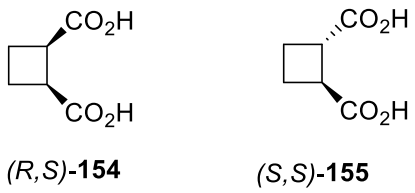

Figure 23. Cyclobutane-1,2-dicarboxylic acid prepared in this Thesis.

These materials consisted on bolaamphiphiles for the preparation of surfactants, triethoxysilane derivatives for the preparation of hybrid materials and C_{16}-(*C*-centered) amides which were studied as organogelators. Thus, in the following parts of the Thesis, the properties and also the morphology of the obtained materials were studied and compared in terms of regiochemistry and stereochemistry using different techniques.

3.3 RESULTS AND DISCUSSION.

3.3.1 Stereoselective synthesis of cyclobutane-1,2-diamines.

To begin with, the four stereoisomers of cyclobutane-1,2-diamine derivatives were prepared in an enantio and diastereocontrolled manner through stereodivergent synthetic routes starting from a readily available optically pure half-ester (*S*,*R*)-**9**[7] as the only chiral precursor. To achieve it, both orthogonally protected amino acids (*R*,*S*)-**156** and (*S*,*R*)-**156** were proposed as key intermediates to prepare precursors **157** and **158** as free carboxylic acids. From **157** and **158**, cyclobutane-1,2-diamines were synthesized (Scheme **19**).

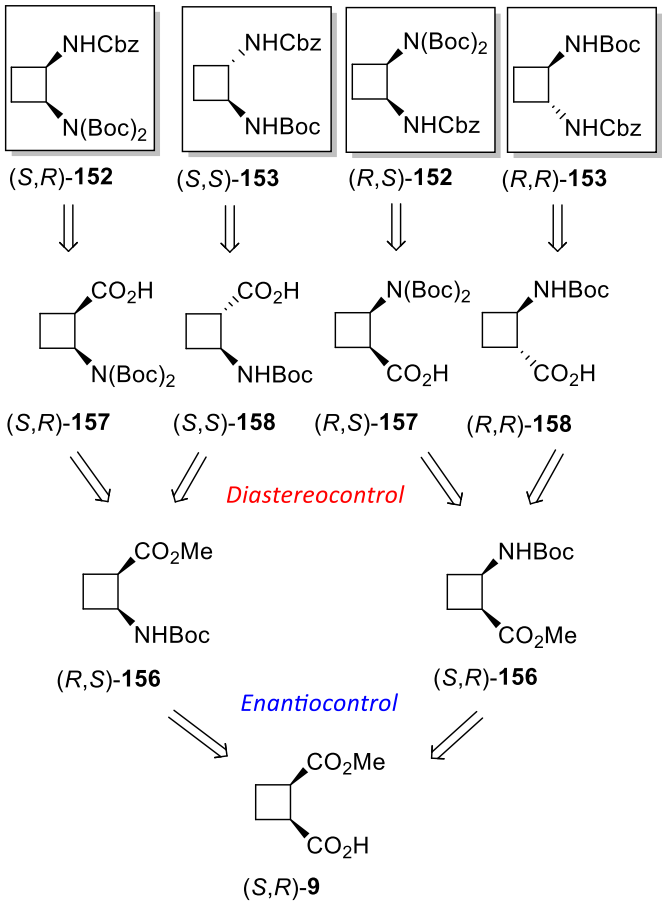

Scheme 19. Retrosynthetic analysis of the orthogonally protected diamines **152** and **153**.

3.3.1.1 Synthesis of chiral precursor (*S*,*R*)-9

In our group, the methodology reported by Huet et al. was optimized and the cyclobutane ring was prepared following a [2+2] photochemical reaction from ethylene and maleic anhydride (**Scheme 20**).[68]

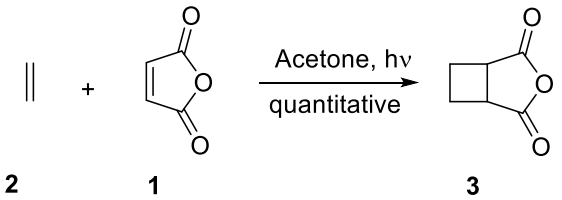

Scheme 20. [2+2] Photoaddition between ethylene and maleic anhydride.

This cycloaddition occured at -35 °C in a Pyrex reactor in the presence of acetone as a photosensitizer and solvent. The system was saturated with ethylene and irradiated during 5 hours using a half pressure mercury lamp. The reaction could be followed by using gas chromatography or ^{1}H NMR.

In the next step, diester **8** was produced through Fischer esterification of the photoadduct in 88% yield**.** Finally, optically active (*S*,*R*)-**9** was obtained through pig liver esterase-induced chemoselective hydrolysis of **8**, in >97% ee and 95% chemical yield following the procedure described by Jones *et al* (Scheme **21**). [69]

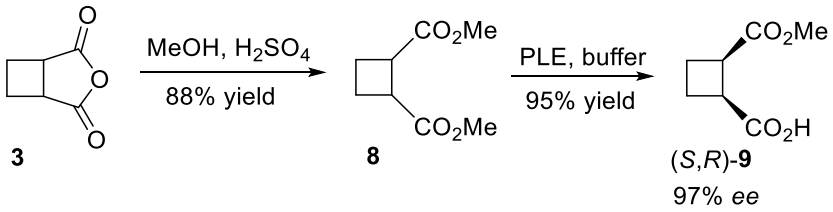

Scheme 21. Synthesic route to achieve (*S*,*R*)-**9** from **3**.

[68]Gorrea, E. *PhD Thesis*, UAB, **2011**.
[69]Sabbioni, G.; Jones, J. B. *J. Org. Chem.* **1987**, *52*, 4565.

3.3.1.2 Enantiocontrolled synthesis of amino acids (*R*,*S*)- and (*S*,*R*)-156

The fully protected amino acid (*R*,*S*)-**156** was prepared stepwise by treatment of (*S*,*R*)-**9** with ethyl chloroformate and triethylamine, followed by reaction with sodium azide. The resultant acyl azide was decomposed by heating to reflux a toluene solution with benzyl alcohol, affording compound (*R*,*S*)-**10** in 72% yield from (*S*,*R*)-**9**.[10] Finally, catalytic hydrogenation in the presence of di(*tert*-butyl) dicarbonate, provided the amino group protected as a *tert*-butyl carbamate, obtaining amino acid (*R*,*S*)-**156** in a 59% global yield (Scheme **22**).

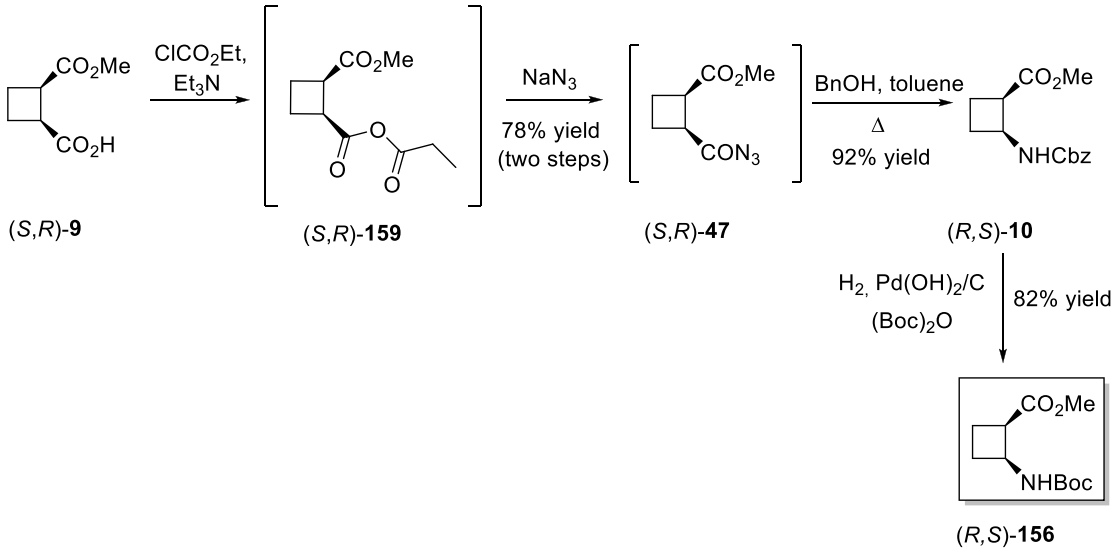

Scheme 22. Synthetic route to (*R*,*S*)-**156**.

Orthogonally protected amino acid (*R*,*S*)-**156** can also be obtained in 51% yield by Curtius rearrangement in neat *tert*-butanol (Scheme **24**). However, due to the poor nucleophilic character of *tert*-butyl alcohol, the yield of the reaction resulted better (72% yield) using benzyl alcohol as nucleophile followed by hydrogenation in the presence of di(*tert*-butyl) dicarbonate, to afford amino group protected as a *tert*-butyl carbamate (Scheme **23**).

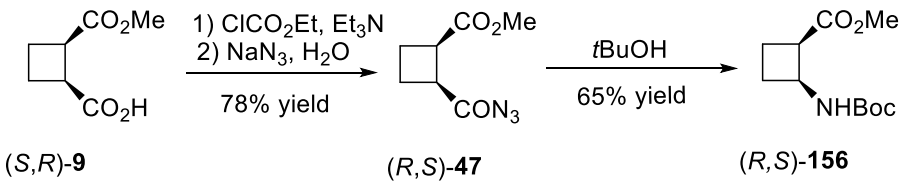

Scheme 23. Synthesis of (*R*,*S*)-**156** through Curtius rearrangement in neat *tert*-butanol.

To prepare enantiomer (*S*,*R*)-**156** it is necessary to modify the synthetic route in order to afford the desired configuration of chiral centres as it is shown in Scheme **24**. To proceed, half-ester (*S,R*)-**9** was protected as a *tert*-butyl ester in 74% yield by treatment of the free carboxylic acid with *tert*-butyl trichloroacetimidate under a nitrogen atmosphere. The saponification of the methyl ester was carried out under mild conditions by using a 0.25 M NaOH solution avoiding epimerization of the chiral centres. The obtained half-ester (*R*,*S*)-**160** was then reacted with ethyl chloroformate followed by treatment with sodium azide to produce the corresponding acyl azide. This was made to react with benzyl alcohol at reflux in toluene for 5 hours in order to obtain the orthogonally protected amino acid (*S*,*R*)-**162**, in 54% overall yield for the three steps. Carboxylic acid was deprotected in 98% yield by reaction with TFA in the presence of triethylsilane and the resulting compound (*S*,*R*)-**16** was transformed quantitatively into the corresponding methyl ester (*S*,*R*)-**10**, by reaction with diazomethane. Benzyl carbamate in (*S*,*R*)-**10** was then hydrogenated at 7 atmospheres of pressure in the presence of di*tert*-butyl dicarbonate and using palladium as catalyst to afford orthogonally protected amino acid (*S*,*R*)-**156** in 77% yield (Scheme **24**).

It is noteworthy to remark that to maintain the orthogonality of the protecting groups during all the synthethic sequence it is required to assure selectivity in the manipulation of the functional groups.

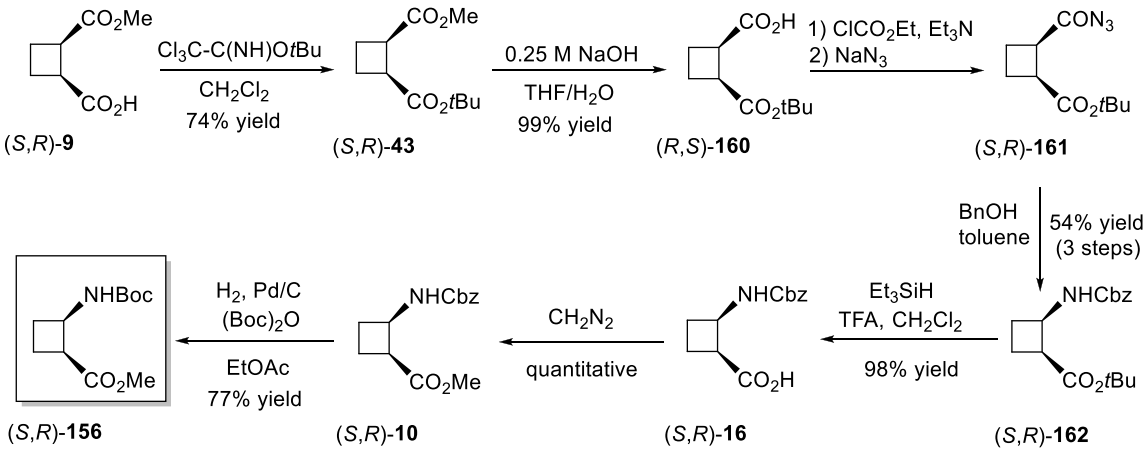

Scheme 24. Enantioselective route to (*S,R*)-**156.**

3.3.1.3 Enantio- and diastereocontrolled synthesis of intermediates 157 and 158

Once the two enantiomers of **156** were prepared, a diastereocontrolled synthetic route from each one was designed to afford both enantiomers of **157** and **158** (Scheme **25**).

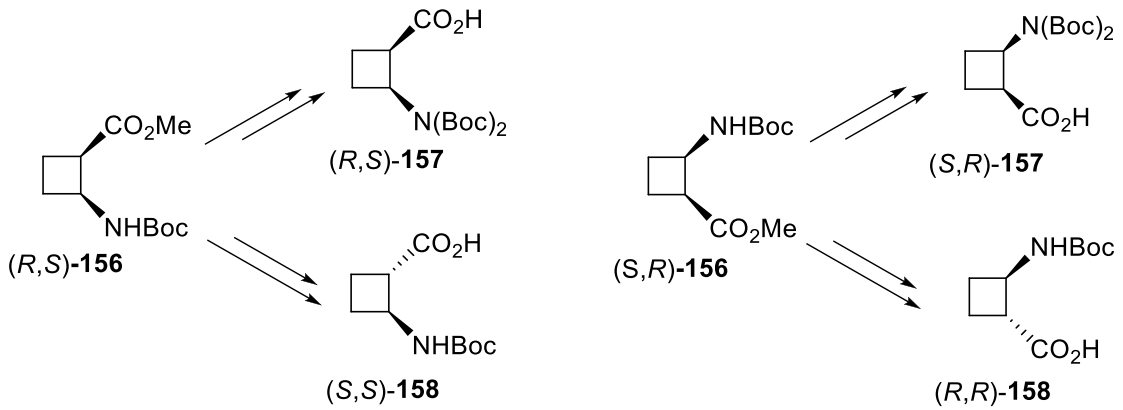

Scheme 25. General scheme to **157** and **158** from **156**.

From **156**, the preparation of *trans* carboxylic acid **158** could be easily achieved by the transformation of the methyl ester into a free amide and subsequent epimerization at the carbonyl α-position as previously described by Aitken and co-workers (Scheme **26**).[70]

[70] Fernandes, C.; Pereira, E.; Faure, S.; and Aitken, D. J. *J. Org. Chem.* **2009,** *74,* 3217.

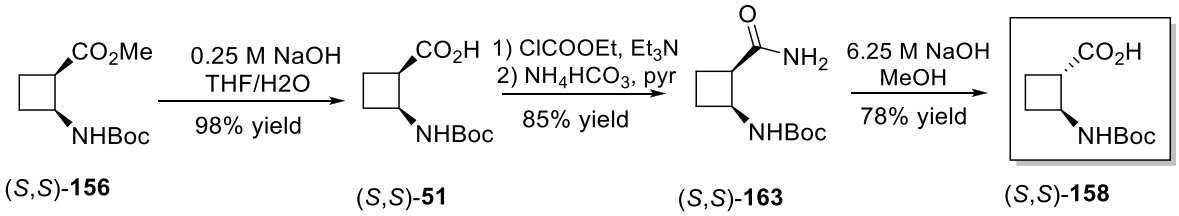

Scheme 26. Synthesis route to free carboxylic acid (*S*,*S*)-**158.**

The epimerization takes place through the formation of a carbanion stabilized by conjugation to the carbonyl group. Subsequent protonation led to the thermodynamically preferred *trans*- isomer. Afterwards, the hydrolysis of the amide and subsequent acidification allowed the formation of carboxylic acid (*S*,*S*)-**158**. Therefore, *trans* monoprotected amino acid (*S*,*S*)-**158** was achieved in 78% yield from (*S*,*S*)-**163** (Scheme **27**).

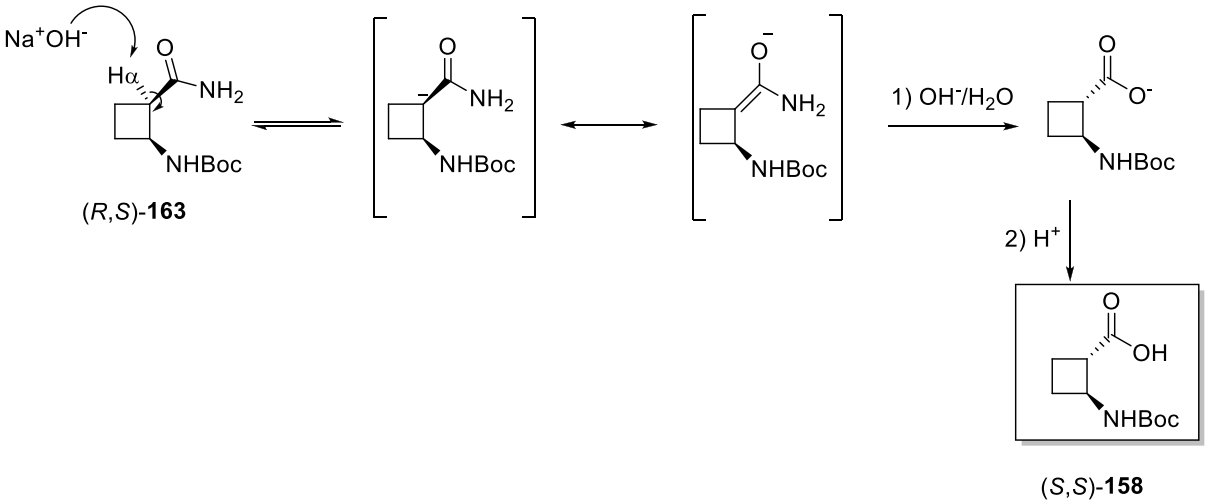

Scheme 27. Mechanism of epimerization reaction to synthesize (*S*,*S*)-**158**.

(*R*,*R*)-**158** was analogously prepared from the corresponding enantiomer (*S*,*R*)-**156** in 71% overall yield.

To afford *cis* free carboxylic acid intermediate (*S*,*R*)-**157**, a short synthetic route was firstly designed. As it is shown in **Scheme 28**, saponification of methyl ester (*S*,*R*)-**10** was achieved under mild conditions to allow the formation of the corresponding free acid in quantitative yield. Curtius rearrangement in neat *tert*-butanol was carried out in order to afford orthogonally protected diamine (*S*,*R*)-**164**.

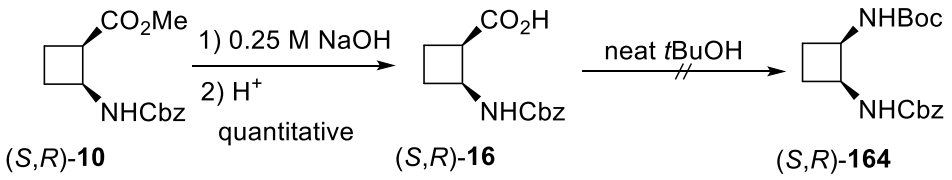

Scheme 28. First approach to *cis* cyclobutane-1,2-diamine.

Nevertheless, when the last product was analyzed by NMR, it was observed that a cyclic urea, previously described in our research group, had been produced.[71] Scheme **29** shows the formation of urea (*S*,*R*)-**54** from acid (*S*,*R*)-**16**. These by-products are produced through intramolecular nucleophilic attack of the carbamate nitrogen to the carbon of the transient isocyanate with concomitant ring-closure, due to the kinetically favorable cyclization to the 5-membered urea ring.

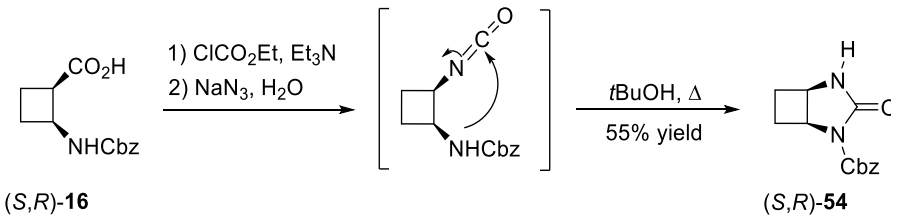

Scheme 29. Formation of cyclic urea (*S*,*R*)-**54.**

Consequently, the synthetic strategy was changed. To proceed, a diprotection of the amine in (*S*,*R*)-**156** as a bis(*tert*-butoxycarbonyl)carbamate was necessary in order to avoid the formation of cyclic ureas during Curtius rearrangement of monoprotected amines. The double protection was achieved by treating (*R*,*S*)-**156** with di*tert*-butyl dicarbonate in the presence of DMAP as catalyst and triethylamine as base. Then, saponification of the methyl ester was carried out to obtain (*R*,*S*)-**157** in satisfactory yields (Scheme **30**).

[71] Gorrea, E.; Nolis, P.; Álvarez-Larena, Á.; Da Silva, E.; Branchadell, V.; Ortuño, R. M. *Tetrahedron: Asymmetry* **2010**, *21*, 339.

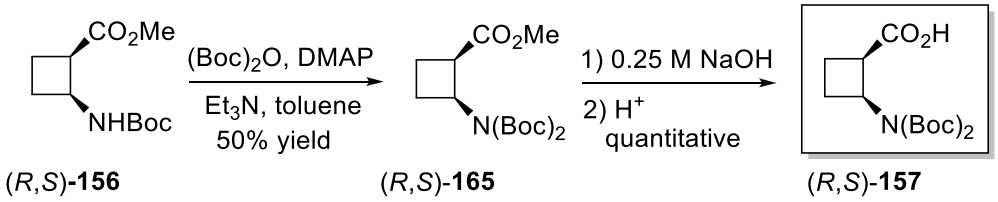

Scheme 30. Synthesis of intermediate **157.**

(*S*,*R*)-**157** was prepared analogously from the corresponding amino acid (*S*,*R*)**-156** in 43% global yield. ^{1}H NMR spectra of both enantiomers of **157** were superimposable, corroborating that both molecules have the same spectroscopic (and chemical) properties.

3.3.1.4 Synthesis of diamines 152 and 153

Orthogonal protection in target molecules **152** and **153** in both enantiomeric forms is crucial for the later selective manipulation of the two amino groups for further introduction of chains and other structural units retaining the chirality in *cis*-diastereomers that would become *meso* in the deprotected *cis*-diamine.

Therefore, the last step described for the synthesis of both enantiomers of target molecules **152** and **153** was a Curtius rearrangement in the presence of benzyl alcohol. Thus, *trans*-diamine (*S*,*S*)-**153** was prepared stepwise by treatment of free carboxylic acid (*S*,*S*)-**158** with ethyl chloroformate and triethylamine, followed by reaction with sodium azide (Scheme **31)**. The resultant acyl azide was decomposed by heating to reflux a toluene solution with benzyl alcohol, affording compound (*S*,*S*)-**153** in 67% yield from (*S*,*S*)-**158**. To afford (*R*,*R*)-**153**, starting from (*R*,*R*)-**158** the same procedure was carried out in 55% global yield over three steps.

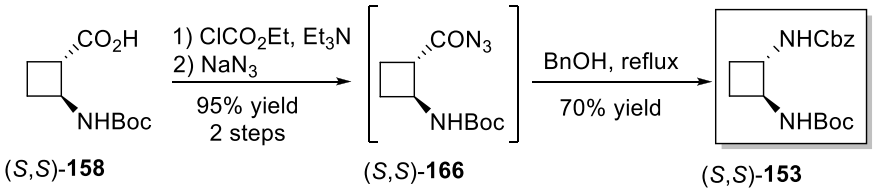

Scheme 31. Synthesis of (*S*,*S*)-**153** from (*S*,*S*)-**158**.

For the preparation of *cis*-diastereomer (*R*,*S*)-**152**, the synthesis was as shown in Scheme **32**. However, the global yield resulted worse due to the sterical hindrance produced by the two *tert*-butyl groups. To afford enantiomer (*S*,*R*)-**152** the same procedure was carried out in 48% global yield over three steps (Scheme **32**).

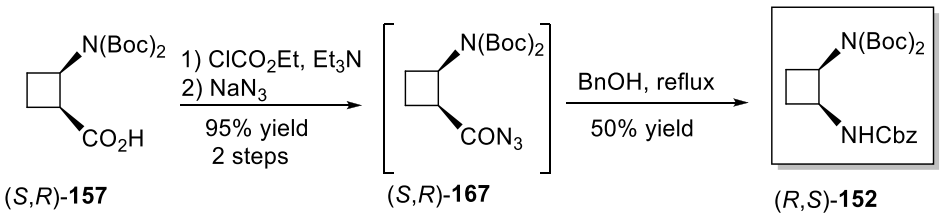

Scheme 32. Synthesis of (*R*,*S*)-**152** from (*R*,*S*)-**157**.

3.3.2 Selective deprotection of cyclobutane-1,2-diamines 152 and 153

The development of orthogonal protecting group strategies makes it possible to remove one set of protecting groups, in any order, using reagents and conditions that do not affect the protecting groups in other sets. An efficient strategy is critical for achieving the synthesis of large, complex molecules possessing a diverse range of reactive functionalities.[72]

For the purpose of proving that the synthesized orthogonally protected cyclobutane 1,2-diamine derivatives could be used for further functionalization, their selective deprotections were carried out (Scheme **33**). Thus, the double elimination of the two *tert*-butoxycarbonyl groups in *cis*-diamine (*R*,*S*)-**152** was achieved yielding amine hydrochloride (*R*,*S*)-**168** in quantitative yields. Similarly, both enantiomers of *trans*-amine hydrochloride **170**, were obtained from diprotected *trans*-diamines (*R*,*R*)-**153** and (*S*,*S*)-**153** in quantitative yields. Alternatively, the benzyl carbamate group in (*S*,*S*)-**153** was hydrogenolyzed in the presence of $Pd(OH)_2/C$ to afford (*S*,*S*)-**172** in 84% yield.

Amines **168** and **170** are suitable for the regioselective introduction of structural units containing additional functional groups. As preliminary instances, *cis*-

[72] Schelhaas, M.; Waldmann, H. *Angew. Chem. Int. Ed.* **1996**, *35*, 2056.

and *trans*-aminothioureas **169** and **171** were synthesized from the free amines (*R*,*S*)-**168** and (*S*,*S*)-**170**, respectively, under treatment of the corresponding ammonium salts with 1 M sodium hydroxide and subsequent reaction with bis(trifluoromethyl)phenyl thioisocyanate. In this way, diastereomeric compounds (*R*,*S*)-**169** and (*S*,*S*)-**171** were obtained in 78 and 75% yield, respectively (Scheme **34**).

The preparation of an alkyl derivative was achieved from (*R*,*R*)-**153** by removal of *N*-Boc protection giving salt (*R*,*R*)-**170**, subsequent neutralization with 1 M NaOH, and later reductive amination of isobutyraldehyde to afford compound (*R*,*R*)-**173** in 38% yield.

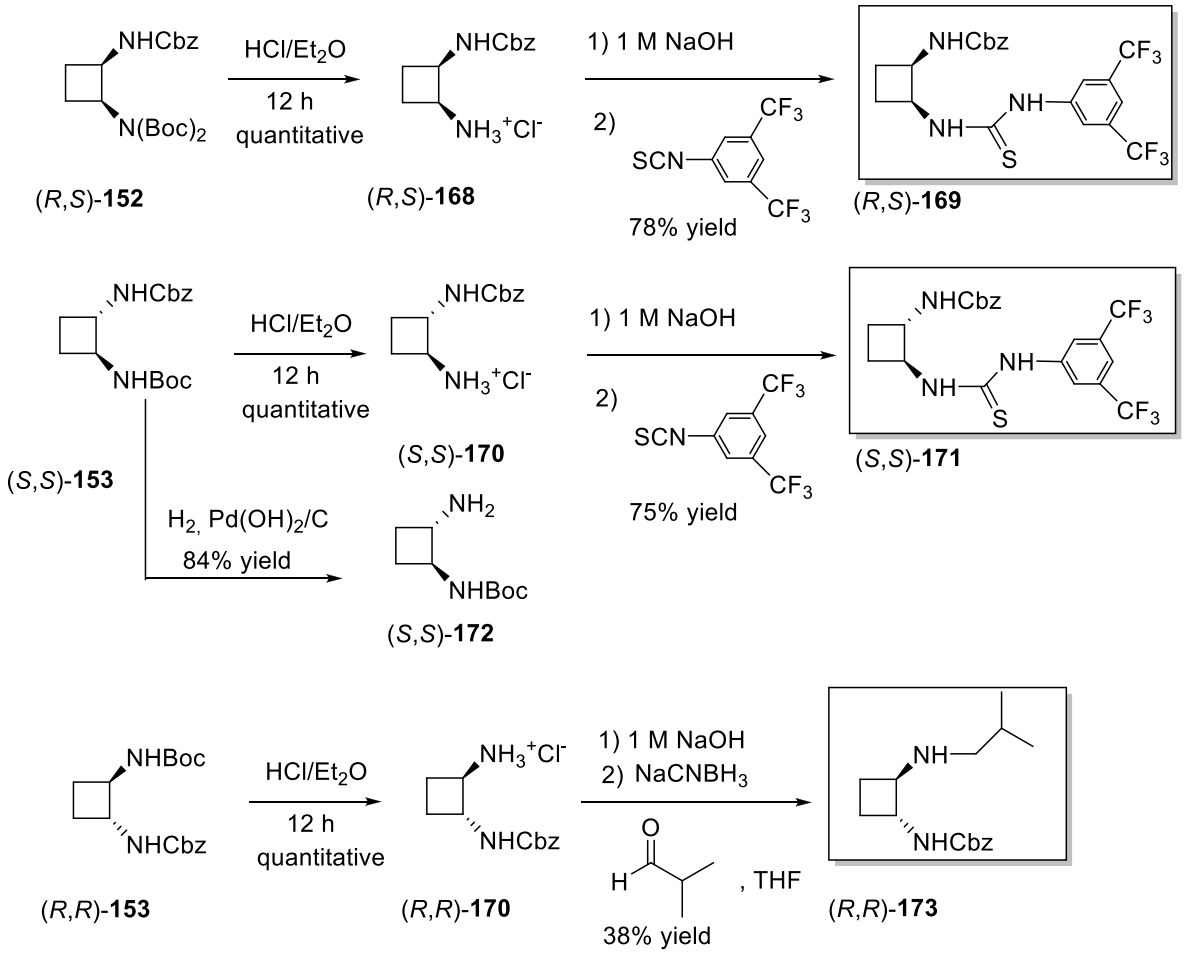

Scheme 33. Some examples on deprotection and regioselective functionalization of diamines.

In summary, an enantio and diastereocontrolled synthesis of the four stereoisomers of cyclobutane-1,2-diamine derivatives has been accomplished. The

versatility of these scaffolds is illustrated in the present Thesis by means of the preparation of functional products with interesting applications such as metal ligands, organocatalysts, surfactants and hybrid materials as described in following chapters.

3.3.3 Stereoselective synthesis of cyclobutane-1,2-dicarboxylic acids 154 and 155.

For the preparation of *cis*-cyclobutane-1,2-dicarboxylic acid (*R*,*S*)-**154** the synthesis started with a [2+2] photochemical cycloaddition between ethylene and maleic anhydride to provide the cycloadduct **3** previously described at the beginning of this Thesis. Then, the cycloadduct was dissolved in water and acetone and the mixture was stirred at room temperature overnight. The progress of the reaction was monitored by ^{1}H NMR following the disappearance of the cycloadduct signals. After three days, the reaction was not completed so further H_20 (9 mL) and HCl (2 mL) were added and the reaction left other three days under stirring. After that, acetone was evaporated under reduced pressure and the residual water lyophilized to give (*R*,*S*)-**154** in quantitative yield (Scheme **34**).

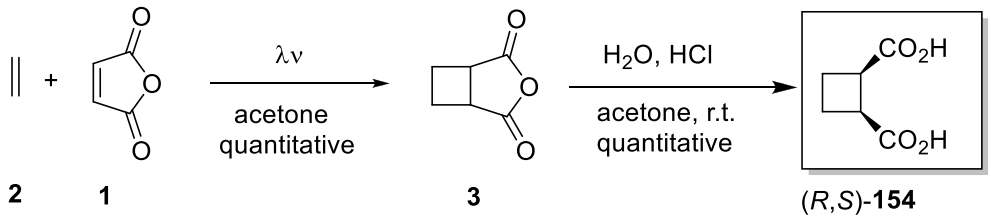

Scheme 34. Synthtethic route to (*R*,*S*)-**154**

The *trans* diastereomer was prepared starting from previously described hemiester (*S*,*R*)-**9**. To proceed, (*S*,*R*)-**9** was dissolved in a THF solution and *t*BuOK was added. The mixture was stirred 1 hour at 0°C to provide enantiopure (*S*,*S*)-**155** in 81% yield (Scheme **35**).

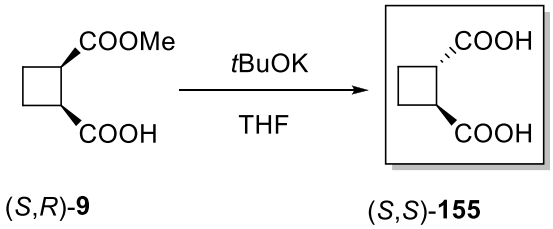

Scheme 35. Synthetic step to (*S*,*S*)-**155** from (*S*,*R*)-**9.**

3.3.4 Synthesis of bolaamphiphiles

Bolaamphiphiles contain two hydrophilic heads connected by a hydrophobic skeleton.[73] Our designed amphiphile joins the presence of 1,2-disubstituted cyclobutane moiety as *chiral core* of the hydrophobic skeleton and two carbon chains with hydrophilic heads. As Figure **24** shows, two scaffolds based on cyclobutane derivatives were used for this purpose.

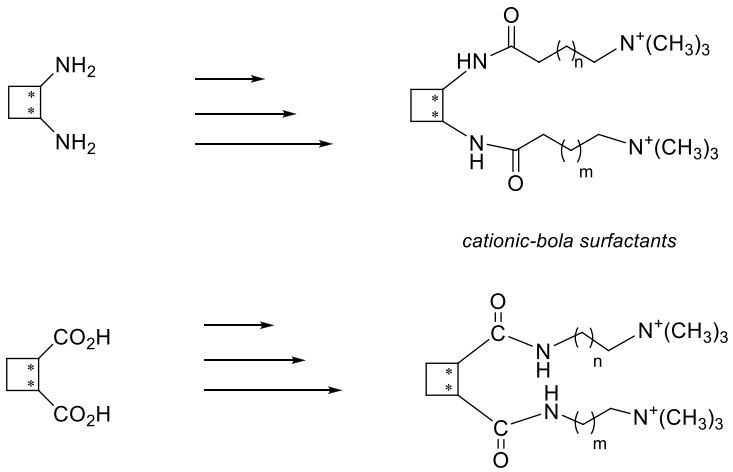

Figure 24. Two different types of amphiphiles synthesized.

Bearing this proposal in mind, in collaboration with Dr. Alessandro Sorrenti, we tackled the stereoselective synthesis of new chiral bola surfactants derived from cyclobutane-1,2-diamine and cyclobutane-1,2-dicarboxylic acid described in Figure **24**, inspired by Hanabusa's previous work.[74]

[73] Sorrenti, A.; Illa, O.; Ortuño, R. *Chem. Soc. Rev.* **2013**, *42*, 8200.
[74] Shirai, H.; Kimura, M.; Hamasaki, N.; Hanabusa, K.; Kobayashi S. *Chem. Mater.* **2012**, *12*, 1523.

3.3.4.1 Synthesis of *cis*- and *trans*- bolaamphiphiles derived from cyclobutane-1,2-diamines

For the preparation and study of surfactants, diamines (*S*,*S*)-**153** and (*S*,*R*)-**152** were chosen in order to study the influence of having substituents in *cis*- and *trans*-configuration. Nevertheless, since identical alkyl chains had to be introduced in order to functionalize the diamines, orthogonal protection was not required. Therefore, changing the amino-protecting group was needed to synthesize new diamine (*S*,*S*)-**174** as Boc dicarbamate. From previously described (*S*,*S*)-**153**, catalytic hydrogenation in presence of di*tert*-butyl dicarbonate, provided new diamine (*S*,*S*)-**174** in a 65% yield. In order to introduce alkyl chains, di*tert*-butyl carbamate was removed by reaction with a 2 M hydrochloric acid solution in diethyl ether and the resulting bisammonium salt (*S*,*S*)-**175** was produced in quantitative yield (Scheme **36**).

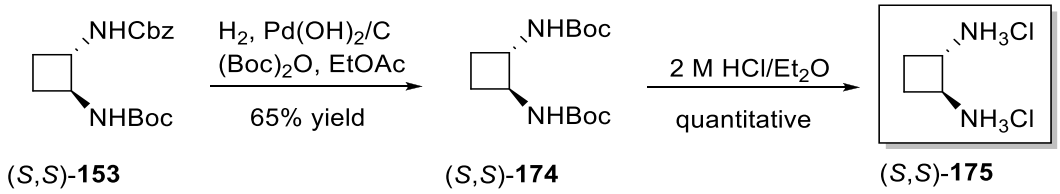

Scheme 36. Synthesis of new diamine (*S*,*S*)-**174** and its deprotection.

There are several methods to synthesize amides.[75] The reaction between an amine and a carboxylic acid using coupling agents gives products with easy purification and, in consequence, better yields. They are widely used in peptide synthesis but due to the need for a variety of peptides, many coupling agents have been developed. The desired peptide often contains stereogenic centers and therefore retention of the optical purity of the compound is also of great importance for any method (Figure **25**).

[75] John S. Carey, J.S.; Laffan, D; Thomsonc, C.; Williams, M. T. *Org. Biomol. Chem.* **2006**, *4*, 2337.

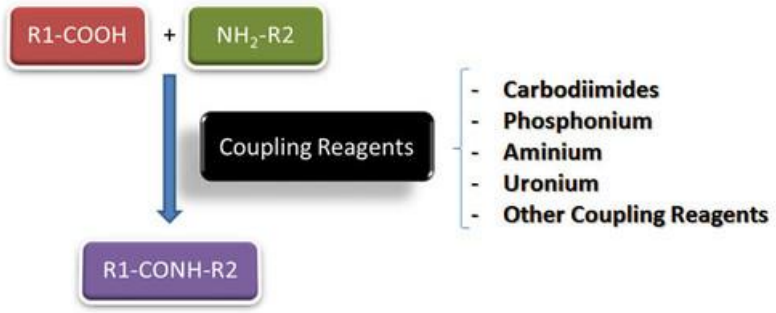

Figure 25. Basic reaction in the amide formation through coupling reagent.

Two different coupling agents were assayed in this Thesis giving similar results: FDPP (pentafluorophenyl diphenylphosphinate) and PyBOP[76] (benzotriazol-1-yl-oxytripyrrolidinophosphonium hexafluorophosphate). However, PyBOP was easier to remove from the crude and it was the most used. Its mechanism of action is shown in Scheme **37**. This reagent is used in tandem with DIPEA as a base, which abstracts the carboxylic acid proton. The generated carboxylate anion attacks the positively charged phosphorous atom, substituting the benzotriazolyl group. The benzotriazolyl anion itself acts as a nucleophile at the acyl centre. The activated acyl group of intermediate is then attacked by the amine giving the amide and the benzotriazol group is released.

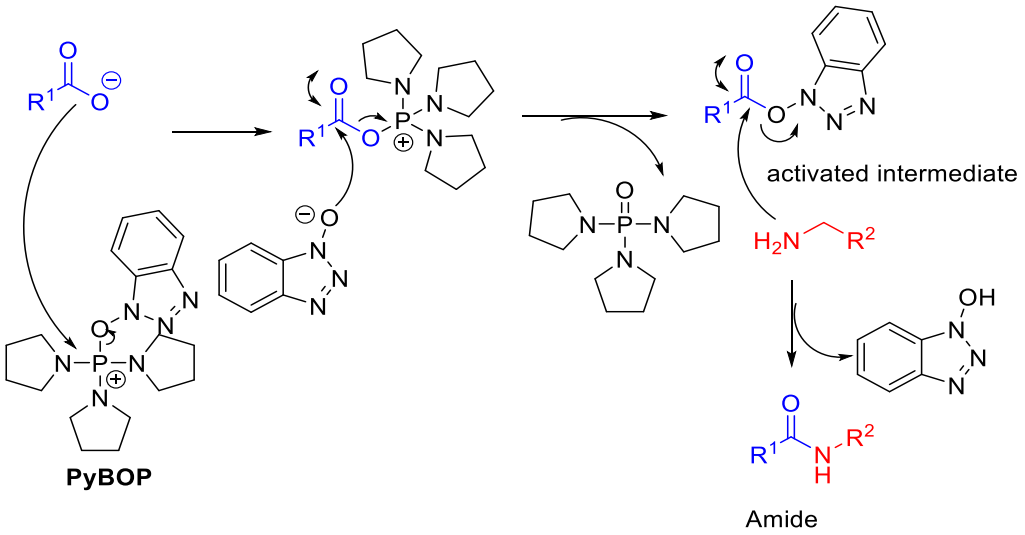

Scheme 37. Reaction mechanism for the PyBOP as coupling agent.

[76] Coste, J.; Le-Nguyen, D.; Castro, B. *Tetrahedron Lett.* **1990**, *31*, 205.

3 Synthesis of the cyclobutane derivatives used as precursors

The cyclic diamine precursor (*S*,*S*)-**175** was coupled with 12-bromododecanoic carboxylic acid in the presence of PyBOP as coupling agent and DIPEA as base in dichloromethane to allow the formation of bromoderivative (*S*,*S*)-**176** in 68% yield. Finally, a solution of (*S*,*S*)-**176** in anhydrous tetrahydrofurane was saturated with trimethylamine and the reaction was stirred at room temperature for 48 hours to provide *trans*-**177** in 60% yield (Scheme **38**).

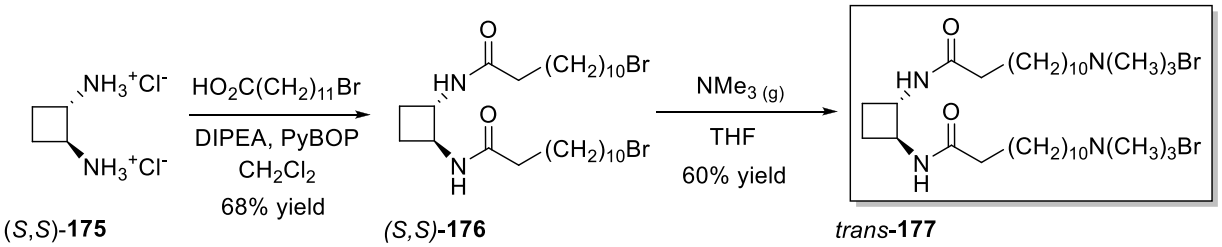

Scheme 38. Synthesis of bolaamphiphile *trans*-**177.**

Bolaamphiphile *trans*-**177** was purified using column chromatography on silica gel followed by a crystallization using dichloromethane in a pentane atmosphere. It was characterized as a white solid and its NMR spectra can be seen in **Figure 26**.

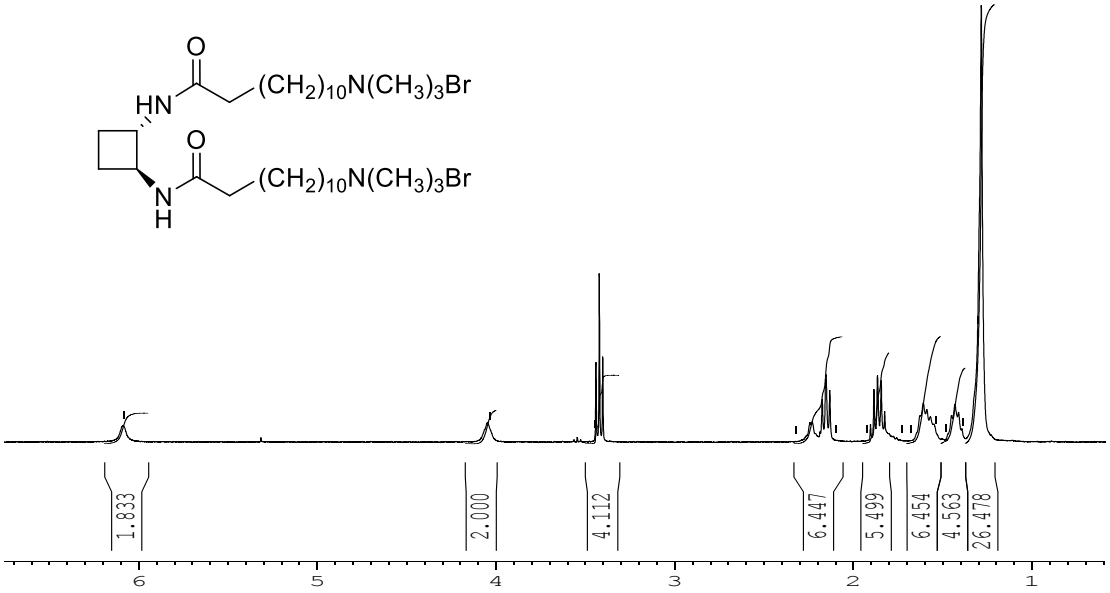

Figure 26. ^{1}H NMR ($CDCl_3$, 250 MHz) spectra of *trans*-**177.**

The synthesis of the peptide bond through an acid chloride was also assayed. First of all, activation of the carboxylic acid was required. This was carried out by addition of a 2 M solution of oxalyl chloride in anhydrous CH_2Cl_2. A few drops of DMF were added and the mixture was stirred under reflux for 2 h in order to generate the acid chloride *in situ*. Then, the resulting acid chloride **178** and triethylamine were added to a solution of diamine **175** in anhydrous dichloromethane to afford bromoderivative **176** in 43% overall yield (Scheme **39**). Observing the yields obtained by the two methods, the reaction with coupling agents resulted better so it was chosen as the methodology to follow in the other cases.

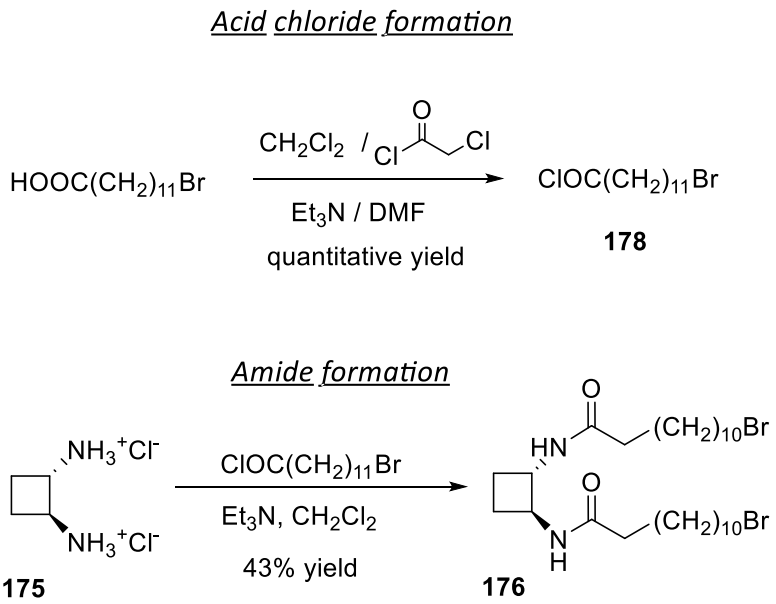

Scheme 39. Two step formation of amide through acid chloride.

To prepare bolaamphiphile *cis*-**177**, the first approach is shown as a retrosynthetic analysis in Scheme **40.** Thus, bolaamphiphile **177** would be synthesized from bromoderivative **179** through nucleophilic substitution of bromide at the *C*-terminal carbon using trimethylamine. In turn, bromoderivative **179** would be prepared by coupling reaction of bromododecanoic carboxylic acid with **180**. The protected amine **181** would be prepared by another coupling reaction of bromododecanoic acid with diamine **168**. Finally, the starting material would be

triprotected diamine (*S*,*R*)-**152**. The bis Boc protection was used in order to avoid the formation of a *cis*-bisammonium salt.

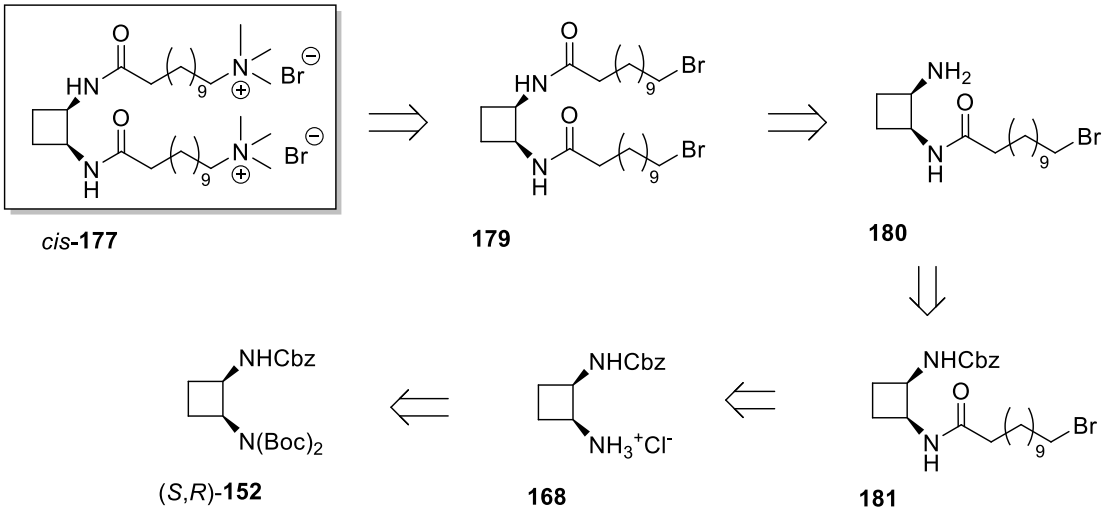

Scheme 40. First approach to prepare bolaamphiphile *cis*-**177.**

Therefore, we tackled this synthethic route. Firstly, di*tert*-butyl carbamate protection of the amino group was removed using a 2 M hydrochloric solution in ether to provide amine hydrochloride **168** in quantitative yield. Then, a coupling reaction with 12-bromododecanoic acid in presence of PyBOP was performed to give bromoderivative **181** in 85% yield. Nevertheless, when catalytic hydrogenation in the presence of palladium hydroxide as catalyst was worked up and checked by NMR we realized that the reaction had not worked and the obtained product was the result of the catalytic reduction of the alkyl halide present in (*S*,*R*)-**181** to give alkane (*S*,*R*)-**182** (Scheme **41**).

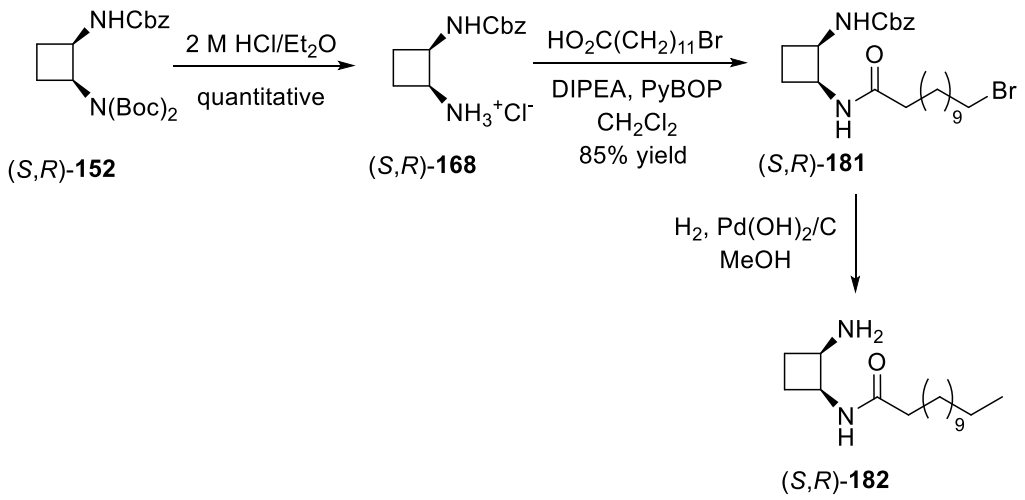

Scheme 41. First synthethic route to achieve *cis*-bolaamphiphile.

Consequently, an alternative synthetic route was proposed similar to the one that was showed previously in **Scheme 38.** Due to the need to introduce the same alkyl chains, the same protecting groups were required in order to afford free cyclobutane-1,2-diamine in one step. To proceed, new *cis* diamine (*R*,*S*)-**183** was achieved from (*R*,*S*)-**152** through catalytic hydrogenation in the presence of di*tert*-butyl dicarbonate in 54% yield. After that, *tert*-butyl carbamate protection was removed with 2 M hydrochloric solution in ether to provide (*R*,*S*)-**184** in quantitative yield. Finally, the use of PyBOP as coupling agent led to the formation of an undesired product difficult to remove. Accordingly, PyBOP was used as coupling agent in the preparation of compound (*R*,*S*)-**179**. Finally, saturating a solution of (*R*,*S*)-**179** in anhydrous THF with trimetylamine provided bolaamphiphile *cis*-**177** in 70% yield (Scheme **42**).

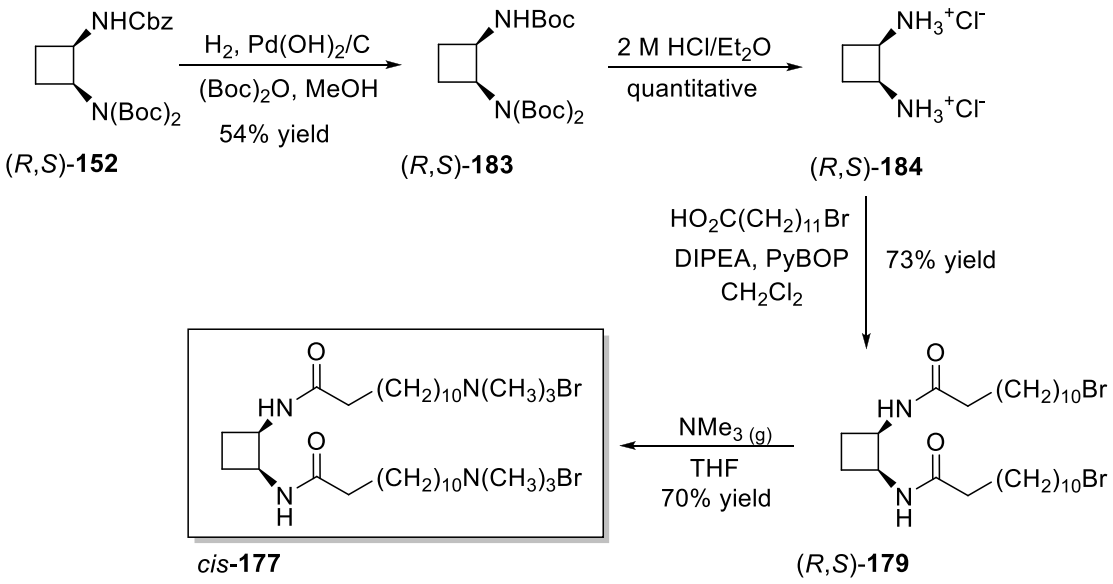

Scheme 42. Synthesis of bolaamphiphile *cis*-**177**.

3.3.4.2 Synthesis of *cis*- and *trans*- bolaamphiphiles derived from cyclobutane-1,2-dicarboxylic acid

To prepare *trans*-**187**, (*S*,*S*)-**155** was coupled with **185** using FDPP as a coupling agent to afford bromoderivative intermediate (*S*,*S*)-**186** in 89% yield. Then, it was dissolved in a mixture of THF/DMF and the solution was saturated with trimethylamine and it was stirred for three days to provide *trans*-**187** as a white solid in 65% yield (Scheme **43**).

In turn, compound **185** was prepared according to a modified literature procedure.[77] Thus, 12-aminododecanol was dissolved in 48% aqueous HBr and the solution was heated to reflux overnight. After the work-up, the combined organic extracts were evaporated to give **185** in 97% yield (Scheme **44**).

[77] Jaegera, D.A.; Josea, R.; Mendoza, A.; Apkarianb, R.P. *Colloids Surf. A* **2007**, *302*, 186.

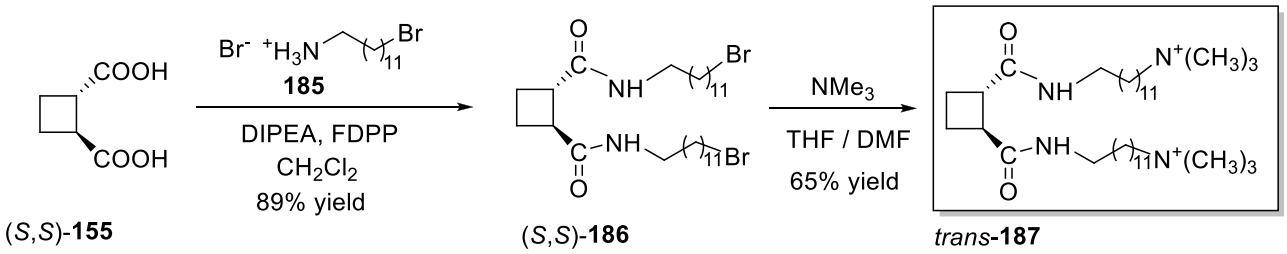

Scheme 43. Synthesis of bolaamphiphiles *trans*-**187**.

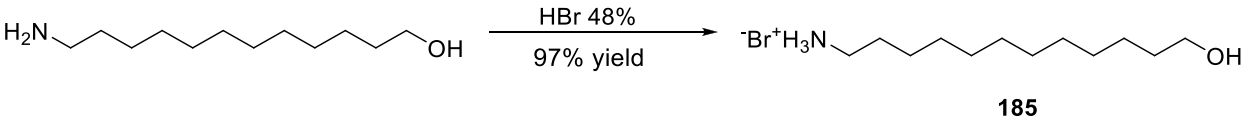

Scheme 44. Synthesis of **185**.

The synthesis of *cis*- diastereomer was carried out by a coupling reaction of (*R*,*S*)-**154** with **185** using FDPP as coupling agent to give bromoderivative intermediate (*R*,*S*)-**188** in 76% yield. Then, a quaternization reaction was carried out to provide bolaamphiphile *cis*-**187** in 85% yield (Scheme **45**).

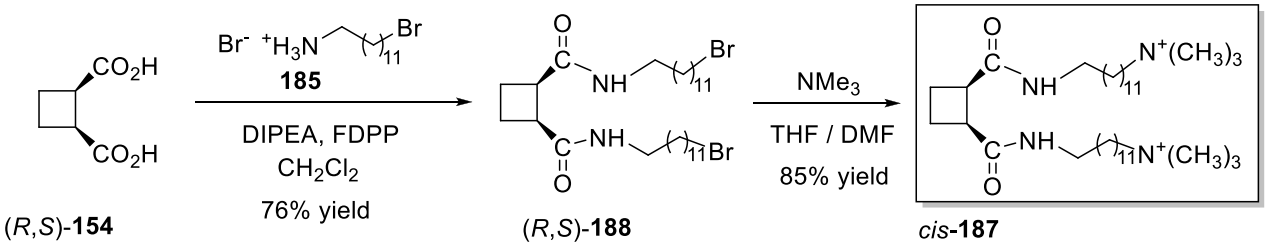

Scheme 45. Synthesis of bolaamphiphiles *cis*-**187**.

3.3.5 Synthesis of *cis*- and *trans*- triethoxysilane derivatives from cyclobutane-1,2-diamine.

Moreau and co-workers reported the synthesis of four chiral diureido derivatives of *trans*-(1*R*,2*R*)- and *trans*-(1*S*,2*S*)-diaminocyclohexane with different carbon chain lengths (n = 3, 4, 5, 10) and the preparation of the corresponding hybrid

bridged silsesquioxanes.[78] Analogously, *cis*- and *trans*- diureido derivatives using cyclobutane-1,2-diamines as chiral scaffolds were synthesized in order to prepare molecular precursors for the hybrid materials described in Chapter 6.

To proceed, the *tert*-butyl carbamate protection of (*S*,*S*)-**174** was removed by reaction with a 2 M solution of hydrochloric acid in ether to provide bisammonium salt (*S*,*S*)-**175.** Then, the reaction with (3-isocyanatopropyl)triethoxysilane in the presence of Et_3N was assayed using different solvents: dichloromethane (CH_2Cl_2) or dichloroethane (CH_2ClCH_2Cl). When using CH_2Cl_2 as solvent the reaction was carried out at 40 ^oC obtaining *trans*-**189** in 10% yield. Using dichloroethane as a solvent, the yield was 52% due to the influence of the temperature because the reaction could be performed at 80 ^oC. Therefore, the reaction was carried out using that solvent to provide triethoxysilanederivative *trans*-**189** with moderated yields (Scheme **46**).

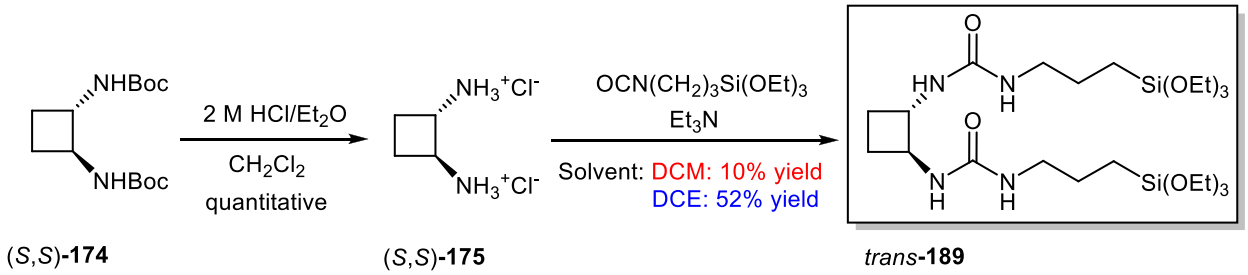

Scheme 46. Synthesis of triethoxysilane derivative *trans*-**189**.

The synthesis of the *cis*-diastereomer was analogous to the previous one. (Scheme **47**). However, the purification of *cis* trietoxysilane derivative was harder to achieve probably due to two effects. On one hand, the sterical hindrance of having substituents in *cis*-disposition could affect the low yield obtained (16%). On the other hand, *cis*-diastereomer seemed to be more unstable than its *trans*-diastereomer analogue and its hydrolysis took place faster, giving some problems during the purification and identification process.

[78] Qinghong, X.; Moreau, J. J. E.; Wong Chi Man, M. W. *J. of Sol-Gel Sci. and Technol.* **2004**, *32*, 111.

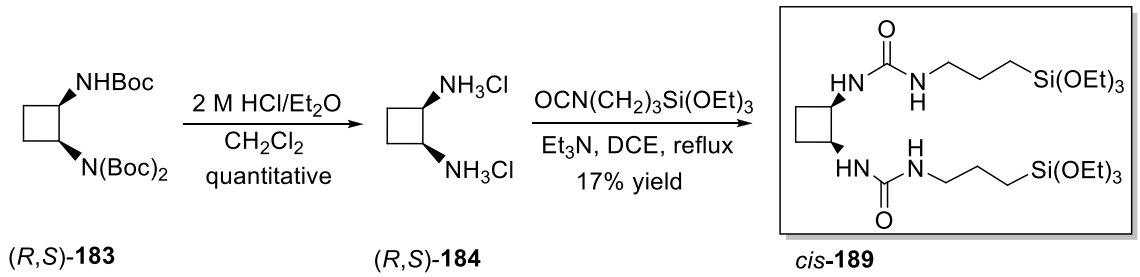

Scheme 47. Synthesis of *cis*-**189**.

3.3.6 Synthesis of *cis*- and *trans*- C_{16}-(*C*-centered) amides based on cyclobutane-1,2-dicarboxylic acid.

For the synthesis of new amido derivatives using cyclobutane-1,2-dicarboxylic acid as scaffold, a well-known method based on coupling agents used previously in our research group was followed to get the target molecules.

From free carboxylic acid (*S*,*S*)-**155**, bisamide *trans*-**190** was prepared through a coupling reaction with hexadecylamine using FDPP as coupling agent in anhydrous dichloromethane and DIPEA as a base in 32% yield (Scheme **48**).

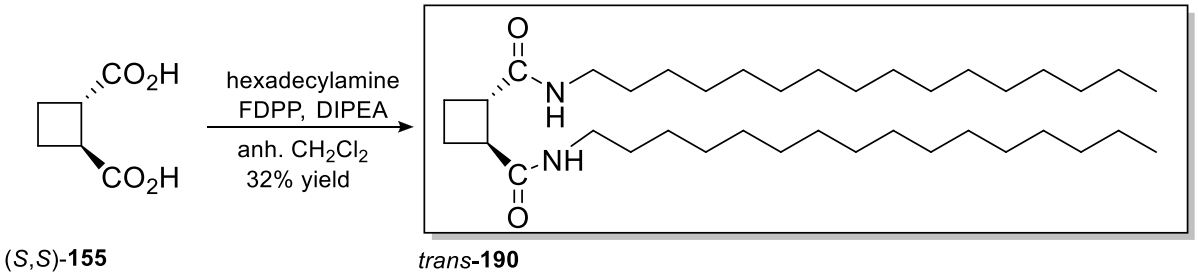

Scheme 48. Synthesis of *trans*-**190.**

In this case FDPP was used as coupling agent because the purification process was easier with this type of products. The reaction with PyBOP was also assayed but the yield was less than 10%. In the mechanism shown in Scheme **49**, the generated carboxylate anion attacks the phosphorous atom, generating the activated acyl group.

Then, the amine acts as a nucleophile: the amide is formed and diphenylphosphinic acid is released.

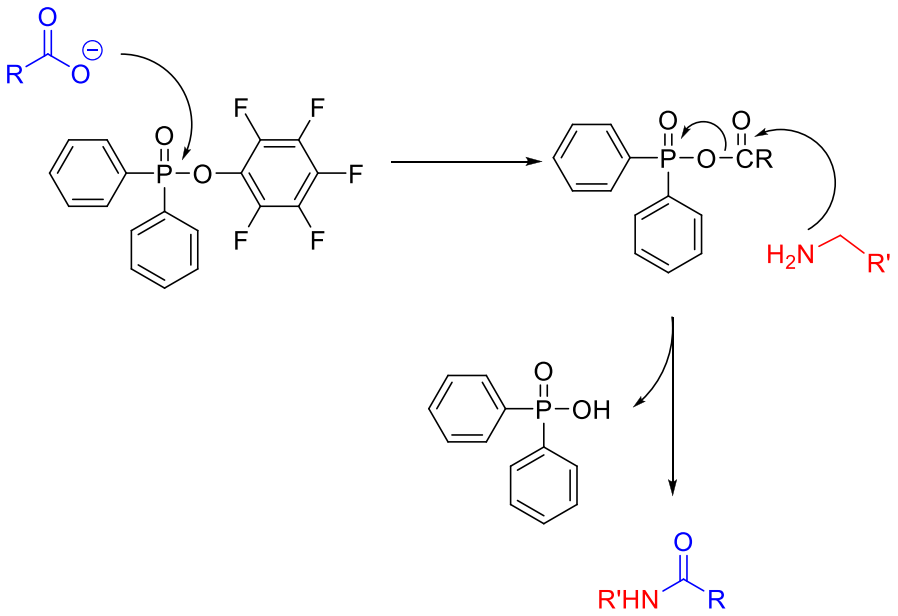

Scheme 49. Reaction mechanism for the FDPP as coupling agent.

With the *cis* diastereomer, an analogous reaction using FDPP as coupling agent from carboxylic diacid (*R*,*S*)-**154** was carried out to afford *cis*-**190**. However, the yield was 22% in front of 32% for its *trans*-diastereomer. Probably, this is again due to the sterical hindrance of having two C_{16} alkyl chains in *cis* disposition (Scheme **50**).

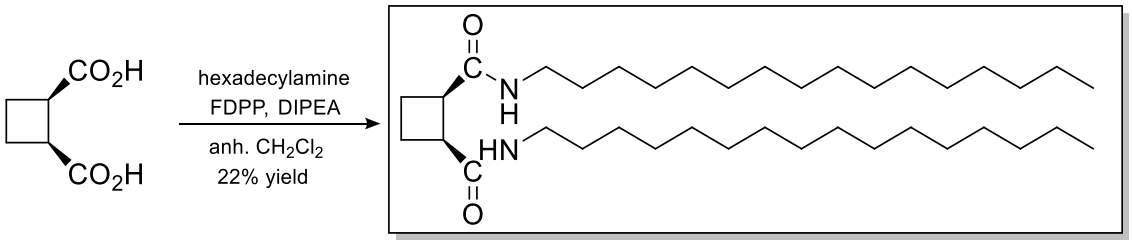

(*R*,*S*)-**154** *cis*-**190**

Scheme 50. Synthesis of *cis*-**190.**

3.4 SUMMARY AND CONCLUSIONS

As described in this chapter, an efficient synthesis of all stereoisomers of cyclobutane-1,2-diamine was achieved through stereodivergent synthetic routes starting from a common chiral precursor (Figure **27**). Furthermore, orthogonal protection of both amino groups was introduced in order to allow a selective deprotection of them.

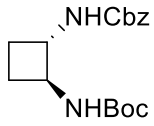

(*S*,*S*)-**153**

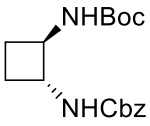

(*R*,*R*)-**153**

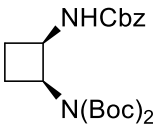

(*S*,*R*)-**152**

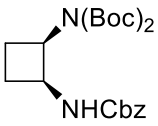

(*R*,*S*)-**152**

Figure 27. Cyclobutane-1,2-diamines synthesized.

In addition, a short synthetic route was performed to provide *cis*- and *trans*-cyclobutane-1,2-dicarboxylic acids in good yields (Figure **28**).

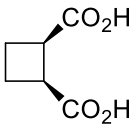

(R,S)-**154**

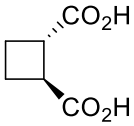

(S,S)-**155**

Figure 28. Cyclobutane-1,2-dicarboxylic acid prepared in this chapter.

Finally, cyclobutane-1,2-diamines and cyclobutane-1,2-dicarboxylic acids were used efficiently as platforms in the preparation of enantiopure derivatives whose properties will be described in the following chapters (Scheme **51**).

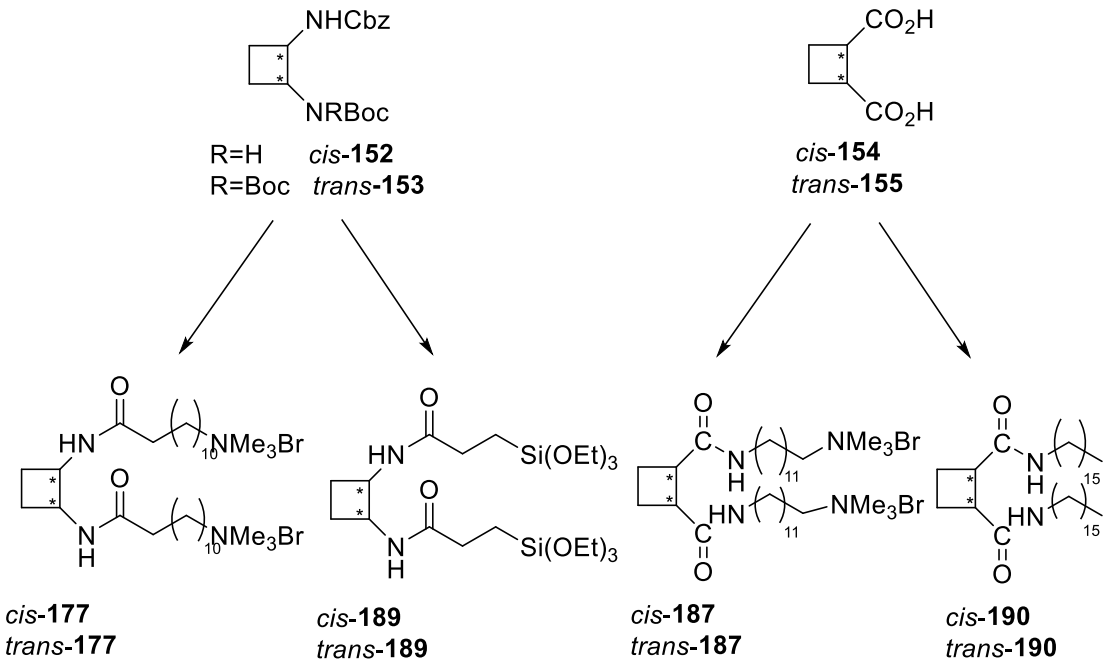

Scheme 51. Schematic representation of the compounds synthesized on this chapter.

CHAPTER IV

Supramolecular study of C_{16}-amido derivatives as organogelators

4.1 INTRODUCTION

4.1.1 Gels: definition and general classification.

One of the major challenges in modern science is the understanding of the mechanisms involved in supramolecular self-assembly and the formation of organogels is an excellent phenomenon to study them.[79]

Many definitions are given but in general, gels belong to an important class of soft materials in which solvent molecules are entrapped within the network structure provided by the gelator molecules under suitable conditions.[80] However, a gel is a material easier to recognize than define. Materials made by means of gelation of organic solvents have received increasing attention over the last 10-15 years,[81] because of their potential applications as functional soft materials in the fabrication of sensors,[82] liquid crystals,[83] electrophoretic and electrically conductive matrices,[84] and in many other industrial fields such as cosmetics, pharmaceuticals,[85] and foods.[86]

A general classification of gels divide them into chemical gels and physical gels (Figure **29**): the internal structure of chemical gels is made of chemical (covalent) bonds,[87] while physical gels are characterized by dynamic cross-links that are constantly created and broken, changing their state between solid and liquid under influence of environmental factors. The gelator present in physical gels may be an inorganic or an organic compound, tipically with molecular mass < 3000. These compounds are generally called ‘‘low molecular weight gelators’’.

[79] Service, R. F. *Science* **2005**, *309*, 95.
[80] Colloid Chemistry, vol. 1. D. Jordan-Lloyd. Chemical Catalogue Company, New York (USA).
[81] Hanabusa, K. *Springer Ser. Mater. Sci.* **2004**, *78*, 118.
[82] Li, S.; John, V. T.; Irvin, G. C.; Bachakonda, S. H.; McPherson, G. L.; O’Connor, C. J. *J. Appl. Phys.* **1999**, *85*, 5965.
[83] Kato, T. *Science* **2002**, *295*, 2414.
[84] Puigmarti-Luis, J.; Laukhin, V.; del Pino, A. P.; Vidal-Gancedo, J.; Rovira, C.; Laukhina, E.; Amabilino, D. B. *Angew. Chem., Int. Ed.* **2007**, *46*, 238.
[85] Kumar, R.; Katare, O.P.; *Pharm. Sci. Tech.* **2005,** *6*, 298.
[86] Pernetti, M.; van Malssen, K.F.; Flöter, E.; Bot, A. *Curr. Opin. Colloid Interface Sci.* **2007**, *12*, 221.
[87] Vlierberghe, S. Van; Dubruel, P.; Schacht, E. *Biomacromolecules* **2011**, *12*, 1387.

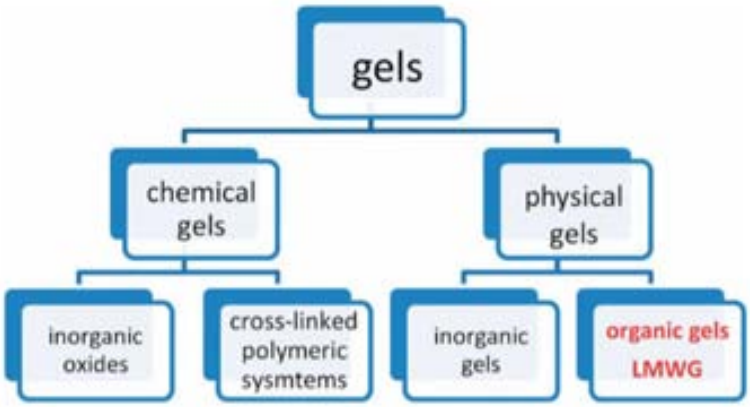

Figure 29. General classification of gels.

It is not yet possible to select a priori a molecule to gel definitively a selected liquid. Discoveries of new gelators or thickeners remain mainly fortuitous. As an aid to defining strategies for the molecular design of new low molecular-mass organogelators, there are different types of molecules acting as organogelators: Fatty acids,[88,89] steroid derivatives,[90] dendrimers,[91] macrocycles,[92] sugar derivatives[93] etc.

4.1.2 Low Molecular Weight Gelators (LMWGs).

LMWGs[94] are especially interesting because they consist of small molecules that can self-assemble due to the fact that they contain hydrogen-bonding functional groups and/or apolar chains, which can induce order or piling through solvophobic van der Waals interactions to form fibrous nanostructures, which can further associate into higher order structures. To follow the procedures in this Thesis it is important to distinguish the terms organogel and xerogel. While an organogel is a gel made of a LMWG and any kind of organic solvent, a xerogel is a solid formed after evaporation of the solvent in a hydrogel or an organogel by drying with unhindered shrinkage.

[88] Polishuk, A. T. *J. Am. Soc. Lubn. Eng.* **1977**, *33*, 133.
[89] Uzu, Y. *J. Jpn. Oil Chem. Soc.* **1975**, *24*, 261.
[90] Ramanathan, N.; Currie, A. L.; Ross Colvin, *J. Nature* **1961**, *4778*, 779.
[91] Hirst, A.; Smith, D. K.; Feiters, M. C.; Geurts, H. P. M.; Wright, A. C. *J. Am. Chem. Soc.* **2003**, *125*, 9010.
[92] Becerril, J.; Burguete, M. I.; Escuder, B.; Galindo, F.; Gavara, R.; Miravet, J. F.; Luis, S. V.; Peris, G. *Chem Eur. J.* **2004**, *10*, 3879.
[93] Gronwald, O.; Shinkai, S. *Chem. Eur. J.* **2001**, *7*, 4329.
[94] Smith, D. K. *Chem. Soc. Rev.* **2009**, *38*, 684.

Xerogels usually retain high porosity (15–50%) and enormous surface area (150–900 m^2 g^1), along with very small pore size (1–10 nm).

The following broad statements about a typical gelator molecule can be made:

(i) The molecule must be partly soluble and partly insoluble in the solvent.

(ii) The molecule must have the potential to form weak intermolecular interactions, such as hydrogen bonds, electrostatic interactions, π–π stacking interactions, hydrophobic forces, non-specific van der Waals forces, and chiral dipole–dipole interactions.

(iii) The non-covalent interactions should be directional, leading to the assembly of anisotropic nanoscale fibres.[95]

(iv) For this reason, often LMWGs are **chiral molecules**. Most LMWGs contain more than one stereogenic centre, so they can exist under several stereoisomers that usually show completely different gelation behaviors. As will be seen throughout this chapter, the spatial arrangement of different diastereoisomers strongly affects their possibility to form weak interactions, such as hydrogen bonds, π–π stacking interactions, van der Waals interactions. Thus, changing the configuration of a single stereocentre may have dramatic effects on the solubility properties, the range of solvents that can be gelated, the stiffness of the gels it forms and its critical gelation concentration, and the temperature at which its gels melt.

David K. Smith and co-worker[96] have recently investigated a two-component acid−amine gelation system in which chirality plays a vital role. A carboxylic acid based on a second generation L-lysine dendron interacts with chiral amines and subsequently assembles into supramolecular gel fibres (Figure **30**).

[95]Aggeli, A.; Nyrkova, I. A.; Bell, M.; Harding, R.; Carrick, L.; McLeish, T. C. B.; Semenov, A. N.; Boden, N. *Proc. Natl. Acad. Sci. U. S. A.*, **2001**, *98*, 11857.
[96]Edwards, W.; Smith. D. K. *J. Am. Chem. Soc.* **2014**, *136*, 1116.

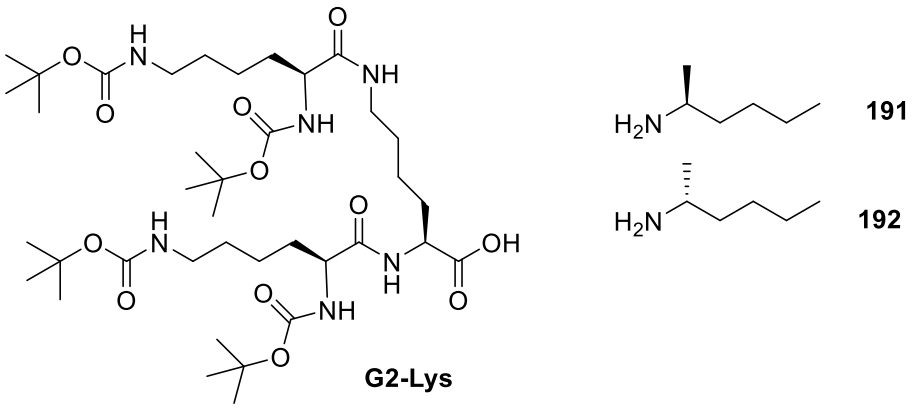

Figure 30. Chiral gelation system of **G2-Lys** and chiral amines **191** and **192**.[96]

In order to study and understand all the possible interactions that are responsible for the formation of supramolecular nanostructures, which are directly related to their possible applications, a wide variety of techniques have gained importance in this field, such as microscopy (SEM, TEM, AFM), NMR spectroscopy, IR spectroscopy, X-Ray spectroscopy, Circular dichroism spectroscopy and computational calculations. Some of them are going to be used in this thesis.

4.1.3 Amide-based LMWGs.

Some examples of LMWGs are going to be outlined as an overview of the different kind of amide-based structures with gelating capability. Fages and co-workers[97] described one of the most simple urea and amide gelator system based on 11-aminoundecanoic acid (**193**). Some of them showed capability of gelating polar aprotic solvents, such as DMF, and apolar solvents, such as toluene (Figure **31**).

[97]Mieden-Gundert, G.; Klein. L.; Fischer, M.; Vögtle, F.; Heuzea, K.; Pozzo, J. L.; Vallier, M.; Fages, F.; *Angew. Chem. Int. Ed.* **2001**, *40*, 3164.

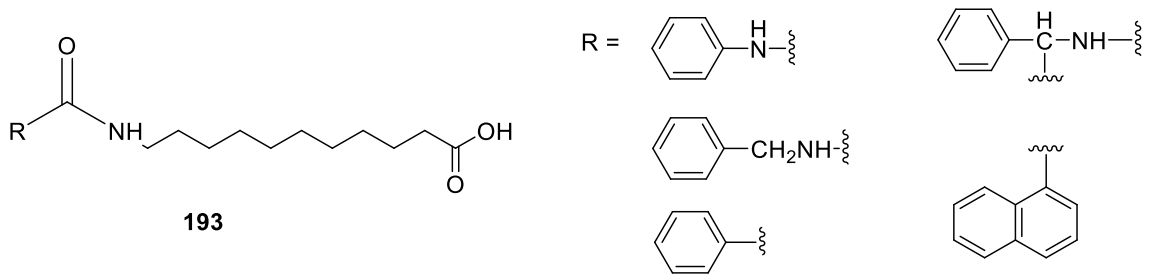

Figure 31. Some of the structures investigated by Fages et al.[97]

Diamides have been also reported, being the derivatives of *trans*-diaminocyclohexane one of the most studied. Organgelators based on *trans*-1,2-diaminocyclohexane were reported by the first time in 1996 by Hanabusa.[98] In his work, he investigated the capability to gelate a wide variety of organic solvents as well as the chiral structure of the aggregate in the gel by FT-IR, CD, molecular modelling studies and TEM. TEM images showed that numerous intertwined aggregates were formed from helical fibers with widths of 40-70 nm. The helicity of the fibers were directly related to the configuration of the chiral center: it was always right-handed for (*R*,*R*)-**194** and left-handed for the enantiomer (*S*,*S*)-**194** (Figure **32**).

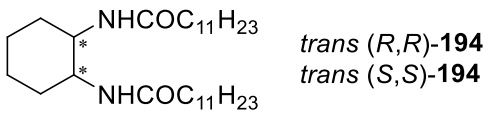

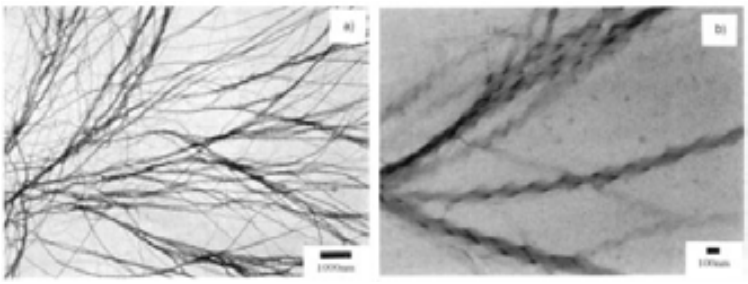

Figure 32. TEM images of (*R*,*R*)-**194** and (*S*,*S*)-**194** in acetonitrile (1 mM).

[98]Hanabusa, K.; Yamada, M.; Kimura, M.; Shirai, H. *Angew. Chem. Int. Ed. Engl.* **1996**, *35*, 1949.

In 2009, Van Esch and Feringa[99] studied the behavior in different solvents of two different organogelators based on cyclohexane-bisamide and bisurea. They demonstrated that for organogel-forming compounds in polar solvents van der Waals interactions played a dominant role whereas in apolar solvents hydrogen-bonding interactions dominated. These results demonstrated that the key point in understanding the dependence of gelation strength on both solvent properties and the anisotropy of intermolecular interactions is essential to recognize that the primary interaction driving the assembly of the gel fibre is itself solvent-dependent.

Amphiphilic gelators based on *trans*-1,2-diaminocyclohexane also found application as nanostructured material with interesting application as a template. In this work,[100] they reported the preparation of a novel TiO_2 material with a hollow-fiber structure like "macaroni" by using **195** as a template. As it can be seen in Figure **33**, the calcined samples under basic conditions possessed hollow structures with outer diameters of 150-600 nm and the maximum length of the titania fibers was around 200 µm.

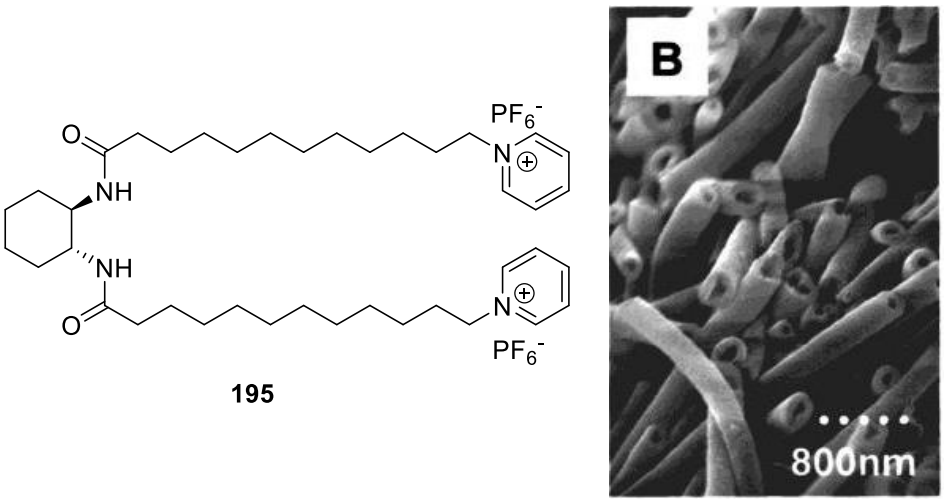

Figure 33. SEM images of the calcined samples prepared with amphiphilic compound **195** under basic conditions.

[99] Zweep, N.; Hopkinson, A.; Meetsma, A.; Browne, W. R.; Feringa, B. L.; van Esch, J. H. *Langmuir* **2009**, *25*, 8802.
[100] Kobayashi, S.; Hanabusa, K.; Hamasaki, N.; Kimura, M.; Shirai, H. *Chem. Mater*. **2000**, *12*, 1523.

4.1.4 Cyclobutane-containing LMWGs

Nevertheless, in the literature very little examples of gelator based on the cyclobutane motif are found. Dastidar,[101] in his works, employed cyclobutane 1,1-dicarboxylic acid in its anionic form and different amines as cations as a two-component organogelator. In fact, multi-component LMWGs are interesting because they afford materials with highly tuneable microscopic and macroscopic properties, due in part to their salt nature, that results in very defined supramolecular structures (Figure **34**).

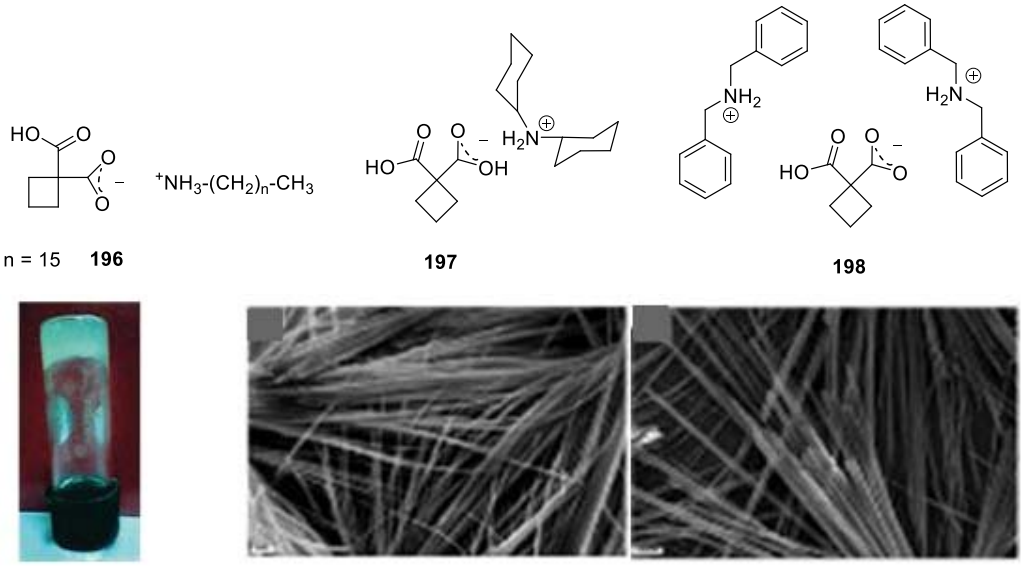

Figure 34. Some examples of two-components LMWGs containing the cyclobutane motif. Compound **196** forms a stable gel in nitrobenzene at 2 mg/mL concentration (left). Compounds **197** and **198** form needle-like supramolecular structures observed by SEM (middle and right).

As it has been seen in Chapter one, the preparation of low molecular weight gelators based on the cyclobutane moiety has been well established in our research group. In particular, low molecular weight gelators based on hybrid peptides studied by Dr. Sergi Celis showed to be good gelators in a broad range of solvents. In addition, their aggregation was studied and it was concluded that they formed chiral aggregates in solution. Moreover, SEM micrographs of them showed well-defined stuctures consisting on bundles of fibers of different lenghts (Figure **35**).

[101] Ballabh, A.; Trivedi, D. R.; Dastidar, P. *Chem. Mater*. **2006**, *18*, 3795.

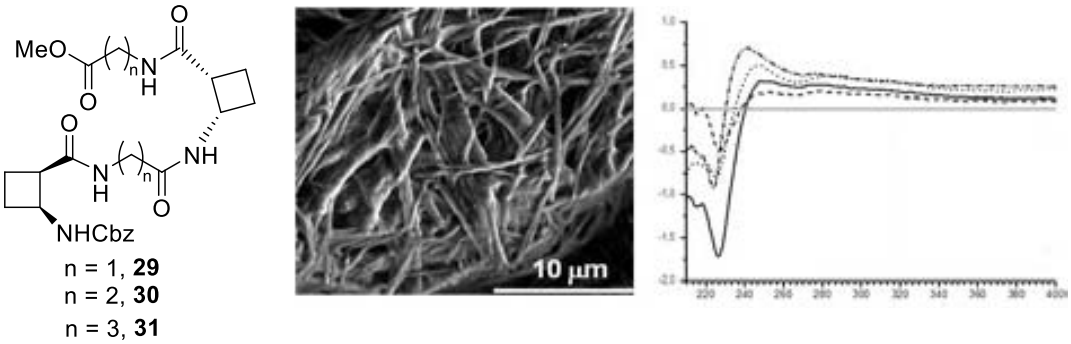

Figure 35. Organogelators based on hybrid peptides synthesized in our group (left). SEM micrograph of organogelator **29**. (center). Circular dicroism spectra of **29** (right).

4.2 OBJECTIVES

In Chapter three of this Thesis, *cis*- and *trans*-C_{16}-*C*-centered amides based on cyclobutane-1,2-dicarboxylic acid were prepared (Figure **36**). Taking into account the acquired experience in our research group in the field of low molecular weight gelators the objectives of this chapter were:

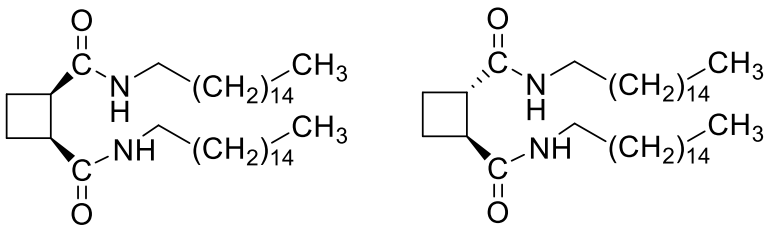

cis-**190** *trans*-**190**

Figure 36. C_{16}-*C*-centered amides synthesized in the previous chapter.

i. To study the capacity of *cis*-**190** and *trans*-**190** to gelate different solvents, as well as to describe the characteristics of these gels.

ii. To carry out a structural study, by NMR experiments, SEM and theoretical calculations of some of the gels formed.

iii. A third objective, in collaboration with Prof. J. C. Estévez from the *Universidad de Santiago de Compostela,* was to compare these results with the ones obtained when cyclohexane is used as a ring as well as the influence of having other substituents as alcohols or ketals in the ring.

4.3 RESULTS AND DISCUSSION

In the introduction of this part, different examples based on diamides with long alkyl chains as organogelators have been presented. Thus, it was decided to perform some quantitative-qualitative study of the gelating properties of *cis*-**190** and *trans*-**190** (Figure **45**). In addition, the research group of Prof. J. C. Estévez from the *Universidad de Santiago de Compostela* synthesized analogue C_{16}-bisamide derivatives with cyclohexane as chiral moiety, *cis*-**199** and *trans*-**199**. On the other hand, they also prepared *cis*-**200** and *trans*-**201** and which incorporate in their structure a ketal in positions 3 and 4 and a hydroxyl group in position 5. This hydroxyl group is protected as a TBDMS ether in **201** (Figure **37**).

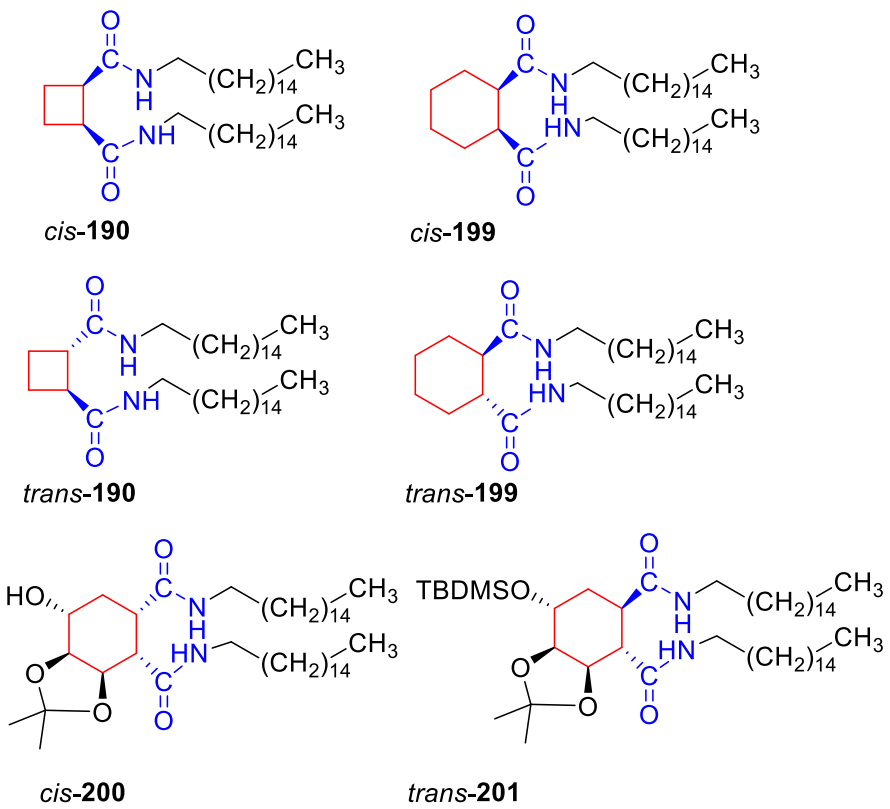

Figure 37. Compounds that incorporate the 1,2-bisamido moiety in their structure.

4.3.1 Preparation of the gels

The study of the gelation properties in these molecules is interesting because the influence of the ring size (cyclohexane vs cyclobutane) and the stereochemistry (*cis* vs *trans*) can be compared. Also, the fact of having pentasubstituted ring with a polar group (OH) which could change the properties of the compound is of interest.

The preparation of the gels was achieved by the following procedure:

i) A small amount (5.0 ± 0.1 mg) of compound is weighed in a 2 mL transparent-glass vial with a septum screw-on cap. When the 5 mg of compound is soluble in a specific solvent, a new vial containing 10 ± 0.1 mg is prepared and the solubility-gelation is checked again. At that point, if the peptide is still soluble, the compound is considered not to be an organogelator because the amount of material needed is too high, in other words, the solution is too concentrated (c = 10 mg/0.5 mL = 20 mg/mL).

ii) In a second step, a certain volume of solvent to be tested is added and the vial is closed. The minimum volume added is 0.05 mL. Then the mixture is heated under the boiling point of the solvent using a balloon system in order to avoid solvent pressure and, once a solution is obtained the mixture is sonicated for 1 to 5 minutes. For high concentrations and also in some solvents, previous sonication is needed for a good solubilization during heating and sonication time is usually shorter than for diluted gels. Then, the mixture is left to stabilize and to reach room temperature.

iii) To state that the mixture is a gel, the tube inversion test is done just by turning the vial upside down (Figure **38**). If the sample is a gel it does not drop. In order to determine the minimum gelation concentration (mgc), a new volume of solvent is added to the gel and the process is repeated until no gel is formed: the last volume added determines the mgc.

Figure 38. Tube inversion test in order to confirm the presence of the gels.

Then, compounds **190**, **199**, **200** and **201** were quantitatively tested as LMWGs in solvents of different dielectric constant. Table **1** summarizes the results and Table **2** shows the appearance of such gels formed at the mgc.

Table **1**. Gelation behavior of compounds **190, 199, 200** and **201** in common solvents.[a]

Compound	Solvent and minimum gelation concentration[b,c]													
	Pentane	Toluene	1,4-dioxane	Et_2O	$CHCl_3$	EtOAc	THF	CH_2Cl_2	iso-PrOH	Acetone	Ethanol	Methanol	MeCN	H_2O
cis-**190**	I	57	I	I	104	I	I	106	I	I	I	I	I	I
trans-**190**	I	25	I	I	I	I	I	I	I	I	I	I	I	I
cis-**199**	I	55	17	I	S	I	I	I	I	I	I	I	I	I
trans-**199**	I	2	3	I	90	I	I	I	I	I	I	I	I	I
cis-**200**	I	30	55	S	S	S	S	S	S	S	S	S	S	S
trans-**201**	I	110	18	S	S	S	S	S	80	S	S	7	S	S

[a] Dielectric constant increases from left to right.
[b] Units: mgc in mM
[c] I: insoluble. S: soluble.

None of these compounds was soluble in water so they were not able to form hydrogels. Compounds **190** and **199** are insoluble in most of the solvents, due to the influence of having two C_{16}-alkyl chains. However, with **200** and **201** there are drastic changes in the solubility in these solvents owing to the presence of a hydroxyl group in position **5** of the cyclohexane. Interestingly, just one nice gel was formed from MeOH at 7 mM for **201**.

On the other hand, **201** formed a gel from iso-PrOH at 80 mM. *cis*-**190** and *trans*-**199** formed gels in $CHCl_3$ but the mgc was too high to be considered good organogels and both were not stable so they were resolubilized at room temperature. Furthermore, an important difference between cyclobutane and cyclohexane derivatives is that all of cyclohexane derivatives formed stable gels in 1,4-dioxane at rather low concentrations but compounds based on cyclobutane were soluble in this solvent when heating but they became insoluble at room temperature.

All of them formed gels in toluene in a wide range of mgc. The best gel was formed at 2 mM from *trans*-**199**. There is another difference if we compare the stereochemistry of the compounds since compounds with *trans* relative configuration seem to be more prone to form gels at lower concentrations.

Table 2. Pictures of the gels of **190**, **199**, **200** and **201** at the mgc.

Compound	Solvent[a,b]					
	Toluene	1,4-dioxane	$CHCl_3$	CH_2Cl_2	iso-PrOH	Methanol
cis-**190**		I			I	I
trans-**190**		I	I	I	I	I
cis-**199**			S	I	I	I
trans-**199**				I	I	I
cis-**200**			S	S	S	S
trans-**201**			S	S		

All gels formed in toluene, dioxane and methanol were stable at room temperature for weeks at their mgc. In addition, they were thermoreversible at concentrations beyond the mgc, while in chlorinated solvents such as dichloromethane and chloroform and with iso-PrOH no evidences of thermoreversibility were found.

On the other hand, some qualitative experimental observations were stated during the preparation of the gels. The gels formed by *cis*-**190** and *trans*-**190** in toluene

resulted to be translucid while the gels formed by *cis*-**199** and *trans*-**199** resulted to be opaque at their mgc. The most transparent were the gels provided by *cis*-**200** in toluene and dioxane. All the gels afforded by *trans*-**201** were opaque.

On the other side, all compounds in 1,4-dioxane, *trans*-**190** and *trans*-**199** in toluene and *trans*-**201** in methanol showed spontaneous gelation without using sonication.

4.3.2 Supramolecular study of the gels formed.

The use of toluene as solvent to form the corresponding gels provided them in a good quality and an easy way. Its high boiling point allowed to solubilize completely the organogelators and made the time to reach room temperature to be longer, allowing a better homogenization. Both cyclobutane and cyclohexane derivatives with *cis* and *trans* configuration provided nice gels in toluene which would be useful to study the influence of the ring size and *cis*/*trans* stereochemistry on the gel properties. Then, toluene gels of *cis*- and *trans*- isomers of **190** and **199** were suitable to compare the different properties and they were chosen for the following supramolecular study.

Their physical properties such as morphology, size and type of supramolecular arrangement were analyzed by scanning electron microscopy (SEM) and IR spectroscopy. In addition, the self-assembly of the molecules is being modelled in order to investigate their tridimensional arrangement. Finally, high-resolution NMR experiments were also carried out, with the aim of studying the dynamics of the sol-gel process.

4.3.2.1 High-resolution NMR spectroscopy

High-resolution NMR spectroscopy is a technique that is widely used to provide evidence for gel formation and to give information about the secondary structures that are adopted.[102]

It is important to recall that in liquid-state NMR studies only the liquid-like fraction of a gel can be observed, but the solid-like part of the gel remains undetected.[103] Signals belonging to the incipient aggregate become very broad because of restricted molecular motion, which increases dipole–dipole interactions and produces an enhanced relaxation relative to the solution-bound species. In fact, large aggregates behave like solids and they are not detected because their very broad signals are constituent of the base line of the spectrum and, therefore, they are not observable. Nevertheless, the spectrum observed from free and pre-aggregated gelators in the gel can provide a qualitative understanding of the possible orientation of a single molecule in an aggregated system.

Thus, these properties allowed us to prove the existence of intermolecular hydrogen bonds and to determine the gelation temperature for compounds *cis*-**190**, *cis*-**199**, *trans*-**190** and *trans*-**199**. Then, in collaboration with Dr. Pau Nolis, from the NMR Service at the Universitat Autònoma de Barcelona, high-resolution NMR experiments were carried out.

The gelation process of a solvent, in which the intermolecular interactions are enhanced by some external stimuli, reduces the mobility of the molecules. There are many gelation inductors but change in the temperature is one of the most applied and adaptable to the NMR. Therefore, if gelation is slow compared to NMR time scale measurement, this dynamic process can be monitored by variable temperature ^{1}H-NMR experiments. By decreasing the temperature, a continuous signal line broadening

[102] Recent examples: (a) Xie Z.; Zhang A.; Ye L.; and Feng Z. *Soft Matter*, **2009**, *5*, 1474–1482. (b) Pasc A.; Akong F. O.; Cosgun S.; and Gérardin C. *Beilstein J. Org.Chem.* **2010**, *6*, 973-977.
[103] Makarević J.; Jokić M.; Perić B.; Tomišić V.; Kojić-Prodić B. and Žinić M. *Chem. Eur. J.* **2001**, *7,* 3328.

is observed and finally a complete signal loss is produced due to the increasing "solid-like" part of the gel, which is NMR invisible.[104]

Furthermore, if the gelation process is monitored in sufficiently slow motion, a differential behavior of signals can be observed which helps to better understand the gel-formation dynamic process. Adequate conditions of sample concentration and appropriate cooling down gradient temperature are crucial in these experiments because the gelation process strongly depends on both interdependent factors.

Regarding our compounds tested as organogelators, for both classes, the gelation is presumed to be driven by two different types of intermolecular interactions: van der Waals (due to the length of the alkyl units) and hydrogen bonding interactions (due to the two amido moieties). Thus, the overall sum of these interactions is assumed to lead to an anisotropic aggregation. Molecules containing amide groups that favour supramolecular interactions are prominent, as for example peptide-based gelators that mimic natural proteins.[105]

In this specific study, a controlled cooling down regime was applied to a 17 mM sample of each of the studied compounds. ^{1}H-NMR spectra were acquired in 1 K steps, starting from 330 K and lowering to 310 K in the case of *cis*- and *trans*-cyclohexane derivatives (Figure **39a**). In the case of *cis*- and *trans*- cyclobutane derivatives, ^{1}H-NMR spectra were acquired also in 1 K steps, starting from 310 K and lowering to 290 K. (Figure **39b**).

Moreover, an equilibration time of three minutes was used in all the compounds as sample thermal equilibration period. The N*H* proton signals were used to follow the gelation process.

[104] Brand, T.; Nolis, P.; Richter, S.; Berger, S. *Magn. Reson. Chem.* **2008**, *45*, 325.
[105] Pashuck, E.T.; Cui, H.; Stupp, S. I. *J. Am. Chem. Soc.* **2010**, *132*, 6041.

(a) Cyclohexane **(b) Cyclobutane**

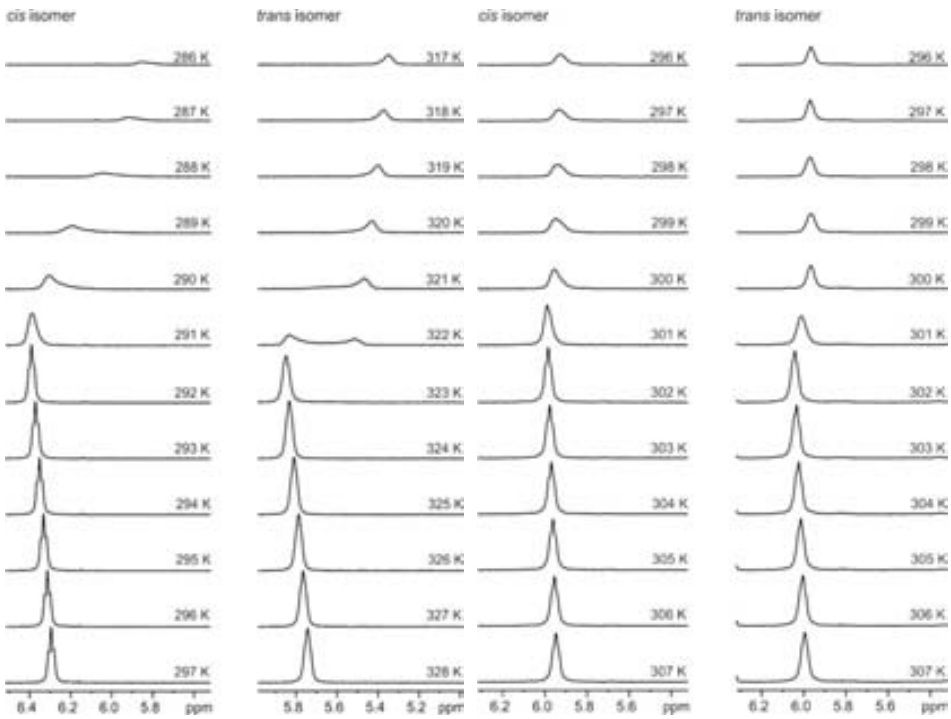

Figure 39. Gelation process monitored by variable-temperature ^{1}H-NMR spectroscopy experiments in 17 mM solutions of (a) *cis*-**199** and *trans*-**199** (b) *cis*-**190** and *trans*-**190**. A 400 MHz Bruker Avance III spectrometer equipped with a cooling unit BCU-Xtreme was used.

Regarding the experiments related to the cyclohexane derivatives, the NH signal of *trans*-**199** decays at 322 K whereas the NH of *cis*-**199** decays at 290 K. This is a great difference which means an important influence of the relative *cis*/*trans* stereochemistry of the cyclohexane derivatives.

Interestingly, the chemical shift of the N*H* of *trans*-**199** in the gelation step is 5.8 ppm and 6.3 ppm for *cis*-**199**. That means that the *cis* isomer has the N*H* and the CO groups of the amide moieties in the same plane favouring the formation of hydrogen bonds. However, the N*H* signal disappears later in the *cis* than in the *trans* isomer. This suggests that the disposition of the C_{16}-alkyl chains in the *trans* isomer is more ordered. Then, *trans* isomer has a worse disposition to form hydrogen bonds but its C_{16}-alkyl chains are more ordered and the Van der Waals interactions are favourable to form gels.

Referring to the cyclobutane derivatives, the N*H* signal of both isomers decays at 301 K and their chemical shift during the gelation process is almost the same, so it can be concluded that there is no influence of the stereochemistry when having cyclobutane as a ring. Thus, comparing the behaviors of all isomers of cyclohexane and cyclobutane derivatives it is worth to remark that having cyclohexane or cyclobutane as carbocycles yields gels with very different behaviors.

In addition, as mentioned before, these experiments were used in order to determine the gelation temperature for compounds *cis*-**190**, *cis*-**199**, *trans*-**190** and *trans*-**199.** The N*H* signal areas were used to follow the gelation process. When each of the N*H* signals was normalized to the highest integral obtained in the spectra series, a new graph was obtained where the normalized integral of the N*H* signal was related to the temperature at which the spectrum was recorded (Figure **40**).

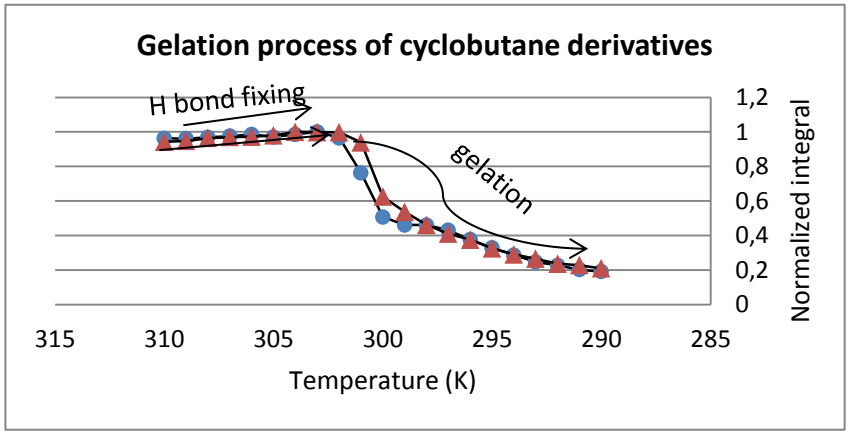

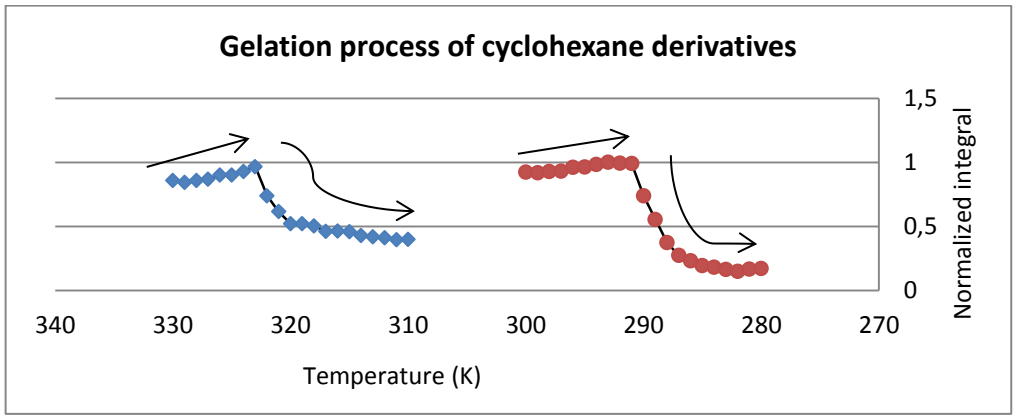

Figure 40. Graphical representation of the normalized NH proton integrals during the gelation process (***trans* in blue and *cis* in red**) for 17 mM solutions of *cis*-**190** and *trans*-**190** (up) and *cis*-**199** and *trans*-**199** (down) in toluene-d_8

The gelation temperature of a material is considered to be the temperature in which the gel is formed. Then, in Figure **40** it can be seen that the temperature of gelation for *cis*- and *trans*- cyclobutane derivatives is the same (T_{gel} : 301 K) whereas it is quite different for the cyclohexane derivatives, being T_{gel} : 291 K for *cis*-**199** and T_{gel} : 323 K for *trans*-**199**. These results suggest that gel formation for *trans*-**199** is more favoured than for *cis*-**199**.

It is important to highlight that the gelation point directly correlates with the chemical shift position of the N*H* signal just prior to gelation point. Thus, for example, at 17 mM for both *cis*/*trans* cyclobutanes derivatives the N*H* position is close to 6.0 ppm (Figure **40**) and both also exhibit the same gelation temperature: 301 K. Nevertheless, in cyclohexane derivatives, *cis* isomer has a lower gelation temperature of 291 K and exhibits a more deshielded N*H* chemical shift position of 6.4 ppm while *trans* isomer has a higher gelation temperature and exhibits a less deshielded NH chemical shift position of 5.8 ppm. This demonstrates that lower gelation point is due to a proper orientation of N*H* hydrogen bond which is directly related to chemical shift position.[106,107] An analogous behavior is observed at the different studied concentrations which are going to be shown along this chapter.

Furthermore, two clear processes can be observed from these graphs for the four stereoisomers. In the first process a continuous increase of the N*H* proton signal area was observed when cooling the sample. The increase in the signal area during the cooling process suggested that the hydrogen bonds were being fixed increasingly in a well-defined position.

On the other hand, as it can be observed, a second process takes place when cooling. Here an abrupt decay in the N*H* protons signal area was noticeable. At this point, having in mind that only the liquid-like part of the sample can be visualized by NMR spectroscopy, the process clearly indicated that the formation of the gel took place. Thus, intermolecular hydrogen-bonding forces became strong enough to create a gel network and the signals were attenuated because the number of molecules

[106] Berglund, B.; Vaughan, R. W. *J. Chem. Phys.* **1980**, *73*, 2037.
[107] Yao, L.; Grishaev, A.; Cornilescu, G.; Bax, A. *J. Am. Chem. Soc.* **2010**, *132*, 10866.

belonging to the rigid (solid-like) part of the gel increased and were not visible in the NMR spectrum.

The same studies were repeated for less concentrated solutions of the four compounds (4.25 mM and 8.5 mM) (Figure **41**). Thus, the temperature effects could be separated from the aggregation phenomena. As expected, the T_{gel} for all compounds was concentration-dependent, being the gel formation easier when increasing the concentration. In the Table **3** the T_{gel} for all the compounds at different concentrations are summarized.

Table 3. Concentration dependence of T_{gel} for *cis*-**190**, *trans*-**190**, *cis*-**199** and *trans*-**199** in toluene.

	Tgel (K)		
Compound	4,25 mM	8,5 mM	17 mM
cis-**190**	290	296	301
trans-**190**	289	296	301
cis-**199**	281	286	291
trans-**199**	312	318	323

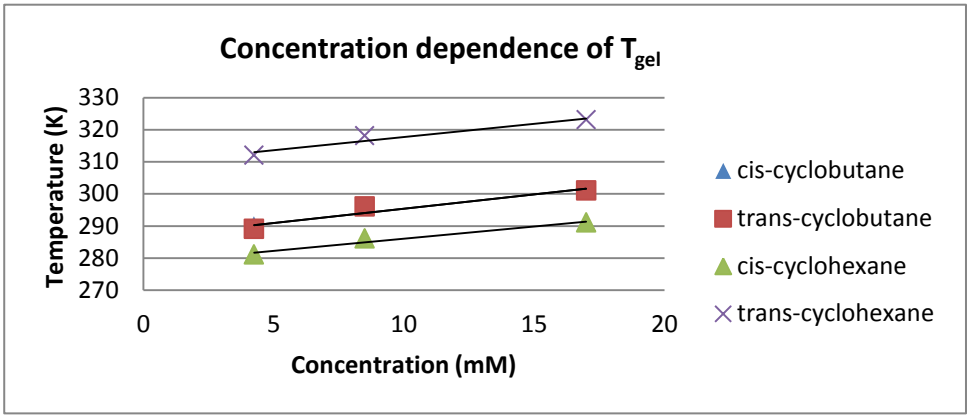

Figure 41. Representation of the concentration dependence of T_{gel} for all the compounds.

4.3.2.3 SEM (Scanning Electron Microscopy)

In collaboration with Dr. Judith Oró from the *Institut de Ciència de Materials de Barcelona* (ICMAB), SEM experiments were carried out to investigate the morphology of the gels obtained from solutions in toluene. Wet gels were disposed on a carbon-film-coated copper grid and dried by standing for 30 minutes on the grid. The resulting xerogels (dry gels) were then introduced into the microscope chamber working at 70 Pa and 5 kV (Figure **42**).

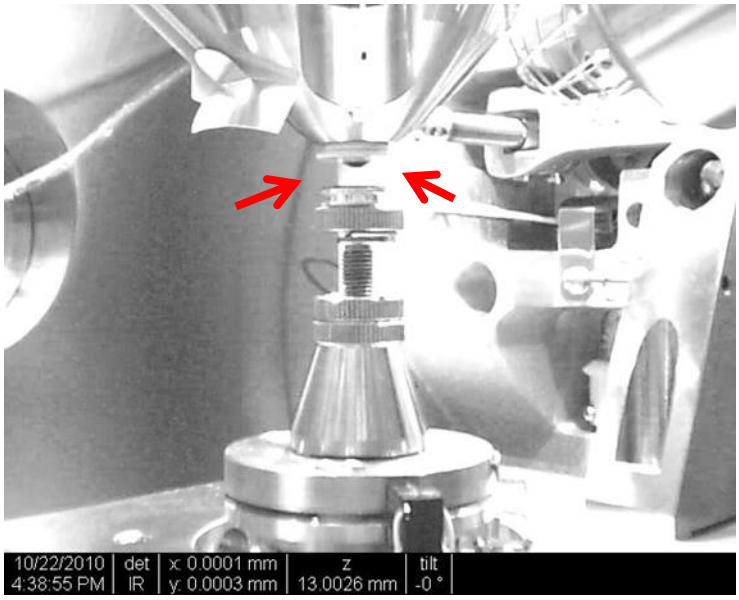

Figure 42. Microscope interior chamber where the samples, previously deposited on a circular support, are placed to be analyzed.

The micrographs were tested at the minimum gelation concentration (mgc) for each organogel. Thus, gel of *cis*-**190** at 57 mM, gel of *trans*-**190** at 25 mM, gel of *cis*-**199** at 55 mM and gel of *trans*-**199** at 2 mM were used to perform SEM experiments. The pictures obtained are shown in Figure **43**.

(a)

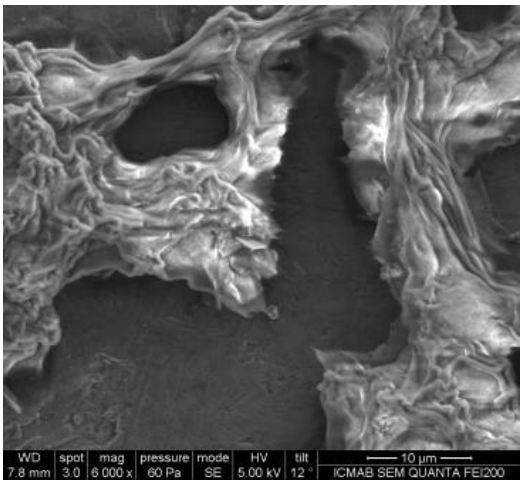
WD spot mag pressure mode HV tilt
7.8 mm 3.0 6 000 x 60 Pa SE 5.00 kV 12 °
10 µm
ICMAB SEM QUANTA FEI200

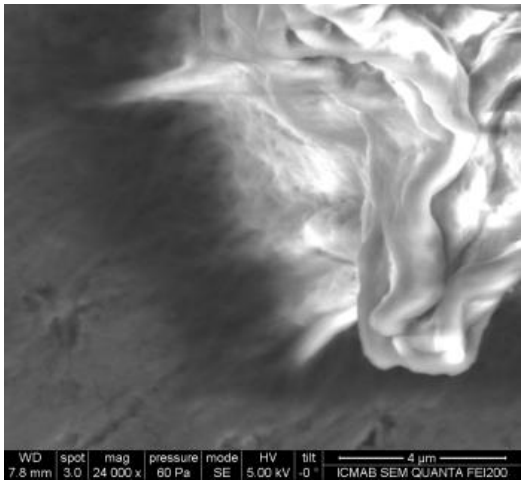
WD spot mag pressure mode HV tilt
7.8 mm 3.0 24 000 x 60 Pa SE 5.00 kV -0 °
4 µm
ICMAB SEM QUANTA FEI200

(b)

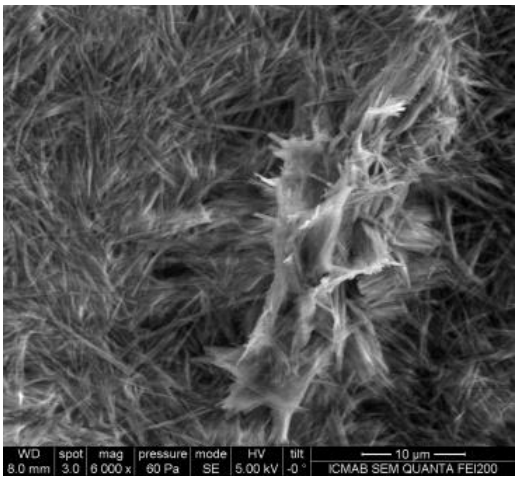
WD spot mag pressure mode HV tilt
8.0 mm 3.0 6 000 x 60 Pa SE 5.00 kV -0 °
10 µm
ICMAB SEM QUANTA FEI200

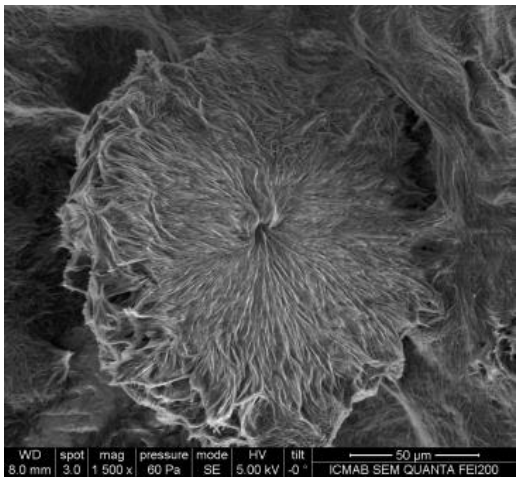
WD spot mag pressure mode HV tilt
8.0 mm 3.0 1 500 x 60 Pa SE 5.00 kV -0 °
50 µm
ICMAB SEM QUANTA FEI200

(c)

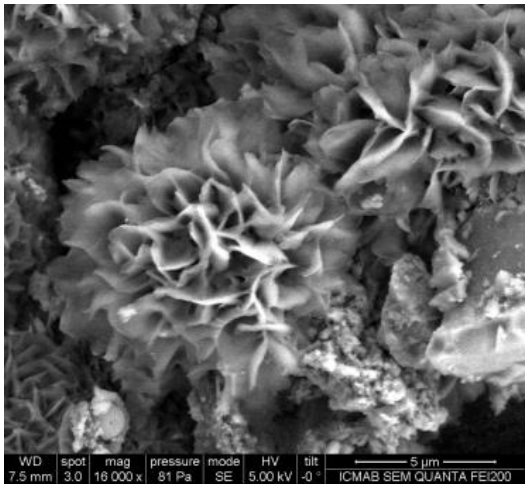
WD spot mag pressure mode HV tilt
7.5 mm 3.0 16 000 x 81 Pa SE 5.00 kV -0 °
5 µm
ICMAB SEM QUANTA FEI200

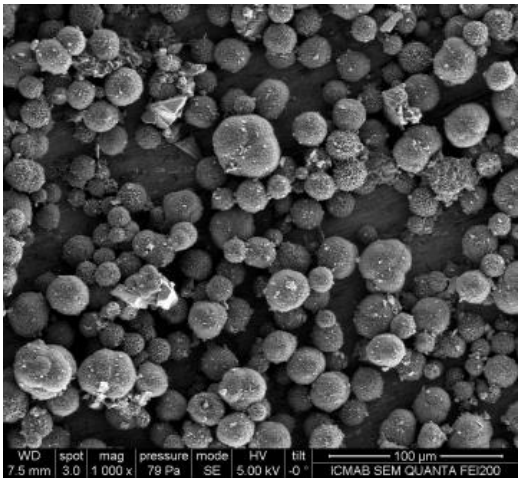
WD spot mag pressure mode HV tilt
7.5 mm 3.0 1 000 x 79 Pa SE 5.00 kV -0 °
100 µm
ICMAB SEM QUANTA FEI200

(d)

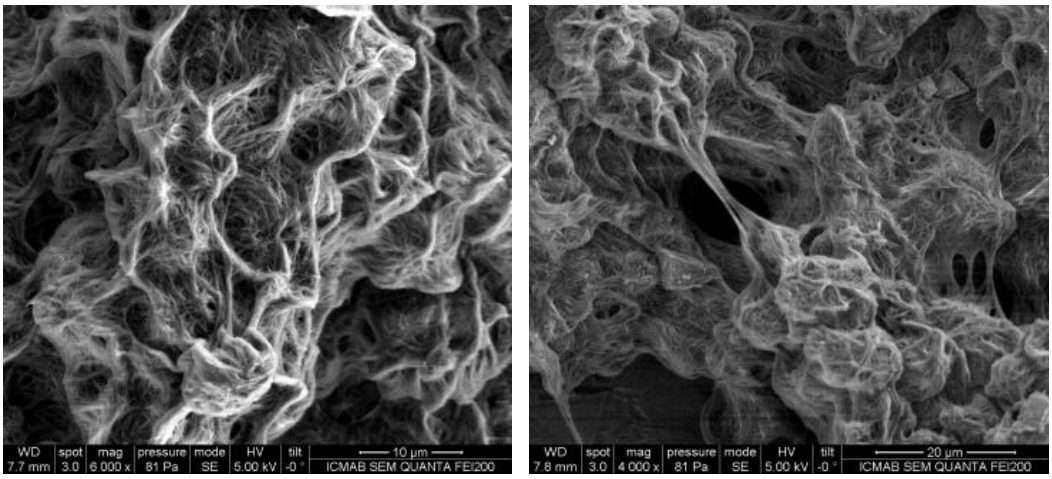

Figure 43. SEM images of the gels in toluene for compounds *trans*-**199** (a)*, cis*-**199** (b) at 60 Pa and *cis*-**190** (c), *trans*-**190** (d) at 81 Pa.

SEM micrographs recorded show the four compounds adopt different structures. For organogels based on cyclohexane, (Figure **43a** and **43b**) these topographic images show xerogel from *trans*-**199** to be composed of fibrillar networks, which consist of intertwined fibres and bundles of variable width. This causes the measured dimensions of these fibres to be highly variable (for example from 5 µm to 100 µm, approximately). In the case of the xerogel from *cis*-**199,** this micrographs are composed by small fibers of less than one micrometre of width and similar lengths around 5 µm. Moreover, these fibers show a facing-up growth and they are self-organized creating different substructures as the one shown in Figure **43b**.

Observing the images for the cyclobutane derivatives, Figure **43c** shows that xerogel from *cis*-**190** is self-organized in spheres of different sizes between 10 and 20 µm. On the other hand, there are big spheres composed by aggregates of two or three smaller spheres. At the same time, these spheres are nanostructured in to a rose-like shape. Finally, Figure **43d** shows the images of the xerogel from *trans*-**190**, again it is formed by disordered fibers from lengths of around 40 µm. Compound **190** gives wide and undefined structures although it is possible to appreciate, inside the material, very small fibres that are intertwined with each other.

In conclusion, it seems that the *cis*/*trans* stereochemistry of the compounds has a great influence in the organization of the structures by SEM. Otherwise, the influence of the number of carbon atoms and the rigidity of the ring (cyclobutane vs cyclohexane) has also importance in the structures formed.

On the other hand, SEM images of xerogel from *trans*-**201** in methanol were also recorded and they are shown in Figure **44**. As it can be observed in the pictures, ordered fibrillar networks were also observed, and similarly to those for the gel obtained from *trans*-**199**, these consisted of intertwined fibres and bundles of variable width in this case in the 1–3 µm range.

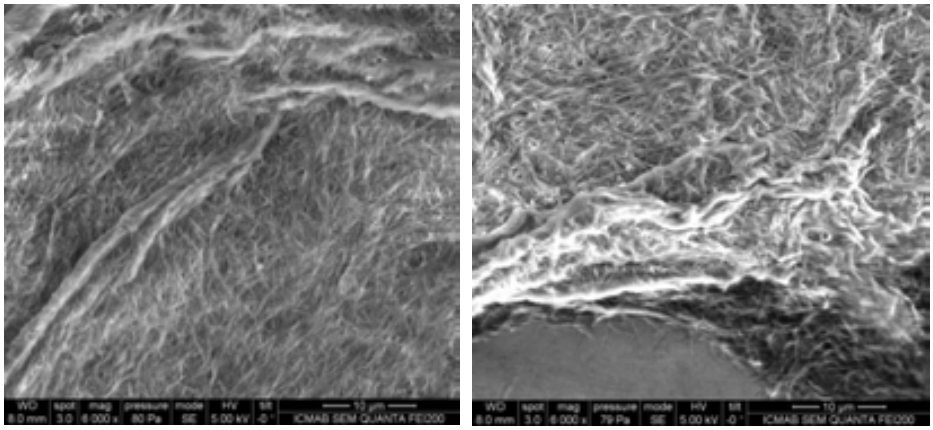

Figure 44. SEM micrographs of xerogel from *trans*-**201** in methanol.

4.3.2.4 IR Spectroscopy

The N-H and C=O regions of the vibrational spectra of *cis*-**190**, *trans*-**190**, *cis*-**199** and *trans*-**199** in the solid state were investigated by IR spectroscopy, as well as the corresponding bands for the xerogels from toluene (in the mgc in KBr). Such data was also recorded in solution (10 mM in toluene). No significant differences were observed between the spectra of all the xerogels.

The N-H and C=O stretching bands were shifted to lower wavenumbers and their intensity was increased slightly when passing from solution to the solid state, in accordance with the formation of aggregates.[108] Results are summarized in Table **4**.

Table 4. N-H and C=O bands in the IR spectra of *cis*-**190**, *trans*-**190**, *cis*-**199** and *trans*-**199** in solution, as xerogels from toluene and as solids.

Compound	NH[a]			CO[a]		
	Solid[b]	Xerogel[c]	Solution[d]	Solid[b]	Xerogel[c]	Solution[d]
cis -**190**	3340 3300	3342 3305	3380	1643	1642	1690
trans -**190**	3272	3283	3287	1644	1642	1700
cis -**199**	3370 3282	3291	3297	1648	1648	1680
trans -**199**	3290	3288	3300	1626	1629	1670

[a] In cm^{-1}.
[b] ATR.
[c] Xerogel from toluene gel at mgc in KBr.
[d] 10 mM solution in $CDCl_3$.

[108] Meersman, F.; Smeller, L.; Heremans, K *Biophys. J.* **2002**, *82*, 2635.

4.4 SUMMARY AND CONCLUSIONS

i) The capacity of *cis*-**190** and *trans*-**190** prepared in this Thesis to gelate different solvents was evaluated in order to see the influence of their stereochemistry in their behavior. Both compounds formed nice gels in toluene being the value of the minimum gelation concentration 57 mM for the *cis*- diastereomer and 25 mM for the *trans*- diastereomer. They were stable at room temperature and thermoreversible. Their gelation process was monitored by variable-temperature ^{1}H NMR spectroscopy experiments and almost no difference between their behavior was experimented so there was no influence of the stereochemistry between these two compounds based on cyclobutane.

ii) Moreover, they were compared with their cyclohexane analogues: *cis*-**199** and *trans*-**199,** which were afforded by Professor J. C. Estévez from the *Universidad of Santiago de Compostela*. As in the case of cyclobutane derivatives, they also formed accurated gels in toluene but also with 1,4-dioxane. Their gelation process was also investigated by NMR experiments and the difference between the chemical shifts of the different diastereomers showed a better ability of the *trans*- diastereomer to form gels due to the good disposition of the alkyl chains to be ordered. Thus, when having compounds with cyclohexane ring, there is an influence of the stereochemistry in the gel formation.

iii) SEM micrographs of all the gels were recorded, showing different morphology adopted by different compounds and corroborating that there is an influence in the organisation of the material when having cyclohexane or cyclobutane ring.

Some of the most relevant differences between all of them are summarized in Table **5**.

Table 5. Relevant differences between **190** and **199**

Compound	Ring	Stable gels	δ_{NH} (ppm)	Tgel in toluene at 17 mM (K)[a]
cis-**190**	C4	toluene	6,0	301
trans-**190**	C4	toluene	6,0	301
cis-**199**	C6	toluene, dioxane	6,3	291
trans-**199**	C6	toluene, dioxane	5,8	323

iv) Finally, two more compounds were studied as organogels: *cis*-**200** and *trans*-**201**, which were based on the *trans*-1,2-disubstituted cyclohexane moiety but also with other substitutents on the ring, a ketal in positions 3 and 4 and a hydroxyl group protected with a TBDMS in position 5 in the case of *cis*-**200** and a hydroxyl group in the case of *trans*-**201**. They also formed gels in toluene and in addition, *trans*-**201** formed one nice gel in methanol at mgc of 7 mM.

CHAPTER V

Physicochemical behavior of novel bolaamphiphiles

5.1 INTRODUCTION

5.1.1 Surfactants: definition, classification and some properties

The compounds called amphiphiles are all of those which possess both hydrophilic and lipophilic properties. Common amphiphiles are surfactants, such as detergents, soaps and fatty acids, or diglycerides, such as phospholipids, the latter being the main components of biomembranes.[109]

The term surfactant refers to "surface acting agent," alluding to the fact that they are amphiphilic molecules that exhibit interfacial activity usually consisting in their ability to lower the surface tension of a liquid or the interfacial tension between two liquids of different polarity due to their property of accumulating at the interface. Most familiar of all surfactants is soap, a simple substance which, in water, clearly demonstrates two effects. It produces foam due to its action at the air-water interface, and it makes the grease transfer from grubby hands into the soapy water as a result of its activity at the water-oil (grease) interface.[110]

However, soap was probably not the first surfactant in the service of humankind since due to their characteristics they are widely used as paints and coatings, textils, construction, food, leather, plastic additives, explosives, pulp and paper and others.[111] It is worth remarking that not all amphiphiles are surface active molecules but more importantly, they create surfaces.[112] In fact, only the amphiphiles with more or less equilibrated hydrophilic and lipophilic tendencies are likely to migrate to the surface or interface. Amphiphiles[110] are usually classified according to different criteria, including the charge of the head group upon its dissociation in water (often used for surfactants), the number and kind of connection of polar

[109] Schramm, L.L. *Surfactants: Fundamentals and Applications in the Petroleum*, Cambridge University Press, Cambridge, **2000**.
[110] L. L. Schramm, *Dictionary of Colloid and Interface Science*, Wiley, New York, **2001**.
[111] Karsa, D. R. *Industrial applications of surfactants IV*. Cambridge: RSC, **1999**.
[112] Fuhrhop, J.H.; Köning, J *Membranes and Molecular Assemblies: the Synkinetic Approach*, Cambridge: RSC, **1994**.

head(s)/hydrophobic tail(s) and the chemical nature of the polar head. Regarding the head group charge, surfactants are classified in[113]:

- ✓ Ionic (cationic or anionic): Anionic surfactants (Figure **45a**), which include soap, are the most widely used for cleaning processes because many of them are excellent detergents. In anionic surfactants the hydrophile comprises some highly electronegative atoms, making these molecules strongly polar. The counterion is usually a small cation such as sodium but occasionally may be a larger cation such as ammonia or quaternary amines. In contrast, cationic surfactants comprise a hydrocarbon long chain as the lipophilic part with a quaternary ammonium group as hydrophile, and a halide ion as counterion (Figure **45b**).

(a) **(b)**

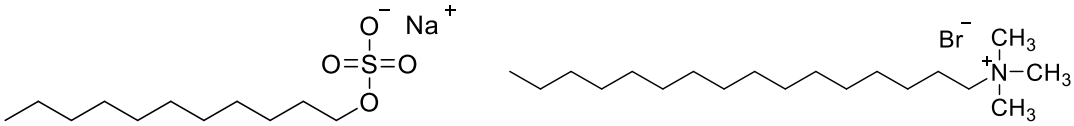

Figure 45. (a) Sodium dodecyl sulfate. (b) cetyltrimethylammonium bromide, hexadecyltrimethylammonium bromide, CTAB.

- ✓ Non-ionic: They do not ionize in aqueous solution because their hydrophilic group can not dissociate. Thus, they not depend on the pH. See for instance octyl glucoside (Figure **46**), which is a detergent frequently used to solubilize integral membrane proteins for studies in biochemistry.

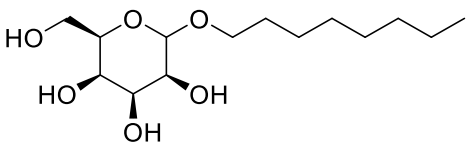

Figure 46. Octyl glucoside.

- ✓ Zwitterionic (whose charge changes depending on pH): Amphoteric surfactants comprize a long hydrocarbon chain (lipophilic) attached to a

[113] Moroi, Y. *Micelles, Theoretical and Applied Aspects,* Ed. Springer **1992**.

hydrophile containing both positive and negative charges, which give it the properties of a zwitterion. Mild and with low irritancy, amphoters are widely used in shampoos (Figure **47**).

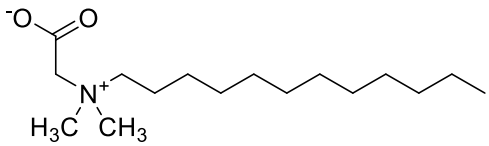

Figure 47. Lauryl betaine

If the classification is based on the number and kind of connection of polar head(s)/hydrophobic tail(s) amphiphiles are classified as (Figure **48**):

- ✓ Conventional single head/single tail amphiphiles.
- ✓ Bolaamphiphiles, which contain two hydrophilic heads connected by a hydrophobic skeleton (e.g. one or two alkyl chains). The present chapter is based on the study and characterization of bolaamphiphiles which are going to be discussed in detail along this introduction.
- ✓ Gemini or ''dimeric'' surfactants made up of two hydrocarbon tails and two ionic groups linked by a spacer.
- ✓ Double and triple chain amphiphiles.
- ✓ Catanionic surfactants are an equimolar mixture of two oppositely charged surfactants (the parent surfactants). Thus, it is uncharged, and one long alkyl chain organic ion acts as a counterion of the other.

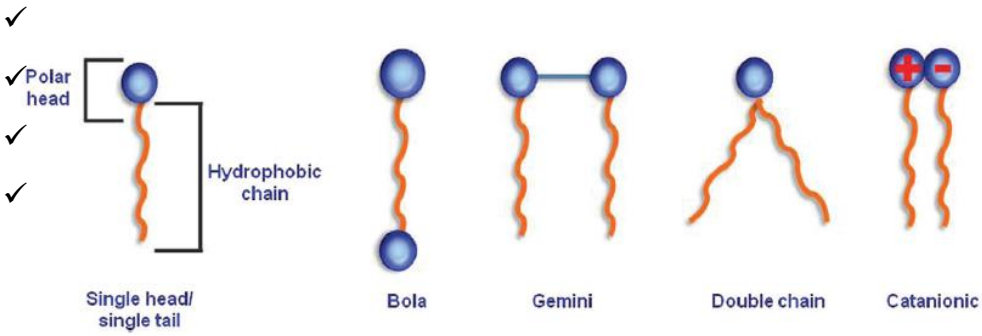

Figure 48. Amphiphile classification.

The proportion of molecules present at the surface or as micelles in the bulk of the liquid depends on the concentration of the amphiphile. At low concentrations, surfactants will favour arrangement on the surface. As the surface becomes crowded with surfactant, more molecules will arrange into micelles. At some concentration the surface becomes completely loaded with surfactant and any further additions must arrange as micelles (Figure **49**). This concentration is called the critical micelle concentration (CMC). To determine the CMC, a property which presents a change in front of the concentration of the surfactant can be used. Some of these properties are surface tension, conductivity and optic and spectroscopic properties such as light scattering or refractive index.[114] In **Figure 49** three phases can be seen: First of all, at very low concentrations of surfactant only slight change in surface tension is detected. Then, additional amount of surfactant decreases surface tension. Finally, at high concentrations, surface becomes fully loaded with no further change in surface tension.[115]

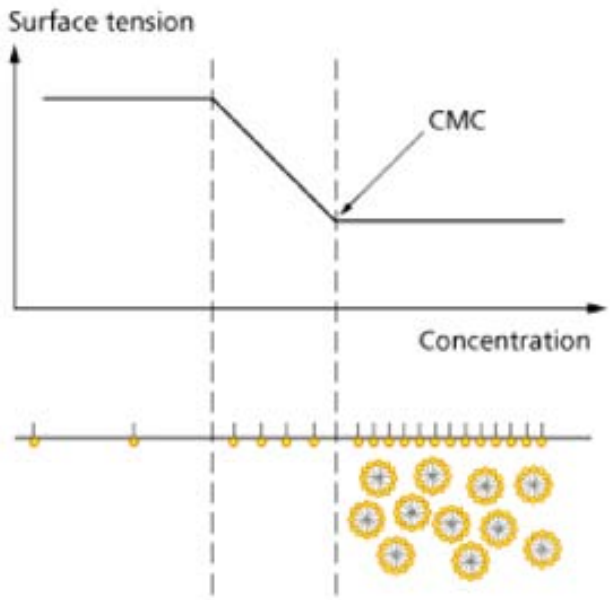

Figure 49. Schematic representation of the organisation of surfactant molecules around the critic micellar concentration (CMC).[116]

[114] Tadros, T.F. *Applied Surfactants: Principles and Applications*, Wiley, New York, **2005**.
[115] Jiménez, D.; Medina, S A.; Gracida, J.N. *Rev. Int. Contam. Ambient.* **2010**, *26*, 65.
[116] Laden, P. *Chemistry and technology of water-based inks*, Chapman and Hall, New York, **1997**.

5.1.2 Self-assembly of surfactants

Amphiphilic surfactants and polymers display characteristic molecular self-assembly behavior in solutions, at interfaces and in bulk, generating nanoscale structures of different shapes. These nanoscale features determine many characteristics of these amphiphiles, relevant for their practical applications in materials, pharmaceutical and biomedical technologies. The ability to generate desired nanoscale morphologies by synthesizing novel amphiphiles would allow the amphiphilic systems to be tailored for specific applications. Critical to achieving this goal is an understanding of the link between the molecular structure of the amphiphiles and their self-assembly behavior.[117]

The self-assembly of surfactants in solution has been widely investigated both experimentally and theoretically, because numerous practical applications take advantage of the resulting molecular aggregates. The structure of these aggregates influences the properties of surfactant solutions, such as for example, their solubilization capacity for hydrophobic substances or their viscous and viscoelastic properties, and consequently, the performance as surfactants in various applications. To select molecules that would yield desired structures such as spherical, globular, spherical bilayer vesicles (Figure **50**), or to custom-design novel amphiphiles to generate desired aggregate morphologies, it is necessary to know how the molecular structure of the surfactant controls the shape and size of the resulting aggregate.

As proposed by Tanford,[118] two opposing forces are responsible for the formation of such assemblies. The hydrophobic effect drives the segregation of the hydrocarbon chains in water, thus providing the impetus for self-organization. On the other hand, repulsive forces (electrostatic and/or hydration) and steric effects between the polar heads prevent the formation of large three-dimensional crystals and hence phase separation.[119] The self-aggregation of amphiphilic molecules has long

[117] Nagarajan, R. Amphiphiles: Molecular Assembly and Applications, ACS Symposium Series; American Chemical Society: Washington , **2011**.
[118] Tanford, C. The Hydrophobic Effect: Formation of Micelles and Biological Membranes, John Wiley & Sons Inc., New York, **1973**.
[119] Fuhrhop, J.H.; Helfrich, W. *Chem. Rev.* **1993**, *93*, 1565.

been known to yield a rich variety of assemblies, depending on the molecular structure of the amphiphile (interplay between the hydrophilic–hydrophobic balance and geometric packing constraints) and on experimental conditions, such as concentration, temperature, pH and ionic strength.[120] Among the most common self-assemblies, of colloid dimensions, formed in water by amphiphilic molecules are micelles and vesicles (Figure **50**).

Other parameters are also important: the structural features of the amphiphiles such as the length of the hydrophobic chain,[121] even-odd carbon number,[122] nature of the counter-ion,[123] chiral centers, spatial geometry of the molecule and also media conditions such as pH,[124] ionic strength and temperature.[125] Molecular aggregates have been studied with the dual objectives of preparing "designer assemblies" and with the aim of developing potential biological applications.

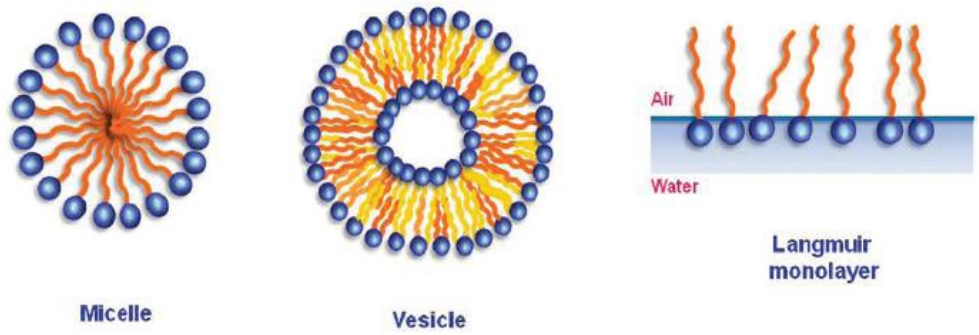

Figure 50. Schematic representation of surfactant aggregates in aqueous solutions.

Micelles are small assemblies of 50–100 unimers that feature an external polar surface made of the hydrophilic head groups and a more or less disordered hydrophobic core formed by the amphiphile tails, usually regarded as a small volume of liquid hydrocarbon. They are thermodynamic equilibrium systems with a loose dynamic structure in which the unimers exchange rapidly with the bulk solution.

[120] Israelachvili, J. N. *Intermolecular and Surface Forces* Academic Press, New York, **1985**.
[121] Brisset, F.; Garelli-Calvet, R.; Azéma, J.; Chebli, C.; Moisand, A.; Rico-Lattes, I. *New J. Chem.* **1996**, *20*, 595.
[122] Shimizu, T.; Masuda, M. *J. Am. Chem. Soc.* **1997**, *119*, 2812.
[123] Fuhrhop, J. H.; Fritsch, C.; Tesche, B.; Schmiady, H. *J. Am. Chem. Soc.* **1984**, *106*, 1998.
[124] Hafkamp, R. J. H.; Feiters, M. C.; Nolte, J. M. *J. Org. Chem.* **1999**, *64*, 412.
[125] Nakashima, N.; Asakuma, S.; Kim, J. M.; Kunitake, T. *Chem. Lett.* **1984**, 1709.

Typically, micelles are formed spontaneously and reversibly by single head/single tail surfactants (with the head substantially bigger that the tail) above CMC, and at temperatures above the Krafft temperature (i.e. the minimum temperature at which aggregation occurs). Most commonly, micelles have spherical shapes, but depending on surfactant geometry, concentration and other experimental variables, they can be ellipsoids or long cylinders (rod-like).[126] Vesicles are spherical or ellipsoidal closed amphiphile bilayer structures with an internal cavity containing the aqueous solution in which they are dispersed. Typical vesicles are formed by natural phospholipids, and in such cases they are referred to as liposomes. However, vesicles are also formed by many synthetic amphiphiles and surfactants able to form bilayers.

The hydrophobic effect is very important in the micelle formation since in aqueous solution dilute concentrations of surfactant act much as normal electrolytes, but at higher concentrations very different behavior results. This behavior is explained in terms of the formation of organized aggregates of large numbers of molecules (micelles), in which the lipophilic parts of the surfactants associate in the interior of the aggregate leaving hydrophilic parts to face the aqueous medium. The formation of micelles in aqueous solution is generally viewed as a compromize between the tendency for alkyl chains to avoid energetically unfavourable contacts with water, and the desire for the polar parts to maintain contact with the aqueous environment.[127]

5.1.3 Bolaamphiphiles

Bolaamphiphiles or bolaform amphiphiles[128,129] consist of two hydrophilic head groups connected by a hydrophobic core and they can be assumed as model compounds for bolalipids from archaebacterial membranes.[130] The terms “bolaform amphiphiles” or “bolaphiles” have also been used but do not make much sense. “Form” does not appear elsewhere in organic nomenclature, and a connection with

[126] Israelachvili, J. N. *Intermolecular and Surface Forces*, Academic Press, New York, **1985**.
[127] Hiemenz, P. C.; Rajagopalan, R. *Principles of Colloid and Surface Chemistry*, Dekker, New York, **1997**.
[128] Escamilla, G. H.; Newkome, G. R. *Angew. Chem., Int. Ed. Engl*. **1994**, *33*, 1937.
[129] Zahna, R. *In Specialist Surfactants*; Robb, I. D., Ed.; *Chapman & Hall*: Glasgow, **1996**.
[130] Danson, M. J.; Hough, D. W.; Lunt, G. G. *The Archaebacteria: Biochemistry and Biotechnology;* Portland Press: London, **1992**.

"phile=friendly" makes sense with respect to a solvent ("amphiphile") or reaction center ("nucleophile") but not in connection with a noun describing a substitution pattern (Figure **51**).

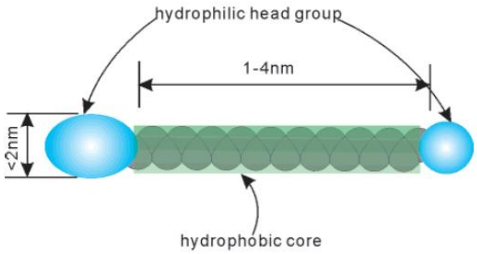

Figure 51. Schematic drawings of a bolaamphiphile. Green colouring indicates hydrophobic parts; blue means hydrophilic.

The aggregation morphologies of bolaamphiphiles are as variable as their molecular structures.[131] These amphiphiles give rise to aggregates such as micelles and multi-layered sheets, vesicles, rings, and a variety of microstructures with cylindrical geometry such as rods, tubules, ribbons, and helices.[132]

Sirieix and co-workers prepared and examined the properties and the self-assembly of symmetrical bolaamphiphiles derived from (*E*)-urocanic acid (3-[1H-imidazolyl-(4)-yl]-propenoic acid) (Figure **52**).[133]

In their study, they showed that the morphologies of the aggregates formed were strongly dependent on three parameters: pH, structure and position of the connecting links obtaining vesicles, spherical or multi-layered aggregates and the formation of fibers due to hydrogen bond interactions.

[131] Shimizu, T. *Macromol. Rapid Commun.* **2002**, *23*, 311.
[132] Nakazawa, I.; Masuda, M.; Okada, Y.; Hanada, T.; Yase, K.; Asai, M.; Shimizu, T. *Langmuir* **1999**, *15*, 4757.
[133] Sirieix, J.; Lauth-de Viguerie, N.; Riviere, M.; Lattes, A. *Langmuir* **2000**, *16*, 9221.

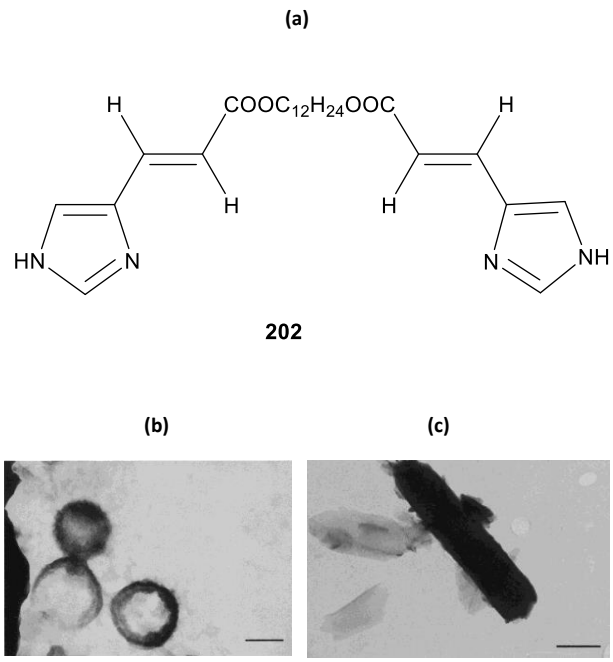

Figure 52. (a) Structure of one of the bolaamphiphiles studied by Sirieix and co-workers **(b)** TEM micrographs of spheres formed from bolaamphiphile **202** in aqueous medium at pH 3. **(c)** Multilayered sheet aggregates formed from bolaamphiphile **202** in aqueous medium at pH 6.5.

On the other hand, Fuhrhop and co-workers synthesized unsymmetric bolaamphiphiles with one amino acid head group (D and L-lysine) and one ammonium head group. Electron micrographs of aqueous gels showed micellar rods (Figure **63a**) and, more interesting, vesicular tubules with a membrane of monomolecular thickness (Figure **53b**).[134]

[134] Fuhrhop, J.-H.; Spiroski, D.; Boettchert, C. *J. Am. Chem. Soc.* **1993**, *115*, 1600.

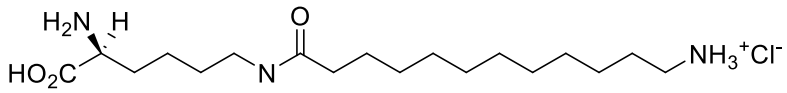

203

(a) **(b)**

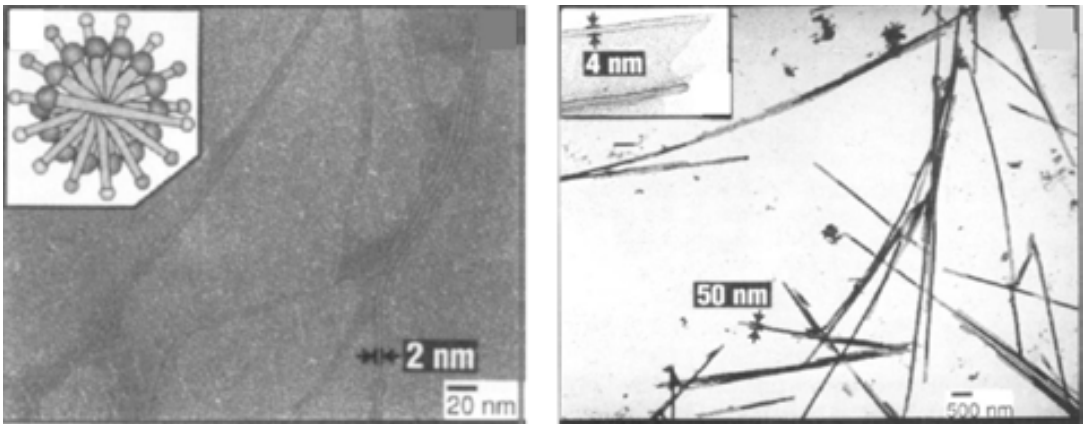

Figure 53. (a) TEM micrographs of molecular monolayers rods made of bolaamphiphile **203** of reference 134 **(b)** TEM micrographs of molecular monolayer tubular made of bolaamphiphile **203** of reference 134.

Kobayashi and co-workers designed bolaamphiphilic gelators based on azobenzene chromophore and they found that they could control their self-assembly reversibly using the spectroscopic properties of the molecule, from fibers to vesicles.[135] The results indicated that the bolaamphiphiles act, although only for specific DMSO–water mixtures, as gelators and form a unique supramolecular helical structure in the gel phase.

The UV-Vis and CD spectra showed that the azobenzene segments adopt H-type face-to-face orientation and the dipole moments are arranged in the right-handed (*R*)-helicity. When boronic acid-appended poly(L-lysine) was added, the gel phase was changed into the sol phase in the macroscopic level and the fibrous aggregate was changed into the vesicular aggregate in the microscopic level (Figure **54**).

[135] Kobayashi, H.; Koumoto, K.; Hwa Junga, J.; Shinkai, S. *J. Chem. Soc., Perkin Trans. 2* **2002**, 1930.

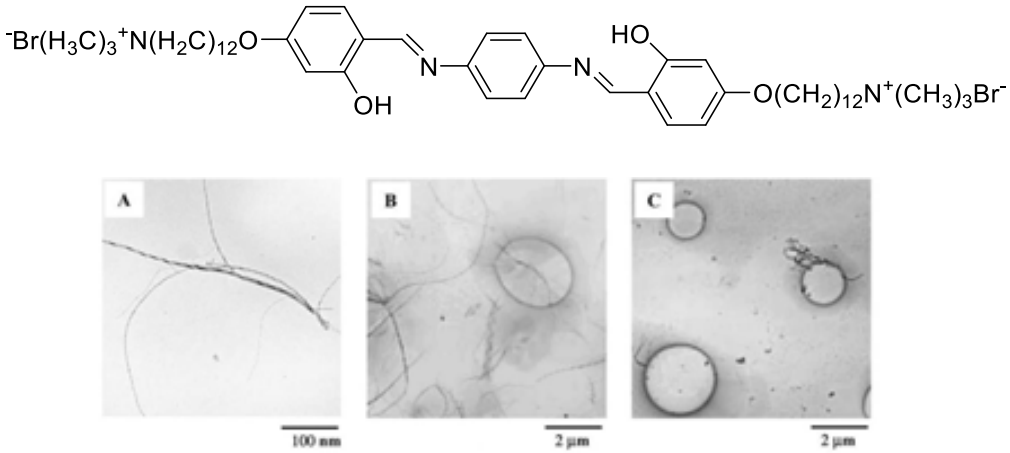

Figure 54. TEM micrographs of bolaamphiphiles from reference 135.

Some chiral bolaamphiphiles derived from biomolecules even form chiral superstructures such as helices. For instance, the group of Shimizu and co-workers[136] observed in their work the spontaneous formation of helically twisted fibers from 2-glucosamide bolaamphiphiles as it is shown in Figure **55**.

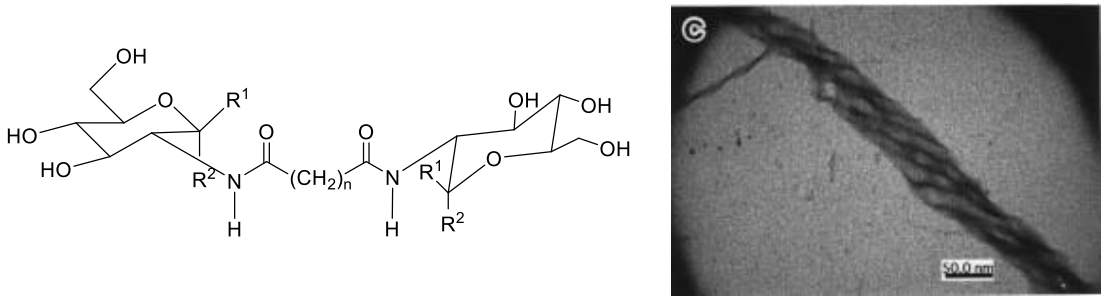

204

Figure 55. Helically twisted fibers formed by **204** observed using TEM in the group of Shimizu et al.[136]

[136] Nakazawa, I.; Masuda, M.; Okada, Y.; Hanada, T.; Yase, K.; Asai, M.; Shimizu, T. *Langmuir* **1999**, *15*, 4757.

5.1.3.1 Applications of bolaamphiphiles

In 2009, Sanders and co-workers[137] tested bolaamphiphile-class surfactants for their ability to stabilize a solubilized membrane protein, Escherichia coli diacylglycerol kinase (DAGK) and to sustain its native function. They obtained satisfactory results and moreover, certain bolaamphiphiles were shown to be lipid-like by providing partial activation of DAGK's catalytic activity. This work represented the first documentation of the potential of bolaamphiphile-class surfactants for use in biochemical and biophysical studies of MPs.[138]

On the other hand, due to their ability to form self-organized aggregate structures, amphiphiles have been used as templates in the synthesis of nano- and mesostructured materials. One of the most important cases is where amphiphile aggregates and silica units interact in a non-covalent way, which makes the silica to organize around the structure directing agent, in this case the supramolecular aggregate. The silica units then react with each other to generate mesostructured materials. Afterwards, the amphiphile is removed by calcination, which leaves a mesoporous material (Figure **56**).[73,139]

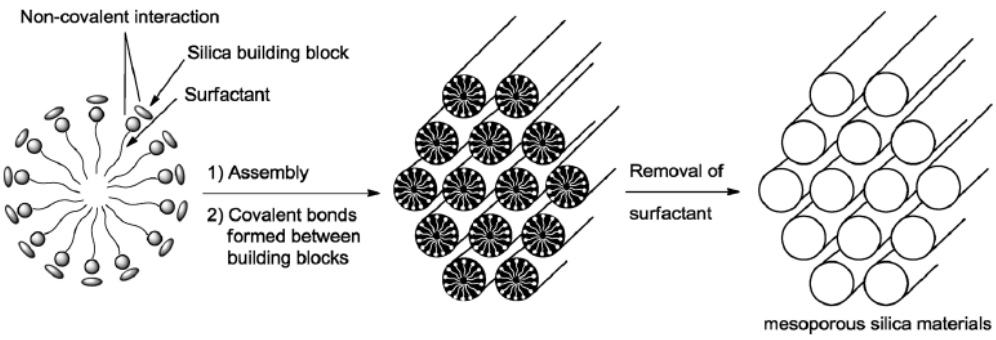

Figure 56. Surfactant-directed formation of mesoporous materials.[73]

[137] Li, Q.; Mittal, R.; Huang, L.; Travis, B.; Sanders, C. R. *Biochemistry* **2009**, *48*, 11606.
[138] De, R. M.; Gambacorta, A. *Prog. Lipid Res.* **1988**, *27*, 153.
[139] Petkovic, N. D.; Stein, A.*Chem. Soc. Rev.* **2013**, *42*, 3721.

Aggregates of synthetic surfactants are also used as soft drug delivery systems and nanostructured lipid carriers.[140] At the end of the 1960s, micelles attracted growing interest for application in drug vectorization. The anisotropic water molecule distribution in the structure of these objects allows the solubilisation of hydrophobic active principles in the micelles and enhances their bioavailability. In addition, active molecules are protected from enzymes that could degrade them and lead to their metabolism in biological media. The major drawback of micellar surfactant vectors is their tendency to break up upon dilution.[141] Vesicles enable the encapsulation of larger amounts of drugs than matrix systems, which means that much smaller amounts of vectors can be administered. Most of these systems have versatile transport properties, and they can vectorize hydrophilic and lipophilic substances.

For example, the group of Heldman and co-workers described the synthesis of bolaamphiphiles of Figure **57** and the characterization of their nanosized vesicles formed from them with potential application for targeted drug delivery in to the brain. The starting material for the synthesis is vernonia oil, which is a naturally epoxidized triacylglycerol obtained from the seeds of Vernonia galamensis.[142] The targeting mechanism is based on the hydrolysis of the amphiphile headgroup by an enzyme abundant in the target tissue, with subsequent release of the encapsulated drug at the target site.[143]

[140] Malmsten, M. *Soft Matter* **2006**, *2*, 760.
[141] Soussan, E.; Cassel, S.; Blanzat M.; Rico-Lattes, I. *Angew. Chem. Int. Ed*. **2009**, *48*, 274.
[142] Gundstone, F.D.; *J. Am. Chem. Soc.* **1954**, 1611.
[143] Grinberg, S.; Kipnis, N.; Linder, C.; Kolot, V.; Heldman, E. *Eur. J. Lipid Sci.Technol* **2010**, *112*, 137.

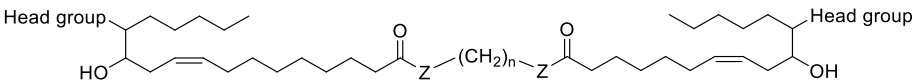

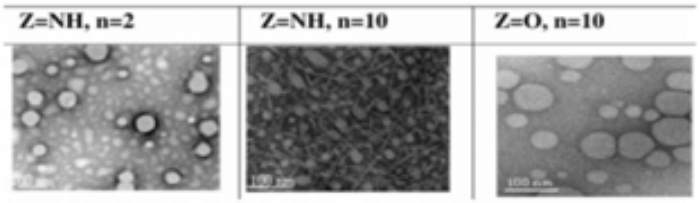

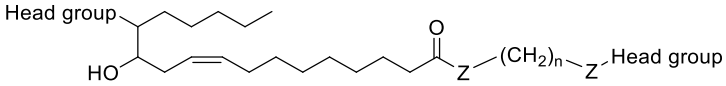

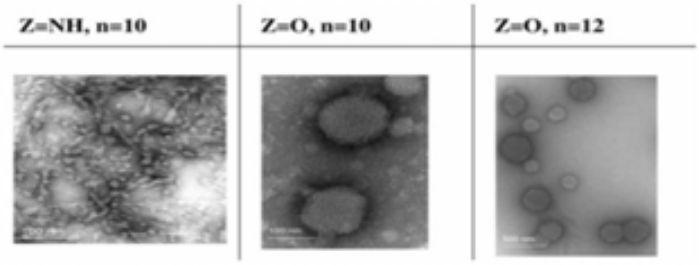

Figure 57. Electron micrographs of aggregated structures of symmetric and asymmetric bolaamphiphiles according to reference 143.

Bolaamphiphiles have also found application in the formation of gold nanoparticles (NPSs).[144] They induce the ordering of these nanoparticles with the presence of bolaamphiphilic moieties in the coating of the nanoparticles (NPSs). The authors introduced and proved experimentally an explanation of how the structures were formed. The model involved elements of geometric packing and ligand reorganization. Upon contact with the hydrophilic surface, ligands rearranged at the surface of the metallic cores of the Bola-AuNPSs so that the bolaamphiphilic moieties (constituting ca. 50% of the coating) were in proximity to the surface, while the hexanethiol moieties moved away from it. The described mechanism is of general relevance for the design of functional NPSs capable of self-assembly (Figure **58**).

[144] Paczesny, J.; Wójcik, M.; Sozanski, K.; Nikiforov, K.; Tschierske, C.; Lehmann, A.; Górecka, E.; Mieczkowski, J.; Hołys, R. *J. Phys. Chem. C* **2013**, *117*, 24056.

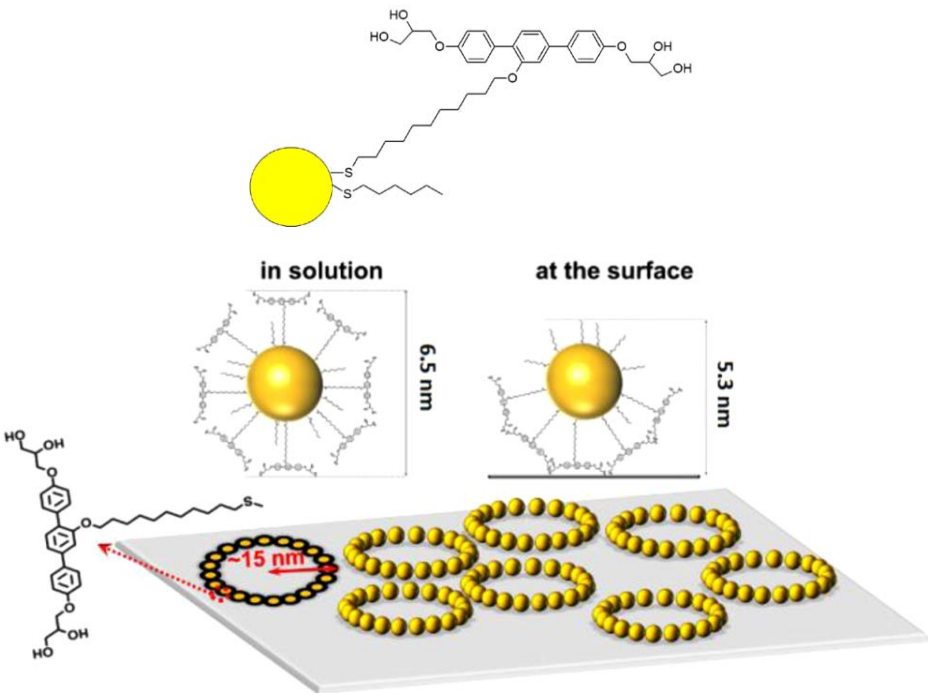

Figure 58. Schematic representation of the mechanism of action of the self-assembly of Bolaamphiphiles-AuNPSs.

Another application is found when spherical monolayer membranes convert to linear or helical fibers, e.g., long rods or tubules, when rigid segments establish an ordered packing or hydrogen bond chains are formed between the headgroups or amide bonds in the hydrophobic core. The most simple case is given by (16-carboxyhexadecyl)trimethylammonium bromide, which forms ribbons of irregular curvature at pH 6.8 with between 3-4 nm thickness corresponding roughly to the length of one molecule. Carboxylcarboxylate hydrogen binding and a charge interaction leading to a U-conformation were made responsible for fiber formation (Figure **59**).[145]

[145] Jaeger, D. A.; Li, G.; Subotkowski, W.; Carron, K. T.; Bench, M.W. *Langmuir* **1997**, *13*, 5563.

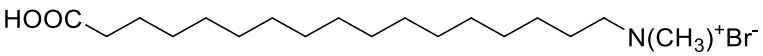

205

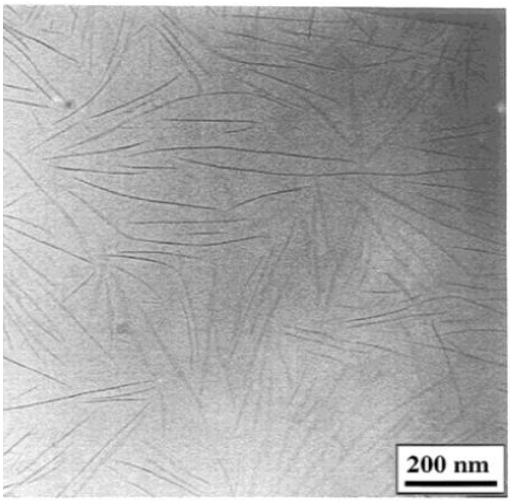

Figure 59. Cryo-TEM of the given α-ammonium-ω-carboxy bolaamphiphile **205**.[46]

5.2 OBJECTIVES.

In this part of the Thesis, the stereoselective synthesis of new chiral bolaamphiphiles derived from cyclobutane-1,2-diamine and cyclobutane-1,2-dicarboxylic acid was carried out (Figure **60**). The main objective was to explore their behavior and properties as surfactants. Special attention was focused on the study of the influence of the relative stereochemistry and the regiochemistry on their aggregation properties.

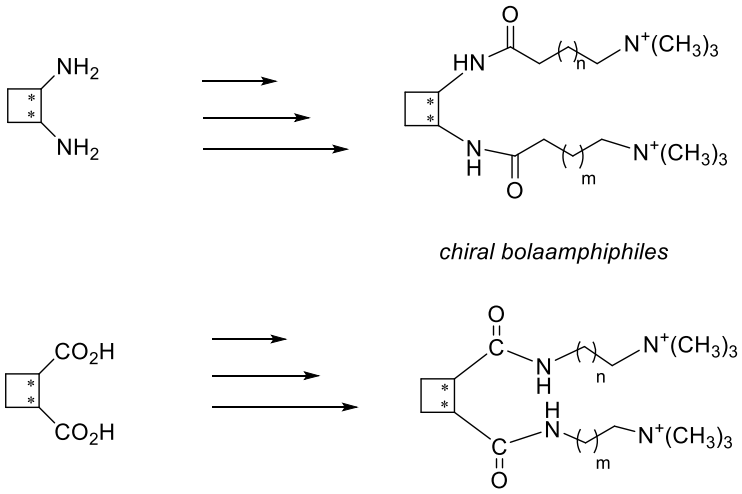

Figure 60. Bolaamphiphiles in this Thesis based on cyclobutane-1,2-dicarboxylic acid and cyclobutane-1,2-diamine to be studied as surfactants.

5.3 RESULTS AND DISCUSSION.

In this chapter, the differences between bolaamphiphiles *cis*-**177**, *trans*-**177**, *cis*-**187**, and *trans*-**187** (Figure **61**) will be discussed. The influence of the relative stereochemistry and the regiochemistry on their aggregation properties was studied.

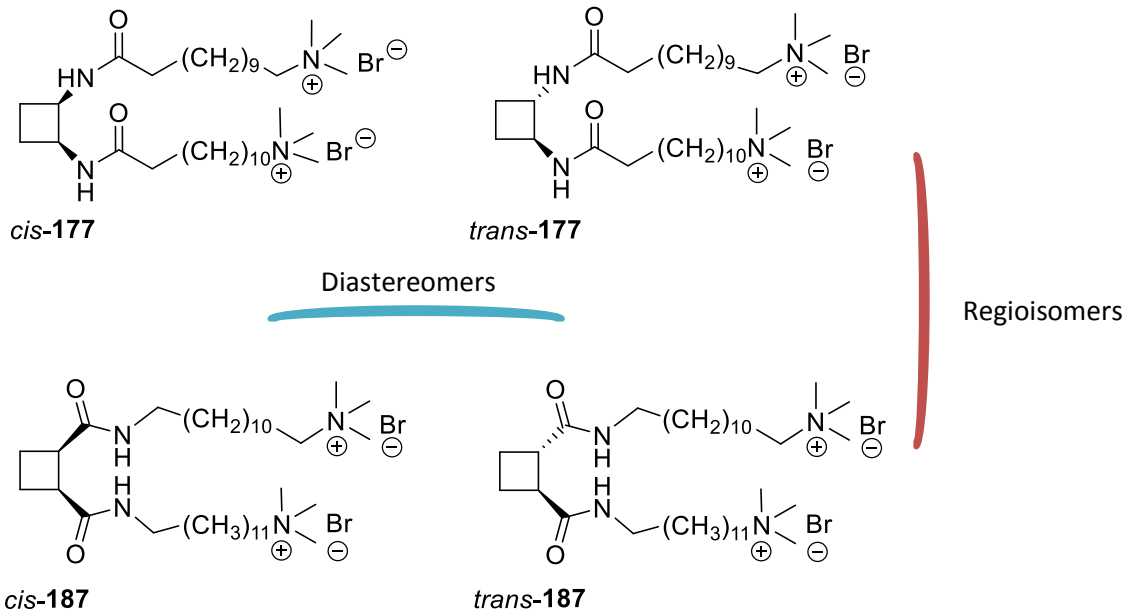

Figure 61. Compounds to be studied in this thesis.

As it has been stated in the introduction of this chapter, the main property to characterize the behavior of an amphiphile in water is the surface tension. The surface tension is a contractive tendency of the surface of a liquid that allows it to resist an external force and surfactants are compounds that lower the surface tension between two liquids. The study of this property for these four compounds was undertaken in collaboration with Dr. Ramon Pons from the *Consejo Superior de Investigaciones Científicas* (CSIC) in Barcelona and Dr. Alessandro Sorrenti from our research group.

The pendant drop technique can be used to determine the interfacial tension between two immiscible liquids. Therefore the balance of gravity, hydrostatic pressure, and surface tension effects, determines the shape of the liquid drop, hanging on a syringe tip. The mechanism is that a drop of liquid is suspended from the end of a tube by surface tension (Figure **62**). The force due to surface tension is proportional to the length of the boundary between the liquid and the tube, with the proportionality constant usually denoted as Υ.[146] Since the length of this boundary is the circumference of the tube, the force due to surface tension is given by the formula:

$$F = \pi d \gamma$$ where d is the tube diameter.

The mass m of the drop hanging from the end of the tube can be found by equating the force due to gravity ($F_g = mg$) with the component of the surface tension in the vertical direction ($F\ \gamma \sin\alpha$) giving the formula $mg = \pi d\gamma \sin\alpha$, where α is the angle of contact with the tube, and g is the acceleration due to gravity. The limit of this formula, as α goes to 90°, gives the maximum weight of a pendant drop for a liquid with a given surface tension, Υ. Then;

$$mg = \pi d \gamma$$

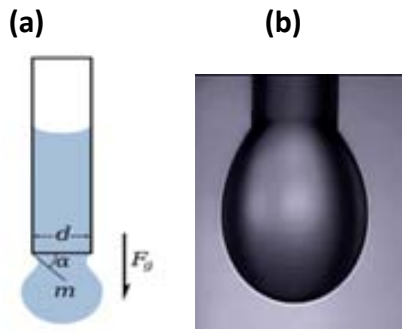

Figure 62. (a) Schematic representation of pendant drop test. **(b)** Pendant drop of one of the compounds studied.

To proceed, different concentrations in water of bolaamphiphiles previously synthesized were prepared for the eight compartments in the equipment (Figure **63**). Once these solutions were prepared, the drop was formed inside the compartment through a needle, which was introduced from the top side of the compartment. Then,

[146] Cutnell, J. D.; Kenneth W. J. *Essentials of Physics*, Wiley, New York, **2006**.

measurements were taken at the initial time of the formation of the drop, and at different times until the equilibrium of the surface tension was observed.

Figure 63. Surface tension measurement device designed by the Department of chemistry and technology of surfactants from CSIC (Barcelona).

5.3.1 Surface tension measurements of bolaamphiphiles *cis*-177 and *trans*-177 derived from cyclobutane-1,2-diamine.

Surfactants based on cyclobutane-1,2-diamine and the effect of the stereochemistry in *cis*- and *trans*- bolaamphiphiles were the first issues to be studied. To do it, solutions in the range of concentrations from 7.4118 to 0.0050 mmol/kg in the case of *trans*-**177** (Table **6**) and in the range from 3.8761 to 0.0037 in the case of *cis*-**177** were prepared (Table **7**). The measurements were taken until 180 minutes in Table **7** for *trans*-**177** and until 300 min for *cis*-**177**, since it was more difficult to stabilize. It was necessary to perform some preliminary tests in order to determine the best range of concentrations to be considered.

Table 6. Surface tension for bolaamphiphile *trans*-**177**.

	Surface tension, Y (mN/m)			
Concentration (mmol/kg)	t = 0 min	t = 60 min	t = 120 min	t = 180 min
7,4118	52,99	51,66	51,10	50,13
2,7046	50,79	48,75	49,20	48,82
0,9869	54,4	51,99	50,71	50,65
0,3233	60,65	53,85	55,04	54,58
0,1186	59,05	54,52	56,40	53,90
0,0421	57,00	53,09	49,86	49,41
0,0147	66,28	60,92	61,58	58,56
0,0050	61,17	58,97	62,64	60,08

Table 7. Surface tension for bolaamphiphile *cis*-**177**.

	Surface tension, Y (mN/m)					
Concentration (mmol/kg)	t = 0 min	t = 60 min	t = 120 min	t = 180 min	t = 240 min	t = 300 min
3,8761	29,98	29,59	27,86	26,90	27,99	27,89
1,9401	31,32	26,47	26,59	25,93	26,01	26,51
0,7177	47,16	41,92	40,86	39,99	38,68	38,97
0,2600	43,06	33,43	31,50	30,44	29,88	29,54
0,0849	55,35	54,07	50,14	50,34	47,60	46,79
0,0300	58,94	51,91	49,58	48,99	47,77	48,50
0,0101	59,67	51,75	52,97	53,23	51,75	51,61
0,0037	62,77	62,00	63,09	61,33	61,97	59,06

Then, the obtained data was plotted in a graph where the surface tension is shown in front of the logarithm of the concentration of amphiphile (Figure **64**). Two different behaviors are observed for both bolaamphiphiles: *trans*-**177** in blue and *cis*-**177** in red. Surfactants are compounds that lower the surface tension of a liquid due to their accumulation in the surface as it was explained in the introduction of this chapter. Taking this statement in mind, observing the blue line in the graph, the surface tension of the water when *trans*-**177** is added remains almost constant. Therefore, *trans*-**177** does not behave as a surfactant since it does not have the capacity to decrease the surface tension of water.

If the red plot is observed, there are different possible behaviors in the graph for *cis*-**177** depending on the points taken. The experiments were repeated with different concentrations providing the same results. In this case, bolaamphiphiles *cis*-**177** has the capacity to reduce the surface tension of the water acting as a surfactant. Nevertheless, it has a strange behavior as a surfactant since the surface tension decreases at 0.2600 mmolal but then it increases again instead of remaining constant. Finally, the surface tension decreases and remains constant. The measurements related to this plot were repeated and it was concluded that there was not an error in the values of surface tension, so it was due to the nature of the surfactant.

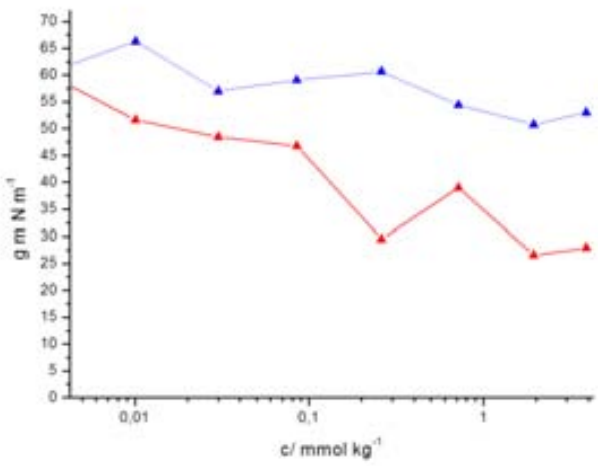

Figure 64. Plots of surface tension, ϒ (mN/m) in front of the concentration (mmol/kg) for *trans*-**177** (blue) and *cis*-**177** (red).

This atypical behavior of *cis*-**177** is confirmed by the conductivity results (Figure **65**). As a general rule, the conductivity of a surfactant tends to decrease with concentration because of the formation of micelles but in this case the conductivity increases with the molality of the solution and that means that no micelles were formed, yielding another type of aggregates. In the case of the bolaamphiphiles, their behavior differs somewhat from that of the single-headed amphiphiles because of the presence of the second hydrophilic group and it is for that reason that they are less investigated than their single-head homologous.[147,148,149]

[147] Estroff, L. A.; Hamilton, A. D. *Angew. Chem. Int. Ed.* **2000**, *39*, 3447.
[148] Estroff, L. A.; Leiserowitz, L.; Addadi, L.; Weiner, S.; Hamilton, A. D. *Adv. Mater.* **2003**, *15*, 38.

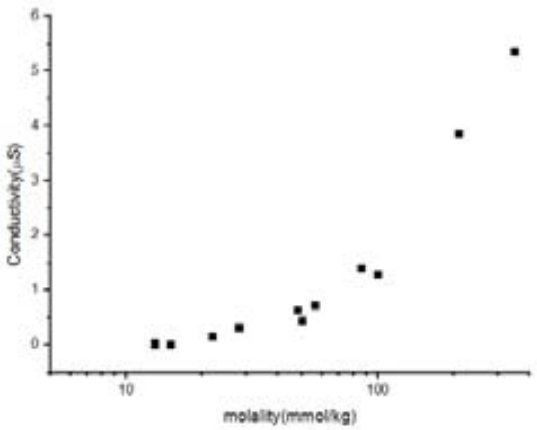

Figure 65. Plots of conductivity (µS) in front of concentration (mmol/kg) of *cis*-**177**.

The aggregate morphologies of bolaamphiphiles are dependent on their head groups and the structure of the hydrophobic chains.[150,151] The surface properties of bolaamphiphiles are also investigated and many new phenomena are observed due to their reverse U-shape conformation in surface phase.[152,153] There is one transition point in the surface tension curve indicating micelle formation in common surfactant systems, (the CMC which has been explained at the beginning of this chapter). However, in some systems, two transition points exist in the surface tension curve. This phenomenon usually can be observed in mixed systems, for instance: hydrocarbon and fluorocarbon chains or polymers and small conventional surfactant. Both amphiphiles form respective micelles at different concentrations; as a result, two transition points in the surface tension curve are observed. In the case of polymer and surfactant system, the surfactant adsorption on the polymer is responsible for the first transition point. This binding occurs abruptly in a similar fashion as micelle formation.[154] The second transition point indicates the surfactant micelle formation as usual. For example, in 2004 Huang and co-workers[155] reported that the two transition points in one surface tension curve can also be observed in the mixed system of a cationic bolaamphiphiles (biphenyl-4,4-bis(oxyhexamethylenetrimethylammonium

[149] Karsa, D. R. *Industrial Applications of Surfactants II*, Springer-Verlag, Heidelberg, 1990.
[150] Bhattacharya, S.; De, S.; Subramanian, M. *J. Org. Chem.* **1998***,63,* 7640.
[151] Bhattacharya, S. De, S. *Chem. Commun*. **1996**, 1283.
[152] Song, J.; Cheng, Q.; Kopta, S.; Stevens, R. C. *J. Am. Chem. Soc.* **2001**, *123*, 3205.
[153] Yan, Y.; Huang, J. B.; Li, Z. C.; Zhao, X. L.; Zhu, B. Y.; Ma, J.M. *Colloid. Surf. A* **2003**, *215*, 263.
[154] Jones, M. N. *J. Colloid Interface Sci.* **1967**, *23*, 36.
[155] Han, F.; Xiao He, X.; Huang, J.; Li, Z. *J. Phys. Chem. B* **2004**, *108,* 5256.

bromide), BPHTAB) and sodium dodecyl sulfate (SDS) (Figure **66**). Using TEM (Transmission electron microscopy) they found that the formation of various kinds of organized assemblies such as vesicles or micelles at different surfactant concentrations were responsible for the existence of two transition points in the surface tension curves.

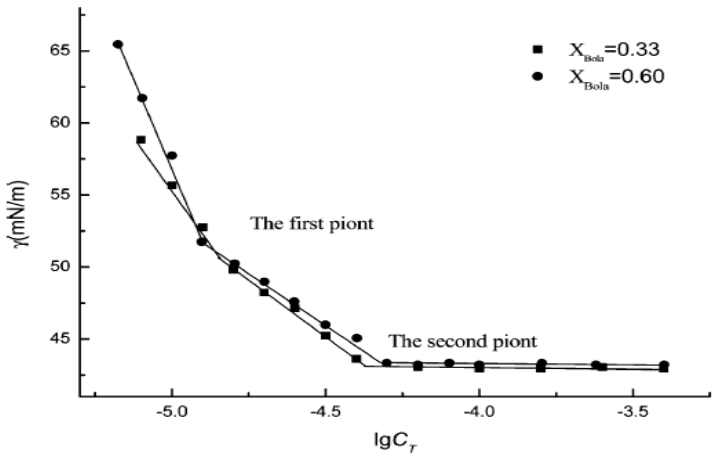

Figure 66. ϒ-log c curves of BPHTAB/SDS mixed systems from ref. 155.

Thus, looking at the plot of *cis*-**177**, it can be said that probably there is an impurity (polymer or some part of the organic fragment with only one hydrophilic group) which causes two CMC points in the surface tension.

Another qualitative feature that could be seen with naked-eye is the fact that *cis*-**177** produced foam when shaking (Figure **67**), which reveals its behavior as surfactant whereas *trans*-**177** did not produce any foam.

Figure 67. Foam generated by surfactant *cis*-**177**.

5.3.2 TEM (Transmission electron microscopy) studies on *cis*-177

TEM was used to determine the supramolecular structures in solution. Different images were recorded using a range of concentrations. Then, 0.5 mmolal, 2.0 mmolal and 4 mmolal solution in water of *cis*-**177** were analyzed after incubation at 0 ^{o}C for 24 hours.

In order to proceed recording images with the microscope, firstly the sample was placed onto a carbon-film-coated copper grid and stained with 2% uranyl acetate. Subsequently, several images were recorded under vacuum. In Figure **68** the micrographs of *cis*-**177** are shown at these three different concentrations.

(a)

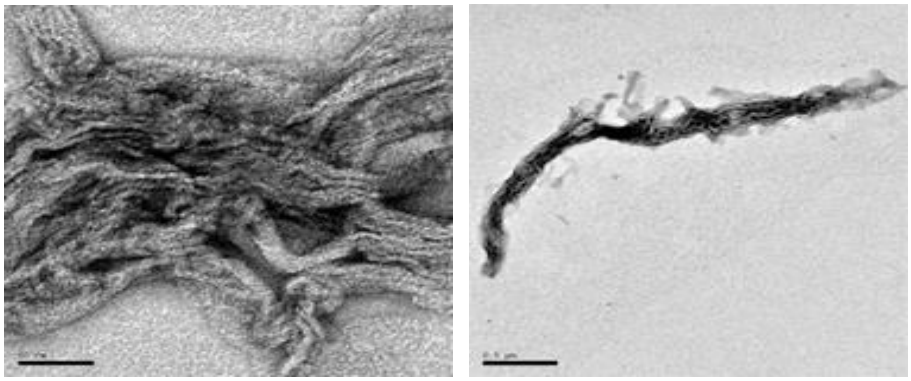

(b)

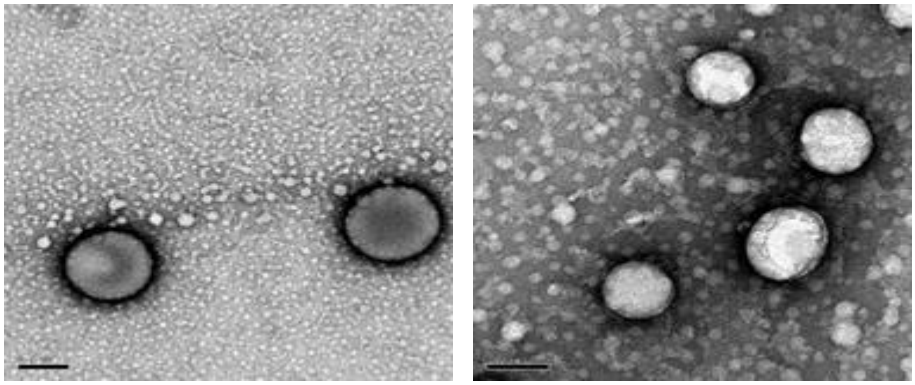

(c)

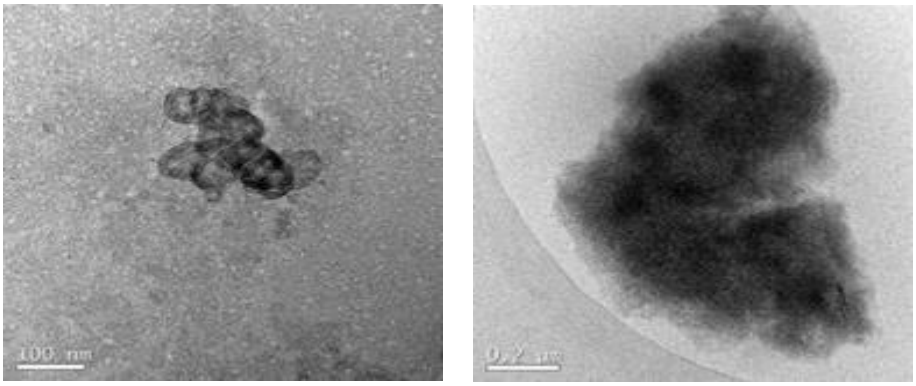

Figure 68. TEM images of *cis*-**177** at (a) 0.55 mmolal, (b) 2 mmolal and (c) 4 mmolal in water after 1 day incubation.

For 0.55 mmolal in water solutions, fibers of lengths above 3 µm are formed and, in most of cases, they are together forming aggregates of different sizes. For solutions of 2 mmol, vesicles from 30 to 400 nm are formed. For the solutions of 4 mmolal, big aggregates around 1 µm are formed. Then, it can be concluded that surfactant *cis*-**177** experiments changes in its aggregate structure depending on its concentration forming fibers, vesicles and big aggregates.

There are some examples in the literature with bolaamphiphiles which have different morphology in solution observed by microscopy.[156,157] Spherical monolayer membranes convert to linear or helical fibers, e.g., long rods or tubules, when rigid segments establish an ordered packing (the cyclobutane moiety in our case) or hydrogen bond chains are formed between the head groups or amide bonds in the hydrophobic core. The most common conversion of spherical vesicles to linear rods or tubules is caused by formation of linear hydrogen-bond chains between the functional groups of the hydrophilic parts or secondary amide linkages in the hydrophobic core. It is controlled by the size of substituents in the neighbourhood of the –CONH– bond and by temperature. If the distance between the amide groups becomes too large to form

[156] Kobayashi, H.; Amaike, M.; Jung, J. H.; Friggeri, A.; Shinkai, S.; Reinhoudt, D. N. *Chem. Commun*. **2001**, 1038.
[157] Wang, X.; Shen, Y.; Pan, Y.; Liang, Y. *Langmuir* **2001**, *17*, 3162.

stable hydrogen bonds or if curvature does not allow linear chains, crystallization or dissolution of the fibers occurs.[158]

5.3.3 TEM studies on *trans*-177

TEM micrographs of bolaamphiphile *trans*-**177** 5.5 mmolal solution in water were also recorded and they are shown in Figure **69**.

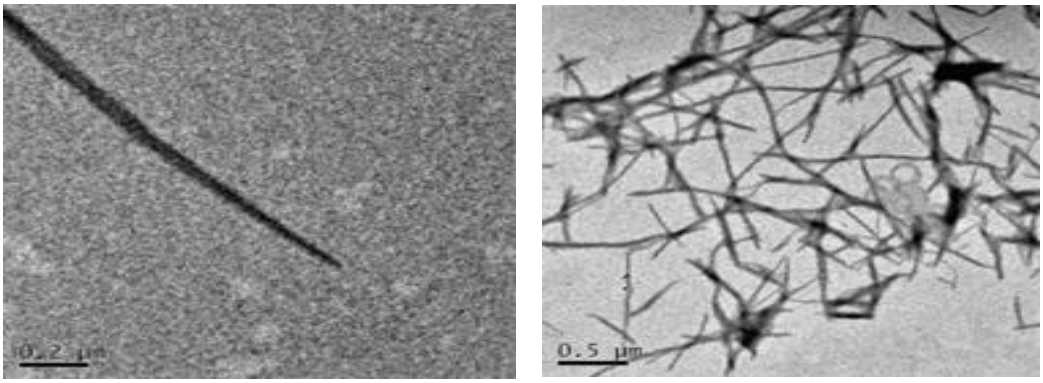

Figure 69. TEM micrographs of *trans*-**177** in H_2O.

Micrographs of bolaamphiphile *trans*-**177** show a fibrilar network composed by single and intertwined fibers with lengths from 0.3 to 4.5 micrometers. It is important to remark that bolaamphiphile *trans*-**177** did not behave as a surfactant since it did not have the capacity to reduce the surface tension of the water (Figure **64**) and this was in a good agreement with the fact that fibrilar structures were found for *trans*-**177** for different sample concentrations. Therefore, in contrast with *cis*-1**77** which showed concentration dependence of the aggregation, the aggregation of its *trans*-diastereomer remained constant with the concentration.

[158] Fuhrhop, J-H.; Wang, T. *Chem. Rev.* **2004**, *104*, 2901.

5.3.4 Organogelator behavior of *trans*-177.

Having seen that *trans*-**177** did not behave as a surfactant, its capacity to form gels with different alcohols was tested. In the literature there are some cases of bolaamphiphiles with the 1,2-diamino moiety which have the ability to form organogels in different solvents. For instance, compound **218** was found to gel *n*-butanol and the mgc was found to be 20 mg/ml (Figure **65**).[159]

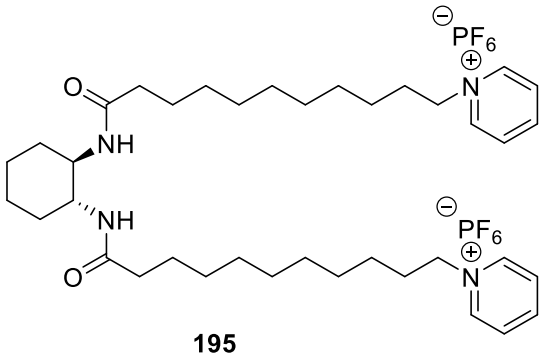

Figure 65. Bolaamphiphile synthesized by Shirai and co-workers according ref. 159.

Another interesting example are the bolaamphiphiles prepared in 2000 by Hanabusa et al.[160] The group synthesized bolaamphiphiles **206** and **207** (Figure **66**) and also their analogues without cationic charges. While the non-cationic compounds gelated alcohols, aprotic and protic solvents, **206** and **207** gelated THF, DMSO and DMF, indicating that the gelation ability was deteriorated by introduction of cationic charges.

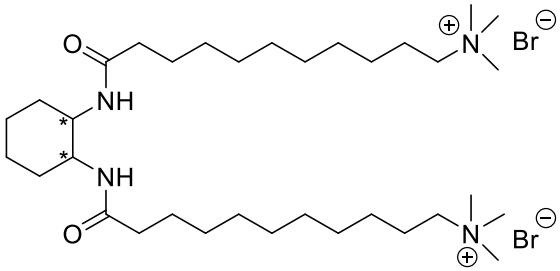

(1*R*, 2*R*)-**206** / (1*R*, 2*S*)-**207**

Figure 66. Bolaamphiphiles synthesized by Hanabusa according to ref. 160.

[159] Kobayashi, S.; Hanabusa, K.; Hamasaki, N.; Kimura, M.; Shirai, H. *Chem Mater* **2000**, *12*, 1523.
[160] Jung, J.H.; Ono, Y.; Hanabusa, K.; Shinkai, S. *J. Am. Chem. Soc.* **2000**, *122*, 5008.

Thus, *trans*-**177** was assayed in ethanol, *n*-butanol, methanol, iso-propanol, DMF, THF and DMSO. It was found to gelate ethanol and DMF at 4 ^{o}C and the gels afforded were transparent and non-thermoreversible. In *n*-butanol and iso-propanol, *trans*-**177** yielded opaque gels, thermoreversible and stable at room temperature for several days. Moreover, the gel in *n*-butanol had a very low value of minimum gelation concentration and its gelation was spontaneous, without needing to sonicate. This means that *trans*-**177** is a very good organogelator of *n*-butanol (Figure **67**). These results are summarized in Table **8**.

Table 8. Results of gelation tests of *trans*-**177**.[a]

Solvent	Properties		
	gel (mgc)[a]	Temperature	Thermoreversible
Etanol	35	277 K	No
n -butanol	10	298 K	Yes
methanol		Soluble	
iso -propanol	70	298 K	Yes
DMF	60	277 K	No
THF		Insoluble	
DMSO		Insoluble	

[a] Value means the minimum gel concentration (mg/ml)

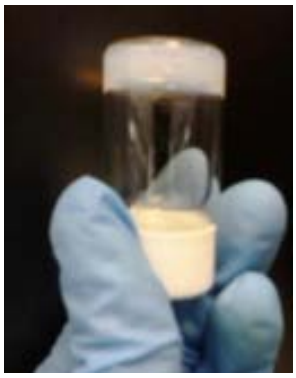

Figure 67. Gel formed by *trans*-**177** in *n*-butanol at 298 K.

SEM micrographs were recorded to investigate the morphology of the gels obtained in *n*-butanol. The micrographs of the xerogels (dry gels) were recorded at 80 kPa of pressure and mgc of 10 mg/ml. The pictures obtained are shown in Figure **68**.

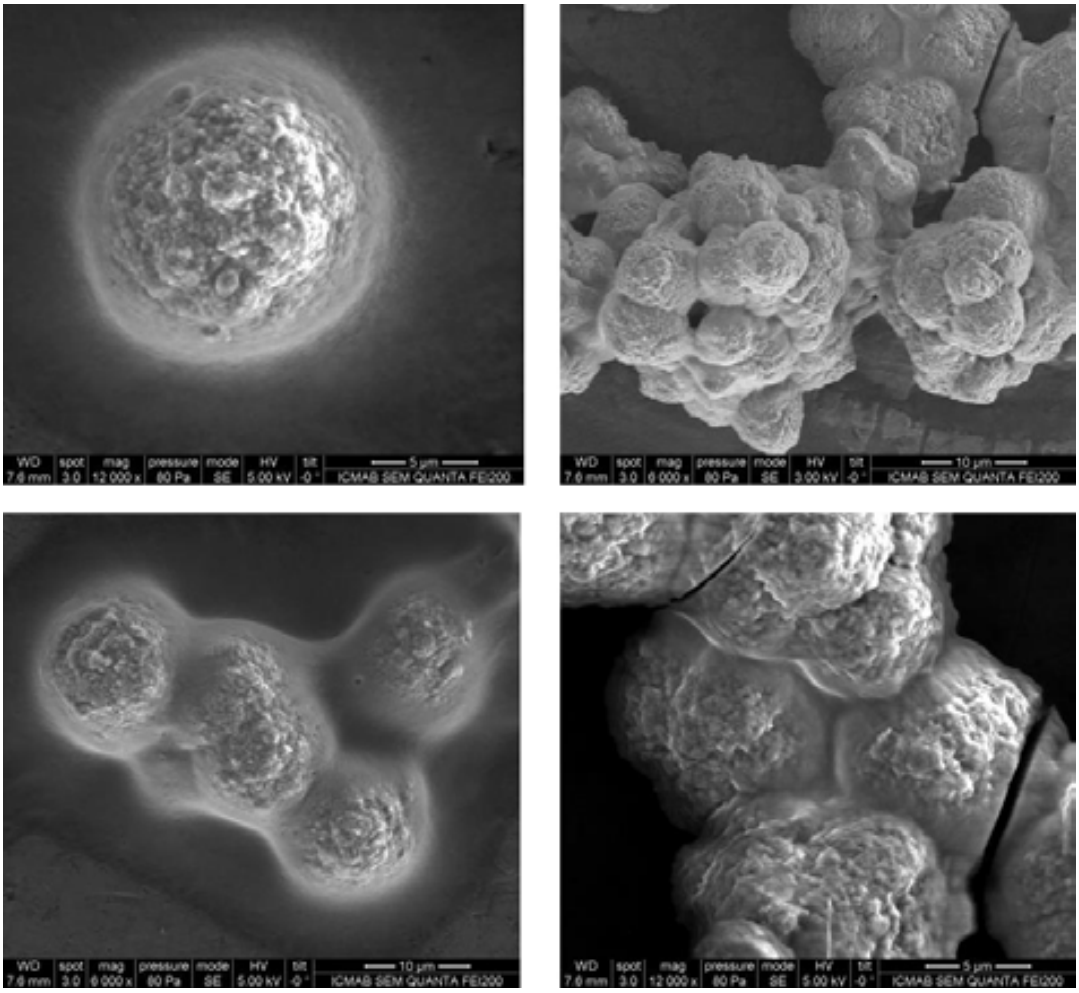

Figure 68. SEM images of the xerogels from *n*-butanol for *trans*-**177**.

The xerogel from *trans*-**177** in *n*-butanol is organized into rough spheres of around 15 µm of diameter. At the same time, these spheres are forming aggregates in a cauliflower-like shape of different sizes ranging from 20 µm to 70 µm in some cases.

5.3.5 Surface tension measurements of bolaamphiphiles *cis*-187 and *trans*-187 derived from cyclobutane-1,2-dicarboxylic acid.

In the previous part of this chapter the effect of stereochemistry in the surface and aggregation properties of *cis*- and *trans*- stereoisomers of **177** were compared. In this second part bolaamphiphiles based on cyclobutane-1,2-dicarboxylic acid will be

characterized in order to see if there are differences with their regioisomers (Figure **69**).

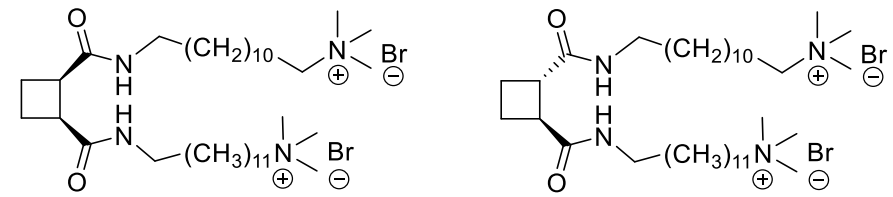

cis-**187** *trans*-**187**

Figure 69. Bolaamphiphiles studied in this chapter.

Again in collaboration with Dr. Ramon Pons from the *CSIC* in Barcelona, the surface tension measurements of solutions of bolaamphiphiles *cis*-**187** and *trans*-**187** were carried out. Then, the obtained data was represented in a graph where the surface tension is shown in front of the logarithm of the concentration of amphiphile (Figure **70**). Similar behavior was observed for both bolaamphiphiles: *cis*-**187** in blue and *trans*-**187** in red. A normal behavior as surfactants, where the tendency of the surface tension (Υ) is to decrease with the addition of surfactant into the solution, can be observed.

The CMC[161] could be determined in these bolaamphiphiles. Before reaching the CMC, the surface tension changes strongly with the concentration of the surfactant. After reaching the CMC, the surface tensions remains relatively constant or changes with a lower slope.[162] Then, the CMC for bolaamphiphiles *cis*-**187** and *trans*-**187** was found to be 7.3 mmol/kg for *cis*-isomer and 2.5 mmol/kg for *trans*-isomer. With these values it can be concluded that both bolaamphiphiles act as surfactants but *trans*-isomer is better than *cis*-isomer since it needs less concentration than its diastereomer to form micelles (Figure **70**).

[161] Jungermann, E. *Cationic Surfactants*, Dekker, New York, **1970**.
[162] Domínguez, A.; Fernández, A.; González, N.; Iglesias, E.; Montenegro, L. *J. Chem. Ed.* **1997**, *74,* 1227.

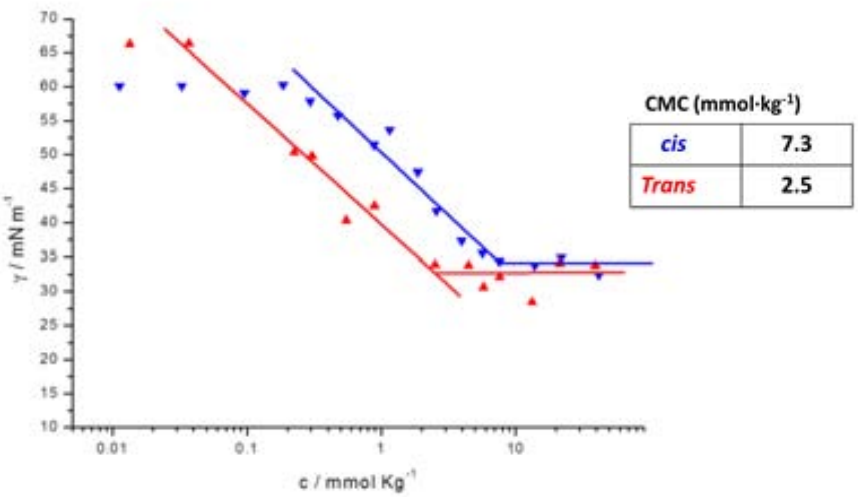

Figure 70. Plots of surface tension, ϒ (mN/m) in front of the concentration (mmol/kg) for *cis*-**187** (blue) and *trans*-**187** (red).

It is important to highlight the remarkable difference in behavior from surfactants *cis*-**187** and *trans*-**187** with their regioisomers *cis*-**177** and *trans*-**177**: Diamide-*C*-centered bolaamphiphiles act as better surfactants than diamide-*N*-centered bolaamphiphiles. Then, it can be concluded that there is a considerable effect of the regiochemistry on the surface behavior.

5.3.6 Aggregation properties of *cis*-187 and *trans*-187

Aggregation properties of bolaamphiphiles *cis*-**187** and *trans*-**187** were also studied using TEM under the same conditions than for previous bolaamphiphiles **177**. Micrographs of both surfactants are shown in Figure **71**.

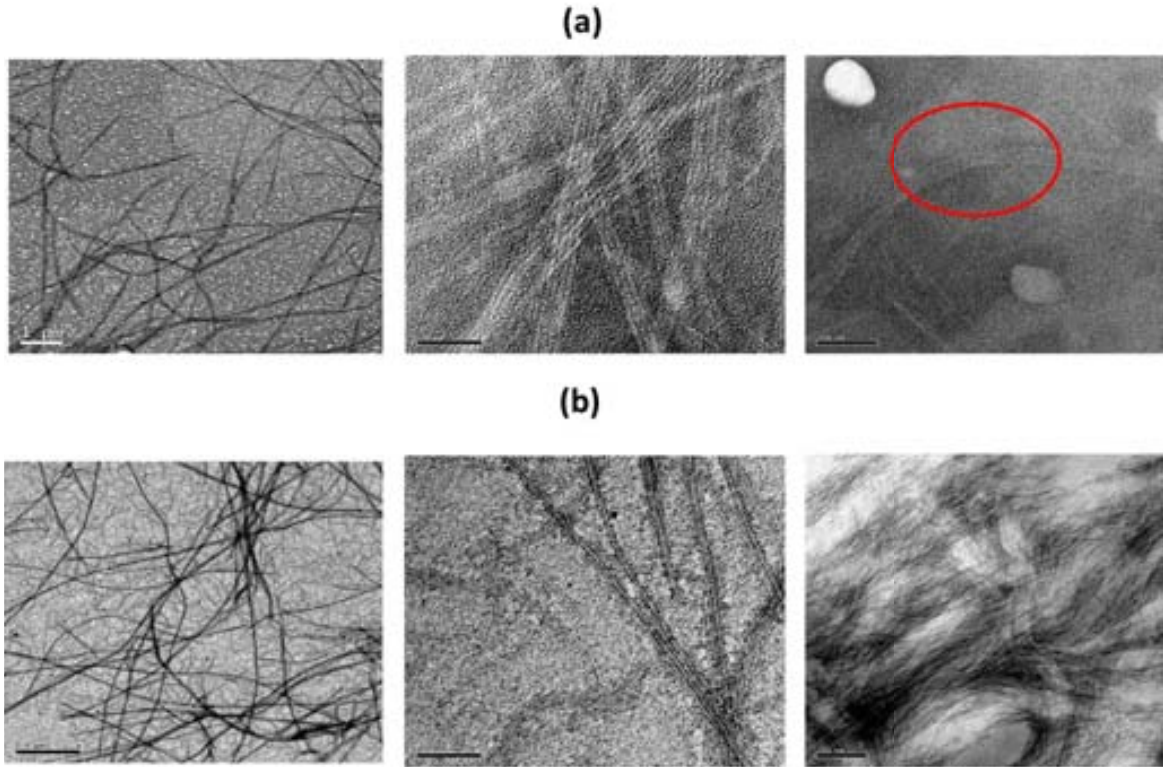

Figure 71. TEM micrographs of surfactants (a) *cis*-**187** and (b) *trans*-**187.**

Observing at the micrographs it can be seen that both surfactants show a fibrillar structure in TEM. The fibers formed by surfactant *cis*-**187** (Figure **71a**) are sheets of 4 nm with a bilayer rearrangement showing in some cases a clear folding of the fibers (remarked in red). *trans*-**187** (Figure **71b**) formed an ordered network of longer fibers with length of more than one micrometer.

4.4 SUMMARY AND CONCLUSIONS

To sum up, the results of the study on the four bolaamphiphiles depicted in Figure **72** show a very important influence of the regiochemistry on the surface properties of bolaamphiphiles:

NH-centered amides *cis*-**177** and *trans*-**177** behave differently in water. On the one hand, *trans*- diastereomer does not have the capacity to decrease surface tension but it acts as a good organogelator in *n*-butanol and its gels were studied by SEM. On the other hand, *cis*-diasteromer acted as surfactant but with a uncommon behavior with two transitions points in their representation of the surface tension in front of the concentration. Its TEM micrographs revealed a difference in their morphology depending on the concentration, which could be related to its peculiar behavior.

C-centered amides *cis*-**187** and *trans*-**187** have a similar behavior in water and they are good and conventional surfactants. Their critical micellar concentration was determined, giving 7.3 mmolal for *cis*- and 2.5 mmolal for *trans*- diastereomer.

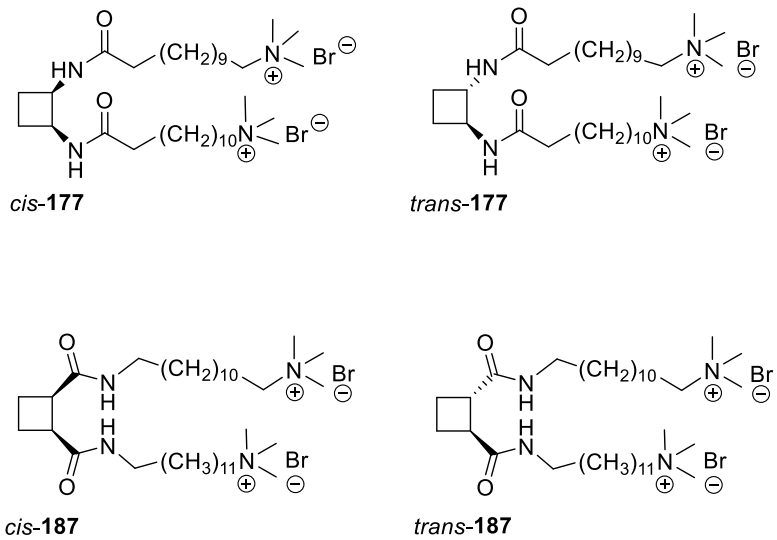

Figure 72. Compounds studied in the present Thesis.

CHAPTER VI

Hybrid materials based on cyclobutane-1,2-diamines

6 Hybrid materials based on cyclobutane-1,2-diamines

6.1 INTRODUCTION

6.1.1 Definition of hybrid material.

Organic–inorganic hybrid materials form a very interesting class of solids which combine the physical properties of the inorganic framework and the intrinsic versatility of the organic component. Numerous organic–inorganic hybrid materials have been developed over the past few decades, providing a wide variety of applications in diverse fields such as optics,[163,164] electronics,[165,166] membranes,[167,168] protective coatings,[169] sensors,[170] and controlled drug delivery.[171] Concomitantly, their use as supports to heterogenize homogeneous catalysts has been an intense field of research in last decade.[172,173]

There are different manners to define the term hybrid material. However, the most wide-ranging definition is the following: a hybrid material that includes two moieties blended on the molecular scale.[174] Commonly one of these compounds is inorganic and the other one organic. These can also be modified as a result of the way the organic and inorganic components are combined together. Thus, Sanchez *et al*.[175,176] proposed a partition in two classes: **Class I materials** where the organic fragment is arranged with the inorganic framework only via non-covalent interactions such as ionic, van der Waals or hydrogen bonds and **Class II materials** where a covalent linkage is present between both areas. This linkage can be a Si–C bond in the case of silica based hybrids or a M–O–C (M = Zr or Ti) sequence for zirconium or titanium

---

[163] Carlos, L. D.; Ferreira, R. A. S.; Bermudez, V. D.; Ribeiro, S. J. L. *Adv. Mater.* **2009**, *21*, 509.
[164] Tani, T.; Mizoshita, N.; Inagaki, S. *J. Mater. Chem.* **2009**, *19*, 4451.
[165] Zhang, Y.; Tang, Q.; Li, H.; Hu, W. *Appl. Phys. Lett.* **2009**, *94*, 2033.
[166] Lu, M.; Xie, B. H.; Kang, J. H.; Chen, F. C.; Yang, Y.; Peng, Z. H. *Chem. Mater.* **2005**, *17*, 402.
[167] Wang, B. Q.; Li, B.; Deng, Q.; Dong, S. J. *Anal. Chem.* **1998**, *70*, 3170.
[168] Mistry, M. K.; Choudhury, N. R.; Dutta, N. K.; Knott, R.; Shi, Z. Q.; Holdcroft, S. *Chem. Mater.* **2008**, *20*, 6857.
[169] Zheludkevich, M. L.; Salvado, I. M.; Ferreira, M. G. S. *J. Mater. Chem.* **2005**, *15*, 5099.
[170] Grate, J. W.; Kaganove, S. N.; Patrash, S. J.; Craig, R.; Bliss, M. *Chem. Mater.* **1997**, *9*, 1201.
[171] Zhang, H.; Pan, D. K.; Zou, K.; He, J.; Duan, X. *J. Mater. Chem.* **2009**, *19*, 3069.
[172] Corma, A.; Garcia, H. *Adv. Synth. Catal.* **2006**, *348*, 1391.
[173] Wight, A. P.; Davis, M. E. *Chem. Rev.* **2002**, *102*, 3589.
[174] Kickelbick, G. *Hybrid Materials*, Wiley, Weinheim, 2007.
[175] Sanchez, C.; Ribot, F. *New J. Chem.* **1994**, *18*, 1007.
[176] Judeinstein, P.; Sanchez, C. *J. Mater. Chem.* **1996**, *6*, 511.

based materials (M = Zr or Ti). The presence of these covalent bonds in the Class II allows the organic parts to remain unaltered under most of the conditions commonly used in homogeneous catalysis. A part of the present Thesis is oriented towards the synthesis of hybrid silica, which constitutes the major inorganic matrix used for immobilizing homogeneous catalysts.[177]

6.1.2 Class II hybrid silica

Organic-inorganic hybrid silica can be obtained from trialkoxysilyl precursors using the sol–gel process which is going to be described later in this chapter. However, the hydrolysis-condensation of mono-silylated compounds usually affords low molecular weight oligomers that remain soluble in certain solvents. Therefore, to obtain a material suitable for catalysis, it is necessary to perform a co-condensation process with a silica precursor such as tetraethylorthosilicate (TEOS) or tetramethoxysilane (TMOS). These materials typically exhibit rather large surface areas.[178]

The drawbacks of the co-condensation method arise from the different rates of hydrolysis between the trialkoxyorganosilane and the silica source (TMOS or TEOS) that translate into the formation of a non-homogeneous solid with contents not well controlled inorganic moieties. To circumvent these problems, the use of bridged silsesquioxanes (BS)[179] allows the formation of hybrid silica with an intrinsic regular distribution of the organic fragments throughout the material (Figure **73**).

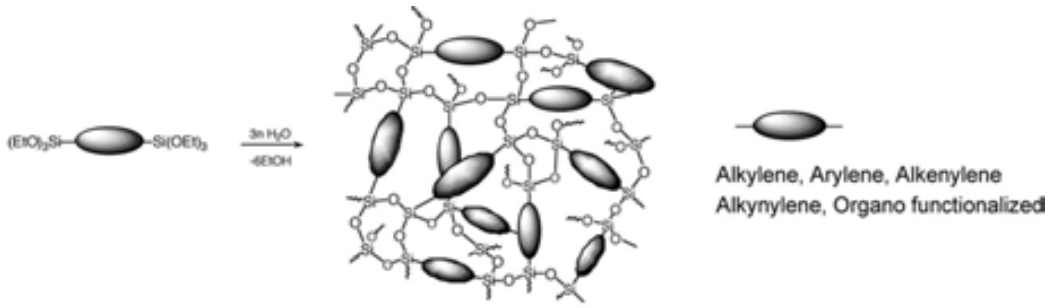

Figure 73. Schematic representation of the formation of bridged silsequioxanes.

[177] Zamboulis, A.; Moitra, N.; Moreau, J. J. E.; Cattoën, X.; Wong Chi Man, M. *J. Mater. Chem.*, **2010**, *20*, 9322.
[178] Adima, A.; Moreau, J. J. E.; Wong Chi Man, M. *Chirality*, **2000**, *12*, 411.
[179] Shea, K. J.; Moreau, J. J. E.; Loy, D. A.; Corriu, R. J. P.; Boury, B. *Functional Hybrid Materials*, Wiley, Weinheim, **2004**.

6.1.3 Structural Engineering

Self-assembly is the major principle of the controlled formation of structural building blocks. There are several basic principles that have to be taken into account for a self-assembly process: the structure and the shape of the building blocks, their interactions like the attractive and repulsive forces, their interactions with solvents, the environment where the reaction is carried out and diffusion processes. Two principles are employed in the synthesis of hybrid materials, the self-assembly of the building blocks of the material itself and the use of templates that can self-assemble and form a shape which is applied in the preparation of materials.

One of the most important cases of templating to synthesize mesoporous materials is that of amphiphile aggregates and silica units interacting in a non-covalent way, which makes the silica organize around the structure directing agent, in this case the supramolecular aggregate. The silica units then react with each other to generate mesostructured materials (Figure **74**). Afterwards, the amphiphile is removed by calcination, which leaves a mesoporous material, usually harder and more stable because of this thermal treatment, with a template pore structure. The removal of the template can also be done by solvent extraction. The whole procedure is also known as soft templating, where soft stands for the use of an organic material as a template.[180,181]

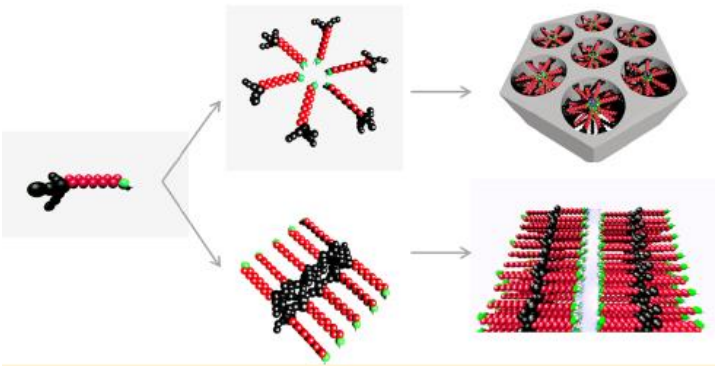

Figure 74. Surfactant-directed formation of mesoporous materials.

[180] Petkovic, N. D.; Stein, A. *Chem. Soc. Rev.* **2013**, *42*, 3721.
[181] Vivero-Escoto, J.L.; Chiang, Ya-Dong; Wu, K. C-W; Yamauchi, Y. *Sci. Technol. Adv. Mater.* **2012**, *13*, 1003.

In the present Thesis, bridged silsesquioxanes were prepared without using any template. Silsesquioxane hybrids offer much larger potentialities and seem very interesting because, owing to the covalent bond between the organic and the inorganic fragments, the auto-assembly of the organic substructure can control the formation of the inorganic silicate components and eventually direct the structure at the meso- or macroscopic level.[182] For both the bridge-silsesquioxane and co-condensation strategies, it is possible to provide a more regular structure to the hybrids by performing the sol–gel reaction in the presence of surfactants, which translates into uniform pore sizes and higher surface areas. [183]

The dual role of monomer and self-directing agent played by organosilane offers, in most examples, the advantages of a template-free and single-step synthesis procedure. As outlined in Figure **75**, precursor structure, sol-gel process, and experimental conditions are crucial in defining the level of ordering of the silsesquioxane. Indeed, the hydrolysis and condensation reactions and the release of sol-gel by-products (water, alcohol) continuously change the chemical structure of the hybrid species (number of Si—OH, Si—OR and Si—O—Si groups), their concentration and the medium. To induce organosilane self-assembly, the main efforts emphasize the key roles of the precursor structure and the preparation method (temperature, solvent, catalyst, addition of water, etc.)

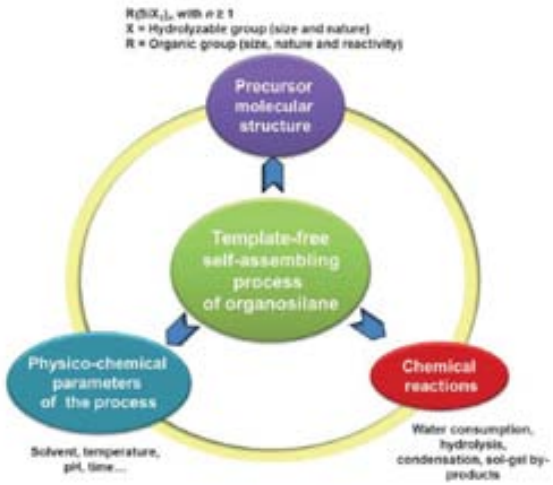

Figure 75. The organosilane self-assembly process is affected by a combination of factors.

[182] Liao, Y.C.; Roberts, J. T. *J. Am. Chem. Soc.* **2006**, *128*, 9061.
[183] Asefa, T.; MacLachlan, M. J.; Coombs, N.; Ozin, G. A. *Nature*, **1999**, *402*, 867.

6.1.4 Mechanism of the formation of hybrid silicas

The synthesis of organic-inorganic hybrid materials by hydrolysis and condensation reactions of bridged organosilica precursors of the type $(R'O)_3Si—R—Si(OR')_3$ has been known for a long time as sol-gel chemistry.[184,185] This process is chemically related to an organic polycondensation reaction in which small molecules form polymeric structures by the loss of substituents. Usually the reaction results in a three-dimentional (3-D) crosslinked network. The fact that small molecules are used as precursors for the formation of the crosslinked materials implies several advantages. For example, a good control of the purity and compositon of the final materials and the use of solvents during the synthesis of the molecular precursors which offers many advantages for their preparation and characterisation. Another important factor is that Si—C bonds have enhanced stability against hydrolysis in the aqueous media usually used in the formation of the hybrid. Compounds with formula $R_{4-n}SiX_n$ (n=1-4, X = OR', halogen) are the most commonly used as molecular precursors, in which the Si—X bond is labile towards hydrolysis reaction providing unstable silanols (Si—OH) that condensate leading to Si—O—Si bonds (Scheme **52**).

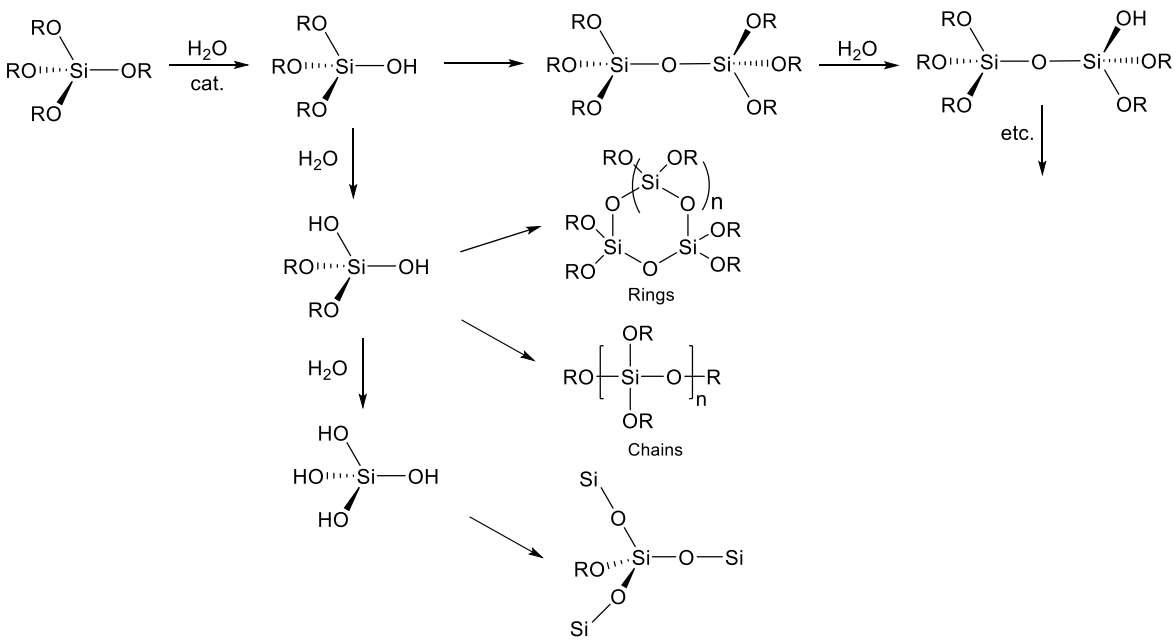

Scheme 52. Fundamental reaction steps in the sol-gel process based on tetralkoxysilanes.

[184] Loy, D. A.; Shea, K. J. *Chem. Rev.* **1995**, *95*, 1431.
[185] Shea, K. J.; Loy, D. A. *Chem. Mater.* **2001**, *13*, 3306.

The process is catalyzed by acids or bases resulting in different reaction mechanisms by the velocity of the condensation reactions (Scheme **53**). Therefore, the pH not only plays a major role in the mechanism, it is also important for the microstructure of the final material. Applying acid-catalyzed reactions an open network structure is formed in the first steps of the reaction leading to later condensation of small clusters. Contrarily, the base-catalyzed reactions lead to highly crosslinked sol particles already in the first steps. Commonly used catalysts are HCl, NaOH or NH_4OH, but fluorides can be also used as catalysts leading to fast reaction rates.

Acid Catalysis:

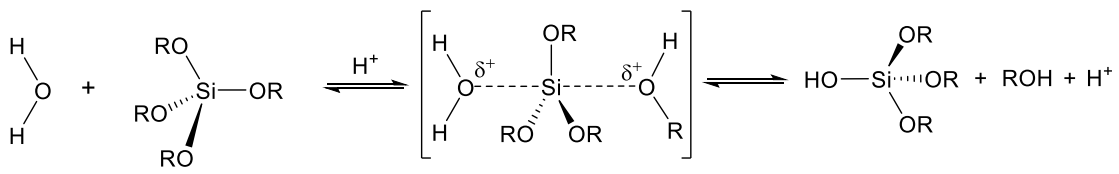

Base Catalysis:

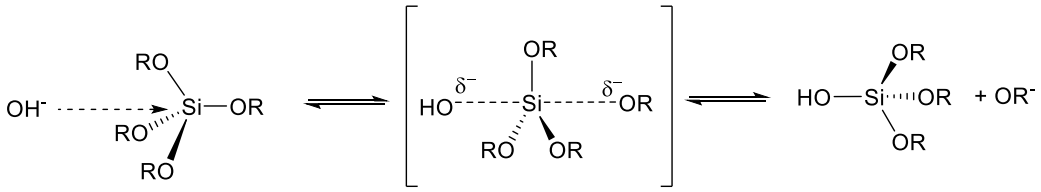

Scheme 53. Differences in mechanism depending on the type of catalyst used in the silicon-based sol—gel process.

The structure of the precursors also has an important influence in the kinetics of the reaction. Generally, larger substituents decrease the reaction rate due to steric hindrance. In addition, the substituents play a mature role in the solubility of the precursor in the solvent. Water is required for the reaction and, if the organic substituents are quite large, usually the precursor becomes immiscible in the solvent.

6.1.5 NMR as a powerful techique to study the structure of hybrid materials.

^{29}Si NMR is the most relevant technique in the field of hybrid materials because it is a powerful tool in the determination of the relative proportions of different silicon species in sol-gel derived materials. Therefore it offers information of the kinetics of the process and the understanding of its fundamental parameters, such as precursor structure and reaction conditions. It is sensitive to the first and the second nearest neighbours and therefore one can distinguish between different silicon atoms in the final material.

Typical for hybrid materials is the nomenclature with letters and numbers. Four different species can be observed in hybrid materials derived by the sol-gel process depending on their substitution pattern at the silicon. In principle one can have one, two, three or four atoms of oxygen surrounding the silicon atom. The abbreviation for these substitution patterns are M (C_3SiO), D (C_2SiO_2), T ($CSiO_3$) and Q (SiO_4). Depending how many Si atoms are connected to the oxygen atoms 3 to 1 a superscript is added to the abbreviation. In addition, these silicon species have different chemical shifts which help to distinguish between them. Therefore, mono-, di-, tri- substituted siloxane bonds were designated as T^1, T^2 and T^3 respectively. Being T^3 the more condensed position since there are the maximum oxygen atoms around silicon atom. The various T^S are defined in Figure **76**.[186]

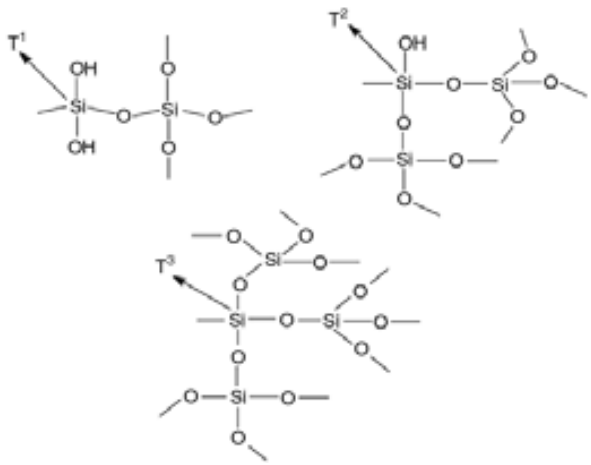

Figure 76. Abbreviations used for Si atoms attached to oxygen atoms in various structural positions.

[186] Da, Z. L.; Zhang, Q. Q.; Wu, D. M.; Yang, D. Y.; Qiu, F. X. *Express Polym. Lett.* **2007**, *1*, 698.

6.1.6 Applications of hybrid silicas

The synthesis of well-ordered organic–inorganic hybrid materials through organosilane self-assembly represents a very exciting field due to their wide range of potential applications in membranes,[187] conductive films,[188] absorbents,[189] catalysis,[190] optoelectronics,[191] and hydrophobic coatings.[192] Evidently, the interest of an ordered hybrid structure is strongly dependent on the application targeted.

For instance, in Figure **77** a membrane system based on hybrid solid can be observed.[193] They include heteroditopic receptors self-organized in solution and in the solid state where molecular recognition sites for the anion and the cation are covalently linked.

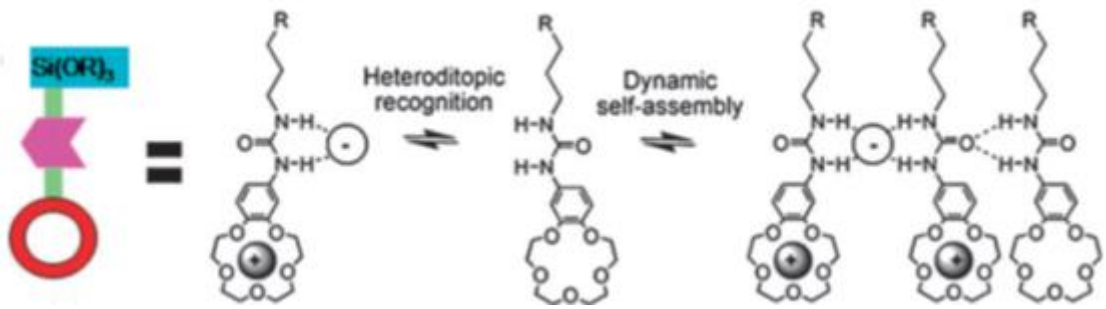

Figure 77. Dynamic self-organization and heteroditopic ion salts recognition by ureido-macrocyclic receptors.[193]

[187] Michau, M.; Barboiu, M.; Caraballo, R.; Arnal-Hérault, C.; Perriat, P.; Van der Lee, A.; Pasc, A. *Chem. Eur. J.* **2008**, *14*, 1776.
[188] Mizoshita, N.; Tani, T.; Inagaki, S. *Adv. Funct. Mater.* **2011**, *21*, 3291.
[189] Mehdi, A. *J. Mater. Chem.* **2010**, *20*, 9281.
[190] Besson, E.; Mehdi, A.; Van der Lee, A.; Chollet, H.; Reyé, C.; Guilard, R.; Corriu, R.J.P. *Chem. Eur. J.* **2010**, *16*, 10226.
[191] Dautel, O. J.; Lere-Porte, J.P.; Moreau, J. J. E.; Man, M. W. C. *Chem. Commun.* **2003**, 2662.
[192] Ke, Q. P.; Li, G. L.; Liu, Y.; He, T.; Li, X. M. *Langmuir* **2010**, *26*, 3579.
[193] Barboiu, M. *Chem. Commun.* **2010**, *46*, 7466.

In the case of optoelectronics there are some examples, for example Dautel and co-workers[194] designed a new approach to control molecular aggregation of π-conjugated chromophores in the solid state. Their objective was to design and synthesize electroluminescent or solar cell hybrid organic-inorganic materials by the sol-gel process applied to a bifunctionalized silane. In this work, the triethoxysilyl fragment was the structure-directing agent. The synthesis of the sol-gel processable precursor was accomplished by introducing the triethoxysilyl group through a transimidation[195] from the imidopyridine derivative rather than the direct addition of the 3-(aminopropyl)triethoxysilane on the 4-bromophthalic anhydride (Scheme **54**).

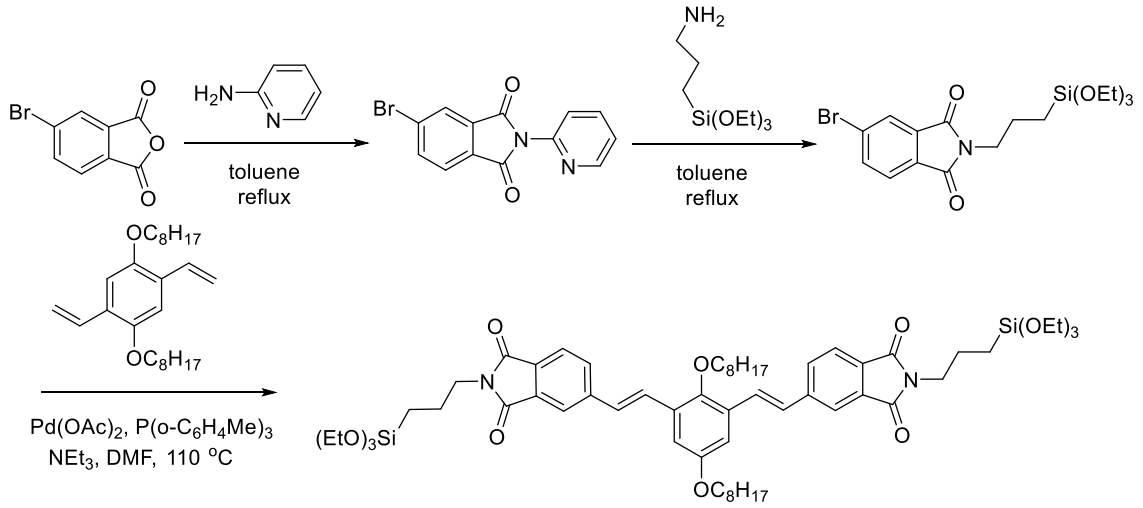

Scheme 54. Synthethic path to the phenylenevinylenediimide silsesquioxane precursor.[195]

6.1.6.1 Diureido derivatives as chiral hybrid silicas

In 2001, Moreau and co-workers[196] reported for the first time the creation of a hybrid material with helical morphology via H-bond mediated hydrolysis of a single precursor. A left- or right-handed helix was auto-generated, according to the configuration of the organic substructure (Scheme **55**). These results showed the first example of self-organized chiral hybrid material (Figure **78**).

[194] Dautel, O. J.; Wantz, G.; Almairac, R.; Flot, D.; Hirsch, L.; Lere-Porte, J.P.; Parneix, J.P.; Serein-Spirau, F.; Vignau, L.; Moreau, J. J. E. *J. Am. Chem. Soc.* **2006**, *128*, 4892.
[195] Wengrovius, J. H.; Powell, V. M.; Webb, J. L. *J. Org. Chem.* **1994**, *59*, 2813.
[196] Moreau, J.J.E.; Vellutini, L.; Wong Chi Man, M.; Bied, C. *J. Am. Chem. Soc.* **2001,** *123,* 1509.

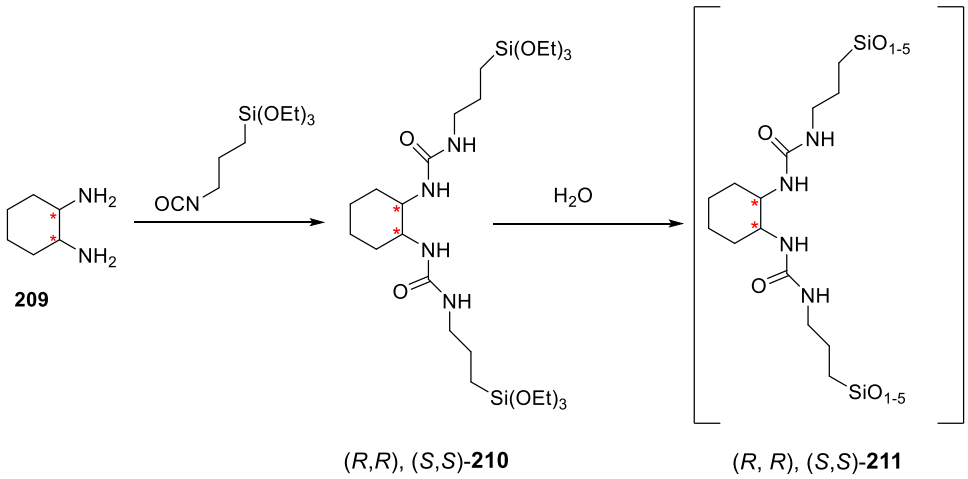

Scheme 55. Formation of diureido hybrid materials from molecular precursors.

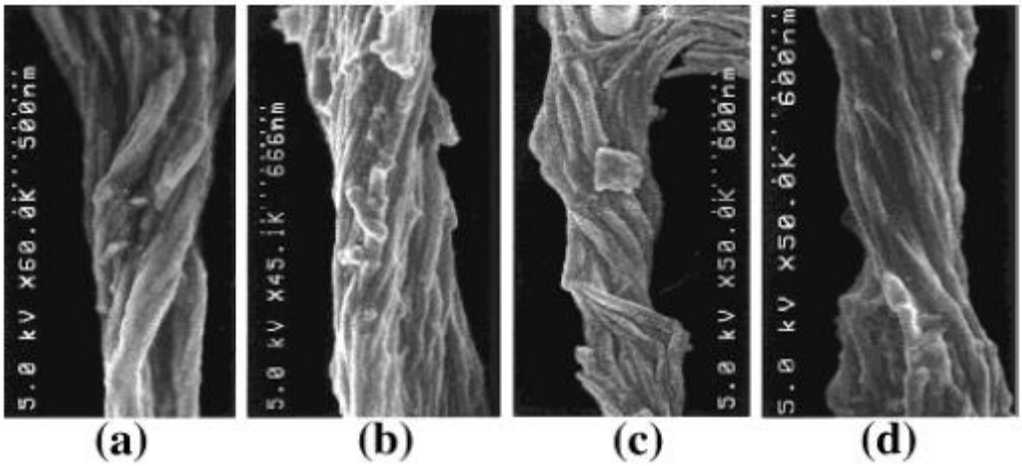

Figure 78. SEM images of hybrid silicas made **(a,b)** from precursor (*R*,*R*) and **(c,d)** from (*S*,*S*) extracted from ref. 196.

6.1.6.2 Applications in metal and non-metal catalysis

Recent interest in the development of environmentally benign synthesis has evoked a renewed pursuit in developing polymer-bound metal catalysts.[197,198] The immobilization of transition metals on organic matrix offers a number of advantages over solution-phase chemistry. In an ideal case, the supported complexes can be recovered from reaction mixtures by simple filtration, they do not contaminate the product solution, they can be recycled and they can increase selectivity. As transition-

[197] Seneci, P. *Solid-Phase Synthesis and Combinatorial Techniques*; John Wiley, New York, N. Y. 2001.
[198] Burgess, K. *Solid-Phase Organic Synthesis*, John Wiley, New York, N. Y. 2000.

metal complexes are often expensive to purchase or prepare, the immobilization on a support, thereby enabling simple extraction and recyclability, makes for commercial advantage as well as easier of manipulation.

A wide variety of organic moieties have been incorporated for structural control and functionalization in hybrid materials, ranging from the relatively simple organic bridges, such as hydrocarbons and heteroatoms, to sophisticated metal complexes.[199,200,201] However, the possibility to generate hybrid materials with different active functions contained in the same organic builders is still in the early stages of exploration. The functionalized monosilanes, $RSi(OR')_3$ are optimal precursors to anchor covalently different active groups onto the external surface of amorphous silica to generate hybrid organic–inorganic heterogeneous catalysts. The possibility to tune these functional heterogeneous catalysts depending on the functionalized monosilanes increases the appeal of this hybrid materials (Figure **79**).

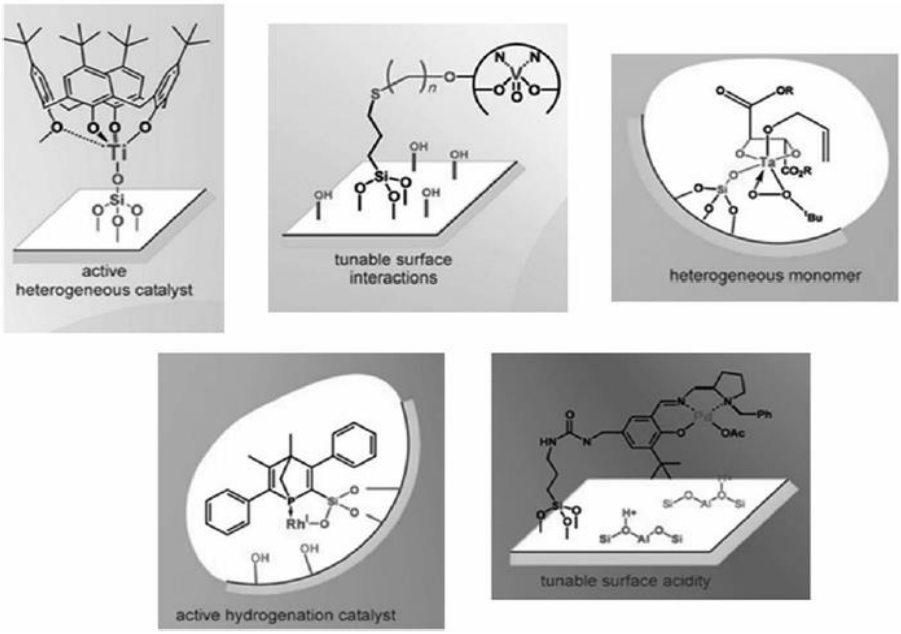

Figure 79. Examples of hybrid catalysts obtained by anchoring of functional monosilanes onto amorphous silica supports.[202]

[199] Hoffmann, F.; Cornelius, M.; Morell, J.; Froba, M. *Angew. Chem. Int. Ed.* **2006**, *45*, 3216 and references therein.
[200] Fujita, S.; Inagaki, S. *Chem. Mater.* **2008**, *20*, 891 and references therein.
[201] Kapoor, M. P.; Inagaki, S.; Ikeda, S.; Kakiuchi, K.; Suda, M.; Shimada, T. *J. Am. Chem. Soc.* **2005**, *127*, 8174.
[202] Notestein, J. M.; Katz, A. *Chem. Eur. J.* **2006**, *12*, 3954.

Bridged silsesquioxanes are also used in the field of non-metallic catalysis. For example, Pleixats and co-workers[203] prepared the materials **212-215** and they evaluated their catalytic activity in the α-tosylation of a range of ketones. In all cases were obtained the product with good yields and the reciclability of **212** was investigated. It was recovered by filtration and reused successfully in a second run for several substrates (Figure **80**).

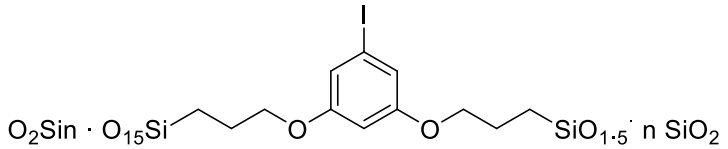

212: n=0; **213** n=2.5

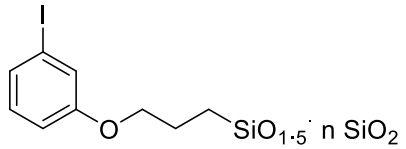

214: n=5; **215**: n=20

Figure 80. Hybrid materials prepared by Pleixats and co-workers[203]

Asymmetric organocatalytic materials based on a prolinamide scaffold were also synthesized by Pleixats's research group.[204] The monosilylated prolinamide precursor **219** and the silica materials **220-222** derived thereof were synthesized as summarized in Scheme **56**. Aminoindane-derived prolinamide **217** was obtained from commercial **216**. Subsequent reaction of **217** with (3-isocyanatopropyl)triethoxysilane in the presence of NEt_3 provided the monosilylated protected prolinamide **218**. After the removal of the protecting group by treatment with cyclohexene and catalytic Pd/C, the organosilane **219** was obtained with good overall yield. From this precursor, four different hybrid silica materials were prepared by sol–gel methodologies.

[203] Guo, W.; Monge-Marcet, A. Cattoën, X.; Shafir, A.; Pleixats, R. *React. Funct Polym* **2013**, *73*, 192.
[204] Monge-Marcet, A.; Cattoën, X.; Alonso, D. A.; Nájera, C.; Wong Chi Man, M.; Pleixats, R. *Green Chem.* **2012**, *14*, 1601.

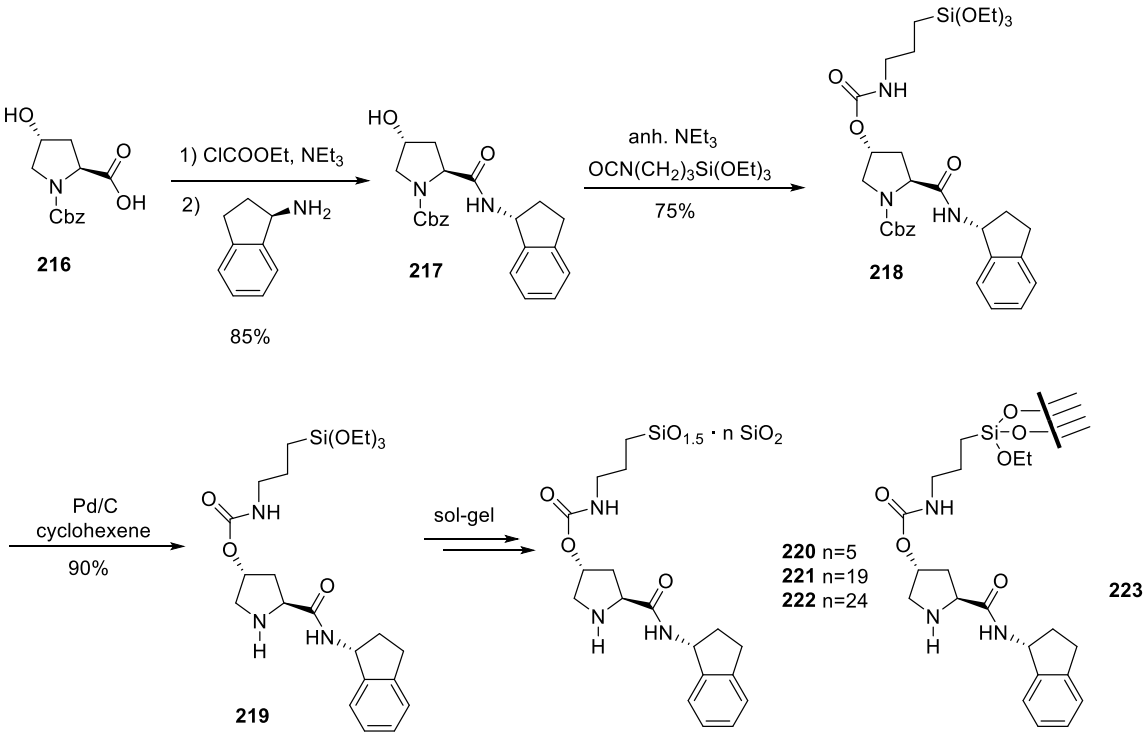

Scheme 56. Preparation of the supported organocatalysts **220-223**.[204]

The catalytic properties of these materials have been compared for direct asymmetric aldol reactions. The best catalytic material results from a simple co-condensation without structure-directing agent. Simple and green conditions are used for the aldol reaction, the process being performed in water at room temperature, with relatively low amounts of supported organocatalysts and in the absence of an acid co-catalyst. Good recyclabilities are observed without the need of catalyst regeneration, with enantioselectivities (ee up to 92%) higher than that of the parent homogeneous catalysts.

6.1.6.3 Materials containing the 1,2-diamine moiety in catalysis.

There are some examples in the literature of hybrid materials containing the cyclohexane-1,2-diamine as chiral moiety. For instance, in Scheme **57**, a mesoporous material containing diaminoacyclohexane groups linked to L-prolinamide fragments

(**224**) showed to be efficient both in terms of yields and enantioselectivities in the non metal catalysis of aldol reaction between *p*-nitrobenzaldehyde and cyclohexanone. The major drawback was the need for a 60% mol catalyst loading.[205]

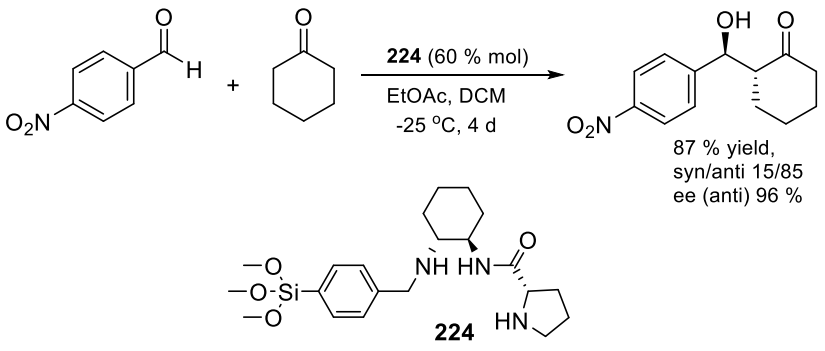

Scheme 57. Aldolisation of p-nitrobenzaldehyde with cyclohexanone using **224** as catalyst.[205]

Baleizao and co-workers[206] prepared a chiral vanadyl salen complex **225** (Figure **81**) and coupled it with TEOS in a co-condensation reaction under basic conditions in the presence of OTAC (octadecyltrimethylammonium chloride). They were able to incorporate up to 2.5% of the salen complex into the material, which still displayed an average degree of mesoporic order. That solid was assayed in the cyanosilylation of benzaldehyde with an enantiomeric excess (ee) of 30%.

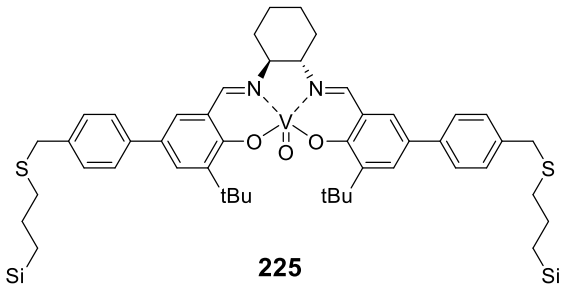

Figure 81. Bissylilated organosilica precursor used in the co-condensaton reascton with TEOS.[223]

In 2001, Bied and co-workers[207] prepared hybrid silicas by co-hydrolysing the monosilylated derivative of (1*R*,2*R*)-diaminocyclohexane and tetraethoxysilane using different reaction conditions, in the presence of primary amines as templates. Then,

[205] Gao, J.; Liu, J.; Jiang, D.; Xiao, B.; Yang, Q. *J. Mol. Catal. A. Chem.*, **2009**, *313*, 79.
[206] Baleizao, C.; Gigante, B.; Das, D.; Alvaro, M.; García, H.; Corma, A. *Chem Commun.* **2003**, 1860.
[207] Bied, C.; Gauthier, D.; Moreau, J. J. E.; Wong Chi Man, M. *J. of Sol-Gel Sci and Tech* **2001**, *20*, 313.

the material containing hybrid chiral ligands was used to immobilize rhodium complexes, **228** with the aim of testing the metal-containing materials in asymmetric catalysis (Scheme **58**).

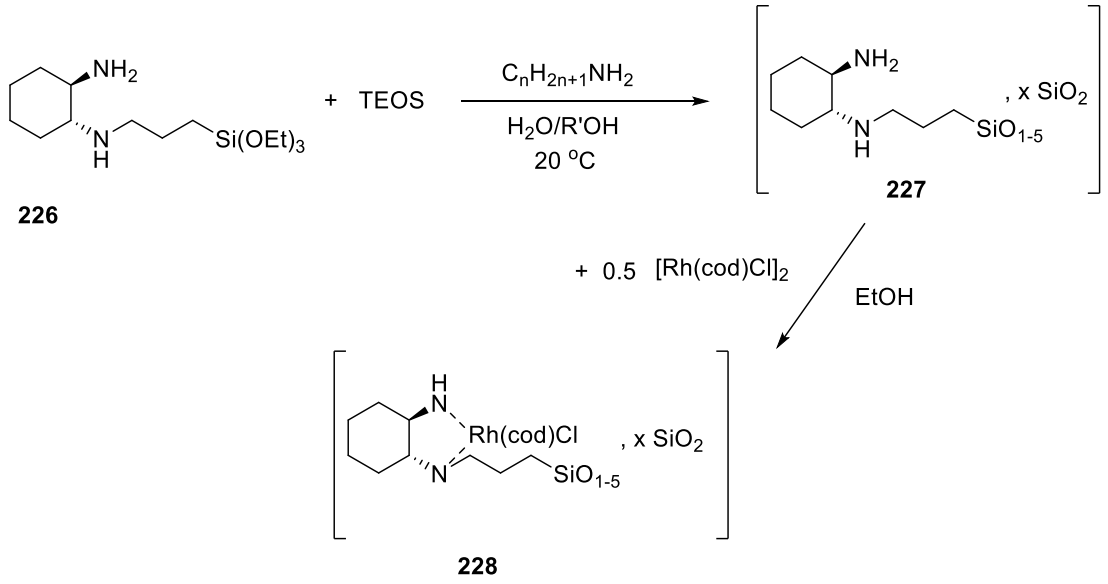

Scheme 58. Synthesis of hybrid material containing rhodium, **228.**[207]

6.2 OBJECTIVES

The main objective of this part was to prepare organic-inorganic hybrid silica materials derived from cyclobutane-1,2-diamines. The influence on the stereochemistry *cis*/*trans* of the molecular precursors in the final materials was going to be investigated as well as the hydrolysis conditions to synthesize these materials.

Therefore, taking into account that there were no precedents in in our research group on hybrid materials, we decided to prepare a new chiral hybrid silicas *cis*-**229** and *trans*-**229** which incorporate the cyclobutane moiety in their structure (Figure **82**).

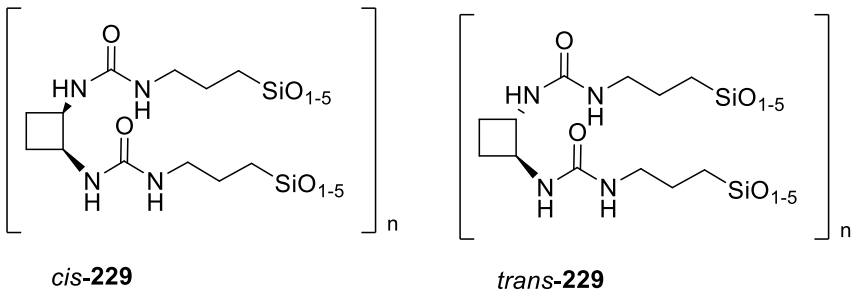

Figure 82. Hybrid silicas to be investigated.

A second objective was to prepare a hybrid material which could incorporate rhodium in order to be used in asymmetric catalysis. Then, *trans*-**230** was synthesized as precursor of *trans*-**230-Rh** to be studied in the asymmetric reduction of acetophenone (Scheme **59**).

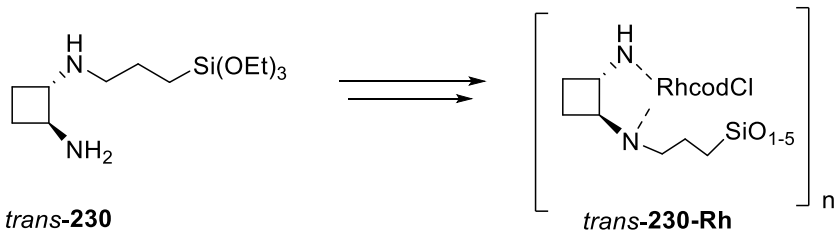

Scheme 59. Rhodium containing hybrid silica synthesized in this Thesis.

6.3 RESULTS AND DISCUSSION

As mentioned before, in the literature there are many examples about how to prepare hybrid materials from a chiral precursor. By rational hydrolysis of the molecular precursor, bridged silsesquioxane with variable morphology have been obtained in a large number of works.[208,209,210]

Moreau and co-workers[211] prepared hybrid materials based on *trans*-(1*R*,2*R*)- and *trans*-(1*S*,2*S*)-diaminocyclohexane as it has been shown in the introduction. They assayed the hydrolysis of the precursors using HCl or NaOH as catalyst obtaining good results and materials with interesting properties. Therefore, this methodology was followed to prepare hybrid materials with a cyclobutane ring as chiral moiety. Diureido derivatives were chosen because of their ability to self-assemble through H-bonds.

6.3.1 Synthesis of organo bridged silsesquioxanes based on cyclobutane-1,2-diamine.

To begin with, the preparation of *cis*-**229** and *trans*-**229** under acid and basic conditions was carried out. As a starting point, *cis*-**189** and trans-**189** were used as precursors, which were previously prepared from a substitution reaction with (3-isocyanatopropyl)triethoxysilane as described in Chapter 3 (Scheme **60**). Furthermore, it is important to highlight that *trans*-**189** is chiral whereas its diastereomer *cis*-**189** despite containing two stereocenters is a meso compound. This feature will be also worth of studying during the process of condensation.

[208] Rabu, P.; Taubert, A. *J. Mater. Chem.* **2010**, 20,
[209] Sanchez, C.; Kitagawa, S.; Sheav, K. *Chem. Soc. Rev.* **2011**, *40*, 2.
[210] Rurack, K.; Martinez-Manez, R. *The Supramolecular Chemistry of Organic–Inorganic Hybrid Materials*, Wiley, Hoboken, New Jersey, **2010**.
[211] Moreau, J. J. E.; Vellutini, L.; Bied, C.; Wong Chi Man, M. *J. of Sol-Gel Sci. and Tech.* **2004**, *31*, 151.

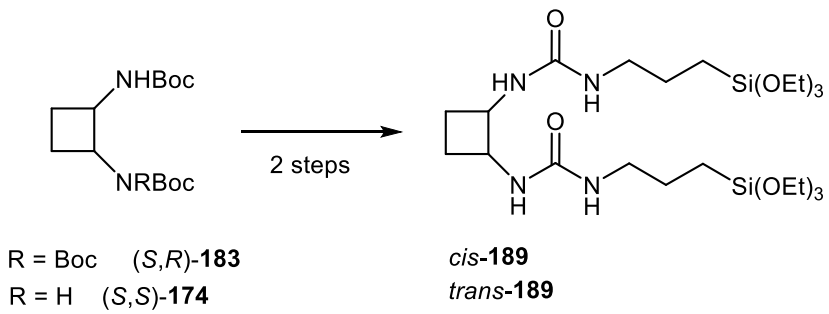

Scheme 60. Precursors *cis*-**189** and *trans*-**189** previously described in Chapter 3.

6.3.1.1 Acid Catalyzed hydrolysis and condensation of *trans*-189

Firstly, the hydrolysis of triethoxysilane *trans*-**189** was investigated under acid catalyzed conditions. To proceed, *trans*-**189** was dissolved in 5 mL of a mixture of miliQ distilled water and HCl in a molar ratio of 0.2 HCl:600 H_2O. The mixture was stirred in an oil bath at 80°C for 2 h and then it was left to stand for 2 days (Scheme **61**).

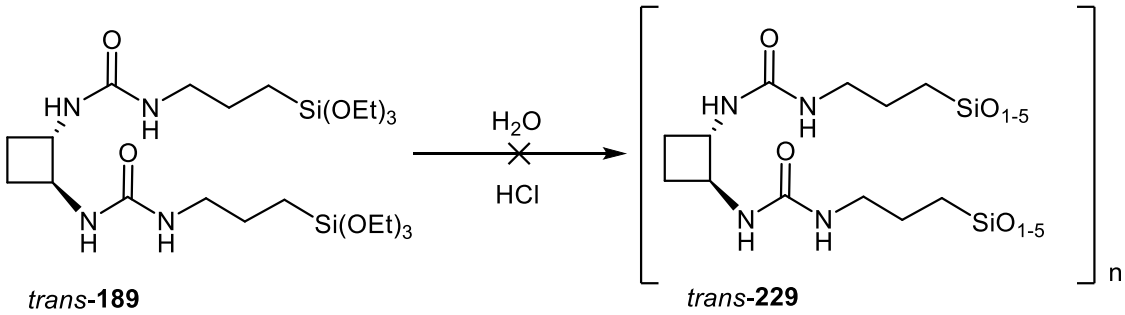

Scheme 61. Synthesis of *trans*-**229** under acid conditions.

Nevertheless, the crude was afforded as colourless oil instead of a solid as expected. Moreover, it was soluble in some organic solvents, so the NMR spectra could be performed in MeOD. Taking into account the characteristics of this product and comparing them with the normal characteristics of hybrid materials, it was deduced that a hybrid material was not formed and the obtained product was silanol *trans*-**231** (Scheme **62**).

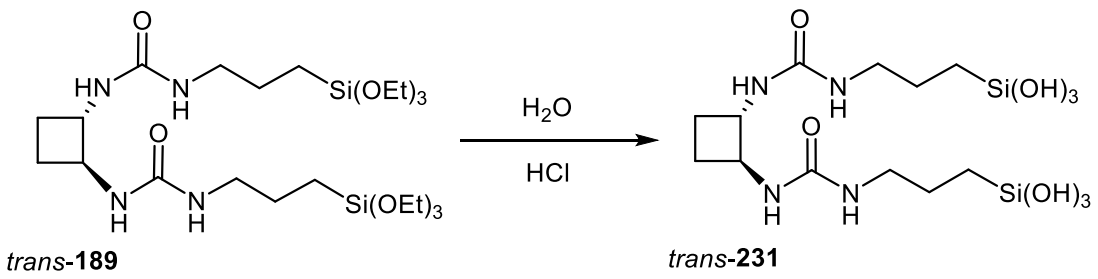

Scheme 62. Acid catalyzed reaction to afford the corresponding silanol *trans*-**231.**

To understand the formation of silanol product it is necessary to return to the mechanistic explanation of the formation of hybrid materials in the introduction. The key principle is based on specific organosilane building blocks self-assembling into hybrid mesostructures or superstructures under appropriate reaction and process conditions.[212] The method used isotropic precursors as starting materials in solution and it took place in three steps illustrated in Figure **83**. Amphiphilic species first result from the *in situ* precursor hydrolysis. They self-assemble in a second step, and organize eventually into a solid mesostructure through condensation. Although the presence of strong Van der Waals binding organic groups is clearly one of the drivers of the self-assembly process, the amphiphilicity also plays an important role. In this mechanism, organosilane *trans*-**189** must be regarded as a latent or hidden "surfactant" or "pre-surfactant", its amphiphilic character being released by hydrolysis. Upon replacing alkoxysilyl (Si-OR) groups by silanol groups (Si-OH), hydrolysis reactions generate a hydrophilic head attached to the hydrophobic organic tail with the cyclobutane as a chiral moiety.

[212] Chemtob, A.; Ni, L.; Croutxé-Barghorn, C.; Boury B. *Chem. Eur. J.* **2014**, *20*, 1.

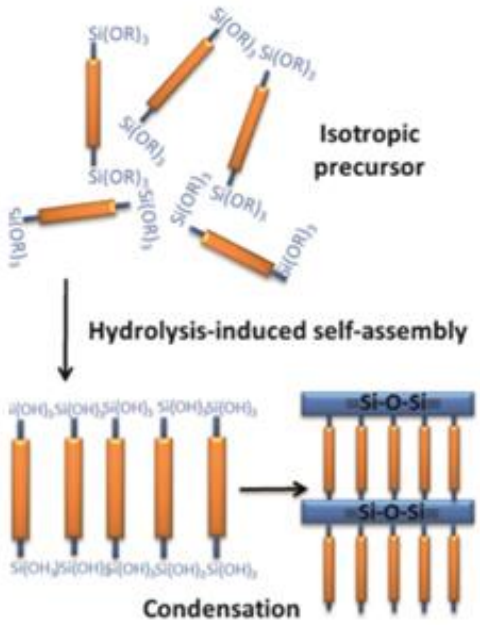

Figure 83. Schematic representation of the pathway towards nanostructured hybrids.

The role of silanols in the achievement of a highly ordered structure is crucial. Ideally, cross-linking between the "silanol heads" only occurs in a last step to lock in the mesophases, through its conversion into a siloxane network. Consequently, there are many factors playing an important role in the condensation of bridged silsesquioxanes: pH, concentration, temperature, solvent, catalyst, addition of water, etc. Barlett and co-workers[213] compared the formation of hybrid films in acid and base conditions. On the basis of their data, it was concluded that in dilute acid-catalyzed solutions, the urea-mediated self-assembly process was not favoured, and formation of the supramolecular species described in Figure **83** did not occur at these concentrations.

Therefore, it was suggested that the protonation of urea nitrogen in very diluted acid solution prevented the formation of hydrogen bonding and, subsequently the self-assembly of urea-urea moieties did not take place, affording the corresponding silanol *trans*-**231** as it has been already shown in Scheme **62**.

[213] Karatchevtseva, I.; Cassidy, D. J.; Wong Chi Man, M.; Mitchell, D. R. G.; Hanna, J. V.; Carcel, C.; Bied, C.; Moreau, J. J. E.; Bartlett, J. R. *Adv. Funct. Mater.* **2007**, *17*, 3926.

To corroborate it, the FTIR spectrum of the product from the acid-catalyzed reaction was performed and it is shown in Figure **84**. This spectrum exhibited bands at around 1685 and 1530 cm^{-1} which are assigned to the so-called amide I ($\upsilon_{c=o}$) and amide II (δ_{N-H}) modes, respectively. Strong hydrogen bonded interactions tipically yield a split between these modes of around 40 cm^{-1}, whereas the absence of hydrogen bonding leads to a split of 130 to 145 cm^{-1}, consistent whith the presence of relatively weak hydrogen bonding interactions in solution.[214] Other key peaks observed in the FTIR spectra at 3400 to 3300 cm^{-1} and 1000 to 1100 cm^{-1} are assigned to N–H/O–H and Si–O stretching modes, respectively. Accordingly, the hypothesis that due to the concentration and the pH of the reaction, the formation of hydrogen bonding was not favoured, preventing the self-assembly among the molecular precursors and leading to the corresponding silanol *trans*-**231** was established.

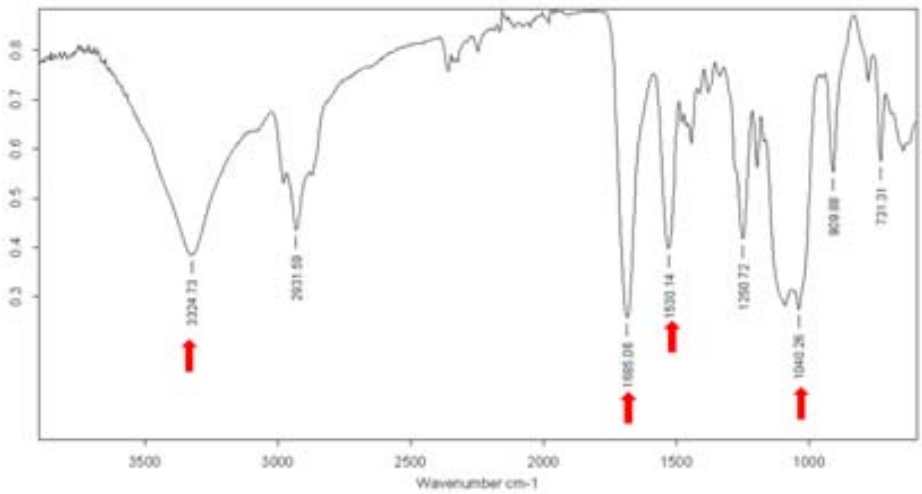

Figure 84. FTIR spectra of silanol *trans*-**231** produced by acid-catalyzed

Hence, it was decided to change the strategy of the hydrolysis and, therefore, basic catalysis was assayed.

[214] Van Esch, J.; Schoonbeek, F.; de Loos, M.; Kooijman, H.; Spek, A.L.; Kellogg, R.M.; Feringa, B.L. *Chem. Eur. J.* **1999**, *5*, 937.

6.3.1.2 Base Catalyzed hydrolysis and condensation of *trans*-189

The base catalyzed hydrolysis of triethoxysilane *trans*-**189** was performed in a mixture of ethanol and water. After that, an aqueous solution of 3 M NaOH was added until pH 12 was maintained and the mixture was heated at 80°C for 4 days under static conditions. The resulting white solid was filtered, washed with water, ethanol and acetone (Scheme **63**).

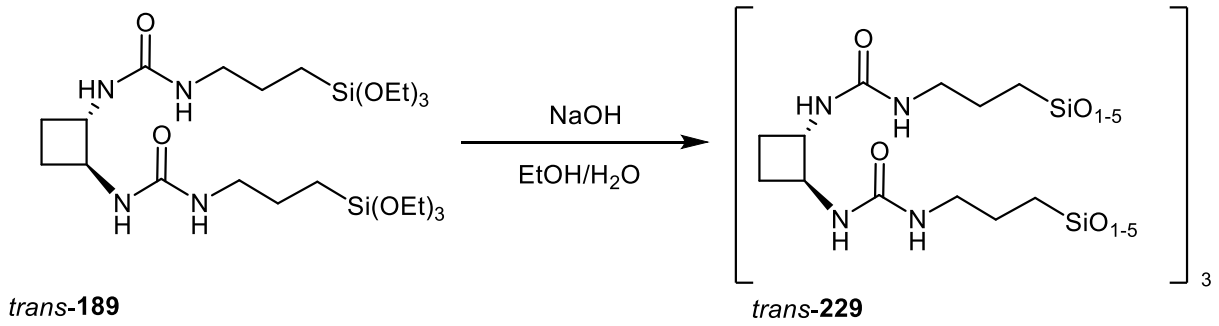

Scheme 63. Synthesis of *trans*-**229** under basic conditions.

During the reaction, differences with acid catalyzed reaction were observed. Firstly, when the water was added a microcrystalline suspension was observed. Secondly, after the product was dried in vacuo a white-yellow solid was observed (Figure **85**). Moreover, in contrast to silanol *trans*-**231**, solid *trans*-**229** was insoluble in water, chloroform, ethanol and acetone. Therefore, solid state NMR spectra were performed in order to characterize the structure of the hybrid.

Figure 85. Appearance of the base catalyzed reaction after addition of water (left) and the resulting yellowish solid (right)

6.3.1.3 CP MAS NMR of *trans*-229

The ^{29}Si and ^{13}C solid state CP MAS NMR spectra of *trans*-**229** confirmed the presence of a covalently bonded organosilicate network. The ^{13}C NMR spectrum (Figure **86**(**a**)) showed a peak at 160 ppm (C=O) and also several sp^3 carbon atoms, which are characteristic of the organic fragments. The ^{29}Si NMR spectrum (Figure **86**(**b**)) exhibited one signal at -69.34 ppm. This indicates that the hybrid material is totally condensed and that silicon atoms are occupying T^3 sites corresponding to the substructure SiC(OSi)$_3$. It could be concluded that all the silicon atoms of hybrid **229** are occupying T^3 sites and therefore, the material is completely condensed. This result was in a good agreement with the literature; hybrid materials have a high condensation degree when the preparation of the materials is carried out in basic conditions.[211]

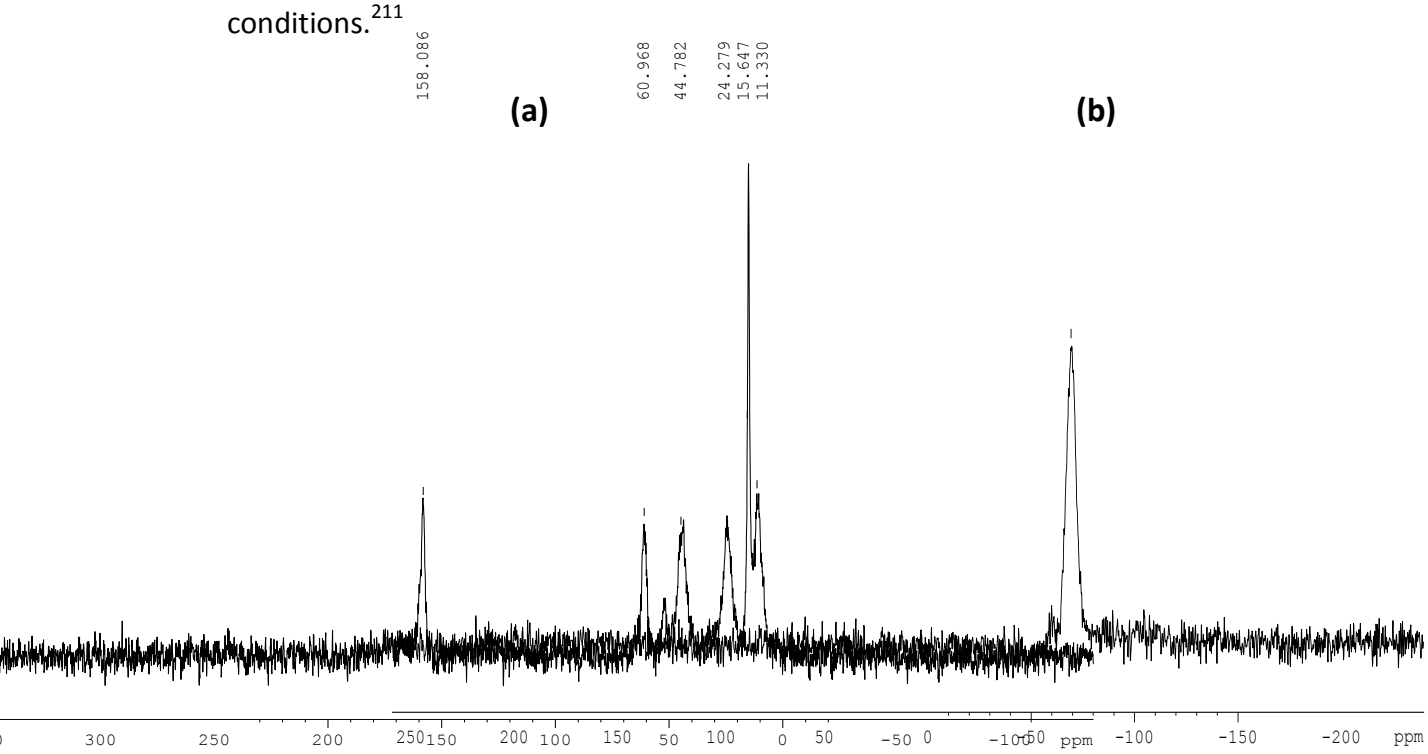

Figure 86. Solid state NMR of *trans*-**229** **(a)** ^{13}C and **(b)** ^{29}Si.

6.3.1.4 SEM studies on *trans*-229

SEM micrographs of hybrid material *trans*-**229** are shown in Figure **87**. Owing to the hydrogen bonding of the urea groups, the organic moieties tend to self-assemble

in water creating supramolecular architectures during the reaction of hydrolysis to give, finally, the arrangement of the organic fragments into a structured solid. Aggregates with lengths ranging from 16 µm to 180 µm were found. *trans*-**229** was structured into a plate-like with the minimum interlamellar distance at around 0.3 µm.

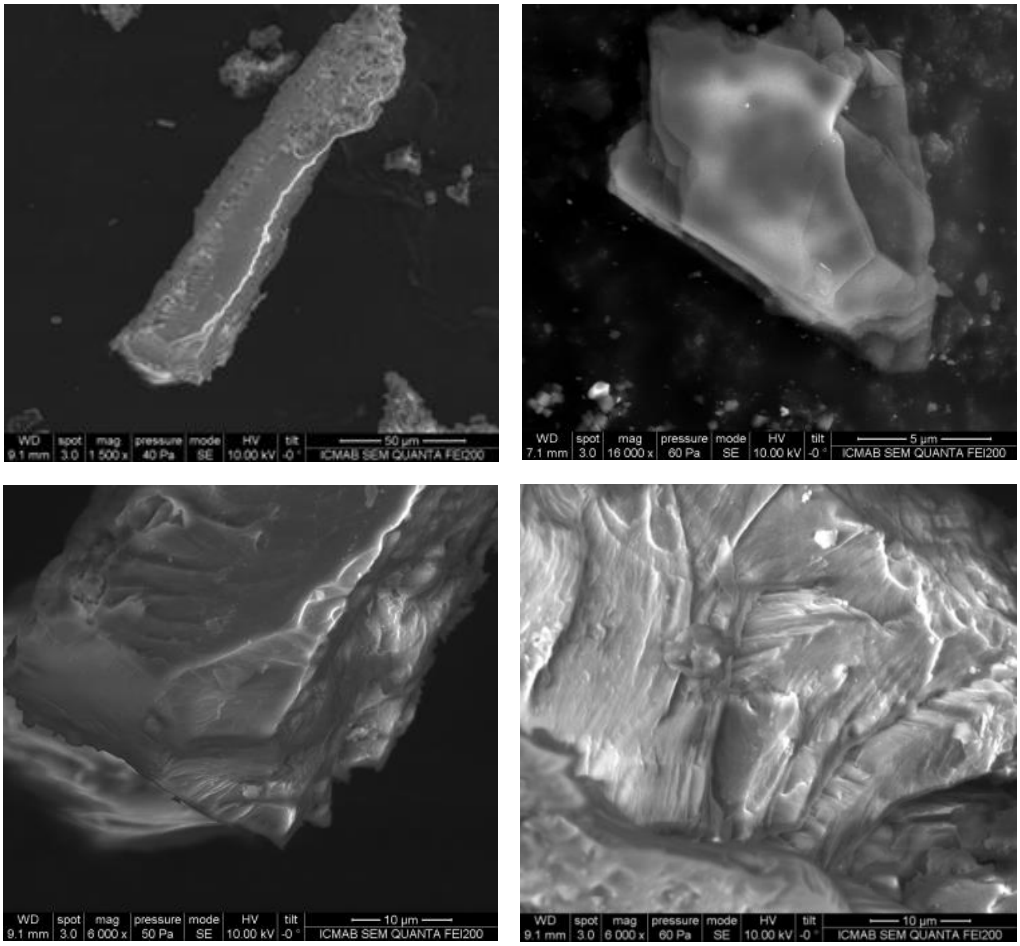

Figure 87. SEM pictures of hybrid *trans*-**229**.

6.3.1.5 Hydrolisis and condensation of *cis*-189

Acid catalyzed hydrolysis of *cis*-**189** was carried out in similar conditions than those used for its diastereomer**.** Notwithstanding, an analogous silanol as that described previously was achieved (Scheme **64**).

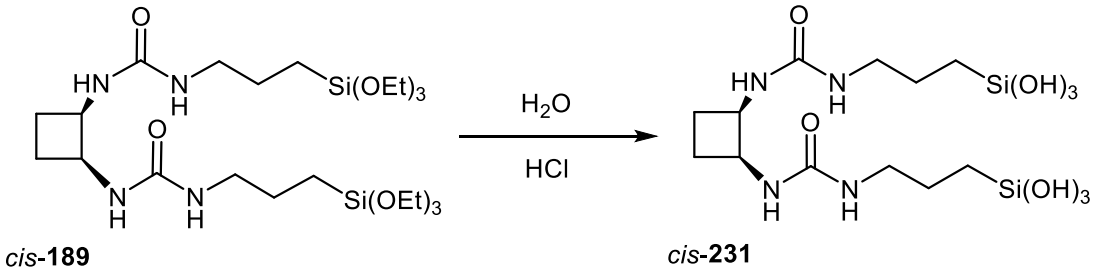

Scheme 64. Synthesis to the corresponding silanol *cis*-**231.**

Taking into account the results obtained for *trans*-**229**, a base catalyzed reaction was performed affording *cis*-**229**. (Scheme **65**).

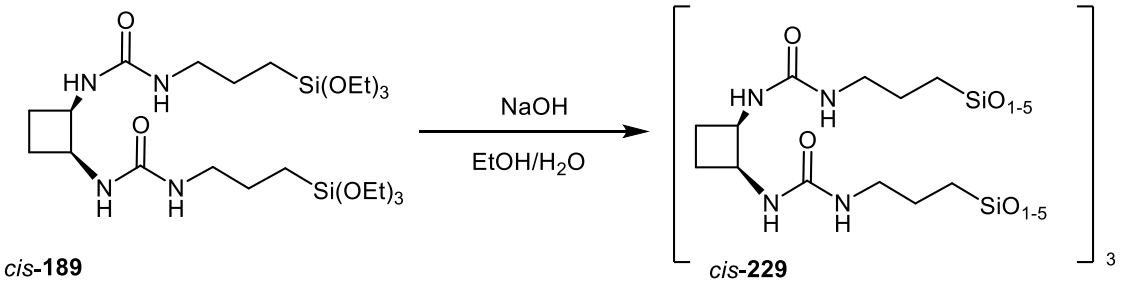

Scheme 65. Synthesis of *cis*-**229** under basic conditions.

6.3.1.6 CP MAS NMR of *cis*-229

Similarly to its *trans*- diastereomer, the ^{29}Si and ^{13}C solid state CP-MAS NMR spectra of *cis*-**229** confirmed the presence of a covalently bonded organosilicate network. The ^{13}C NMR spectrum (Figure **88a**) showed a peak at 157 ppm (C=O) and also several sp^3 carbon atoms, which are characteristic of the organic fragments. The ^{29}Si NMR spectrum (Figure **88b**) exhibited one signal at -74.74 ppm. This indicates that

the hybrid material is totally condensed similarly to what was observed for the *trans*-diastereomer. This means that there is not a diastereomeric influence on the condensation process.

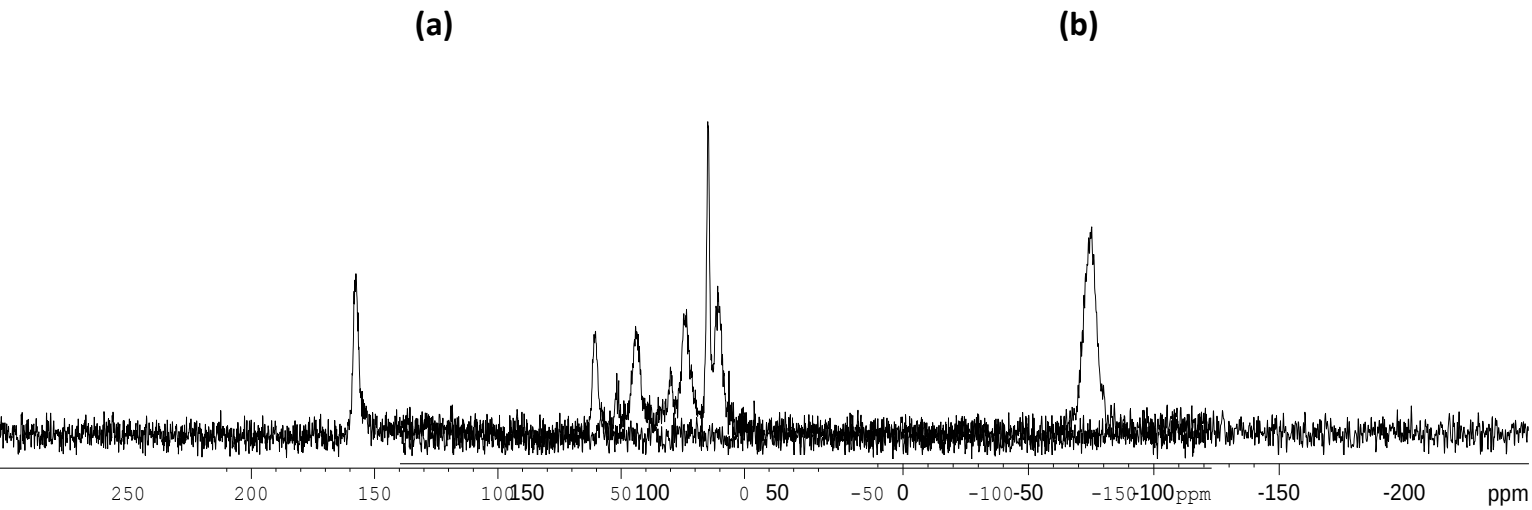

Figure 88. Solid state NMR of *cis*-**229** **(a)** ^{13}C and **(b)** ^{29}Si.

6.3.1.7 SEM studies on *cis*-229

As it can be observed in Figure **89**, SEM images of compound *cis*-**229** showed to adopt a fiber-like structure and it formed dense ordered fibers with regular size. The length of the fibers was in the micrometer range and their width ranged from 53 nm to 746 nm. On the other hand, big aggregates of 150 µm^2 of area composed by bundles of fibres were formed (Figure **89a**).

Interestingly, a right-handed helical shape was observed for *cis*-**229** (Figure **89d**). The helicity of these materials could not be explained as a transcription of chirality from the starting molecular precursor since *cis*-**189** was a *meso* compound and it had not chiral activity. Therefore, there is an example of generation of chirality through the formation of hybrid materials. Transcription of chirality from molecular precursors to materials was described by Moreau and co-workers,[196] they observed that the *R*,*R* and the *S*,*S* derived materials exhibited respectively left-handed and right-handed helicity. On the other hand, there are some examples in the literature that clearly demonstrate that the expression of chirality in amphiphile self-assemblies

cannot be straightforwardly correlated with the chiral information embedded in the monomer but it depends on the organization of the whole aggregate. For example, the group of G. Mancini has widely investigated chiral recognition in biomembrane models, in particular micelles and liposomes, either from synthetic enantiopure amphiphiles as well as from natural lipids, exploiting suitable probes of chirality.[215] Interestingly, they found that chiral recognition in amphiphile aggregates can occur in the hydrophobic region, in sites far from the stereogenic centres of the chiral head groups, where enantioselectivity cannot be observed at the molecular level. Other investigations made use of racemic (1:1) mixtures of rapidly interconverting enantiomers (e.g. biphenylic derivatives and bilirubin) as markers of chirality.[216]

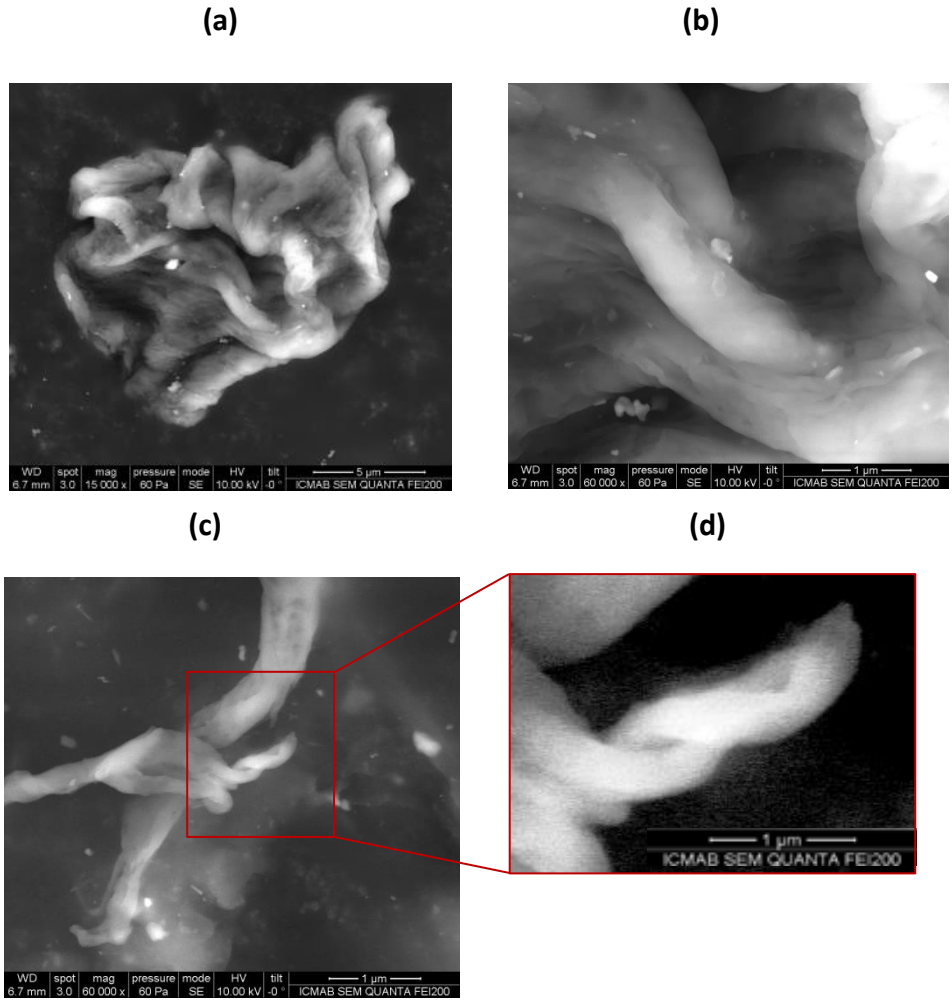

Figure 89. SEM images of *cis*-**229**.

[215] Borocci, S.; Ceccacci, F.; Cruciani, O.; Mancini, G.; Sorrenti, A. *Synlett*, **2009**, 1023.
[216] Bombelli, C.; Bernanrdini, C.; Elemento, G.; Mancini, G.; Sorrenti, A.; Villani, C. *J. Am. Chem. Soc.* **2008**, *130*, 2732.

In conclusion, hybrid materials derived from diastereoisomers *cis*-**189** and *trans*-**189**, being the first one the *meso* compound, presented different structures. SEM micrographs from the *meso* derivative *cis*-**229** showed a structure formed by fibers presenting an example of generation of helicity. In contrast, plate-like shape structures were formed for *trans*-**229**.

6.3.2 Synthesis and complexation of a new hybrid chiral material with rhodium

The focus was then moved to the preparation of a new heterogeneous enantioselective catalyst and the incorporation of a metal in the chiral hybrid matrix was investigated.

Inspired by the Bied's previous work showed in the introduction of this Chapter,[207] we designed the synthesis of a new chiral material based on cyclobutane-1,2-diamine. To prepare it, *trans*-**190** was used as the diamine precursor and the first synthetic approach was carried out.

To proceed, the double elimination of the two *tert*-butoxycarbonyl groups in (*S,S*)-**174** was achieved quantitatively yielding amine hydrochloride (*S,S*)-**175.** Then, (*S,S*)-**175**, (3-isocyanatopropyl)triethoxysilane, and freshly distilled triethylamine were mixed in a sealed tube to perform the reaction under pressure and in an oil bath at 87°C overnight. Nevertheless, when the crude was checked by NMR it was found that the SN2 reaction had not worked and the starting material (*S,S*)-**175** was then recovered (Scheme **66**).

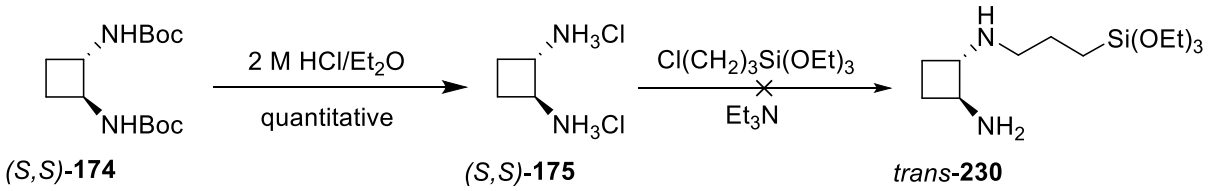

Scheme 66. First synthethic route to synthesize *trans*-**230**.

The proposed explanation was that triethylamine was not strong enough to completely deprotonate the hydrocloride (*S,S*)-**175** in order to have the diamino group

free to act as a nucleophile. Then, another synthethic approach based on a two-step deprotection of the diamino groups in (*S,S*)-**153** was carried out. From (*S,S*)-**153** the *tert*-butyl carbamate protection was removed by reaction with a 2 M solution of hydrochloric acid to provide quantitatively ammonium chloride (*S,S*)-**170.** Then, the benzyl carbamate group in (*S,S*)-**170** was hydrogenolyzed in the presence of Pd/C to afford (*S,S*)-**175** in 80% yield. Finally, the nucleophilic substitution was successfully performed giving free amine *trans*-**230** (Scheme **67**).

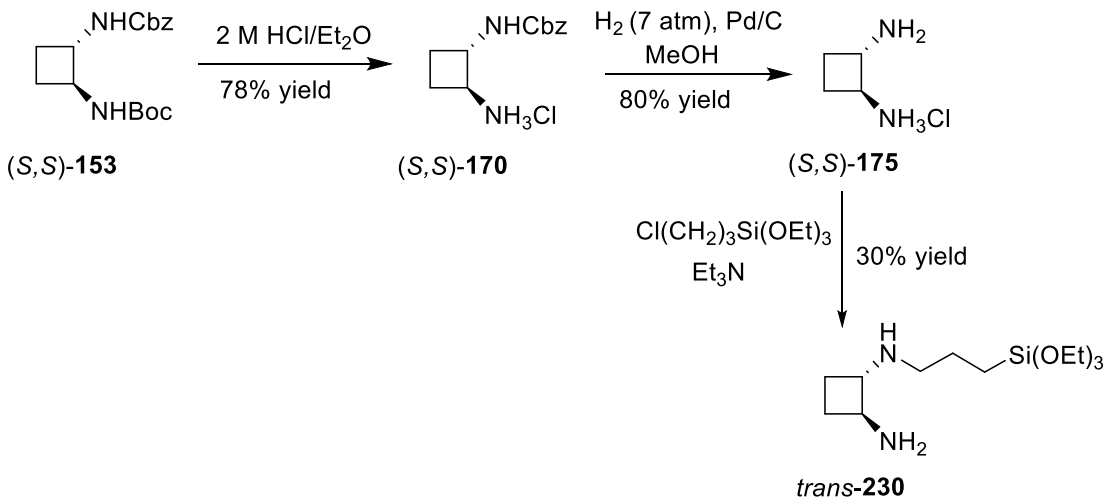

Scheme 67. Synthetic route to achieve *trans*-**230**.

Molecular precursor *trans*-**230** was then used to prepare a new hybrid material containing a chiral ligand based on the 1,2-diamine moiety. Afterwards, the chiral ligand was used to immobilize rhodium complexes with the purpose of examinating the activity of the material in asymmetric catalysis. To proceed, in a Schlenk tube under nitrogen atmosphere, a solution containing *trans*-**230** and $[Rh(cod)Cl]_2$ in dry ethanol was stirred at 20 ^{o}C for 1 hour and then, ethanol, distilled water and a 0.1 M solution of NH_4F as catalyst were added. The reaction was then kept at 50 ^{o}C for 12 h and then cooled at room temperature. An orange solid was formed after after two days, which was left to stand for 5 days to provide hybrid *trans*-**230-Rh** (Scheme **68**).

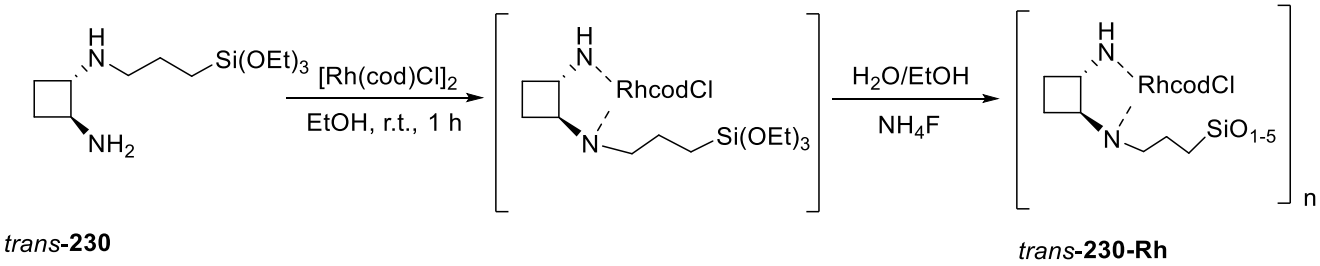

Scheme 68. Synthetic route to *trans*-**230-Rh**

6.3.2.1 Spectroscopic study of *trans*-230-Rh

Spectroscopic data indicate that the organic moiety was incorporated into the silicate framework. The bands at 3321 and 2933.5 cm^{-1} in the IR spectrum are characteristic of the N-H and C-H bonds and it indicates that the organic diamine is immobilized in the material. In the ^{13}C NMR spectrum (Figure **90a**), the signals at 25-30 and 50-60 ppm are characteristic of the organic moiety. The signal at 10 ppm which corresponds to a carbon linked to silicon indicates that the diamine is incorporated without cleavage to the Si-C bond. Moreover, there was an additional broad signal at 78 ppm which corresponds to vinyl carbons linked to the rhodium metal and indicates the cyclooctadiene ligand remained in the coordination sphere of the metal. The signal observed in the ^{29}Si NMR spectrum at -69 ppm (Figure **90b**) correspond respectively to the substructure T^3 $CSi(OSi)_3$. It indicates that the material is totally condensed without presence of non-condensed OH or OEt groups.

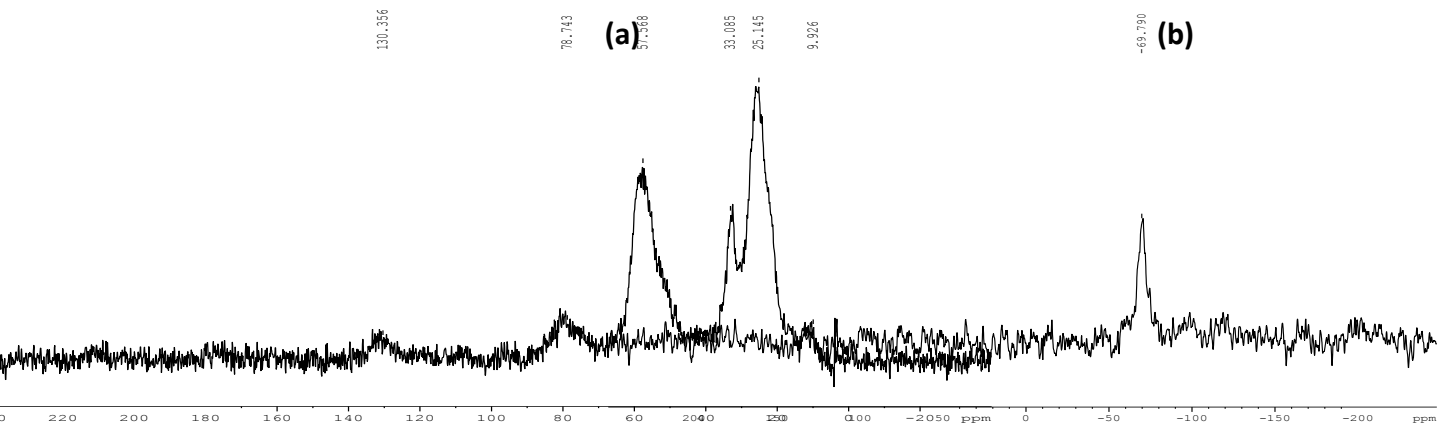

Figure 90. (a) ^{13}C NMR and **(b)** ^{19}Si NMR of hybrid *trans*-**230-Rh**

On the other hand, the presence of rhodium (I) in the solid was investigated by SEM and analysed by ICP-MAS as described below.

6.3.2.2 SEM/EDX analyses

Scanning electron microscopy with energy dispersive X-ray spectroscopy (SEM/EDX) is the best known and most widely-used of the surface analytical techniques. It is based on the interaction of X-ray excitation and a sample with the fundamental principle that each element has a unique atomic structure allowing a unique set of peaks on its X-ray spectrum.[217] To stimulate the emission of characteristic X-rays from a specimen, a beam of X-rays is focused into the sample being studied. At rest, an atom within the sample contains ground state (or unexcited) electrons in discrete energy levels or electron shells bound to the nucleus. The incident beam may excite an electron in an inner shell, ejecting it from the shell while creating an electron hole where the electron was. An electron from an outer, higher-energy shell then fills the hole, and the difference in energy between the higher-energy shell and the lower energy shell may be released in the form of an X-ray. The number and energy of the X-rays emitted from a specimen can be measured by an energy-dispersive spectrometer. As the energy of the X-rays are characteristic of the

[217] Goldstein, J. *Scanning Electron Microscopy and X-Ray Microanalysis*, Springer, Weinheim, 2003.

difference in energy between the two shells, and of the atomic structure of the element from which they were emitted, this allows the elemental composition of the specimen to be measured (Figure **91**).

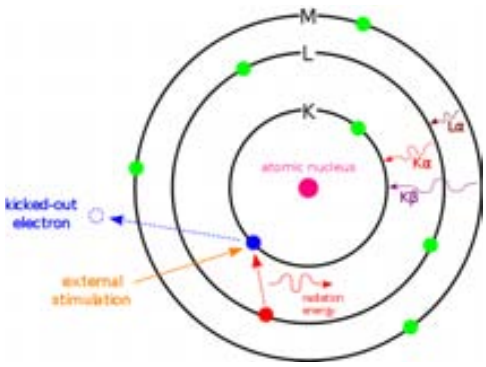

Figure 91. Principle of Energy-dispersive X-Ray spectroscopy (EDS, EDX, or XEDS)

SEM, accompanied by X-ray analysis, is considered a relatively rapid, inexpensive, and basically non-destructive approach to surface analysis. It is often used to survey surface analytical problems before proceeding to techniques that are more surface-sensitive and specialized.

The presence of rhodium in hybrid *trans*-**230-Rh** was confirmed by SEM (Figure **92**, Table **9**). The Rh/Si ratio found in the hybrid material (1:1) was similar than that expected on the basis of the stoichiometry of the polycondesantion mixture. On the other hand, the rhodium/chlorine ratios (which are superimposed in Figure **92** due to the similar energy of absorption of rhodium and chlorine atoms in keV) were found to be close to one. The exact structure of the rhodium complex probably corresponds to a Rh^{+} species.

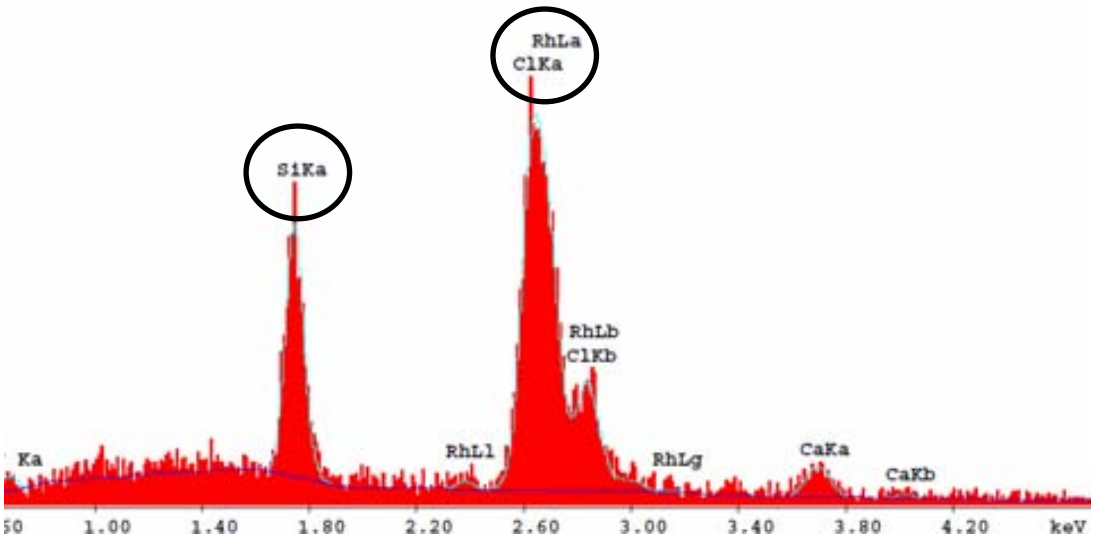

Figure 92. EDX spectrum for *trans*-**230-Rh**

Table 9. Rh/Si and Rh/Cl ratios in *trans*-**230-Rh** determined by SEM.

Analyses	Rh / Si ratio of *trans*-**230-Rh**	Rh / Cl ratio of *trans*-**230-Rh**
	SEM	**SEM**
1	1 : 1	1 : 1
2	1.2 : 1	1 : 1.2
3	1 : 1.5	1 : 1.5

SEM images of hybrid *trans*-**230-Rh** are shown in Figure **93** and they exhibited a featureless solid with aggregates composed basically by fibers with different lengths and widths.

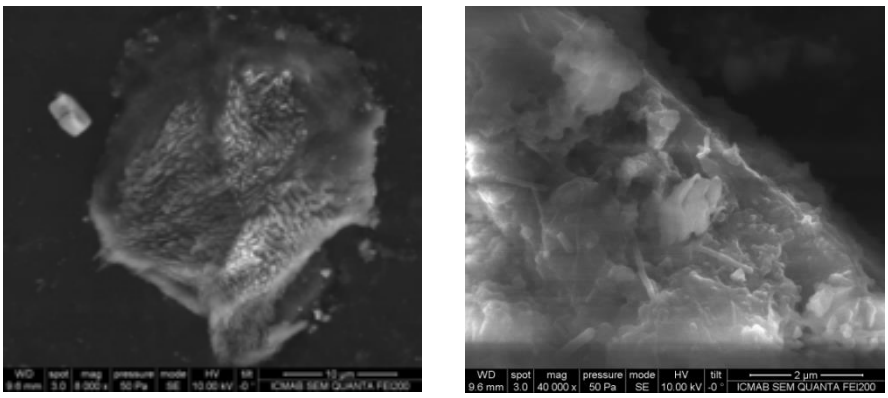

Figure 93. SEM images of hybrid *trans*-**230-Rh.**

6.3.2.3 ICP-MAS study

The quantitative presence of rhodium was then detected by ICP-MAS. Inductively coupled plasma mass spectrometry is a type of mass spectrometry which is capable of detecting metals and several non-metals at concentrations as low as one part in 10^{12} (part per trillion). In ICP-MS sampled material is transferred by an argon flow into inductively coupled plasma in which an effective temperature of 7000 K results in atomisation and ionisation of the material. Subsequently, the ions are extracted into a mass spectrometer, with which the elemental composition of the material is determined.

The mass spectrum obtained showed an important peak at m/z 103 which confirmed the presence of rhodium in the sample. In addition, the percentatge of rhodium in the sample was determined to be 19%. The molecular formula of the compound was not determined but with the ^{19}Si NMR spectra we know that every silicon atom is surrounded by three –OSi groups. Moreover, with ^{13}C NMR and SEM/EDX analyses we determined that there was the fragment RhCl(cod) in the molecule. Thence, we could suppose that the molecular formula of the fragment is approximately: $C_{15}H_{28}ClN_2O_3RhSi$ (Figure **94**).

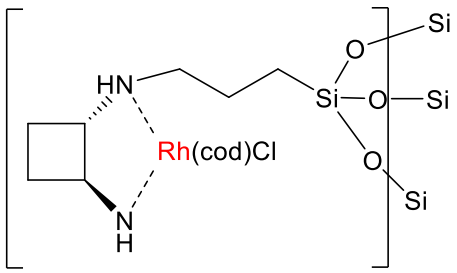

Formula of **230-Rh**: $C_{15}H_{28}N_2O_3RhSi$ (Mol. Wt.: 415)

% Rhodium = 102 (Mol. Wt Rh)/415 = 25 %

Figure 94. Structure of complex *trans*-**230-Rh**

Taking it into account, if we divide the atomic mass of rhodium by the molecular mass of the molecular formula shown in Figure **94** the result is 25% of

rhodium, which is in good agreement with the results obtained by ICP-MAS. There was a little loss of rhodium probably by leaching.

6.3.3 Catalytic activity of *trans*-230-Rh in the enantioselective reduction of acetophenone

The asymmetric hydrogenation of ketones employing small organic molecules as hydrogen donors (for example, formic acid and especially 2-propanol) constitutes a practical alternative to the use of reducing agents. In this process Ru, Rh, and Ir chiral catalysts are particularly useful and have been intensively studied.[218] A hybrid chiral ligand containing rhodium, *trans*-**230-Rh**, synthesized in this thesis was assayed as catalyst in some preliminary tests as it is shown in Scheme **69**. There are some examples in the literature for the enantioselective reduction of prochiral ketones.[219,220,221]

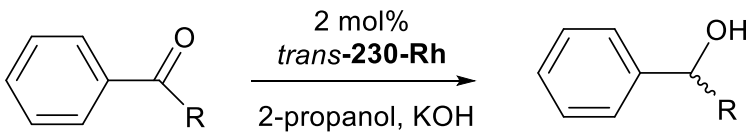

Scheme 69. Hydride transfer reduction of aromatic ketones using *trans*-**230-Rh** as catalyst.

Thus, the catalytic activity of *trans*-**230-Rh** in the hydride-transfer reduction of acetophenone was examined. As it was mentioned before, this catalyst is analogous to the one described with cyclohexane by Bied and co-workers. The experiment was performed using 2 mol% of rhodium, the amount of solid catalyst was adjusted according to its rhodium content and 2-propanol was both the solvent of the reaction and the hydride donor.

[218] Noyori, R.; Hashiguchi, S. *Acc. Chem. Res.* **1997**, *30*, 97.
[219] Maggie, I.; Sachin, G.; Sheryl, Wiskur, L. *J. Org. Chem.*, **2012**, *77*, 3570.
[220] Noyori, R.; Hashiguchi, *S. Acc. Chem. Res.* **1997**, *30*, 97.
[221] Gamez, P.; Fache, F.; Lemaire, M. *Tetrahedron: Asymmetry* **1995**, *6*, 705.

Then, the catalytic activity of *trans*-**230-Rh** was studied and the alcohol was obtained in a rate of conversion of 85% after 12 h of reaction at 85 ^{o}C. Concerning the selectivity, the reduction of acetophenone using a non-chiral catalyst $[Rh(cod)Cl]_2$ was also assayed in order to compare both catalytic systems. The *ee* of the obtained 1-phenylethanol was measured by HPLC on a chiral columm (Daicel chiracel OD) and using as eluent a mixture of hexane:2-propanol (98:2) and with a flow of 0.5 mL/min. The retention times for *S*-(-) and *R*-(+) were 30 and 38 min respectively. As it can be seen in Figure **95**, there was no induction of selectivity for the reduction of acetophenone with *trans*-**230-Rh**.

(a)

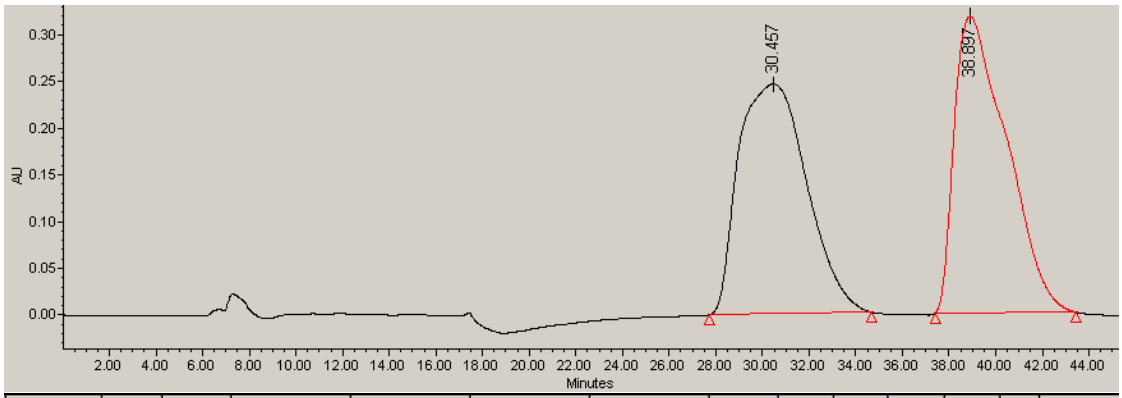

Retention Time (min)	Purity1 Angle	Purity1 Threshold	PDA/FLR Match1 Spect. Name	PDA/FLR Match1 Angle	PDA/FLR Match1 Threshold	PDA/FLR Match1 Lib. Name	Area (µV*sec)	% Area	Height (µV)	Int Type	Amount	Units	Peak Type
30.459							47985183	49.57	240339	bb			Unknown
38.897							48817356	50.43	314904	bb			Unknown

(b)

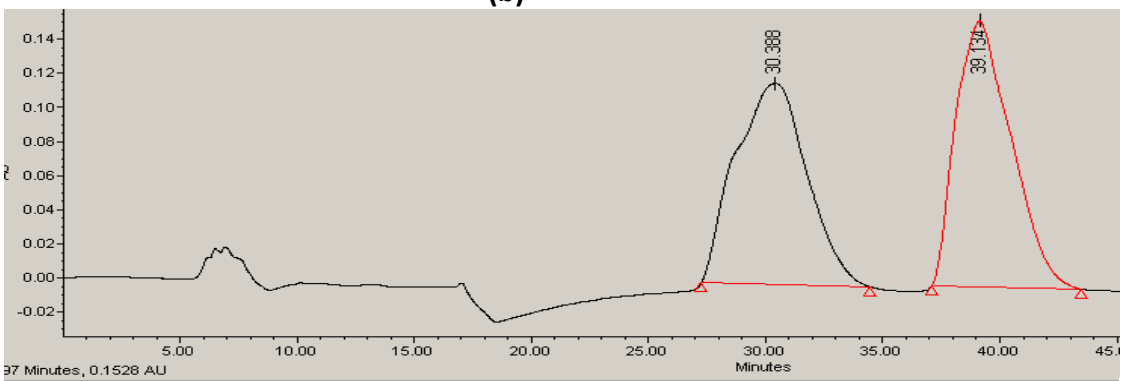

Retention Time (min)	Purity1 Angle	Purity1 Threshold	PDA/FLR Match1 Spect. Name	PDA/FLR Match1 Angle	PDA/FLR Match1 Threshold	PDA/FLR Match1 Lib. Name	Area (µV*sec)	% Area	Height (µV)	Int Type	Amount	Units	Peak Type
30.388							25040357	49.40	117835	bb			Unknown
39.134							25651788	50.60	155921	bb			Unknown

Figure 95. HPLC chromatogram of reduction of acetophenone catalyzed by **(a)** $[Rh(cod)Cl]_2$ and by **(b)** *trans*-**230-Rh**

As explained before, this catalyst is analogue to the one described by Bied and co-workers using cyclohexane derivatives.[207] In their work, a rate of conversion between 80 and 90% was reached after 20 h of reaction and 85 ^{o}C and the alcohol was obtained with a low ee between 10% and 16%. Comparing these results to the ones obtained in our laboratory, it can be concluded that *trans*-**230-Rh** is better than the catalyst of that work in terms of catalytic activity but worse in terms of enantioselectivity.

Zassinovich and co-workers proposed a catalytic cycle for such a reaction.[222] Considering our catalyst *trans*-**230-Rh** this would be the mechanism: a pentacoordinated rhodium (I) hydride complex containing cyclobutane-1,2-diamino moiety as ligand (**B**) was assumed to be the key intermediate. In the suggested catalytic cycle**,** deprotonation of propan-2-ol by KOH should occur on the solvated complex (**A**). Acetone extrusion from the 2-propoxy ligand in **B** generates the hydride derivative (**C**) that, in the stereodetermining step, should preferentially add to the *re or si* face of acetophenone (**D**) to give the **E**. Displacement of 1-phenylethanol by propan-2-ol would then restore the starting complex (Scheme **70**).

In 2005, Somanathan and co-workers[223] prepared a number of bidentate and tridentate ligands derived from cyclohexane-1,2-diamine and they were tested with Ru(II) and Rh(I) for catalytic activity in the transfer hydrogenation reaction of ketones. Interestingly, when ligands were used with $[RhCl(cod)]_2$ as a source of metal, excellent yields were obtained of the alcohol (80-90%), but as a racemic mixture. This is in agreement with Lemaire's observation, where bulky COD induces geometry of the complex in which rhodium is too far from the metal and it is unable to induce enantioselectivity in the formation of the alcohol.[224]

It is important to highlight that this was a preliminary test and due to the lack of time it was not possible to test other sources of metal with other ligands than COD.

[222] Zassinovich, G.; Mestroni, G. *Chem. Rev.* **1992,** *92,* 1051.
[223] Aidé-Cortez, N.; Flores-López, C. Z.; Rodríguez-Apodaca, R.; L. Z. Flores-López, Parra-Hake, M.; Somanathan, R. *Arkivoc* **2005**,162.
[224] Bernard, M.; Guiral, V.; Delbeeq, F.; Fache, F.; Sauet, P.; Lemaire, M. *J. Am. Chem. Soc.* **1998**, *120*, 1441.

The improvement of the activity of the catalyst through different methods is under active investigation in our laboratory.

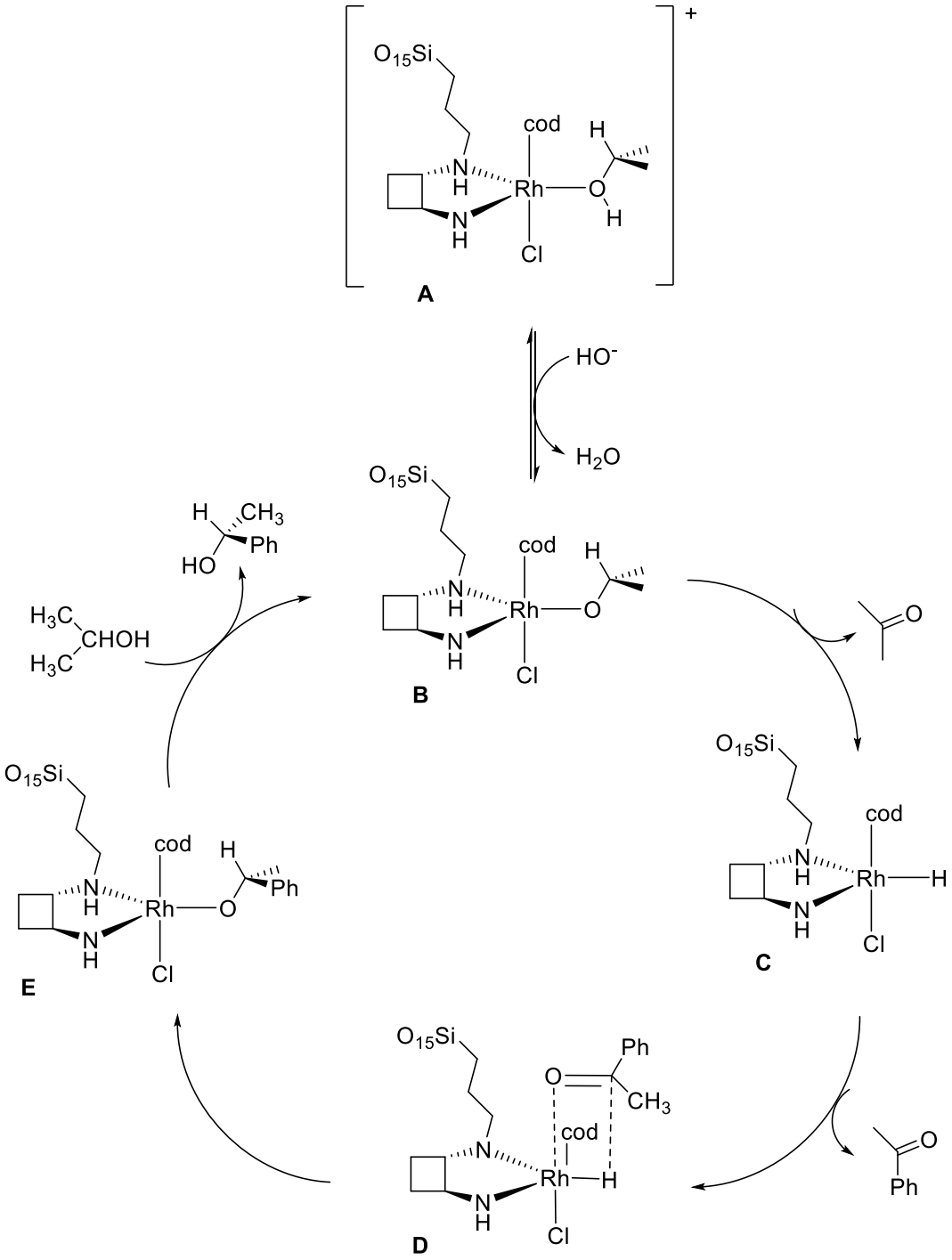

Scheme 70. Proposed catalytic cycle for transfer hydrogenation of ketones using rhodium complexes with 1,2-disubstituted cyclobutane as chiral ligand.

6.4 SUMMARY AND CONCLUSIONS

i. Two new hybrid materials *cis*-**229** and *trans*-**229** based on cyclobutane-1,2-diamine were prepared stereoselectively and with moderate overall yields.

ii. The acid-catalyzed and base catalyzed hydrolysis or *cis*- and *trans*-triethoxysilane derivatives were assayed: the acid hydrolysis led to silanols *cis*-**231** and *trans*-**231**. The base catalyzed hydrolysis led to the corresponding hybrid materials *cis*-**229** and *trans*-**229**.

iii. NMR in solid state, IR and SEM techniques were employed to study the structure of these materials.

The results showed that the structures formed have a strong dependence on the conditions of hydrolysis. By ^{13}C and ^{19}Si NMR in solid state, *cis*-**229** and *trans*-**229** showed the presence of only T^3 sites corresponding to a fully condensed system. Moreover, by SEM it was observed that *trans*-**229** presented a plate like structure while *cis*-**229** presented bundles of fibers with examples of helicity. This was especially interesting because it shows that creation of chirality from meso precursors was achieved.

iv. A new hybrid chiral material with rhodium, *trans*-**230-Rh** was prepared in moderate yields.

v. *trans*-**230-Rh** was fully characterized by CP MAS NMR (^{13}C and ^{19}Si), IR, SEM, EDX and ICP-MAS.

The NMR in solid state showed a material totally condensed with predominantly T^3 sites. On the other hand, the presence of rhodium was identified by using EDX analysis, which ratios between Si and Rh are in a good agreement with the stoichiometric ratios of polycondensation (1 a 1). Finally, the mass spectrum obtained by ICP-MAS showed an important peak at *m/z* 103 corresponding to the presence of

rhodium in the sample. The quantitative analyses of rhodium in the sample showed a 25% of rhodium, which was in good agreement with the calculated value.

vi. This catalyst was assayed in the enantioselective reduction of acetophenone and the *ee* was determined by chiral HPLC. Although the catalytic activity was good because the conversion was 85% in 12 hours, the catalyst did not show induction of enantioselectivity, leading to a racemic mixture of 2-phenylethanol.

As a general conclusion, the synthesis of three hybrid materials (one of them containing rhodium) was achieved by using the knowledge of our laboratory. Different experimental techniques were used to study their structure and their preliminary activity in metal catalysis was tested showing a high catalytic activity but without enantioselective induction.

CHAPTER VII

Synthesis of cyclobutane ligands and applications in the stabilization of ruthenium nanocatalysts

7 Synthesis of cyclobutane ligands and applications in the stabilization of ruthenium nanocatalysts

7.1 INTRODUCTION

7.1.1 Background.

Nanoparticles are defined as particles with size in the range of 1 to 100 nm at least in one of the three dimensions.[225] Because of this very small size scale, they possess an immense surface area per unit volume, a high proportion of atoms in the surface and near surface layers, and the ability to exhibit quantum effects. As it is shown in Figure **96**, the number of publications including the prefix nano- in their title has grown during the past decades to satisfy the needs of specific applications.

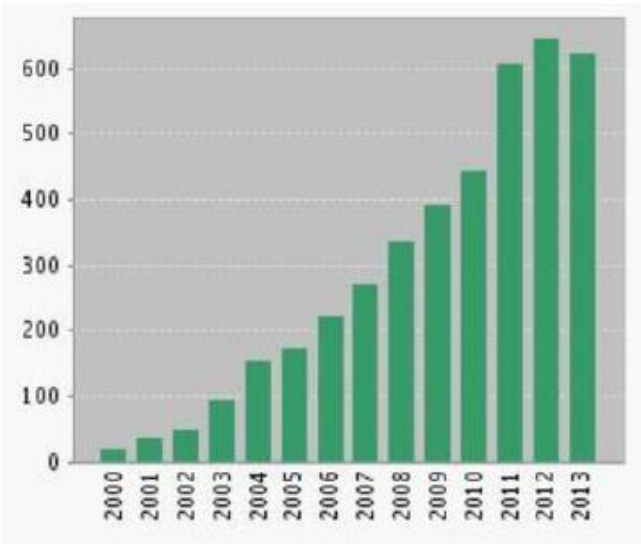

Figure 96. Number of articles including the prexif nano- in their title (from Web of Science).

The history of metal nanoparticles begins with Faraday's study of gold colloids. In his Bakerian Lectures of 1857, Michael Faraday proposed that microscopic particles of gold are responsible for the beautiful coloration of the famed ruby–gold decorative glasses.[226] A fine example is the famous Lycurgus Cup in the British Museum (Figure **97**).

[225] Schmid, G. *Nanoparticles. From Theory to Applications*, Wiley-VCH, Weinheim, **2003**.
[226] Barber, D. J.; Freestone, I. C. *Archaeometry* **1990**, *32*, 33.

Figure 97. The Lycurgus Cup dates from Roman times. The glass appears green in daylight (reflected light), but red when light is transmitted from the inside of the vessel.

Metallic nanoparticles have mainly been studied because of their strong optical absorption in the visible region. Moreover, these particles are found to show application in catalysis,[227] oligonucleotide recognition,[228] size- and shape- dependent optical properties,[229] electronic properties,[230] optical devices,[231] and medicinal applications.[232]

However, the physical and chemical properties of nanoparticles depend on several factors such as (i) the particle size and the size dispersity; (ii) the structure of the particles; (iii) the surface of the particles; (iv) the shape of the particles; and (v) the organization of the particles into a nanomaterial and their dispersability. In turn, these factors will depend on the successful control, including reproducibility, of the synthetic process and the stability of the particles.

The most common tools used for stabilizing nanoparticles have been so far polymers, but they may not be usable in selected chemical or physical applications. For this reason, the use of ligands coordinated at the surface of the particles has been

[227] Hayakawa, K.; Yoshimura, T.; Esumi, K. *Langmuir* **2003**, *19,* 5517.
[228] Elghanian, R.; Storhoff, J.J.; Mucic, R.C.; Letsinger, R.L.; Mirkin, C.A. *Science* **1997**, *277*, 1078.
[229] Link, S.; El-Sayed, M.A. *J. Phys. Chem. B* **1999**, *103*, 4199.
[230] Kamat, P.V. *Chem. Rev.* **1993**, *93*, 267.
[231] Gaponik, N.P.; Talapin, D.V.; Rogach, A.L. *J. Mater. Chem.* **2000**, *10*, 2163.
[232] Hirsch, L.R.; Stafford, R.J.; Bankson, J.A.; Sershen, S.R.; Rivera, B.; Price, R.E.; Hazle, J.D.; Halas, N.J.; West, J.L. *Proc. Natl. Acad. Sci. USA* **2003**, *100*, 13549.

considerably developed in the past few years.[233,234,235] The presence of ligands prevents the particles from coalescing and allows their self-assembly onto various surfaces.

7.1.2 Nanoparticles in catalysis

Heterogeneous metal catalysis, which benefits from easy removal of catalyst materials and possible use of high temperatures, suffered for a long time from lack of selectivity and understanding of the mechanistic aspects that are indispensable for parameter improvements. Homogeneous metal catalysis is very efficient and selective, and it is used in a few industrial processes, but it suffers from the impossibility of removal of the catalyst from the reaction media and its limited thermal stability.

These demanding conditions bring a new research impetus for catalyst development at the interface between homogeneous and heterogeneous catalysis with supported and biphasic catalysts, including also studies which will help to establish the desired optimized catalytic systems.[236]

In this context, the use of transition-metal nanoparticles (NPs) in catalysis is crucial as they mimic metal surface activation and catalysis at the nanoscale and thereby bring selectivity and efficiency to heterogeneous catalysis

7.1.3 Synthesis of metal nanoparticles.

Metal nanoparticles can be prepared by two distinct ways, by subdivision of bulk metals (a physical method) or by the growth of particles starting from metal atoms, which are obtained from molecular or ionic precursors (a chemical method)

[233] Jansat, S.; Picurelli, D.; Pelzer, K.; Philippot, K.; Gómez, M.; Muller, G.; Lecante, P.; Chaudret, B. New J. Chem. **2006**, 30, 115.
[234] Nath, S.; Jana, S.; Pradhan, M.; Pal, T. *Journal of Colloid and Interface Science* **2010**, *341*, 333.
[235] Chen, S.; Murray, R. W. *Langmuir* **1999**, *15*, 682.
[236] Astruc, D. *Nanoparticles and Catalysis,* Wiley, Weinheim, Germany, **2007**.

(Figure **98**). The latter preparative method is more suitable to obtain small and uniform nanoparticles than the former. In the latter method, control of the atom aggregation is the most important step to control the size and uniformity of the metal nanoparticles. In the present Thesis, metal nanoparticles are going to be prepared by the chemical method from a molecular precursor in solution in the presence of suitable stabilizers.

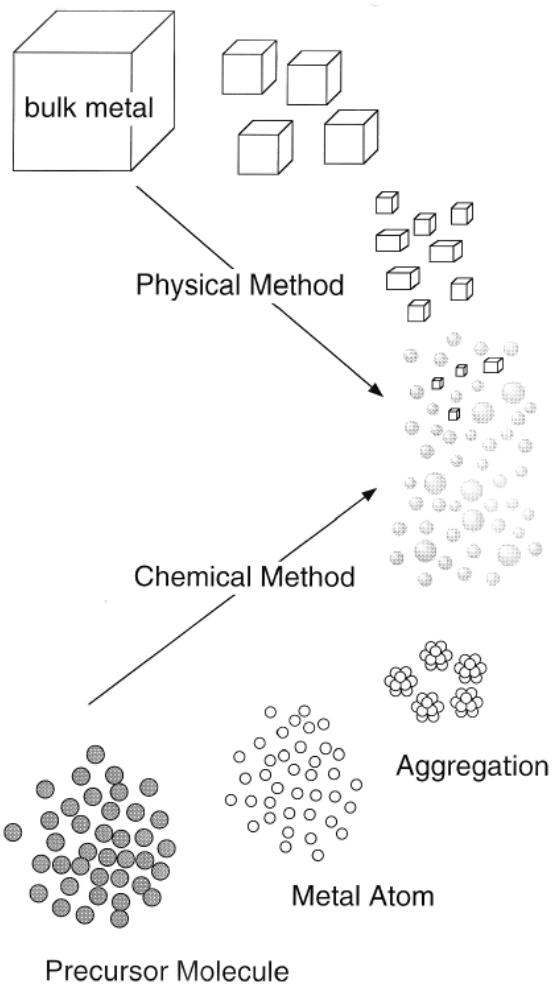

Figure 98. Schematic illustration of preparative methods of metal nanoparticles.

Stable transition metal colloidal suspensions can be obtained by a wide range of procedures which allows one to choose the most suitable method for a specific application: thermal, photochemical, or sonochemical decomposition of organometallic compounds,[237,238] synthesis by condensation of atomic metal vapor,[239]

[237] Belapurkar, A. D.; Kapoor, S.; Kulshreshtha, S. K.; Mittal, J. P. *Mater. Res. Bull*. **2001**, *36*, 145
[238] Vinodgopal, K.; He, Y.; Ashokkumar, M.; Grieser, F. *J. Phys. Chem. B,* **2006,** *110,* 3849.

chemical reduction of metal salts, which was the most widely used method to generate colloidal suspensions of metals,[240] or by the displacement of ligands from organometallic compounds. This is the method used in this Thesis for the preparation of ruthenium nanoparticles, where some zerovalent organometallic complexes can be converted into colloidal suspension of metals by reduction or ligands displacements. This methodology provides well-controlled NPs regarding size, dispersion, and shape, the control of which depends on the ligands used for their stabilization.[241,242]

7.1.4 Stabilization of metal nanoparticles.

Today, catalysis is the essential application of metal nanoparticles although they find also application in such diverse fields as photochemistry, nanoelectronics, or optics and biomedicine. As catalysts, these systems show a great potential because of the large surface area of the particles. The original catalytic approach is to use coloidal metallic particles finely dispersed in organic or aqueous solution or a solvent mixture. One of the main characteristics of colloidal particles is their small size. Unfortunately, these metallic nanoparticles are unstable with respect to agglomeration to the bulk. In most cases, this aggregation leads to the loss of the properties associated with the colloidal state of these metallic particles. For example, during catalysis the coagulation of colloidal particles used as catalyst leads to a significant loss of activity. The stabilization of metallic colloids and thus the means to preserve their finely dispersed is a crucial aspect to consider during their synthesis.[243]

---

[239] Bradley, J. S. In *Clusters and Colloids: From Theory to Application*, Ed. VCH, New York, **1994**.
[240] Boutonnet, M.; Kizling, J.; Stenius, P.; Maire, G. *Colloids Surf.* **1982**, *5*, 209.
[241] Pan, C.; Pelzer, K.; Philippot, K.; Chaudret, B.; Dassenoy, F.; Lecante, P.; Casanove, M. J. *J. Am. Chem. Soc.* **2001**, *123*, 7584.
[242] Philippot, K.; Chaudret, B. *C. R. Chim.* **2003**, *6*, 1019.
[243] Roucoux, A.; Schulz, J.; Patin, H. *Chem. Rev.* **2002,** *102,* 3757

7.1.4.1 Electrostatic stabilization

Ionic compounds such as halides, carboxylates, or polyoxoanions, dissolved in generally aqueous solution can generate the electrostatic stabilization. The adsorption of these compounds and their related counterions on the metallic surface generates an electrical double-layer around the particles (Figure **99**). This results in a Coulombic repulsion between the particles. However, they are very sensitive to any phenomenon able to disrupt the double layer like ionic strength so it is crucial to control these parameters to guarantee an effective electrostatic stabilization.

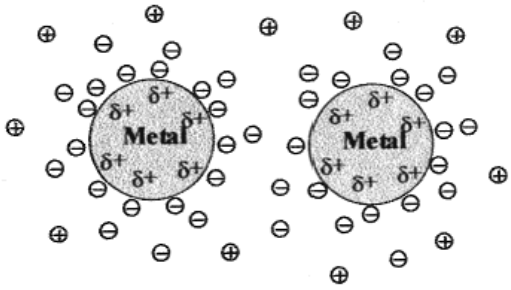

Figure 99. Schematic representation of electrostatic stabilization of metal colloid particles.

7.1.4.2 Steric stabilization

Metal nanoparticles can be also prevented from aggregating using macromolecules such as polymers or oligomers. The adsorption of these molecules at the surfaces of the particles provides a protective layer. Nevertheless, the nature of the macromolecules adsorbed influence the thickness of the protective layer and it can thus modify the stability of the colloidal metal particles (Figure **100**).

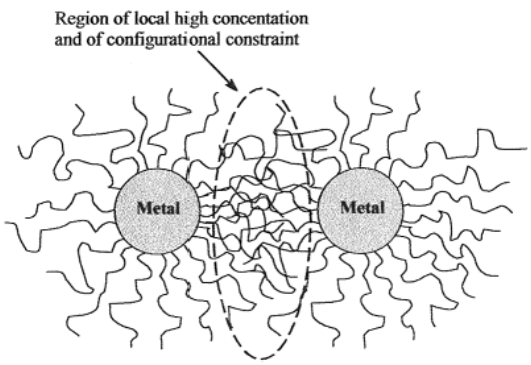

Figure 100. Schematic representation of steric stabilization of metal colloid particles.

7.1.4.3 Ligand stabilization.

The term *ligand stabilization* has been chosen to describe the use of traditional ligands to stabilize transition metal colloids. This stabilization occurs by the coordination of metallic nanoparticles with ligands such as phosphines, thiols, amines, etc.

The investigation of this part of the Thesis was carried out in collaboration of the group of Prof. Montserrat Gómez from the Université Paul Sabatier in Toulouse. For the past few years, the research of Prof. Gómez has been focused on the preparation of well-defined metallic nanoparticles stabilized by different classical ligands.[244,245,246] One of their main objectives is to better understand how the ligand can affect the stabilization of the NPs depending on its interaction with the metallic surface.

For instance, in a work of her group from 2008[247] in order to elucidate the presence of π-interactions between the ligand and the metallic surface, 4-(3-phenylpropyl)pyridine was chosen as a NPs stabilizer for its simple structure containing a pyridine group, which, upon σ-coordination could favour the flat phenyl approach to the metallic surface (Scheme **71**).

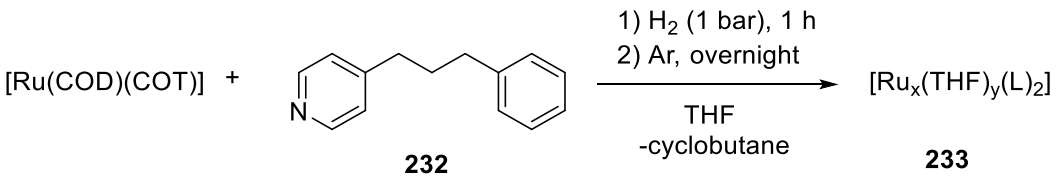

Scheme 71. Synthesis of Ru nanoparticles **233** stabilized by **232** synthesized by the group of Prof. Gómez.[247]

[244] Gómez, M.; Philippot, K.; Collière, V.; Lecante, P.; Muller, G.; Chaudret, B. *New J. Chem.* **2003**, *27*, 114.
[245] Ramirez, E.; Jansat, S.; Philippot, K.; Lecante, P.; Gómez, M.; Masdeu, A.; Chaudret, B. *J. Organomet. Chem.* **2004**, *689*, 4601.
[246] Jansat, S.; Picurelli, D.; Pelzer, K.; Philippot, K.; Gómez, M.; Muller, G.; Lecante, P.; Chaudret, B. *New J. Chem.* **2006**, *30*, 115.
[247] Favier, I.; Massou, S.; Teuma, E.; Philippot, K; Chaudret, B.; Gómez, M. *Chem. Commun.*, **2008**, 3296.

Small and homogeneously dispersed nanoparticles showing a quite narrow size distribution around a mean diameter of 1.3 ± 0.3 nm, were obtained under these conditions (Figure **101**). This result contrasted with the formation of large and agglomerated particles that they observed using simple pyridine as stabilizer. This suggested that the presence of a phenyl group in 4-(3-phenylpropyl)pyridine participates in the stabilization of the particles favouring their dispersion probably as a result of the coordination of the phenyl group on the metallic surface.

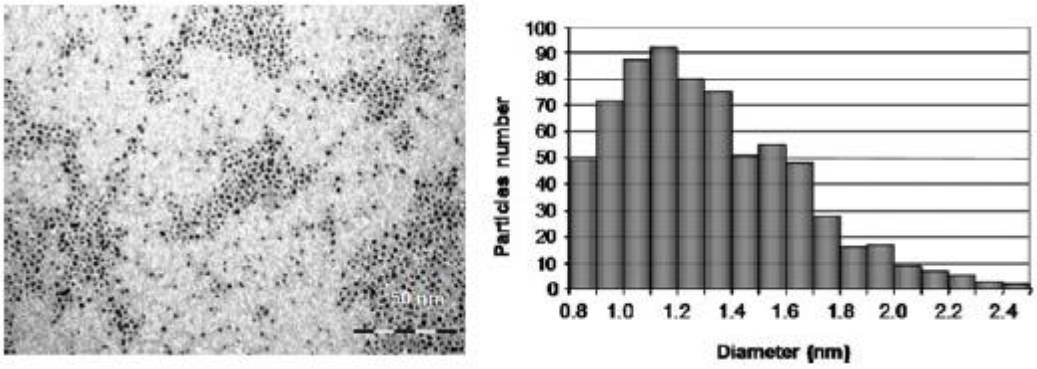

Figure 101. TEM micrograph of RuL nanoparticles and size distribution histogram (ϕmean = 1.27 ± 0.33 nm for 696 particles).

They also have used other metal transition nanoparticles. For instance, palladium nanoparticles stabilized by chiral diphosphite ligands were synthesized[248] showing high activity and enantioselectivity in the asymmetric allylic alkylation of racemic substrates such as 3-acetoxy-1,3-diphenyl-1-propene and 3-acetoxy-1-cyclohexene with dimethyl malonate under basic Trost conditions.[249]

Other research groups have focused on the stabilization of ruthenium nanoparticles using chiral ligands. For instance, Van Leeuween and co-workers studied the application of ruthenium nanoparticles (RuNPs) stabilized by the *N*-heterocyclic carbenes (NHC) *N*,*N*'-di(tertbutyl)imidazol-2-ylidene (I^{t}Bu) and 1,3-bis(2,6-diisopropylphenyl)imidazol-2-ylidene (IPr) as catalysts in the hydrogenation of several

[248] Favier, I.; Gómez, M.; Muller, G.; Axet, M. R.; Castillón, S.; Claver, C.; Jansat, S.; Chaudret, B.; Philippot, K. *Adv. Synth. Catal.* **2007**, *349*, 2459.
[249] Trost, B. M.; Murphy, D. J. *Organometallics* **1985**, *4*, 1143.

substrates.[250] The RuNHC nanoparticles were active catalysts in the hydrogenation of aromatics and they shown an interesting ligand effect, being RuIPr NPs generally more active than RuItBu ones (Scheme **72**).

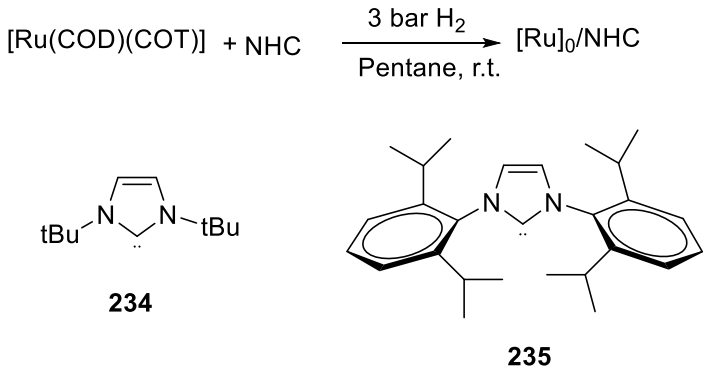

Scheme 72. *N*-heterocyclic carbenes and reaction conditions used for the synthesis of RuNHCs nanoparticles by the group of Prof. Van Leeuwen.[250]

[250] Gonzalez-Galvez, D.; Lara, P.; Rivada-Wheelaghan, O.; Conejero, S.; Chaudret, B.; Philippot, K.; Van Leeuwen, P. W. N. M. *Catal. Sci. Technol.* **2013**, *3*, 99.

7.2 OBJECTIVES

The last part of this Thesis was foccused on the preparation of ruthenium nanoparticles stabilized by chiral ligands which could be tested in heterogeneous catalysis.

Cyclobutane pyrrolidines **237**, **238** and **239** (Scheme **73**) were synthesized for the first time by Dr. Jordi Aguilera in his PhD thesis with the aim to evaluate them as stabilizers for ruthenium nanoparticles in the future. In the current chapter, these compounds were prepared following the synthethic methodology used in the past by Dr. Jordi Aguilera.

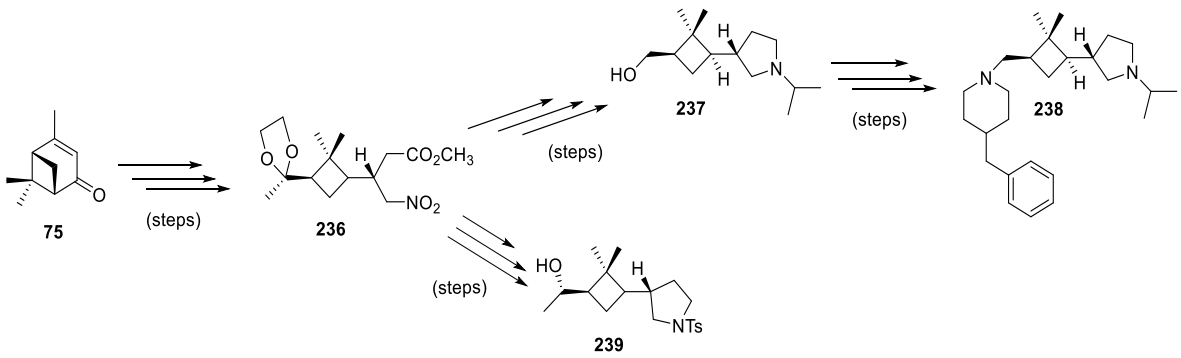

Scheme 73. Pyrrolidines **237, 238** and **239** tested in this Thesis.[251]

237, 238 and **239** were used as ligands to stabilize ruthenium nanoparticles. To do so, a short stay in the laboratory of Prof. Gómez in Toulouse allowed me to synthesize and characterize the stabilized ruthenium nanoparticles. Finally, these systems were tested as catalysts in the reduction of acetophenone.

[251] Aguilera, J. *PhD Thesis*, UAB, 2010.

7.3 RESULTS AND DISCUSSION.

7.3.1 Synthesis of pyrrolidines 237 and 238 from intermediate nitroester 236.

The use as precursors of chiral bicyclic terpenoids derivatives such as (-)-verbenone, has been traditionally the preferred choice as starting materials in our laboratory. This is due to the fact that these molecules are available with high purity and enantiomeric excess at reasonable prices.

Thus, starting from (-)-verbebone as chiral precursor, intermediate nitroester **236** was stereoselectively prepared in good yields.[252] Then, nitroester **236** was heated to reflux for two hours in the presence of ammonium formate, 10% Pd/C and four equivalents of acetone, affording the *N*-isopropyl γ-lactam **240** in quantitative yield. Then the acid hydrolysis of the ketal in **240** led quantitatively to methyl ketone **241** which was transformed into methyl ester **242** by treatment with NaOBr in dioxane (Lieben degradation) and subsequent methylation using diazomethane. The reaction of **242** with a large excess of $LiBEt_3H$ in refluxing THF overnight afforded **237**, where the amide carbonyl and the methyl ester had been reduced (78% yield). This alcohol can be transformed into diamine **238** by activation of the alcohol as mesylate and subsequent nucleophilic substitution by 4-benzylpiperidine (Scheme **74**).[253]

[252] Moglioni, A. G.; Brousse, B. N.; Álvarez-Larena, Á.; Moltrasio, G. Y.; Ortuño, R. M. *Tetrahedron: Asymmetry* **2002**, *13*, 451.
[253] Aguilera, J.; Moglioni, A.; Mor, A.; Ospina, J.; Illa, O.; Ortuño, R.M. *Tetrahedron* **2014**, *70*, 6546.

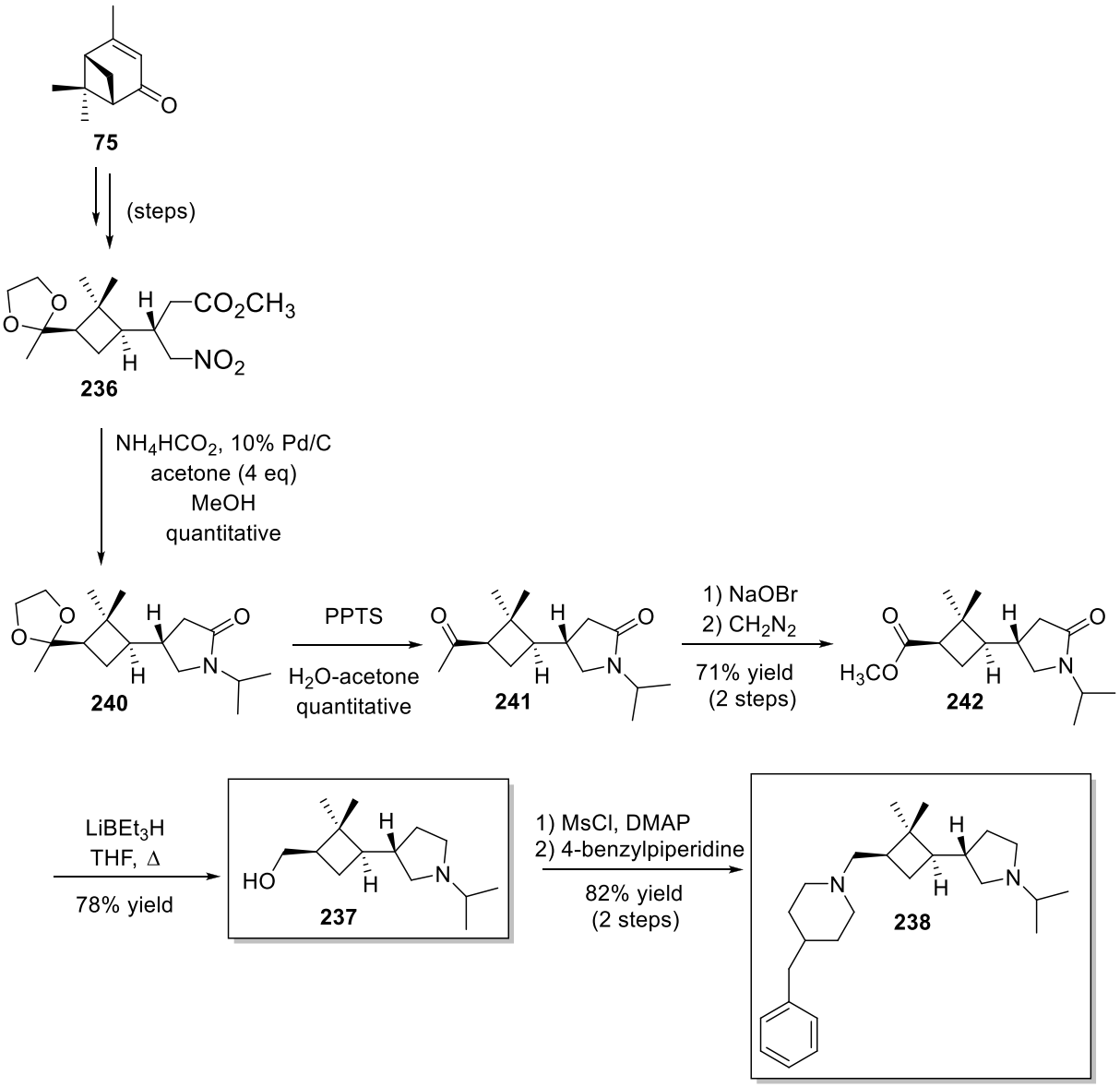

Scheme 74. Cyclobutane pyrrolidines prepared in this thesis.[251]

7.3.2 Synthesis of pyrrolidine 239

The synthesis of pyrrolidine **239** was carried out via Mitsunobu reaction.[254] The Mitsunobu protocol involves the reaction of an alcohol and an acidic pronucleophile (NuH) in the presence of a phosphane, very often PPh_3, and an azodicarboxylate to afford compounds containing a newly formed C-O, C-S, C-N or C-C bond. To proceed,

[254] Mitsunobu, O.; Yamada, Y. *Bull. Chem. Soc. Japan* **1967**, *40*, 2380.

nitroester **236** was reduced to the corresponding aminoalcohol **243** using $LiBH_4$ in THF/MeOH to reduce the ester to alcohol followed by catalytic hydrogenation to reduce the nitro group to amine. Then, the amine group was protected as a sulphonamide since this common protection for amine groups results often in crystalline compounds more resistant to nucleophilic attack than carbamates. The chemoselective tosylation of the amine in **244** using 1 equivalent of TsCl in pyridine provided **245** in a 71% yield. This compound was submitted to the Mitsunobu conditions using PPh_3 and DIAD in cold THF to afford the *N*-tosyl pyrrolidine **246** in excellent yield Then, the ethylene glycol ketal in **246** was hydrolysed under mild conditions using PPTS as an acid catalyst, and the resulting methyl ketone was treated with $NaBH_4$ without any chiral auxiliary to test the intrinsic stereoselectivity of the cyclobutane pyrrolidine. The resultant alcohols mixture (ratio 10:1 according to integration in ^{1}H-NMR spectrum) was enriched in the secondary alcohol with absolute *S* configuration (**Scheme 75**).[255]

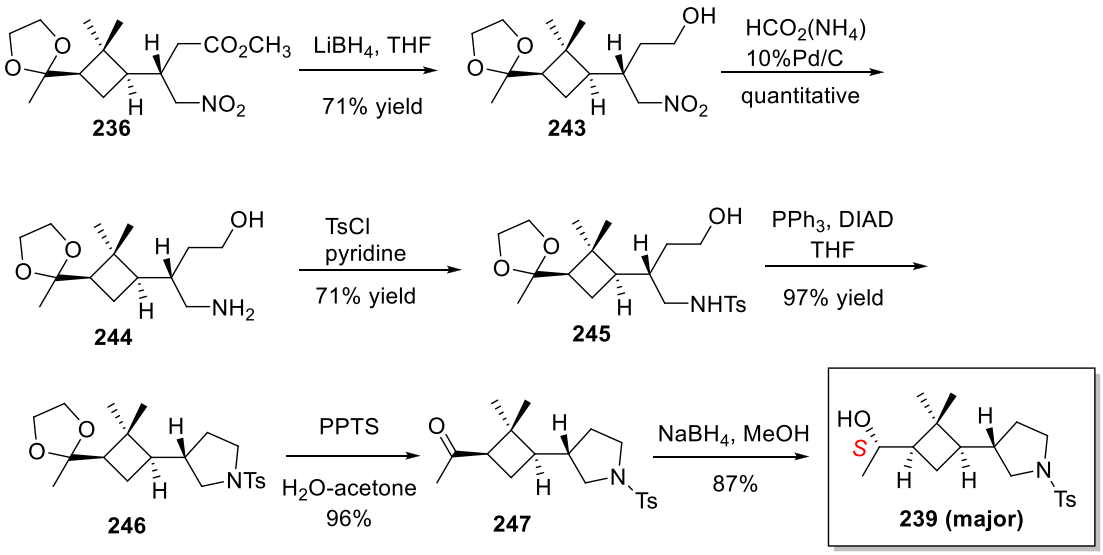

Scheme 75. Synthesis of *N*-tosyl pyrrolidine **239**.

[255] Hergueta, A.R.; López, C.; Fernández, F.; Caamaño, O.; Blanco, J. M. *Tetrahedron: Asymmetry* **2003**, *14*, 3773.

7.3.3 Synthesis of rutenium nanoparticles stabilized by 237, 238 and 239.

As it has been mentioned before, **237**, **238** and **239** (**Figure 102**) were tested as chiral ligands in the stabilization of Ru nanoparticles in collaboration with the laboratory of Professor Gómez. Due to the presence in the molecule of three controlled stereocenters in a very constraint conformation due to the cyclobutane moiety, it was thought that these molecules could not only stabilize nanoparticles but confer an asymmetric environment that could be interesting for their use in the catalytic synthesis of optically active compounds.

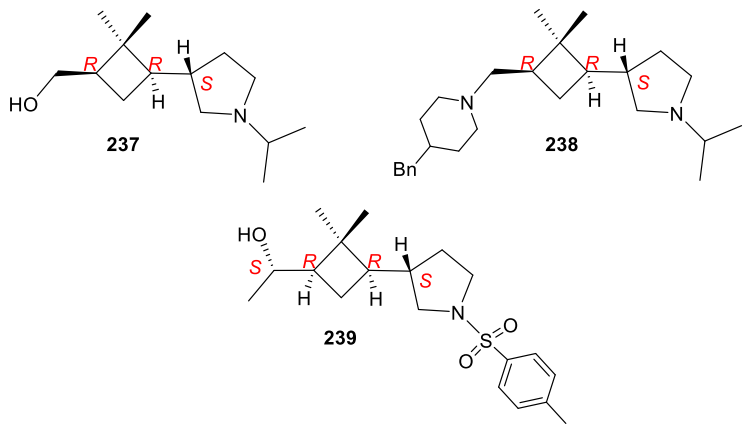

Figure 102. Cyclobutane pyrrolidines that will be tested as chiral ligands in this Thesis.

Thus, when the synthesis of *N*-alkyl ciclobutane γ-lactams was achieved, I moved to Toulouse to collaborate with Dr. Montserrat Gómez in the preparation of ruthenium nanoparticles using our ligands as stabilizers. Ligand **248** (Scheme **85**) was considered as a reference because of its ability to both strongly coordinate at the metallic surface and promote hydrogenation.[256]

First of all, Ru(NP) were synthesized according the methodology previous described by Chaudret and co-workers.[257] Ruthenium nanoparticles (colloids **RuNP$_1$–RuNP$_3$**) were synthesized from [Ru(COD)(COT)] (1,5-cyclooctadiene)(1,3,5-

[256] Favier, I.; Lavedan, P.; Massou, S.; Teuma, E.; Philippot, K.; Chaudret, B.; Gómez, M. *Top. Catal.* **2013**, *56*, 1253.
[257] Philippot, K.; Chaudret, B. *C. R. Chimie* **2003**, *6*, 5626.

cyclooctatriene)ruthenium(0) as metal precursor and the appropriate chiral ligand **237**, **238**, **239** and **248** (Scheme **76**).

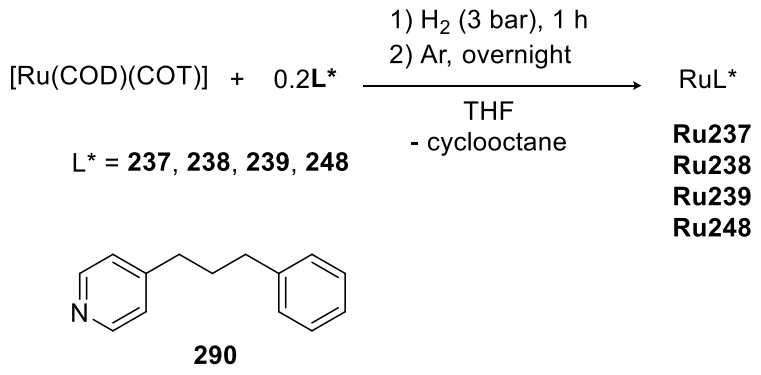

Scheme 76. Synthesis of RuNP stabilized by ligands **237**, **238, 239** and **248**.

The procedure was as follows: Ru(COD)(COT) was weighted in a glove box and it was dissolved in anhydrous THF inside a Fisher-Porter bottle. First of all, hydrogenation in order to afford bulk ruthenium was carried out in 60 minutes. Afterwards, the reaction was stirred overnight under argon atmosphere. A change in the colour due to the formation of ruthenium metal and consequent release of cyclooctane gas could be observed in Figure **103**. Finally, the solvent was removed and the product was washed with pentane in order to remove the excess of ligands and to precipitate the nanoparticles. Subsequently, the nanoparticles were isolated as a black powder after pentane precipitation (Figure **104**).

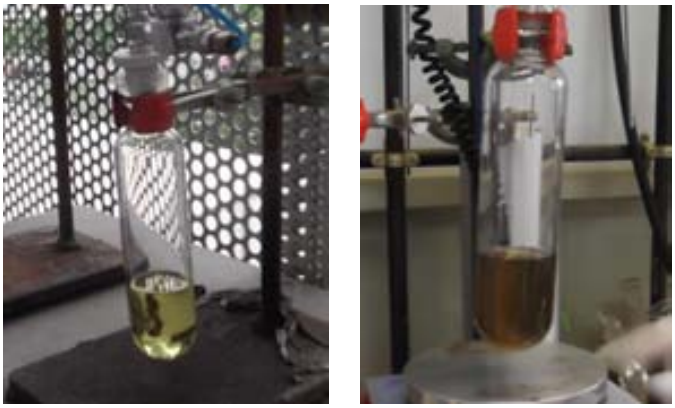

Figure 103. Change in the colour of the solution from yellowish (left) to brown (right) due to the formation of ruthenium metal.

Figure 104. Ruthenium nanoparticles obtained.

7.3.4 Characterisation of ruthenium nanoparticles.

For **Ru239** under conditions described previously, TEM micrographs revealed the presence of small, spherical, and homogeneously dispersed nanoparticles showing a narrow size distribution around a mean diameter of 2.0 nm (Figure **105**).

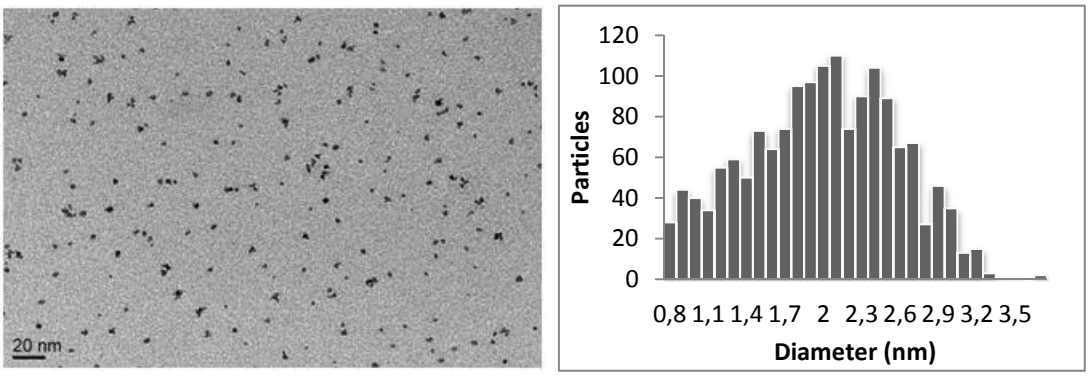

Figure 105. TEM micrograph of **Ru239** nanoparticles and size distribution histogram (ϕmean = 2.0 ± 0.6 nm for 1560 particles).

For **Ru238**, dispersed nanoparticles without signs of agglomeration but leaning to give self-organisations were observed. However, they were not homogeneous in size as it can be seen in the histogram of Figure **106**.

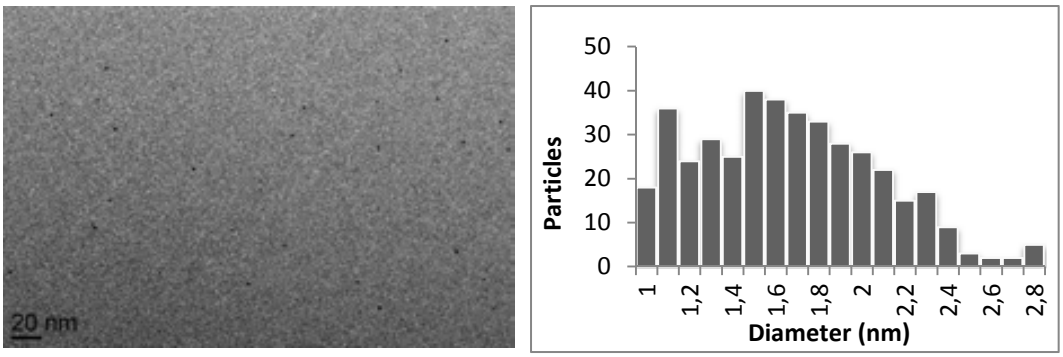

Figure 106. TEM micrograph of **Ru238** nanoparticles and size distribution histogram (ϕmean = 1.6 ± 0.4 nm for 407 particles).

These results contrasted with the formation of large and agglomerated particles that were observed using **237** as stabilizer (Figure **107**). Colloid **Ru237** contains nanoparticles which are not well dispersed on the TEM grid in opposition to what is observed for **Ru238** and **Ru239**. As a consequence of their agglomeration, the size of **Ru237** nanoparticles could not be precisely determined because of their close proximity.

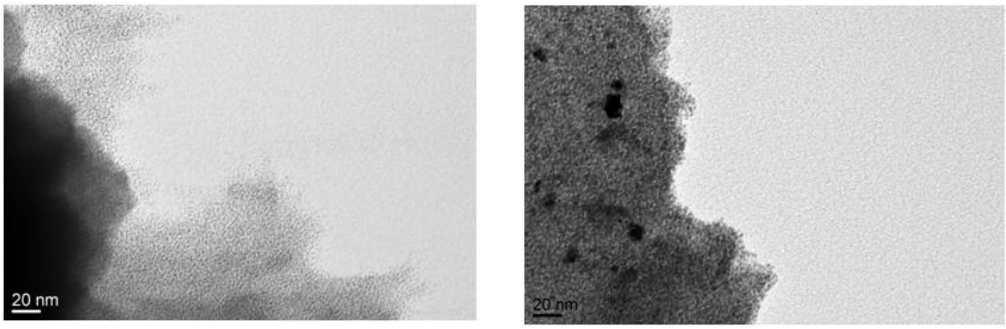

Figure 107. TEM micrograph of **Ru237** nanoparticles.

This different behavior could be associated to the positive effect of the aromatic groups on the stabilization of nanoparticles for **Ru238** and **Ru239** (but not for **Ru237**).[270]

7.3.5 Ruthenium nanoparticles in heterogeneous catalysis.

These nanoparticles were tested in the reduction reaction of acetophenone. Enantioselective reduction of prochiral ketones to optically active secondary alcohols is an important subject in synthetic organic chemistry because the resulting chiral alcohols are extremely useful, biologically active compounds.

Acetophenone (**A**) was used as the substrate in order to compare the selectivity of the hydrogenation process when other functional groups (carbonyls) are present. As shown in Scheme **77** three possible reaction products can be formed: if the aromatic ring is first hydrogenated, cyclohexylmethylketone, **B**, is obtained, while chiral (racemic) phenylethanol, **C**, would be formed if the carbonyl group is hydrogenated first. Further hydrogenation of either **B** or **C** would finally produce cyclohexylethanol, **D**. In addition, hydrogenolysis products can be obtained, such as ethylbenzene and ethylcyclohexane.

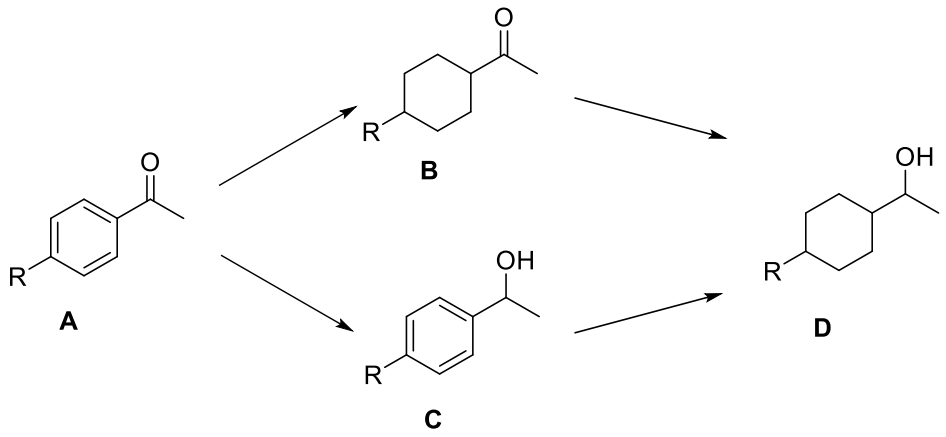

Scheme 77. Acetophenone hydrogenation.

The chemoselective reduction of aromatic ketones to benzyl alcohols can be carried out effectively by direct hydrogenation and hydrogen transfer reactions, both employing homogeneous catalysts,[258] but the selective hydrogenation of the aromatic

[258] Van Leeuwen, P. W. N. M. *Homogeneous Catalysis—Understanding the Art, Kluwer Academic Publishers*, Dordrecht, Netherlands, **2004**.

ring is more complicated. This reaction has been studied in detail,[259,260] usually producing a mixture of the three products when heterogeneous catalysts are used and the reaction is not complete. The formation of these three hydrogenation products is interesting, since the aromatic ring was more prone to be hydrogenated than the carbonyl group. This is also characteristic of the catalysis with metal nanoparticles, they have been proved to be efficient and selective catalysts for reactions which are catalyzed by molecular complexes such as olefin hydrogenation or C-C coupling, for example, but also for reactions which are not catalyzed by molecular species such as aromatic hydrocarbon hydrogenation.[261]

Thus, ruthenium nanoparticles stabilized by ligands **237, 238, 239,** and **248** were applied in the hydrogenation of different unsaturated substrates (Scheme **78**). The results are summarized in Table **10**.

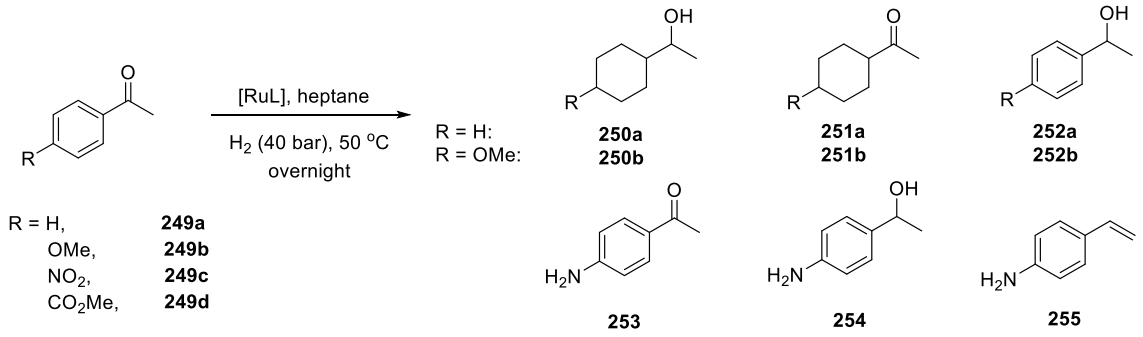

Scheme 78. Ru-catalyzed hydrogenation of acetophenone-based substrates

[259] Denicourt-Nowicki, A.; Leger, B.; Roucoux, A. *Phys. Chem. Chem. Phys.* **2011**, *13*, 13510.
[260] Wang, Y.; Yao, J.; Li, H. R.; Su, D. S.; Antonietti, M. *J. Am. Chem. Soc.*, **2011**, *133*, 2362.
[261] Widegren, J. A.; Finke, R. G. *J. Mol. Catal. A: Chem.* **2003**, *191*, 187.

Table 10. Ru-catalyzed hydrogenation of acetophenone-based substrates **249a-d**.[a]

Entry	R	Compound	Catalyst	Conv.(%)[b]	Selectivity[b] **250/251/252**	Selectivity[b] **253/254/255**
1	H	**249a**	**Ru239**	100	58/42/0	-
2	H	**249a**	**Ru238**	42	0/100/0	-
3	H	**249a**	**Ru237**	100	70/30/0	-
4	H	**249a**	**Ru248**	82	33/62/5	-
5	OMe	**249b**	**Ru239**	92	79/0/21	-
6	OMe	**249b**	**Ru248**	100	100/0/0	-
7	OMe	**249b**	**Ru238**	<5	-	-
8	NO_2	**249c**	**Ru239**	100	-	97/0/3
9	NO_2	**249c**	**Ru237**	100	-	45/29/26
10	NO_2	**249c**	**Ru248**	81	-	100/0/0
11[c]	CO_2Me	**249d**	**Ru239**	0		
12[c]	CO_2Me	**249d**	**Ru237**	0		
13[c]	CO_2Me	**249d**	**Ru248**	0		

[a] Reaction conditions: 1 mmol of substrate in 25 mL of heptane at 50 °C, overnight, 40 bar H_2 and the corresponding preformed nanoparticles, **Ru237**, **Ru238**, **Ru239** and **Ru248**; substrate/Ru/L = 100/1/0.2. [b] Determined by GC-MS; for acetophenone, **249a**, the hydrogenated products correspond to **250a-253a**; for 4-methoxyacetophenone, **250b**, to **250b-252b**. [c] CH_2Cl_2 as solvent (substrate was not soluble in heptane).

For acetophenone, **250a**, (entries 1-4), preformed **RuL** nanoparticles were appropriate to hydrogenate the aromatic ring (only 5% of 1-phenylethanol, **252a**, was produced), obtaining a mixture of 1-cyclohexylethanol, **250a**, and cyclohexylethanone, **251a**, being **Ru237** and **Ru239** the most active systems in favouring the full hydrogenation of acetophenone (entries 1 and 3). However, **Ru238** exhibited lower activity, leading to the exclusive formation of cyclohexylethanone, **251a** (entry 2). The

catalytic system **Ru248** was less active and less selective than **Ru237** and **Ru239** (entry 4).

Using 4-methoxyacetophenone, **249b**, as substrate, **Ru239** and **Ru248** were more active than for the hydrogenation of acetophenone, **249a**, due to the electron-donating behavior of the methoxyl group, giving more than 70% of the full hydrogenated product **250b** (entries 5-6); in particular, **Ru248** gave exclusively **250b** (entry 6). However **Ru238** catalyst was inactive (entry 7). Unfortunately, no asymmetric induction was observed for the chiral alcohols (**250a** or **250b**; **252a** or **252b**).

The hydrogenation of 4-nitroacetophenone, **249c**, led to the exclusive formation of aniline derivatives without reduction of the aromatic cycle (entries 8-10). The catalytic system **Ru239** was more selective, essentially giving 4-aminoacetophenone, **253**, analogously to **Ru248** (entries 8 and 10, respectively). But **Ru237** was not chemoselective, favouring the reduction-elimination process to form 4-aminostyrene, **255**, as by-product (entry 9). When methyl 4-acetylbenzoate was used as substrate, no hydrogenation products could be observed (entries 11-13), due to the electron-withdrawing character of the acetyl group, in agreement with the behavior of 4-nitroacetophenone, **249c** (entries 8-10).

7.3.5.1 Influence of the nanoparticles nature : preformed, formed in situ or under one pot conditions.

Taking previous results into consideration, the possible influence of the nature of the ruthenium nanoparticles was investigated (Table **11**). To do so, the conditions with which the nanoparticles were formed were compared: preformed, formed in situ or under one pot conditions. Under *one pot* conditions means to mix all reactant together at the same time and *in situ* means to mixe the organometallic precursor [Ru(cod)(cot)], the corresponding ligand and acetophenone in heptane at room temperature, followed by pressurisation of H_2 (40 bar) and heating at 50 °C. The results

obtained with **Ru248** catalytic systems (entries 7-8) showed that the *in situ* methodology led to more active catalytic species than those from preformed Ru nanoparticles, giving *ca.* equimolar mixture of **250** and **251** (entry 8), probably due to the formation of smaller nanoparticles when they are generated *in situ* without being isolated, than when preformed Ru nanoparticles are used as catalytic precursors. However for Ru systems containing ligands **239** (entries 1-2) and **237** (entries 5-6), no important differences were observed between both approaches. Independently of the way to generate the catalyst, Ru/**238**-based systems remained less active (entries 3-4), presumably related to the trend to give self-organizations between nanoparticles hindering the substrate access to the metallic surface as it has been shown previously in TEM images.

Table 11. Influence of the catalyst generation in the hydrogenation of acetophenone, **249a**.[a]

Entry	Catalyst	Conv.(%)[b]	Selectivity[b] **250a/251a/252a**
1[c]	**Ru239**	100	58/42/0
2[d]	*In situ* Ru/**239**	100	57/43/0
3[c]	**Ru238**	42	0/100/0
4[d]	In situ Ru/**238**	15	0/100/0
5[c]	**Ru237**	100	70/30/0
6[d]	In situ Ru/**237**	100	73/27/0
7[c]	**Ru248**	82	33/62/5
8[d]	In situ Ru/**248**	100	51/49/0

[a] Reaction conditions: 1 mmol of acetophenone (120 mg) in 25 mL of heptane at 50 °C, overnight, 40 bar H_2. [b] Determined by GC. [c] Results from Table 1. [d] Catalyst generation from 3 mg (0.01 mmol) of [Ru(cod)(cot)] and 0.002 mmol of ligand (0.45 mg of **237,** 0.8 mg of **238**, 0.7 mg of **239**, and 0.4 mg of **248**) mixed in heptane at room temperature just before the addition of substrate and pressurisation with dihydrogen; acetophenone/Ru/L = 100/1/0.2.

Finally, the hydrogenation capability of these catalytic systems for the hydrogenation of more challenging substrates, such as 4-methylanisole and 4-chloroanisole was tested. Disappointingly, they were not active under the same conditions described for the hydrogenation of acetophenone-based substrates (see Scheme 8 and Table 1). However, the Ru/**239** catalytic system efficiently hydrogenated (*E*)-4-phenylbut-3-en-2-one, **256**, although a mixture of compounds coming from the C=C and C=O bonds hydrogenation was obtained (Scheme **79**), favouring the hydrogenation of the aromatic ring (compounds **257** and **258**). Starting from the non-conjugated analogous substrate, 4-phenylbutan-2-one, **261**, only the formation of the saturated alcohol **262** was observed, inducing a low enantiomeric excess (15%) (Scheme **79b**).

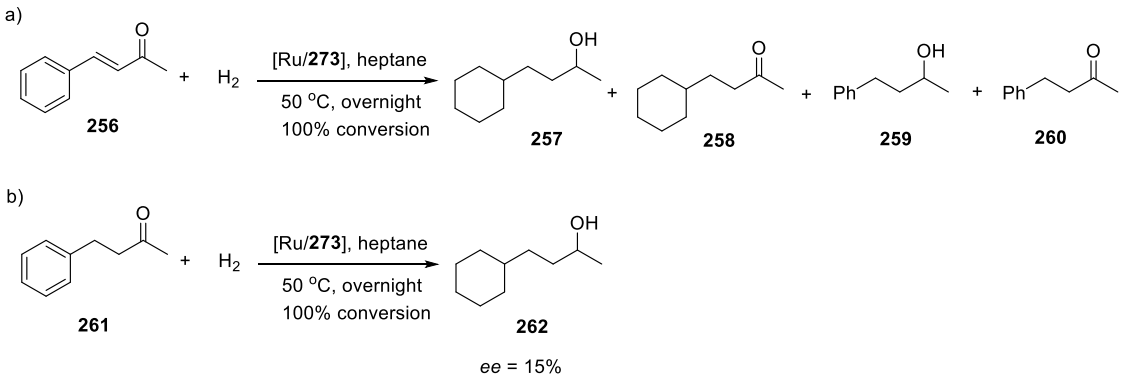

Scheme 79. Hydrogenation of (*E*)-4-phenylbut-3-en-2-one, **256** (a) and 4-phenylbutan-2-one, **261** (b) catalyzed by the *in situ* generated Ru/**239** system.

7.4 SUMMARY AND CONCLUSIONS

i) Cyclobutane pyrrolidines **237**, **238** and **239** using (-)-verbenone as starting material were synthesized using stereoselective and high yielding transformations by means of methodologies previously set up in our laboratory (Scheme **108**).

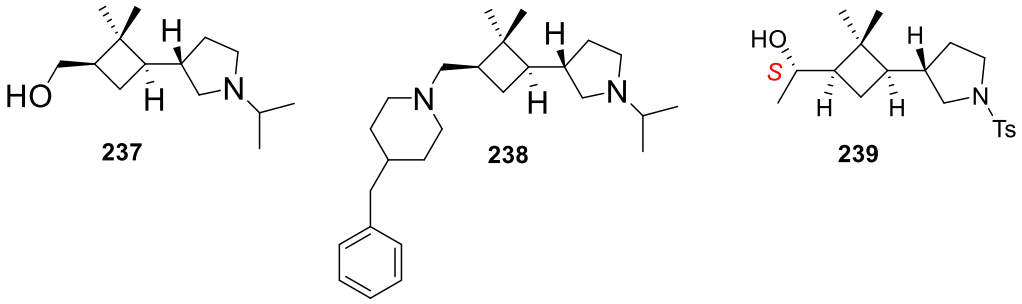

Figure 108. Optically pure cyclobutane pyrrolidine synthesized.

ii) In collaboration with the laboratory of Prof. Montserrat Gómez in Université Paul Sabatier in Toulouse, compounds **237**, **238**, **239** were tested as stabilizers in the formation of ruthenium metal nanoparticles. Small and homogeneously dispersed nanoparticles showing a quite narrow size distribution when **237** was used as stabilizer were obtained. In contrast, using **238** nanoparticles tend to self-association and large and agglomerated particles were observed using pyrrolidine **239** as stabilizer.

iii) Finally, RuNP were tested in heterogeneous catalysis in the reduction of acetophenone. Preformed Ru nanoparticles **Ru237** and **Ru239** favored the full hydrogenation of acetophenone. However, **Ru238** exhibited lower activity leading to the exclusive formation of cyclohexylethanone. With 4-nitroacetophenone, **Ru239** showed high activity and selectivity, essentially giving the aniline derivative without reduction of the aromatic cycle. In contrast with, **Ru238** was the less active system, probably related to the trend to give self-organization. Thus, the ligands **237** and **239** were the best in terms of

stabilization, leading to active catalytic systems but, unfortunately, without asymmetry induction for the chiral alcohols. It is remarkable the selectivity of these systems towards hydrogenation of arenes and nitrobenzene derivatives giving selectively the corresponding cyclohexane or aniline derivatives.

These results are under active investigation in our laboratory and modifications are being carried out in order to improve the results on catalysis.

CHAPTER VIII

General conclusions

8. GENERAL CONCLUSIONS

The experience previously acquired in our laboratory on stereoselective synthetic strategies has been used in this Thesis as a base to prepare and to study new optically active compounds containing the cyclobutane moiety.

An efficient enantio and diastereocontrolled **synthesis of the four stereoisomers of cyclobutane-1,2-diamine derivatives** has been achieved. Their orthogonal protection secures the regioselective functionalization of both amino groups retaining the chirality in the case of *cis*-compounds that otherwise would become *meso*. Then, the versatility of some of these scaffolds has been used in the preparation of the following compounds or materials.

Low molecular weight gelators, which have shown the ability to gelate toluene among other solvents. In collaboration with Prof. J.C. Estévez from the *Universidad de Santiago de Compostela*, these organogelators based on cyclobutane structures have been compared with the ones formed by the cyclohexane analogues. The behavior and the morpholohy of these gels have been studied by ^{1}H NMR at variable temperature, scanning electron microscopy and IR. They showed high dependence on their regiochemistry: *C*-centered or *N*-centered amides and on the stereochemistry *cis*/*trans* in the case of the six-membered ring.

New bolasurfactants. Bolaamphiphiles based on 1,2-cyclobutane diamines have been compared with the ones based on 1,2-dicarboxylic acid and their behavior as surfactants has been studied in collaboration of Dr. Ramon Pons from the *Consejo Superior de Investigaciones Cientificas* in Barcelona. *C*-centered bolaamphiphiles have shown a normal behavior as surfactant and their CMC has been determined using surface tension measurements. *N*-centered bolaamphiphiles showed different behavior depending on their stereochemistry *cis*/*trans*. *cis*-Diastereomer did not have the ability to reduce the surface tension but it acted as organogelator. *trans*-Diastereomer had an uncommon behavior as surfactant with two possible CMC values and their structure at different concentrations was studied by TEM.

Hybrid silicas derived from cyclobutane-1,2-diamine. They have been studied by ^{13}C and ^{19}Si NMR in solid state and by SEM and they showed to be materials totally condensed and with different morphology depending on their stereochemistry *cis*/*trans*. Moreover, a right-handed helix was evidenced by SEM and as far as we know is one of the first examples of creation of chirality from *meso* precursors to chiral materials. On the other hand, cyclobutane-1,2-diamine has been also used as precursor to a silica able to coordinate rhodium in order to prepare a chiral material for catalysis. It has been used in the reduction of acetophenone without induction of chirality but with encouraging outcomes to improve these results in the future.

Ruthenium nanoparticles stabilized by cyclobutane ligands have been prepared in collaboration of Prof. Montserrat Gómez of the *Université Paul Sabatier* in Toulouse. These nanoparticles were tested as catalysts in reduction reactions showing good catalytic activity and selectivity. Unfortunately, only in some cases a moderate enantiomeric excess was found.

CHAPTER IX

Experimental section

9.1 GENERAL METHODOLOGY

9.1.1 Spectroscopy and spectrometry

^{1}H-NMR (at 250, 360, 400, 500 or 600 MHz), **^{13}C-NMR** (at 62.5, 90, 100, 125 or 150 MHz) were recorded at *Servei de Ressonànica Magnètica Nuclear de la Universitat Autònoma de Barcelona*.

The spectrometers used were:

- AC 250 Brucker for ^{1}H at 250 MHz and ^{13}C at 62.5 MHz.
- AVANCE 360 Bruker for ^{1}H at 360 MHz and ^{13}C at 90 MHz.
- ARX 400 Brucker for ^{1}H at 400 MHz and ^{13}C at 100 MHz at different temperatures.
- AVANCE 500 Bruker with a CP-MAS line, for ^{1}H at 400 MHz and ^{13}C at 100 MHz, for the NMR in the solid state.

Chemical shifts of each signal are given in ppm, using as reference the next values:

$CDCl_3$: δ 7.26 and 77.16 for ^{1}H and ^{13}C respectively.

Methanol-d_4 (H_2O): δ 3.31 (4.87) and 49.00 for ^{1}H and ^{13}C respectively.

The *abbreviations* used to describe multiplicity are:

m	multiplet
s	singlet
br.s.	broad singlet
c.a.	complex absorption
dd	double doublets
ddt	doublet of doublet of triplets

q quartet

NMR signals were assigned with help of DEPT, HMBC, HMQC experiments. The numerology used to assign each signal has been also used for nomenclature.

Infrared spectra (IR) in solid state and in solution were recorded on a Sapphire-ATR Spectrophotometer and peaks are reported in cm^{-1}.

High resolution mass spectra (HRMS) were recorded at *Servei d'Anàlisi Química de la Universitat Autònoma de Barcelona* in a Bruker micrOTOFQ spectrometer using ESI-MS (QTOF).

Inductively coupled plasma *mass* spectrometry *(ICP-MAS)* *was* performed at *Servei d'Anàlisi Química de la Universitat Autònoma de Barcelona* in a mass spectrometer inductively coupled Agilent, model 7500ce.

Circular Dichroism spectra were recorded with a JASCO-715 spectropolarimeter and were processed by use of the associated software.

9.1.2 Chromatography

Column chromatography was always performed with Baker® silica gel for flash chromatography (mean pore: 60 Å; particle size: 0.04-0.06 mm, 230-400 mesh ASTM), using nitrogen as driving gas.

All reactions were monitored by thin-layer chromatography (TLC) using ALUGRAM® SIL G/UV_{254} pre-coated aluminium sheets. Layers of 0.20 mm of thickness covered with silica gel 60 with fluorescent indicator UV_{254}.

Several methods were used to visualize the spots:

- Irradiation under a LED UV-light (UV_{254}), using a VILBER LOURMAT® lamp, VL-4LC model.
- Staining thin-layers under acid solution of para-anisaldehyde or vanillin in ethanol 96%.

- Staining thin-layers under basic solution of $KMnO_4$ in water.

9.1.3 Microscopy

TEM images were acquired with a Hitachi H-7000 microscope on samples stained with 2% uranyl acetate in the *Servei de Microscopia* at the University. Carbon-filmcoated copper grids were used.

SEM images were acquired with Quanta 200 ESEM FEG apparatus equipped with a field-emission gun (FEG) in the Institut de Ciència de Materials de Barcelona (ICMAB). Wet gels were disposed on a carbon-film-coated copper grid and introduced into the microscope, working under a pressure of 130 Pa. To obtain data from xerogels (dry gels), wet gels were dried by standing for 30 min on the grid before being introduced into the microscope working at 60-80 Pa and 5 kV. In the SEM/EDX analyses the same apparatus equipped with an Energy Dispersive X-ray (EDX) system for chemical analysis was used.

9.1.4 General tools

Optical rotations, $[\alpha]_D$, were measured using an automatic polarimeter PROPOL™, Dr. Wolfgang Kernchen model, at 22±2 ºC and using a JASCO-715 spectropolarimeter and determined by the associated software.

Melting points were determined on a hot stage using a Kofler apparatus, REICHERT AUSTRIA™ model.

Micro-distillations were carried out in a BÜCHI™ distiller, GKR-51 model.

Lyophilization of samples were done using a POLYSCIENCE™ lyophilizator, KR-80A model and a TELSTAR™ lyophilizator, LyoQuest-85 model.

Hydrogenations were carried out in an autoclave hydrogenation T-reactor Swagelok™, with a pressure capacity from 1 to 20 at (kg/cm^2).

HPLC analysis were performed using a Waters 2690 with a Photodiodearray and a detector Waters™ 996.

Photochemical reactions were performed in a pyrex T-shaped photochemical reactor from TRALLERO&SCHLEE™. Irradiation is emitted from a mercury lamp of 125 W medium pressure PHILLIPS® and a mercury lamp of 400 W medium pressure ELECTRO DH™. Refrigeration at -40 ºC comes from a C40P TERMO SCIENTIFIC™ refrigerator, Phoenix II model.

Reagents were used directly from commercial sources and Solvents were directly used due to their high quality. If necessary, reagents were conveniently purified and the solvents were distilled under nitrogen atmosphere using standard procedures described at Vogel's, Textbook of practical Organic Chemistry, Ed. Logman Scientific and Technical, UK, 1989.

Deuterated solvents were used directly from commercial source Eurisotop™.

In the synthesis of nanoparticles, all manipulations were performed using standard Schlenk techniques under argon atmosphere. Unless stated otherwise, commercially compounds were used without further purification. [Ru(cod)(cot)] was purchased from NanoMeps. GC analyses were carried out on an Agilent GC6890 equipped with flame ionization and mass detectors, using a SGE BPX5 column composed by 5% of phenylmethylsiloxane.

9.2 EXPERIMENTAL PROCEDURES

3-Oxabicyclo [3.2.0] heptane-2,4-dione, 3

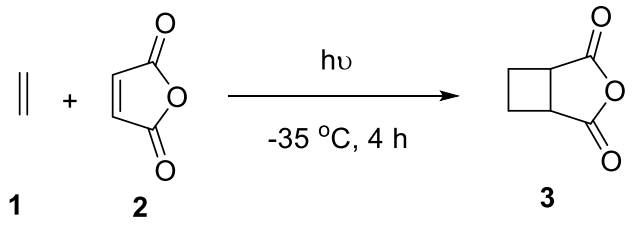

A solution of maleic anhydride (1.52 g, 15.3 mmol) in acetone (500 mL) was cooled to -35 °C. The solution was saturated with ethylene and the system was irradiated through a Pyrex filter for 4 h. The solvent was removed under vacuum to afford pure compound **3** as a white solid (1.93 g, 15.3 mmol, quantitative yield).

Spectroscopic data for compound 3:

^{1}H NMR (250 MHz, $CDCl_3$): δ 2.35 (c.a., 2H), 2.74 (c.a., 2H), 3.52 (c.a., 2H, H_1, H_2).

Spectroscopic data are consistent with those reported in reference:

Tufariello, J. J.; Milowsky, A. S.; Al-Nuri, M.; Goldstein, S. *Tetrahedron Lett*., **1987**, *28*, 267.

Dimethyl (1*R*,2*S*)-cyclobutane-1,2-dicarboxylate, 8

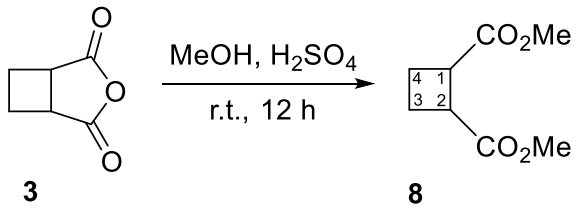

A solution of **3** (1.92 g, 15.1 mmol) and concentrated H_2SO_4 (1.0 mL) in methanol (50 mL) was stirred at 50 °C for 5 h. Dichloromethane (100 mL) was added to the organic phase and it was successively washed with water (2 x 50 mL) and brine (1 x 50 mL). The organic layer was then dried over $MgSO_4$, filtered off and concentrated in order to provide the corresponding crude as yellowish oil (2.15 g, 12.5 mmol, 83%

yield). Generally, the product is obtained pure enough to carry on the next step of the synthesis. However, it can be distilled under vacuum at 150 °C.

Spectroscopic data for compound 8:

^{1}H NMR (250 MHz, $CDCl_3$): δ 2.10 (c.a., 2H), 2.29 (c.a., 2H), 3.31 (c.a., 2H, H_1, H_2), 3.58 (s, 6H, Me).

Spectroscopic data are consistent with those reported in reference:

Sabbioni, G.; Jones, J. B. *J. Org. Chem.* **1987**, *52*, 4565.

(1*S*,2*R*)-2-methoxycarbonylcyclobutane-1-carboxylic acid, 9

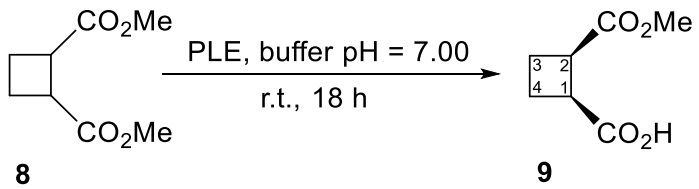

Diester **8** (3.61 g, 21.0 mmol) was dissolved in 250 mL of a buffer previously prepared from 0.1 M KH_2PO_4 at pH = 7. Pig liver esterase (PLE) (98 mg) was added to the solution and the mixture was stirred at room temperature for 18 h. The reaction was maintained at pH 7 by adding a 1 M solution of NaOH. Then, the reaction mixture was washed with diethyl ether (2 x 100 mL), and 5% HCl was added to reach pH 2-3. The acid solution was extracted with ethyl acetate (4 x 150 mL) and the organic extracts were dried over magnesium sulfate. The solvent was evaporated under vacuum to dryness obtaining half-ester (*S*,*R*)-**9** as a colourless liquid (3.15 g, 19.9 mmol, 95% yield).

Spectroscopic data for compound (*S*,*R*)-9:

^{1}H NMR (250 MHz, $CDCl_3$): δ 2.23 (c.a., 2H), 2.41 (c.a., 2H), 3.43 (c.a., 2H, H_1, H_2), 3.69 (s, 3H, Me).

Spectroscopic data are consistent with those reported in reference:

Sabbioni, G.; Jones, J. B. *J. Org. Chem.* **1987**, *52*, 4565.

Methyl (1*R*,2*S*)-2-azidocarbonylcyclobutane-1-carboxylate, 47

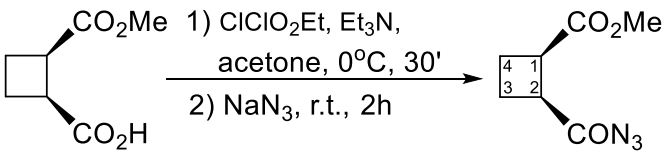

To an ice-cooled solution of half-ester (*S*,*R*)-**9** (5.73 g, 36.2 mmol) in anhydrous acetone (80 mL), triethylamine (6.5 mL, 47.1 mmol, 1.3 eq) and ethyl chloroformate (4.5 mL, 47.1 mmol, 1.3 eq) were subsequently added. The mixture was stirred at 0 °C for 30 minutes. Then, sodium azide (5.9 g, 90.6 mmol, 2.5 eq) in 100 mL of water was added and the resultant solution was stirred at room temperature for 1.5 h. The reaction mixture was extracted with dichloromethane (4x100 mL), and the organic extracts were dried over magnesium sulfate. Solvents were removed under reduced pressure to give acyl azide (*R*,*S*)-**47** as a colourless oil (5.18 g, 28.3 mmol, 78% yield), which was used in the next step without further purification. WARNING: This product should be carefully manipulated because of its explosive nature.

Spectroscopic data for compound (*R*,*S*)-47:

^{1}H RMN (250 MHz, acetone-d_6): δ 2.27 (c.a., 4H, H_3, H_4), 3,54 (m, 2H, H_1, H_2), 3.68 (s, 3H, Me).

IR (ATR) **:** 3024, 2952, 1905 (N_3), 1708, 1172 cm^{-1}

Spectroscopic data are consistent with those reported in reference:

Martín-Vilà, M.; Muray, E; P. Aguado, G.; Alvarez-Larena, A.; Branchadell, V.; Minguillón, C.; Giralt, E.; Ortuño, R.M. *Tetrahedron*: Asymmetry, **2000**, *11,* 3569.

Methyl (1*R*,2*S*)-2-(*tert*-butoxycarbonylamino)cyclobutane-1-carboxylate, 156

METHOD A:

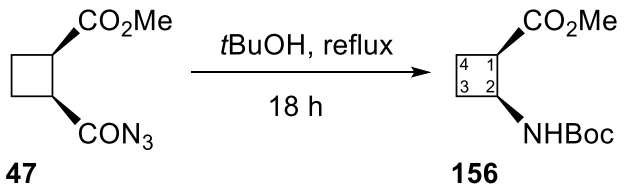

To acyl azide (*R*,*S*)-**47** (5.18 g, 28.3 mmol), 30 mL of *tert*-butanol were added as the solvent and the reagent. The mixture was heated to reflux and stirred for 18 h. Then, the solvent was evaporated under *vacuum*, and the residue was purified by column chromatography (9:1 hexane-EtOAc as eluent) affording diprotected aminoacid (*R*,*S*)-**156** as a white solid (4.21 g, 18.4 mmol, 65% yield).

METHOD B:

Step 1: Methyl (1*R*,2*S*)-2-(benzyloxycarbonylamino)cyclobutane-1-carboxylate, 10

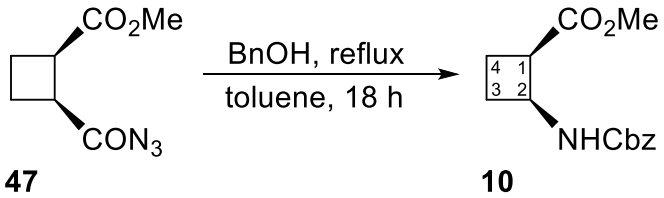

A solution of (*R*,*S*)-**47** (2.54 g, 13.8 mmol) and benzyl alcohol (1.43 mL, 16.6 mmol, 1.2 eq) in toluene (50 mL) was heated to reflux for 18 hours (the reaction progress was monitored by IR following the signals for the acyl azide at 1906 cm^{-1} and the related isocyanate at 2260 cm^{-1}). Toluene was removed under reduced pressure and then the excess of benzyl alcohol was eliminated by lyophilisation. The residue

was chromatographed on silica gel (dichloromethane as eluent) to afford carbamate (*R*,*S*)-**10** as a white solid (3.39 g, 12.8 mmol, 92% yield).

Spectroscopic data for compound (*R*,*S*)-**10:**

^{1}H NMR (250 MHz, $CDCl_3$): δ 1.97 (c.a., 2H), 2.18-2.43 (c.a., 2H), 3.39 (m, 1H, H_1), 3.66 (s, 3H, Me), 4.46 (m, 1H, H_2), 5.08 (s, 2H, CH_2-Ph), 5.64 (broad s., 1H, N*H*), 7.34 (m, 5H, H_{ar}).

Spectroscopic data are consistent with those reported in reference:

Martín-Vilà, M.; Muray, E; P. Aguado, G.; Alvarez-Larena, A.; Branchadell, V.; Minguillón, C.; Giralt, E.; Ortuño, R.M. *Tetrahedron*: Asymmetry, **2000**, *11,* 3569.

Step 2: Methyl (1*R*,2*S*)-2-(*tert*-butoxycarbonylamino)cyclobutane-1-carboxylate, 156

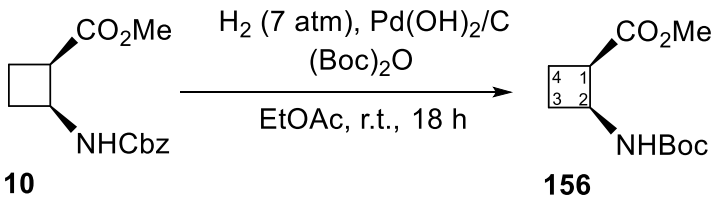

Carbamate (*R*,*S*)-**10** (3.04 g, 11.5 mmol) in ethyl acetate (15 mL) was hydrogenated under 7 atmospheres of pressure in the presence of 20% $Pd(OH)_2/C$ (0.35 g) and Boc_2O (3.2 mL, 13.9 mmol, 1.2 eq) overnight. The reaction mixture was filtered through Celite® and solvent was removed under vacuum and the residue was purified by column chromatography (dichloromethane as eluent) affording carbamate (*R*,*S*)-**156** as a white solid (2.17 g, 9.5 mmol, 82 % yield).

Spectroscopic data for compound (*R*,*S*)-156:

^{1}H NMR (250 MHz, $CDCl_3$): δ 1.38 (s, 9H, *t*Bu), 1.87-1.97 (c.a., 2H), 2.25 (c.a., 2H), 3.35 (m, 1H, H_1), 3.67 (s, 3H, Me), 4.41 (m, 1H, H_2), 5.33 (br. s., 1H, N*H*).

Spectroscopic data are consistent with those reported in reference:

Izquierdo, S.; Rúa, F.; Sbai, A.; Parella, T.; Álvarez-Larena, A.; Branchadell, V.; Ortuño, R.M. *J. Org. Chem.*, **2005**, *70,* 7963.

(1*S*,2*R*)-1-*tert*-butyl-3-methyl cyclobutane-1,2-dicarboxylate, 43

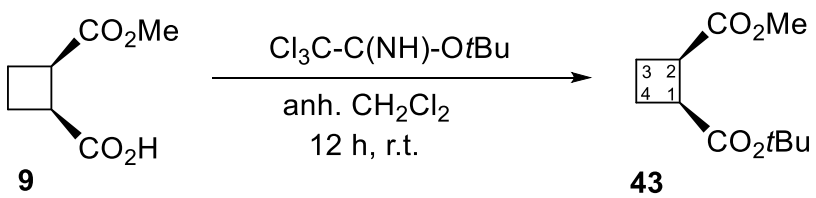

tert-Butyl 2,2,2-trichloroacetimidate (3.6 mL, 19.85 mmol) was added to a solution of half-ester (*S*,*R*)-**9** (1.57 g, 9.93 mmol) in anhydrous dichloromethane (50 mL) under nitrogen atmosphere and the mixture was stirred overnight. The mixture was evaporated to dryness under reduced pressure. The reaction crude was purified by column chromatography on neutral silica gel (1:3 ethyl acetate-hexane) to afford pure (*S*,*R*)-**43** (1.57 g, 7.32 mmol, 74% yield).

Spectroscopic data for compound (*S*,*R*)-43:

^{1}H NMR (250 MHz, $CDCl_3$): δ 1.43 (s, 9H, *t*Bu), 2.16 (c.a., 2H), 2.35 (c.a., 2H,), 3.32 (c.a., 2H, H_1, H_2), 3.68 (s, 3H, Me).

Spectroscopic data are consistent with those reported in reference:

Izquierdo, S.; Martin-Vila, M.; Moglioni, A. G.; Branchadell, V.; Ortuno, R. M., *Tetrahedron: Asymmetry*, **2002**, *13*, 2403.

(1*R*,2*S*)-2-(*tert*-butoxycarbonyl)cyclobutane-1-carboxylic acid, 160

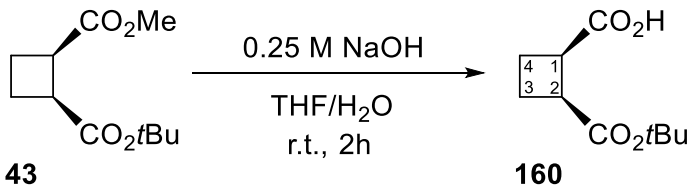

To an ice-cooled solution of ester (*S*,*R*)-**43** (1.57 g, 7.33 mmol) in a 1:10 THF-water mixture (40 mL), 0.25 M sodium hydroxide aqueous solution (70 mL, 18.32 mmol, 2.5 eq) was added and the resultant mixture was stirred for 2 h. (Reaction progress was monitored by TLC). The reaction mixture was washed with dichloromethane (50 mL), and 5% HCl aqueous solution was added to the aqueous phase to reach pH 2. The acid solution was extracted with ethyl acetate (4 x 80 mL) and dried over magnesium sulfate. Solvent was removed at reduced pressure to afford crude (*R*,*S*)-**160** as a yellowish oil (1.46 g, 7.29 mmol, 99% yield) without need of further purification.

Spectroscopic data for compound (*R*,*S*)-160:

^{1}**H NMR** (250 MHz, $CDCl_3$): δ 1.46 (s, 9H, *t*Bu), 2.22 (c.a., 2H), 2.38 (c.a., 2H), 3.38 (m, 2H, H_1, H_2)

<u>Spectroscopic data are consistent with those reported in reference:</u>

Izquierdo, S.; Martin-Vila, M.; Moglioni, A. G.; Branchadell, V.; Ortuno, R. M., *Tetrahedron: Asymmetry*, **2002**, *13*, 2403.

tert-Butyl(1*S*,2*R*)-2-(benzyloxycarbonylamino)cyclobutane-1-carboxylate, 162

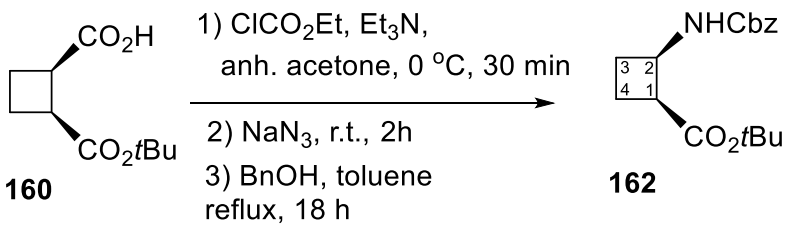

To an ice-cooled solution of half-ester (*S*,*R*)-**160** (1.46 g, 7.3 mmol) in anhydrous acetone (40 mL), triethylamine (1.3 mL, 9.5 mmol, 1.3 eq) and ethyl chloroformate (1.3 mL, 9.5 mmol, 1.3 eq) were subsequently added. The mixture was stirred at 0 °C for 30 minutes. Then, sodium azide (1.19 g, 18.2 mmol, 2.5 eq) in 25 mL of water was added and the resultant solution was stirred at room temperature for 1.5 h. The reaction mixture was extracted with dichloromethane (4 x 20 mL), and the organic extracts were dried over magnesium sulfate. The crude was dissolved in toluene (50 mL) and benzyl alcohol (1.43 mL, 16.6 mmol, 1.2 eq) was added. Then the mixture was heated to reflux for 18 hours (the reaction progress was monitored by IR following the signals for the acyl azide at 1906 cm^{-1} and the corresponding isocyanate at 2260 cm^{-1}). Toluene was removed under reduced pressure and then the excess of benzyl alcohol was eliminated by lyophilisation. The residue was chromatographed on silica gel (1:4 ethyl acetate-hexane as eluent) to afford carbamate (*S*,*R*)-**162** (1.19 g, 3.90 mmol, 54% yield).

Spectroscopic data for compound (*S*,*R*)-162:

^{1}H NMR (250 MHz, $CDCl_3$): δ 1.43 (s, 9H, *t*Bu), 1.95 (m, 2H), 2.20 (m, 1H), 2.34 (m, 1H), 3.25 (m, 1H, H_1), 4.49 (m, 1H, H_2), 5.08 (s, 2H, CH_2-Ph), 5.65 (d, 1H, *J*= 9.4 Hz, N*H*), 7.34 (m, 5H, H_{ar}).

<u>Spectroscopic data are consistent with those reported in reference:</u>

Izquierdo, S.; Martin-Vila, M.; Moglioni, A. G.; Branchadell, V.; Ortuno, R. M., *Tetrahedron: Asymmetry*, **2002**, *13*, 2403.

(1*S*,2*R*)-2-(Benzyloxycarbonylamino)cyclobutane-1-carboxylic acid, 16

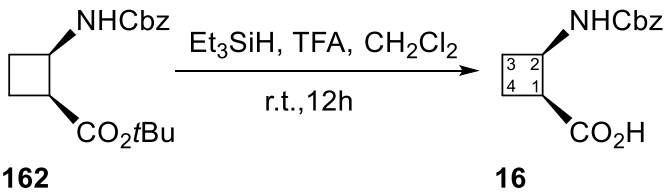

A mixture containing compound (*S*,*R*)-**162** (3.37 g, 11.0 mmol), TFA (11.7 mL, 152.1 mmol, 13 eq) and triethylsilane (2.5 mL, 30.0 mmol, 2.5 eq) in anhydrous dichloromethane (25 mL) was stirred at room temperature overnight. Solvent was evaporated and excess of TFA acid was removed by lyophilisation affording acid (*S*,*R*)-**16** as a yellowish oil (2.70 g, 10.8 mmol, 98% yield). If necessary, the crude can be purified by column chromatography (7:3 ethyl acetate-hexane as eluent).

Spectroscopic data for compound (*S*,*R*)-16:

^{1}H NMR (250 MHz, $CDCl_3$): δ 2.04 (m, 2H), 2.36 (m, 2H), 3.40 (m, 1H, H_1), 4.54 (m, 1H, H_2), 5.09 (d, *J*= 12.6 Hz, 2H, CH_2-Ph), 5.83 (br. s., 1H, N*H*), 7.35 (m, 5H, H_{ar}).

Spectroscopic data are consistent with those reported in reference:

Izquierdo, S.; Martin-Vila, M.; Moglioni, A. G.; Branchadell, V.; Ortuno, R. M., *Tetrahedron: Asymmetry*, **2002**, *13*, 2403.

Diazomethane distillation from Diazald®

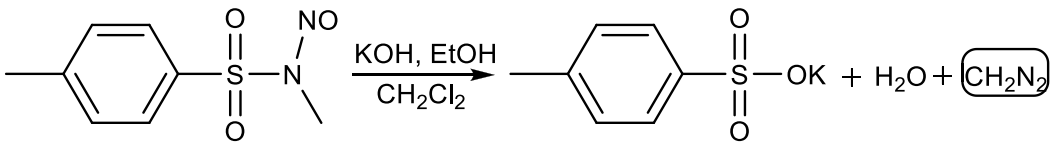

Diazomethane reacts instantaneously with carboxylic acids to yield methyl esters quantitatively. However, it must be prepared from a precursor and care must be taken when handling this very reactive reagent:

· Diazomethane is a yellow gas at room temperature, liquifies at –23 °C, and freezes at –145 °C. It is extremely toxic.

· All edges of glassware used for diazomethane should be carefully fire-polished and ground-glass joints cannot be employed. Care should be taken in cleaning the glassware used for diazomethane to avoid scratching the surfaces. Contact of diazomethane with alkali metals or drying agents such as calcium sulfate can result in

an explosion. The recommended drying agent for diazomethane is potassium hydroxide pellets.

· All diazomethane reactions should be performed in an efficient fume hood and behind a sturdy safety shield. Reactions of diazomethane are best performed at room temperature or below.

· Solutions of diazomethane should not be frozen because the rough edges of crystals could cause explosions.

Procedure:

To a mixture containing Diazald (5 g, 23 mmol) in dichloromethane (60 mL), a mixture of KOH in EtOH 96% (0.8 g in 70 mL) is added. The system is stirred for 10 minutes at room temperature before it is heated to 50 °C to promote the distillation of **CH_2N_2** (as a yellow gas) over the reactant to be methylated. When the distillation is finished, the heating is turned off and the system is allowed to reach room temperature. Then the distillation apparatus is removed.

Silica gel is added slowly and carefully to the solution that initially contained the diazald to eliminate the diazomethane excess.

The excess of diazomethane in the flask that contains the methylated product is carefully removed using a gentle nitrogen flow.

Methyl-(1*S*,2*R*)-2-(benzyloxycarbonylamino)cyclobutane-1-carboxylate, 10

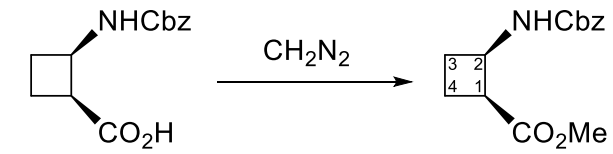

16 **10**

Acid (*S*,*R*)-**16** (0.38 g, 1.51 mmol) was methylated by the action of an excess of diazomethane (5 eq) in a dichloromethane solution to provide orthogonally protected amino acid (*S*,*R*)-**10** (0.40 g, 1.51 mmol, quantitative yield).

Spectroscopic data for compound (*S*,*R*)-10:

^{1}H NMR (250 MHz, $CDCl_3$): δ 1.97 (c.a., 2H), 2.18-2.43 (c.a., 2H), 3.39 (m, 1H, H_1), 3.66 (s, 3H, Me), 4.46 (1H, m, H_2), 5.08 (s, 2H, CH_2-Ph), 5.64 (broad s, 5H, H_{ar})

Spectroscopic data are consistent with those reported in reference:

Izquierdo, S.; Martin-Vila, M.; Moglioni, A. G.; Branchadell, V.; Ortuno, R. M., *Tetrahedron: Asymmetry*, **2002**, *13*, 2403.

Methyl-(1*S*,2*R*)-2-(*tert*-butoxycarbonylamino)cyclobutane-1-carboxylate, 156

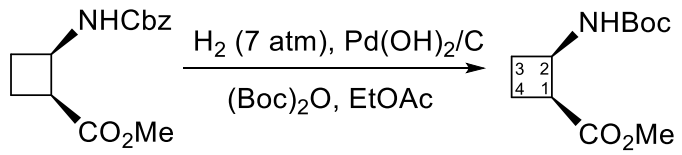

10 **156**

Carbamate (*S*,*R*)-**10** (0.39 g, 1.48 mmol) in ethyl acetate (15 mL) was hydrogenated under 7 atmospheres of pressure in the presence of 20% $Pd(OH)_2/C$ (39 mg) and Boc_2O (0.41 mL, 1.78 mmol, 1.2 eq) overnight. The reaction mixture was filtered through Celite® and solvent was removed under vacuum and the residue was purified by column chromatography (1:4 ethyl acetate-hexane as eluent) affording the desired carbamate (*S*,*R*)-**156** as a white solid (0.26 g, 1.13 mmol, 77% yield).

Spectroscopic data for compound (*S*,*R*)-156:

^{1}H NMR (250 MHz, $CDCl_3$): δ 1.42 (s, 9H, *t*Bu), 1.98 (c.a., 2H), 2.22 (m, 1H), 2.34 (m, 1H), 3.39 (m, 1H, H_1), 3.71 (s, 3H, Me), 4.45 (m, 1H, H_2), 5.32 (br. s., 1H, N*H*).

Spectroscopic data are consistent with those reported in reference:

Fernandes, C.; Gauzy, C.; Yang, Y.; Roy, O.; Pereira, E.; Faure, S.; Aitken, D. J. *Synthesis,* **2007**, *14*, 1992.

(1*S*,2*R*)-methyl 2-(bis(*tert*-butoxycarbonyl)amino)cyclobutanecarboxylate, 165

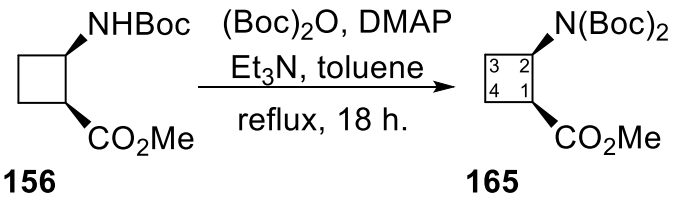

Carbamate (*S*,*R*)-**156** (0.10 g, 0.44 mmol) was dissolved in anhydrous toluene (20 mL) under a nitrogen atmosphere. Then, DMAP (30.6 mg, 0.25 mmol) and triethylamine (0.14 mL, 1.00 mmol) were added. Then, di-*tert*-butyl dicarbonate (199.78 mg, 1.02 mmol) was added. The mixture was refluxed for 18 hours. After that, the solvent was evaporated under vacuum and the crude was purified by column chromatography on silica gel using a mixture of hexane-ethyl acetate 4:1 to afford (S,R)-**165** (0.07 g, 0.20 mmol, 46% yield) as a colorless oil.

Spectroscopic data and physical constants for compound (*S*,*R*)-165:

[α] $^{20}_{D}$ + 11 (*c* 3, methanol).

IR (ATR) 2978.9, 1700, 1650, 1367.8, 1352.3, 1118.5 cm^{-1}.

^{1}H NMR ($CDCl_3$, 360 MHz) δ 1.45 (s, 18H, *t*Bu), 1.87 (m, 1H), 2.22 (c.a., 2H), 2.60 (m, 1H), 3.36 (m, 1H, H_1), 3.62 (s, 3H, Me), 4.56 (q, *J* = 12.5 Hz, 1H, H_2).

^{13}C NMR ($CDCl_3$, 90 MHz) δ 18.4, 26.7 (C_3, C_4), 28.1 ($C(CH_3)_3$), 44.5 (C_1), 51.5 (C_2), 51.7 (Me), 82.4 ($C(CH_3)_3$), 152.5 (CO_e), 173.2 (CO_c).

HRMS (ESI) Calculated for $C_{16}H_{27}NO_6Na$ $[M+Na]^+$: 352.1731. Found: 352.1735.

(1*S*,2*R*)-2-bis(*tert*-butoxycarbonylamino)cyclobutane-1-carboxylic acid, 157

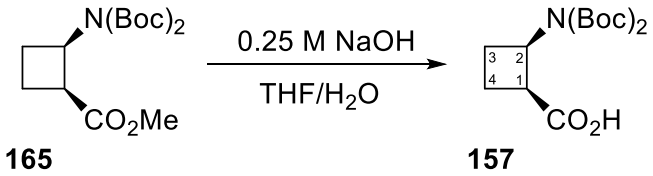

Methyl ester (*S*,*R*)-**165** (0.79 g, 0.32 mmol) was dissolved in a 1:10 mixture of THF-water (55 mL). Then, 0.25 M NaOH (34 mL, 2.5 eq, 8.6 mmol) was added. The mixture was stirred at 0 ^{o}C for 3 hours. After that, the solution was acidified to pH 2 with 2 M HCl. Then, the mixture was extracted with CH_2Cl_2 (4 x 50 mL). The organic layers were combined and dried with anhydrous $MgSO_4$. The solvent was evaporated and (*S*,*R*)-**157** (0.73 g, 0.30 mmol, 93% yield) was obtained as a white solid.

Spectroscopic data and physical constants for compound (*S*,*R*)-157:

[α] $^{20}_{D}$ = + 20 (*c* 1, CH_2Cl_2).

IR (ATR) 3155.7, 2951.6, 2660.7, 1737.7, 1709.2, 1657.2, 1562.4 cm^{-1}.

^{1}H NMR ($CDCl_3$, 360 MHz) δ 1.49 (s, 18H, *t*Bu), 1.96 (c.a., 1H), 2.25 (c.a., 2H), 2.60 (m, 1H), 3.47 (m, 1H, H_1), 4.61 (q, *J*=14 Hz, 1H, H_2).

^{13}C NMR ($CDCl_3$, 90 MHz) δ 27.1 (C_4), 28.1 ($C(CH_3)_3$), 29.9 (C_3), 44.7 (C_1), 51.8 (C_2), 83.0 ($C(CH_3)_3$), 152.9 (CO_c), 176.2 (CO_a).

HRMS Calculated Mass for $C_{15}H_{25}NO_6Na$ $[M+Na]^+$: 338.1574. Found: 338.1579.

tert-Butyl ((1_R_,2_S_)-2-(benzyloxycarbonylamino)cyclobutane)(_tert_-butoxycarbonyl)carbamate, 152

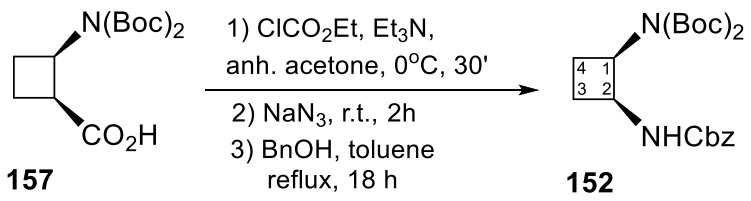

Carboxylic acid (*S*,*R*)-**157** (0.26 g, 0.82 mmol) was dissolved in anhydrous acetone (50 mL). Then, ethyl chloroformate (0.09 mL, 0.91 mmol) and triethylamine (0.11 mL, 0.82 mmol) were added. The system was stirred at 0 °C and under a nitrogen atmosphere for 30 minutes. Then, NaN_3 (0.082 g, 1.29 mmol) was dissolved in water (5 mL). The system was stirred at room temperature for 2 hours. After that, water (10 mL) was added and extractions with CH_2Cl_2 were done (3 x 15 mL). The organic layer was dried with anhydrous $MgSO_4$ and the solvent was evaporated. The acyl azide was obtained as yellow oil which was used directly in the following step. Then, acyl azide was dissolved in anhydrous toluene (20 mL) and benzyl alcohol (0.17 mL, 1.68 mmol) was added. The mixture was refluxed for 18 hours. After that, the solvent was evaporated under vacuum and the excess of benzyl alcohol was lyophilized. The reaction crude was purified by column chromatography using silica gel (Ethyl acetate-hexane; 1:2) to afford (*R*,*S*)-**152** (0.17 g, 0.41 mmol) as a yellowish oil in 50% yield.

Spectroscopic data and physical constants for compound (*R*,*S*)-152:

[α] $^{20}_{D}$ + 17 (*c* 0.8, methanol).

IR (ATR) 2917.8, 2849.5, 1727.6, 1466.9, 1244.2 cm^{-1}.

^{1}H NMR ($CDCl_3$, 250 MHz) δ 1.48 (s, 18H, *t*Bu), 2.25 (c.a., 1H), 2.44 (c.a., 3H), 4.47 (m, 1H, H_2), 4.76 (m, 1H, H_1), 5.08 (broad s., 2H, CH_2-Ph), 6.10 (broad s., 1H, N*H*), 7.34 (m, 5H, H_{ar}).

^{13}C NMR ($CDCl_3$, 62.5 MHz) δ 23.3, 26.2 (C_3-C_4), 28.0 ($C(CH_3)_3$), 51.1 (C_2), 53.3 (C_1), 66.4 (CH_2-Ph), 82.9 ($C(CH_3)_3$), 127.9, 128.4 (C_{ar}), 136.8 (CO), 153.2 (CO), 155.8 (CO).

HRMS Calculated Mass for $C_{22}H_{32}N_2O_6Na$ $[M+Na]^+$: 443.2153. Found: 443.2161.

(1*R*,2*S*)-2-(*tert*-butoxycarbonylamino)cyclobutane-1-carboxylic acid, 51

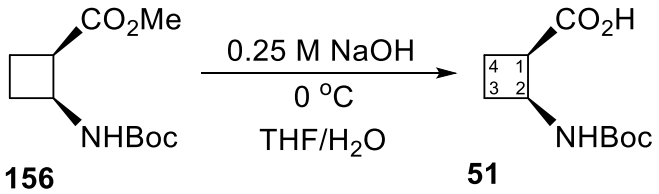

To an ice-cooled solution of ester (*R*,*S*)-**156** (0.79 g, 3.4 mmol) in a 1:10 THF-water mixture (55 mL), 0.25 M sodium hydroxide aqueous solution (34 mL, 8.6 mmol, 2.5 eq) was added and the resultant mixture was stirred for 2 h. (Reaction progress was monitored by TLC). The reaction mixture was washed with dichloromethane (20 mL), and 5% HCl aqueous solution was added to the aqueous phase to reach pH 2. The acid solution was extracted with ethyl acetate (4 x 50 mL) and dried over magnesium sulfate. Solvent was removed at reduced pressure to afford crude (*R*,*S*)-**51** as a white crystalline solid (0.72 g, 3.34 mmol, 98% yield) without need of further purification.

Spectroscopic data for compound (*R*,*S*)-51:

^{1}H NMR (250 MHz, $CDCl_3$): δ 1.45 (s, 9H, *t*Bu), 1.70-2.35 (c.a., 4H, H_3, H_4), 3.36 (m, 1H, H_1), 4.35 (m, 1H, H_2), 5.57 (broad s, 1H, N*H*).

<u>Spectroscopic data are consistent with those reported in reference:</u>

Izquierdo, S.; Rúa, F.; Sbai, A.; Parella, T.; Álvarez-Larena, A.; Branchadell, V.; Ortuño, R.M. *J. Org. Chem.*, **2005**, *70,* 7963.

tert-Butyl (1*S*,2*R*)-2-carbamoylcyclobutanecarbamate, 163

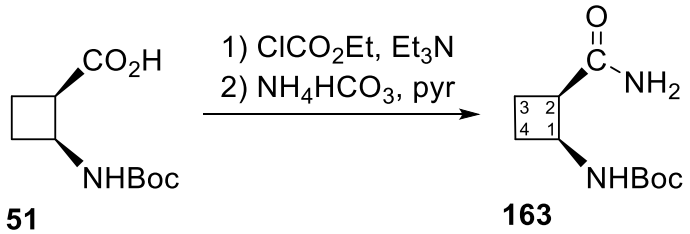

A mixture containing the free acid (*R*,*S*)-**51** (2.01 g, 9.34 mmol) in anhydrous acetone (50 mL), ethyl chloroformate (1.8 mL, 10.5 mmol) and triethylamine (0.19 mL, 1.4 mmol) was stirred at 0 °C and under a nitrogen atmosphere for 30 minutes. Then, ammonium bicarbonate (2.21 g, 28.01 mmol, 3.0 eq) and pyridine (1.9 mL, 23.34 mmol, 2.5 eq) were added and the mixture was stirred at room temperature for 2 h. EtOAc was added and the solution was washed with water (4 × 15 mL) and then dried under vacuum to give the desired product. Flash chromatography (3:2 EtOAc-hexane) provided the free amide (*S*,*R*)-**163** as a white powder (1.70 g, 7.94 mmol, 85% yield).

Spectroscopic data for compound (*S*,*R*)-163:

^{1}H NMR (250 MHz, $CDCl_3$): δ 1.42 (s, 9H, *t*Bu), 1.83-2.41 (c.a., 4H), 3.49 (m, 1H, H_2), 4.41 (m, 1H, H_1), 5.33 (br. s., 2H, NH_2), 5.53 (br. s., 1H, NH).

<u>Spectroscopic data are consistent with those reported in reference:</u>

Fernandes, C.; Pereira, E.; Faure, S.; Aitken, D. J., *J. Org. Chem.* **2009**, *74*, 3217.

(1*S*,2*S*)-2-(*tert*-butoxycarbonylamino)cyclobutane-1-carboxylic acid, 158

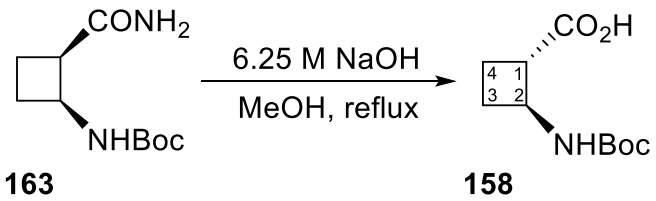

A solution of (*R*,*S*)-**163** (0.14 g, 0.65 mmol) in MeOH (15 mL) was treated with 6.25 M NaOH aqueous solution (5.2 mL) and the mixture was heated to reflux overnight. The methanol was then removed by careful evaporation under reduced pressure and the residual aqueous phase was washed with EtOAc (3 × 20 mL). The aqueous phase was then cooled at −5 °C, while concentrated HCl was added slowly until pH = 2. The aqueous phase was then extracted with EtOAc (3 × 60 mL) and the combined organic extracts were dried with $MgSO_4$ and concentrated under vacuum. After flash chromatography (EtOAc as eluent) the free acid (*S*,*S*)-**158** was obtained as a white powder (0.11 g, 0.51 mmol, 78% yield).

Spectroscopic data and physical constants for compound (*S*,*S*)-158:

^{1}H NMR (250 MHz, $CDCl_3$): δ 1.44 (s, 9H, *t*Bu), 1.88-2.22 (c.a., 4H, H_3, H_4), 3.10 (m, 1H, H_1), 4.14 (m, 1H, H_2), 6.28 (broad s, 1H, N*H*).

Spectroscopic data are consistent with those reported in reference:

Fernandes, C.; Pereira, E.; Faure, S.; Aitken, D. J. *J. Org. Chem.* **2009**, *74*, 3217.

Benzyl *tert*-butyl ((1*S*,2*S*)-cyclobutane-1,2-diyl)dicarbamate, 153

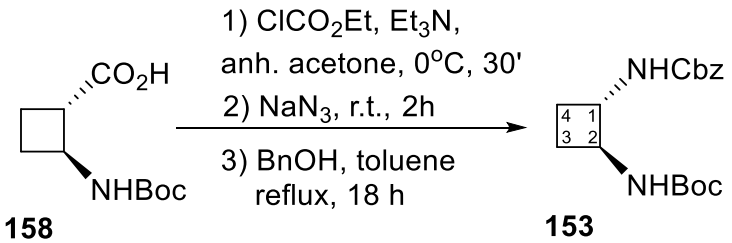

Acid carboxylic (*S*,*S*)-**158** (0.40 g, 1.9 mmol) was dissolved in anhydrous acetone (40 mL). Then, ethyl chloroformate (0.2 mL, 2.1 mmol) and triethylamine (0.26 mL, 1.9 mmol) were added. The system was stirred at 0 °C under a nitrogen atmosphere for 30 minutes. Then, NaN_3 (0.19 g, 1.6 eq, 3.0 mmol) dissolved in water (5 mL) was added. The system was stirred at room temperature for 2 hours. After that, water (15 mL) was added and extractions with CH_2Cl_2 were done (3 x 30 mL). The organic layer was dried with anhydrous $MgSO_4$ and the solvent was evaporated. 0.36 g (1.5 mmol, 80 % yield)

of the acyl azide were obtained as a yellow oil which was used directly in the following step. Acyl azide (0.36 g, 1.5 mmol) was dissolved in anhydrous toluene (80 mL). Then, 0.4 mL (3.9 mmol) of benzyl alcohol were added. The mixture was refluxed for 18 hours. After that, the solvent was evaporated under vacuum and the excess of benzyl alcohol was lyophilized. The reaction crude was purified by column chromatography using silica gel (Ethyl acetate-hexane; 1:3) to obtain (*S*,*S*)-**153** (0.41 g, 1.3 mmol, 70% yield) as a yellow oil. WARNING: Acyl azide intermediate should be carefully manipulated because of its explosive nature.

Spectroscopic data and physical constants for compound (*S*,*S*)-153:

[α] $^{20}_{D}$ +9 (*c* 1, CH_2Cl_2).

M.p. 140-142 ^{o}C (CH_2Cl_2).

IR (ATR) 3338.7, 2978.2, 2481.9, 1676.1, 1637.7, 1618.7, 1420.0 cm^{-1}.

^{1}H NMR ($CDCl_3$, 250 MHz) δ 1.45 (s, 9H, *t*Bu), 1.50 (c.a., 2H), 2.16 (c.a., 2H), 3.88 (m, 2H, H_1, H_2), 4.93 (broad s., 1H, N*H*), 5.10 (s, 2H, CH_2-Ph), 5.83 (broad s., 1H, N*H*), 7.37 (m, 5H, H_{ar}).

^{13}C NMR ($CDCl_3$, 62.5 MHz) δ 23.5, 23.8 (C3, C4), 28.5 (C(CH_3)$_3$), 52.8, 54.1 (C_1, C_2), 66.9 (CH_2-Ph), 80.0 (*C*(CH_3)$_3$), 128.4 (C_{ar}), 128.7 (C_{ar}), 136.6 (C_{ipso}), 155.4 (CO), 156.1 (CO).

HRMS (ESI) Calculated Mass for $C_{17}H_{24}N_2O_4Na$ $[M+Na]^+$: 343.1626. Found: 343.1628.

Methyl 2-bis(*tert*-butoxycarbonylamino)-*(*1R*,2S*)*-cyclobutan-1-carboxylate, 165

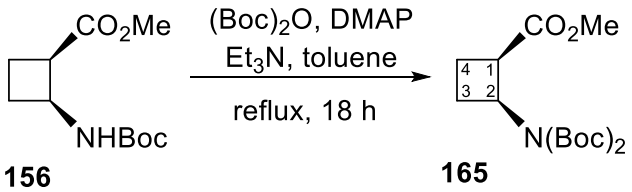

Carbamate (*R*,*S*)-**156** (0.6 g, 1.58 mmol) was dissolved in anhydrous toluene (60 mL) under a nitrogen atmosphere. Then, DMAP (110 mg, 0.9 mmol) and triethylamine (0.5 mL, 3.6 mmol) were added. Then, di-*tert*butyl dicarbonate (0.8 g, 3.67 mmol) was added. The mixture was refluxed for 18 hours. After that, the solvent was evaporated under vacuum and the crude was purified by column chromatography on silica gel using a mixture of hexane-ethyl acetate 4:1 to afford pure (*R*,*S*)-**165** (0.26 g, 0.8 mmol, 50% yield) as a colorless oil.

Spectroscopic data and physical constants for compound (*R*,*S*)-165:

[α] $^{20}_{D}$ -10 (*c* 2, methanol).

IR (ATR) 2981.3, 2716.3, 2000.0, 2113.8, 1779.8, 1731.6, 1701.1, 1355.9, 1251.0 cm^{-1}

^{1}H NMR ($CDCl_3$, 250 MHz) δ 1.44 (s, 18H, *t*Bu), 1.87 (m, 1H), 2.21 (m, 2H), 2.57 (m, 1H), 3.35 (m, 1H, H_1), 3.61 (s, 3H, Me), 4.56 (q, *J*=12.5 Hz, 1H, H_2).

^{13}C NMR ($CDCl_3$, 62.5 MHz) δ 18.1, 26.3 (C_3, C_4), 27.7 ($C(CH_3)_3$), 44.1 (C_1), 51.1 (Me), 51.3 (C_2), 82.0 ($C(CH_3)_3$), 152.1 (CO_c), 172.9 (CO_e).

HRMS (ESI) Calculated for $C_{16}H_{27}NO_6Na$ $[M+Na]^+$: 352.1731. Found: 352.1731.

(1R,2S)-2-bis(*tert*-butoxicarbonylamino)cyclobutane-1-carboxylic acid, 157

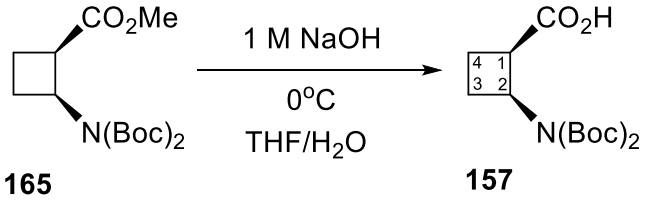

Methyl ester (*R*,*S*)-**165** (0.20 g, 0.61 mmol) was dissolved in a 1:10 THF-water mixture (20 mL). Then, 1 M NaOH (6.1 mL, 10 mmol) was added. The mixture was stirred at 0 °C for 3 hours. After that, the solution was acidified to pH 2 with 2 M HCl. Then, the mixture was extracted with CH_2Cl_2 (3 x 15 mL). The organic layers were combined and dried with anhydrous $MgSO_4$. The solvent was evaporated and (*R*,*S*)-**157** (0.19 g, 0.61 mmol, quantitative yield) was obtained as a white solid.

Spectroscopic data and physical constants for compound (*R*,*S*)-157:

[α] $^{20}_{D}$ - 23 (*c* 1, methanol).

IR (ATR) 2979.0, 1703.6, 1350.4, 1120.9 cm^{-1}

^{1}H NMR ($CDCl_3$, 250 MHz) δ 1.46 (s, 18H, *t*Bu), 1.97 (m, 1H), 2.21 (c.a., 1H), 2.31(c.a., 1H), 2.62 (m, 1H), 3.42 (m, 1H, H_1), 4.58 (q, *J* =14 Hz, 1H, H_2).

^{13}C-NMR ($CDCl_3$, 62.5 MHz) δ 19.3 (C_4), 27.4 ($C(CH_3)_3$), 28.5 (C_3), 44.9 (C_1), 51.9 (C_2), 83.1 ($C(CH_3)_3$), 153.0 (CO_c), 179.1 (CO_a).

HRMS Calculated Mass for $C_{15}H_{25}NO_6Na$ $[M+Na]^+$: 338.1574. Found: 338.1581.

tert-butyl ((1_S_,2_R_)-2-(benzyloxycarbonylamino)cyclobutane)(_tert_-butoxycarbonyl)carbamate, 152

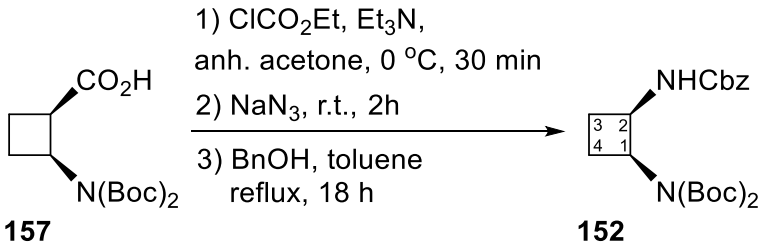

Carboxylic acid (*R*,*S*)-**157** (0.16 g, 0.5 mmol) was dissolved in anhydrous acetone (20 mL). Then, ethyl chloroformate (0.05 mL, 0.55 mmol) and triethylamine (0.07 mL, 0.50 mmol) were added. The system was stirred at 0°C under a nitrogen atmosphere for 30 minutes. Then, of NaN_3 (0.05 g, 1.6 eq, 0.79 mmol) dissolved in water (5 mL) was added. The system was stirred at room temperature for 2 hours. After that, water (10 mL) was added and extractions with CH_2Cl_2 were done (3 x 15 mL). The organic layer was dried with anhydrous $MgSO_4$ and the solvent was evaporated. The corresponding acyl azide (0.10 g, 0.4 mmol, 80 % yield) was obtained as a yellow oil and it was used directly in the following step. WARNING: This product should be carefully manipulated because of its explosive nature.

Acyl azide (0.10 g, 0.4 mmol) was dissolved in anhydrous toluene (50 mL). Then, benzyl alcohol (0.1 mL, 1.03 mmol) was added. The mixture was refluxed for 18 hours. After that, the solvent was evaporated under vacuum and the excess of benzyl alcohol was lyophilized. The reaction crude was purified by column chromatography using silica gel (Ethyl acetate-hexane; 1:2) to afford (*S*,*R*)-**152** (0.10 g, 0.24 mmol, 60% yield) as a yellowish oil.

Spectroscopic data and physical constants for compound (*S*,*R*)-152:

[α] $^{20}_{D}$ -15 (*c* 1.94, CH_2Cl_2).

IR (ATR) 3053.7, 2985.6, 2305.2, 2050.8, 1719.4, 1421.9, 1264.6 cm^{-1}.

^{1}H NMR ($CDCl_3$, 250 MHz) δ 1.48 (s, 18H, *t*Bu), 1.96 (c.a., 1H), 2.24 (c.a., 3H), 4.47 (c.a., 1H, H_1), 4.75 (c.a., 1H, H_2), 5.08 (broad s., 2H, CH_2-Ph), 6.12 (broad s., 1H, N*H*), 7.34 (m, 5H, H_{ar}).

^{13}C NMR ($CDCl_3$, 62.5 MHz) δ 23.7, 26.6 (C_3-C_4), 28.4 (C(CH_3)$_3$), 51.5, 53.7 (C_1, C_2), 66.8 (CH_2-Ph), 83.4 (*C*(CH_3)$_3$), 128.4, 128.8, 128.3 (C_{ar}), 137.2 (C_{ipso}), 153.7 (CO), 156.2 (CO).

HRMS (ESI) Calculated Mass for $C_{22}H_{32}N_2O_6Na$ $[M+Na]^+$: 443.2153. Found: 443.2156.

(1*R*,2*R*)-2-(*tert*-butoxycarbonylamino)cyclobutane-1-carboxylic acid, 158

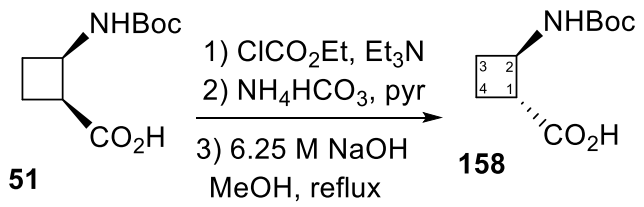

A mixture containing the free acid (*R*,*S*)-**51** (2.5 g, 8.67 mmol) in anhydrous acetone (50 mL), ethyl chloroformate (1.8 mL, 10.5 mmol) and triethylamine (0.19 mL, 1.4 mmol) was stirred at 0 °C and under a nitrogen atmosphere for 30 minutes. Then, ammonium bicarbonate (2.21 g, 28.01 mmol, 3.0 eq) and pyridine (1.9 mL, 23.34 mmol, 2.5 eq) were added and the mixture was stirred at room temperature for 2 h. EtOAc was added and the solution was washed with water (4 × 15 mL) and then dried under vacuum to give the desired product. Flash chromatography (3:2 EtOAc-hexane) provided the free amide intermediate as a white powder (2.20 g, 10.22 mmol, 85% yield). Then, this amide intermediate (0.22 g, 1.03 mmol) was dissolved in MeOH (5 mL) and was treated with 6.25 M aqueous NaOH solution (1.7 mL, 10.26 mmol, 10 eq) and the mixture was heated to reflux overnight. The methanol was then removed by careful evaporation under reduced pressure and the residual aqueous phase was washed with EtOAc (3 × 20 mL). The aqueous phase was then cooled at −5 °C, while concentrated HCl was added slowly until pH = 2. The aqueous phase was then extracted with EtOAc (3 × 60 mL) and the combined organic extracts were dried with

$MgSO_4$ and concentrated under vacuum. After flash chromatography (EtOAc as eluent) (*R*,*R*)-**158** was obtained as a white powder (0.16 g, 0.74 mmol, 71% yield).

Spectroscopic data for compound (*R*,*R*)-158:

^{1}H NMR (250 MHz, $CDCl_3$): δ 1.44 (s, 9H, *t*Bu), 1.78 (c.a., 2H), 2.22 (c.a., 2H), 3.14 (m, 1H, H_1), 4.10 (m, 1H, H_2), 5.02 (br. s., 1H, N*H*).

Spectroscopic data are consistent with those reported in reference:

Fernandes, C.; Gauzy, C.; Yang, Y.; Roy, O.; Pereira, E.; Faure, S.; Aitken, D. J. *Synthesis,* **2007**, *14*, 1992.

Benzyl *tert*-butyl ((1*R*,2*R*)-cyclobutane-1,2-diyl)dicarbamate, 153

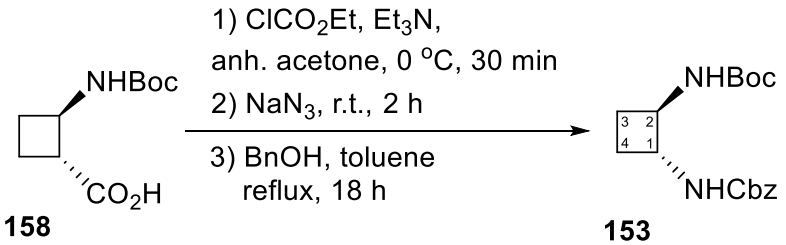

Carboxylic acid (*R*,*R*)-**158** (0.30 g, 1.4 mmol) was dissolved in anhydrous acetone (20 mL). Then, ethyl chloroformate (0.15 mL, 1.55 mmol) and triethylamine (0.19 mL, 1.4 mmol) was added. The system was stirred at 0 °C and under a nitrogen atmosphere for 30 minutes. Then, NaN_3 (0.14 g, 1.6 eq, 2.21 mmol) dissolved in water (5 mL) were added. The system was stirred at room temperature for 2 hours. After that, water (10 mL) was added and extractions with CH_2Cl_2 were done (3 x 20 mL). The organic layer was dried with anhydrous $MgSO_4$ and the solvent was evaporated. Acyl azide (0.27 g, 1.1 mmol, 78 % yield) was obtained as a yellow oil which was used directly in the following step. WARNING: This product should be carefully manipulated because of its explosive nature.

Acyl azide (0.27 g, 1.1 mmol) was dissolved in anhydrous toluene (80 mL). Then, benzyl alcohol (0.29 mL, 2.87 mmol) was added. The mixture was refluxed for 18 hours. After that, the solvent was evaporated under vacuum and the excess of benzyl

alcohol was lyophilized. The reaction crude was purified by column chromatography using silica gel (Ethyl acetate-hexane; 1:2) to achieve (*R*,*R*)-**153** (0.32 g, 1.0 mmol, 71 % yield) as a white solid.

Spectroscopic data and physical constants for compound (*R*,*R*)-153:

[α] $^{20}_{D}$ - 10 (*c* 1.4, methanol).

M.p. 141-142 ºC (CH_2Cl_2).

IR (ATR) 3343.8, 2972.2, 1674.8, 1519.3, 1274.5, 1161.2 cm^{-1}.

^{1}H-NMR ($CDCl_3$, 360 MHz) δ 1.42 (s, 9H, *t*Bu), 1.46 (c.a., 2H), 2.13 (c.a., 2H), 3.86 (m, 2H, H_1, H_2), 4.97 (broad s., 1H, N*H*), 5.08 (broad s., 2H, CH_2-Ph), 5.29 (broad s., 1H, N*H*), 7.34 (m, 5H, H_{ar}).

^{13}C-NMR ($CDCl_3$, 90 MHz) δ 23.8, 28.2 (C_3-C_4), 28.5 ($C(CH_3)_3$), 53.2 (C_2), 53.8 (C_1), 66.8 (CH_2-Ph), 79.7 ($C(CH_3)_3$), 128.3, 128.7 (C_{ar}), 136.6 (C_{ipso}), 155.3 (CO), 155.8 (CO).

HRMS calculated Mass for $C_{17}H_{24}N_2O_4Na$ $[M+Na]^+$: 343.1626. Found: 343.1632.

(1*S*,2*S*)-2-(benzyloxycarbonylamino)cyclobutanaminium chloride, 170

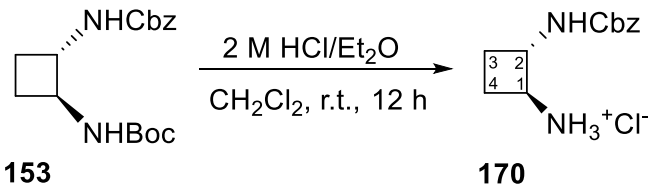

Diamine (*S*,*S*)-**153** (0.25 g, 0.9 mmol) was dissolved in CH_2Cl_2 (10 mL) Then, 2 M HCl solution in diethyl ether (5.5 mL, 14 mmol) was added. The reaction was stirred at room temperature overnight. After that, the solvent was evaporated under vacuum. (*S*,*S*)-**170** (230 mg, 0.9 mmol, quantitative yield) was obtained as a brown oil and it could be used in the next reaction without further purification.

Spectroscopic data and physical constants for compound (*S*,*S*)-170:

[α] $^{20}_{D}$ + 4 (*c* 1, methanol).

IR (ATR) 2952.9, 2142.4, 1687.0, 1527.2, 1249.0 cm^{-1}

^{1}H NMR (MeOD, 360 MHz) δ 1.80 (c.a., 2H), 2.21 (c.a., 2H), 3.59 (m, 1H, H_1), 4.10 (m, 1H, H_2), 5.08 (m, 2H, CH_2-Ph), 7.33 (m, 5H, H_{ar}).

^{13}C NMR (MeOD, 62.5 MHz) δ 20.7, 22.7 (C_2-C_3), 51.0 (C_1), 52.8 (C_2), 66.9 (CH_2-Ph), 128.2, 128.4, 128.8 (C_{ar}), 137.4 (C_{ipso}), 157.4 (CO_c).

HRMS calculated Mass for $C_{12}H_{17}ClN_2O_2Na$ $[M+Na]^+$: 221.1285. Found: 221.1287.

(1*R*,2*R*)-2-(benzyloxycarbonylamino)cyclobutane-1-aminium chloride, 170

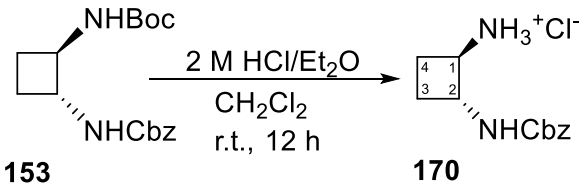

Diamine (*R*,*R*)-**153** (0.13 g, 0.40 mmol) was dissolved CH_2Cl_2 (10 mL). Then, 2 M HCl solution in diethyl ether (2.4 mL, 6.22 mmol) were added. The reaction was stirred at room temperature overnight. After that, the solvent was evaporated under vacuum. (*R*,*R*)-**170** (0.39 mg, 0.10 mmol, quantitative yield) was obtained as a brown oil and it could be used in the next reaction without further purification.

Spectroscopic data and physical constants for compound (*R*,*R*)-170:

[α] $^{20}_{D}$ - 4 (*c* 1, methanol).

IR (ATR) 2952.3, 1688.1, 1527.9, 1273.8 cm^{-1}.

^{1}H NMR (MeOD, 250 MHz) δ 1.79 (c.a., 2H), 2.16 (c.a., 2H), 3.59 (m, 1H, H_2), 4.11 (m, 1H, H_1), 5.04 (m, 2H, CH_2-Ph), 7.30 (m, 5H, H_{ar}).

(1*S*,2*R*)-2-(benzyloxycarbonylamino)cyclobutane-1-aminium chloride, 168

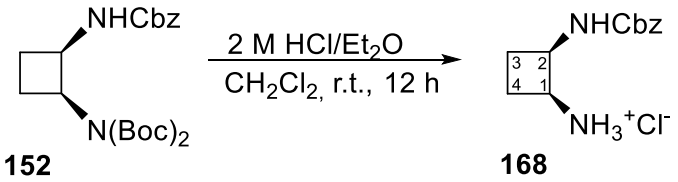

Diamine (*S*,*R*)-**152** (0.084 g, 0.20 mmol) was dissolved in CH_2Cl_2 (10 mL). Then, 2 M HCl solution in diethyl ether (1.22 mL, 3.11 mmol) was added. The reaction was stirred at room temperature overnight. After that, the solvent was evaporated under vacuum. (*S*,*R*)-**168** (0.049 mg, 0.19 mmol, quantitative yield) was obtained as a brown oil and it could be used in the next step without further purification.

Spectroscopic data and physical constants for compound (*S*,*R*)-168:

[α] $^{20}_{D}$ +18 (*c* 2.8, methanol).

IR (ATR) 3344.3, 3053.6, 2986.8, 2305.3, 2163.6, 2050.7, 1979.7, 1708.8, 1519.2, 1421.7 cm^{-1}.

^{1}H NMR (MeOD, 250 MHz) δ 2.05 (m, 1H), 2.30 (c.a., 3H), 3.89 (m, 1H, H_2), 4.15 (m, 1H, H_1), 4.36 (m, 1H, N*H*), 5.10 (m, 1H, CH_2-Ph), 7.36 (m, 5H, H_{ar}).

^{13}C NMR (MeOD, 62.5 MHz) δ 23.4, 24.6 (C_3, C_4), 50.9 (C_2), 53.3 (C_1), 67.8 (CH_2-Ph), 128.7, 128.8, 129.2 (C_{ar}), 137.6 (C_{ipso}), 157.9 (CO_c).

HRMS Calculated Mass for $C_{12}H_{17}ClN_2O_2Na$ $[M+Na]^+$: 221.1285. Found: 221.1284.

Tert-butyl ((1*S*,2*S*)-2-aminocyclobutane)carbamate, 172

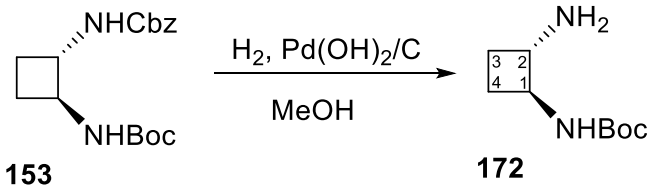

Diamine (*S*,*S*)-**153** (0.1 g, 0.31 mmol) was dissolved in the minimum amount of methanol. Then, $Pd(OH)_2/C$ (300 mg, 30 % weight) was added. The reaction mixture was stirred at room temperature for 12 hours under 7 atm pressure of hydrogen. Then the crude was filtered through Celite™ and this was washed abundantly with ethyl acetate. Solvents were evaporated under vacuum and (*S*,*S*)-**172** (0.05 g, 0.26 mmol, 84% yield) was obtained as a colorless oil.

Spectroscopic data and physical constants for compound (*S*,*S*)-172:

[α] $^{20}_{D}$ + 10 (*c* 1, CH_2Cl_2).

^{1}H NMR (MeOD, 360 MHz) δ 1.43 (c.a., 9H, *t*Bu), 2.01 (c.a., 2H), 3.12 (broad s, 1H, H_2), 3.61 (m, 1H, H_1).

^{13}C NMR ($CDCl_3$, 62.5 MHz) δ 22.0, 24.0 (C_3, C_2), 27.3 ($C(CH_3)_3$), 54.7 (C_2), 55.1 (C_1), 78.6 ($C(CH_3)_3$), 156.3 (CO_c).

Benzyl ((1*S*,2*S*)-2-(3'-(3'',5''-bis(trifluoromethyl)phenyl)thioureido)cyclobutane)carbamate, 171

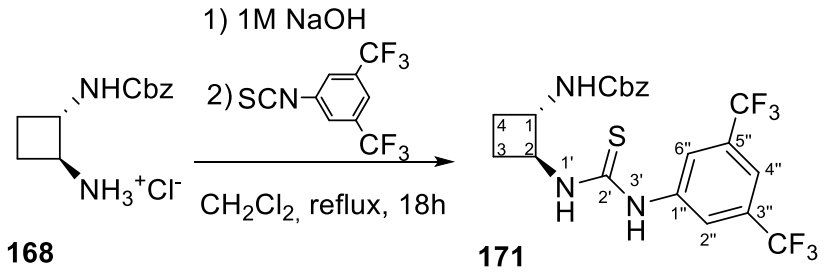

Diamine (*S*,*S*)-**168** (0.15 g, 0.68 mmol) was dissolved in CH_2Cl_2 (10 mL). This solution was washed with a 1 M aqueous solution of NaOH (3 x 10 mL). The organic layer was dried with anhydrous magnesium sulfate and the solvent was evaporated under vacuum. After that, the free amine was dissolved in anhydrous CH_2Cl_2 (7 mL) under a nitrogen atmosphere. 3,5-bis(trifluoromethyl)phenyl thioisocianate (0.130 mL, 1.5 eq, 0.71 mmol) was added. The reaction mixture was refluxed overnight. Then, the solvent was evaporated under vacuum and the reaction crude was purified by column chromatography using silica gel and using a mixture of hexane-ethyl acetate 2:1. (*S*,*S*)-**171** (240 mg, 0.51 mmol, 75% yield over two steps) as a colorless oil were obtained.

Spectroscopic data and physical constants for compound (*S*,*S*)-171:

[α] $^{20}_{D}$ - 16 (*c* 1, methanol).

IR (ATR) 3355.0, 2003.2, 1698.0, 1382.6, 1278.9 cm^{-1}.

^{1}H NMR ($CDCl_3$, 250 MHz) δ 1.65 (c.a., 2H), 2.30 (c.a., 2H), 3.99 (broad s, 1H, H_2), 4.62 (broad s, 1H, H_1), 5.04 (c.a., 2H, CH_2-Ph), 5.47 (m, 1H, N*H*), 7.26 (c.a., 5H, H_{ar}), 7.55 (m, 1H, $H_{4''}$), 7.96 (c.a., 2H, $H_{2''}$, $H_{7''}$).

^{13}C NMR ($CDCl_3$, 62.5 MHz) δ 22.9, 29.5 (C_3-C_4), 53.4 (C_1), 56.5 (C_2), 67.2 (CH_2-Ph), 118.1 (C and CH Ar and CF_3), 121.3, 123.2, 124.3, 128.0, 128.6, 131.3, 131.7, 132.0, 132.4, 135.6, 139.9, 156.5 (CO_c), 180.1 (CS).

HRMS Calculated Mass for $C_{21}H_{19}F_6N_3O_2SNa$ $[M+Na]^+$: 514.0994. Found: 514.0994.

Benzyl ((1*R*,2*S*)-2-(3'-(3'',5''-bis(trifluoromethyl)phenyl)thioureido)cyclobutane) carbamate, 169

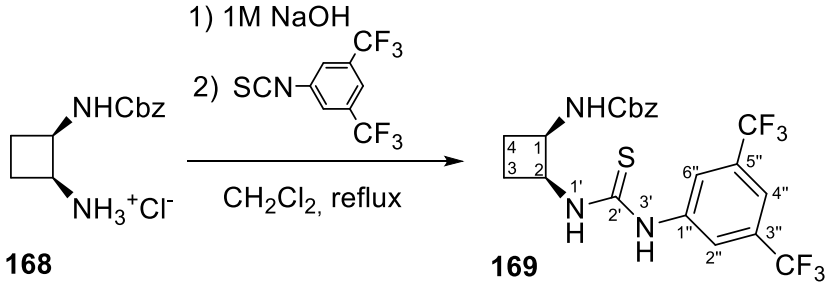

Diamine (*R*,*S*)-**168** (0.070 g, 0.18 mmol) was dissolved in CH_2Cl_2 (10 mL). This solution was washed with a 1 M aqueous solution of NaOH (3 x 10 mL). The organic layer was dried with anhydrous magnesium sulfate and the solvent was evaporated under vacuum. After that, the free amine was dissolved in anhydrous CH_2Cl_2 (7 mL) under a nitrogen atmosphere. 3,5-bis(trifluoromethyl)phenyl thioisocianate (0.034 mL, 0.19 mmol) was added. The reaction mixture was refluxed overnight. Then, the solvent was evaporated under vacuum and the reaction crude was purified by column chromatography using silica gel and using a mixture of hexane-ethyl acetate 2:1. Carbamate (*R*,*S*)-**169** (0.069 g, 0.14 mmol, 78% yield over two steps) was obtained as a colorless oil.

Spectroscopic data and physical constants for compound (*R*,*S*)-169:

[α] $^{20}_{D}$ + 2 (*c* 2, CH_2Cl_2).

IR (ATR) 3053.6, 2360.1, 1723.7, 1422.0, 1264.3 cm^{-1}.

^{1}H NMR ($CDCl_3$, 250 MHz) δ 2.04-2.39 (c.a., 4H), 3.91 (m, 1H, H_2), 4.33 (m, 1H, H_1), 5.03-5.07 (c.a., 2H, CH_2-Ph), 5.42 (m, 2H, N*H*), 7.30 (c.a., 5H, H_{ar}), 7.61 (m, 1H, $H_{4''}$), 8.00-8.41 (c.a., 2H, $H_{2''}$, $H_{6''}$).

^{13}C NMR ($CDCl_3$, 62.5 MHz) δ 23.7, 25.6 (C_4-C_3), 30.2 (C_2), 54.6 (C_1), 67.9 (CH_2-Ph), 119.0 (C and CH Ar and CF_3), 122.1, 124.2, 125.1, 128.5, 128.8, 128.9, 129.2, 132.5, 136.1, 140.9, 157.7 (CO_c), 181.6 (CS).

HRMS Calculated Mass for $C_{21}H_{19}F_6N_3O_2SNa$ $[M+Na]^+$: 514.0994. Found: 514.1003.

Benzyl (1*R*,2*R*)-2-(isobutylamino)cyclobutane carbamate, 173

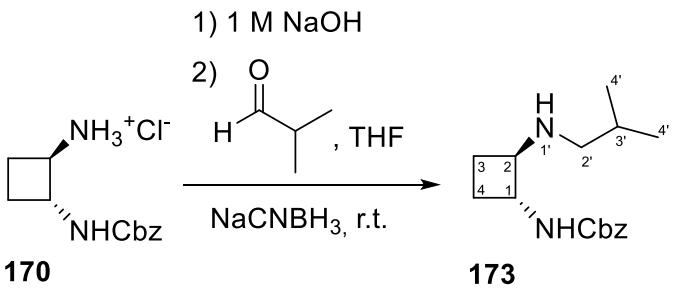

Diamine (*R*,*R*)-**170** (0.065 mg, 0.25 mmol) was dissolved in CH_2Cl_2 (5 mL). This solution was washed with a 1 M aqueous solution of NaOH (3 x 10 mL). The organic layer was dried with anhydrous magnesium sulfate and the solvent was evaporated under vacuum. After that, the free amine was dissolved in anhydrous THF (10 mL) under a nitrogen atmosphere and isobutyraldehyde (0.11 mL, 5 eq, 1.2 mmol) was added. The reaction mixture was stirred at room temperature for an hour. After that, sodium cyanoborohydride (23 mg, 1.6 eq, 0.37 mmol) was added. The reaction mixture was stirred at room temperature overnight. Then, the solvent was evaporated under vacuum. The crude residue was dissolved in CH_2Cl_2 (10 mL) and it was washed with a saturated aqueous solution of sodium bicarbonate (3 x 10 mL). The organic layer was dried with magnesium sulfate and the solvent was evaporated under vacuum. The crude was purified by column chromatography with silica gel and using a mixture of hexane-ethyl acetate 2:1. Carbamate (*R*,*R*)-**173** (26 mg, 0.094 mmol, 38% yield over two steps) was obtained as a colorless oil.

Spectroscopic data and physical constants for compound (*R*,*R*)-173:

[α] $^{20}_{D}$ - 2 (*c* 1.9, CH_2Cl_2).

IR (ATR) 2955.1, 2870.7, 2001.2, 2050.1, 1703.3, 1521.8, 1263.4 cm^{-1}.

^{1}H NMR ($CDCl_3$, 360 MHz) δ 0.90 (d, *J*=5.8 Hz, 6H, $2H_{4'}$), 1.25 (c.a., 2H), 1.73 (c.a., 1H), 2.05-2.17 (c.a., 2H), 2.31 (c.a., 2H), 3.16 (m, 1H, H_2), 3.91 (m, 1H, H_1), 5.08 (s, 2H, CH_2-Ph), 7.34 (c.a., 5H, H_{ar}).

^{13}C NMR ($CDCl_3$, 62.5 MHz) δ 20.8 (C4'), 23.1, 23.8 (C_3, C_4), 28.4 (C_2), 53.2 ($C_{2'}$), 54.8 (C_1), 62.1 (C_2), 67.0 (CH_2-Ph), 128.3, 128.7 (C_{ar}), 136.7 (C_{ipso}), 155.7 (CO_c).

HRMS Calculated Mass for $C_{16}H_{24}N_2O_2Na$ $[M+Na]^+$: 227.1911. Found: 227.1912.

(22*R*,19*S*)-*N*^{22},*N*^{19}-dihexadecylcyclobutane-22,19-dicarboxamide, *cis*-190

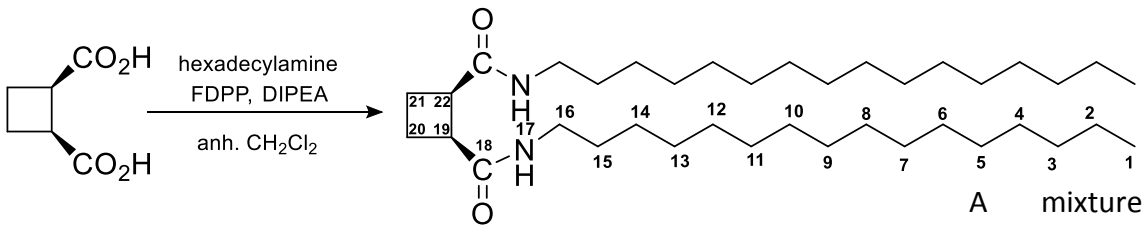

154 **190**

A mixture containing acid (*R*,*S*)-**154** (0.1 g, 0.69 mmol), FDDP (600 mg, 1.6 mmol) and DIPEA (1 mL, 5.7 mmol) in anhydrous dichloromethane (10 mL) was stirred for 10 minutes under nitrogen atmosphere. Then, hexadecylamine (370 mg, 1.53 mmol) and DMF (0.7 mL) was added. After that, more CH_2Cl_2 was added and the organic phase was washed with $NaHCO_3$, dried with $MgSO_4$ and concentrated to give a yellow solid. Purification by flash chromatography (EtOAc/Hexane; from 8:2 to 10:0) afforded *cis*-**190** (90 mg, 0.22 mmol, 22% yield) as a white solid that can be crystallized in MeOH.

Spectroscopic date and physical constants for compound *cis*-190

M. p.: 70 – 72 °C (MeOH)

IR (ATR): 3377.1, 3282.4, 2849.9, 1648.3, 1590.7, 1547.8 cm^{-1}

^{1}H NMR (500 MHz, $CDCl_3$) δ 0.93 (t, *J*= 6.7 Hz, $3H_1$), 1.29 (c.a., 24H, H_{14}, H_{13}, H_{12}, H_{11}, H_{10}, H_9, H_8, H_7, H_6, H_5, H_4, H_3), 1.59-1.65 (c.a., H_{15}), 2.35-2.49 (c.a., 1H, H_{20}), 2.52-2.60 (c.a., 1H, H_{20}), 3.32 (t, *J*= 6.8 Hz, H_{16}), 3.94 (broad s., 1H, H_{19}), 9.23 (broad s., 1H, NH_{17})

^{13}C NMR (125 MHz, $CDCl_3$) δ 14.4 (C_1), 23.0 (C_{20}), 26.4 (C_2), 27.2 (C_3), 28.8 (C_4), 29.5 (C_5), 29.7 (C_6), 29.8 (C_{12}), 29.9 (C_8), 30.0 (C_9, C_{10}, C_{11}), 30.1 (C_{13}), 32.3 (C_{14}), 41.3 (C_{16}), 41.5 (C_{19}), 177.0 (C_{18})

HRMS Calculated Mass for $C_{38}H_{74}N_2O_2Na$ $[M+Na]^+$: 613.5643. Found: 613.5625.

(19*S*,22*S*)-*N*^{19},*N*^{22}-dihexadecylcyclobutane-19,22-dicarboxamide, *trans*-190

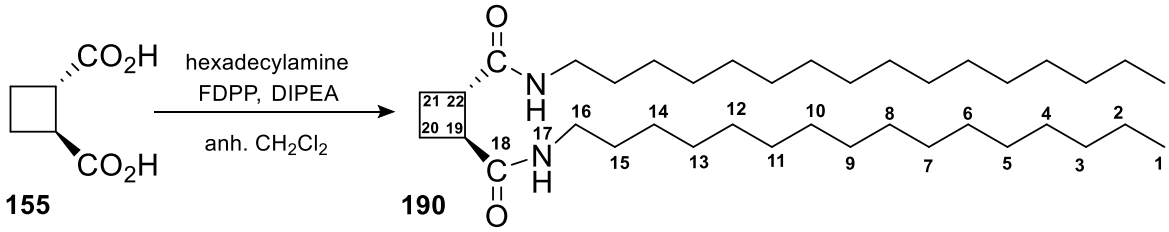

A mixture containing acid (*S*,*S*)-**155** (100 mg, 0.69 mmol), FDPP (600 mg, 1.6 mmol) and DIPEA (1 mL, 5.7 mmol) in anhydrous dichloromethane (10 mL) was stirred for 10 minutes under nitrogen atmosphere. Then, hexadecylamine (370 mg, 1.53 mmol) and DMF (0.7 mL) were added. After that, more CH_2Cl_2 was added and the organic phase was washed with $NaHCO_3$, dried with $MgSO_4$ and concentrated to give a yellow solid. Purification by flash chromatography (EtOAc/Hexane; 1:2) afforded *trans*-**190** (0.13 g, 0.22 mmol, 32% yield) as a white solid that can be crystallized in a mixture of MeOH-pentane.

Spectroscopic date for compound *trans*-190

[α] $^{20}_{D}$ - 90.5 (*c* 0.35, CH_2Cl_2)

M. p.: 113 – 114 °C (MeOH-pentane)

IR (ATR): 3290.1, 2916.5, 1628.6.

^{1}H NMR (500 MHz, $CDCl_3$) δ 0.89 (t, *J*=7.3 Hz, 3H, H_1), 1.27 (broad s., 24 H, H_{14}, H_{13}, H_{12}, H_{11}, H_{10}, H_9, H_8, H_7, H_6, H_5, H_4, H_3), 1.48-1.53 (t, *J* = 7.3 Hz, H_{15}), 2.00-2.01 (c.a., 1H, H_{20}), 2.10-2.16 (c.a., 1H, H_{20}), 3.13 (c.a., 1H, H_{19}), 3.24 (ddt, *J'*=1.2 Hz, *J''*=6.1 Hz, *J'''*=11.9 Hz, 2H, H_{16}), 6.4 (t, *J*=5.3 Hz, NH_{17})

^{13}C NMR (125 MHz, $CDCl_3$) δ 14.5 (C_1), 20.9 (C_{20}), 23.05 (C_2), 27.4 (C_3), 29.70 (C_4), 29.8 (C_5), 29.9 (C_6), 30.00 (C_7, C_8), 30.1 (C_9, C_{10}), 30.1 (C_{11}, C_{12}, C_{13}, C_{14}), 32.3 (C_{15}), 39.9 (C_{16}), 43.6 (C_{19}), 174.2 (C_{18}).

HRMS Calculated Mass for $C_{38}H_{74}N_2O_2$ $[M + Na]^+$: 613.5643. Found: 613.5631.

***tert*-butyl (1*S*,2*S*)-cyclobutane-1,2-diyldicarbamate, 174:**

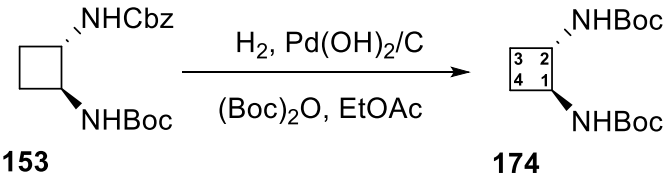

Diamine (*S*,*S*)-**153** (0.17 g, 0.53 mmol) in ethyl acetate (15 mL) was hydrogenated under 7 atmospheres of pressure in the presence of 30% $Pd(OH)_2/C$ (6 mg) and Boc_2O (0.12 mL, 0.55 mmol, 1.2 eq) overnight. The reaction mixture was filtered through Celite® and solvent was removed under vacuum and the residue was purified by column chromatography (1:2 ethyl acetate-hexane as eluent) affording the desired diamine (*S*,*S*)-**174** as a white solid (0.10 g, 0.35 mmol, 65% of yield).

Spectroscopic data and physical constants for compound (*S*,*S*)-174.

[α] $^{20}_{D}$ - 15.2 (*c* 0.58, MeOH)

IR (ATR): 3346, 2974, 1681, 1521, 1254, 1169 cm^{-1}

^{1}H NMR (250 MHz, $CDCl_3$) δ 1.45 (c.a., 18 H, *t*Bu), 2.04-2.23 (c.a., 2H, H_3, H_4), 3.83 (broad s, 2H, H_1, H_2), 5.05 (broad s, 2H, N*H*)

^{13}C NMR (62.5 MHz, $CDCl_3$) δ 24.1 (C_3, C_4), 29.2 ($C(CH_3)_3$), 53.8 (C_1, C_2), 80.1 ($C(CH_3)_3$), 156.1 (CO_c)

HRMS Calculated for $C_{14}H_{26}N_2O_4Na$ $[M + Na]^+$: 309.1785. Found: 309.1785.

C_{12}-NH-centered-bromoalkyl, 176:

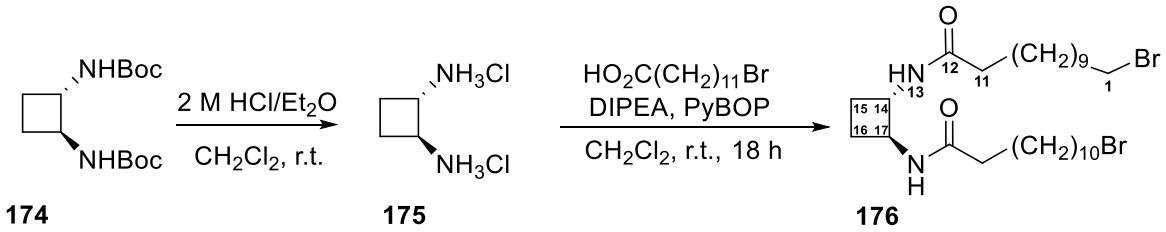

Diamine (*S*,*S*)-**174** (0.1 g, 0.4 mmol) was dissolved in CH_2Cl_2 (5 mL). Then, a 2 M HCl solution in diethyl ether (4 mL, 8 mmol) was added. The reaction was stirred at room temperature overnight. After that, the solvent was evaporated under vacuum. 65 mg (0.40 mmol, quantitative yield) of an intermediate diamine in the form of a chloride salt were obtained as a brown oil. This compound was used in next step without further purification. Diamine (*S*,*S*)-**175** (50 mg, 0.31 mmol) was dissolved in anhydrous dichloromethane (12 mL) and bromododecanoic acid (150 mg, 0.54 mmol), DIPEA (0.4 mL, 2.30 mmol) and PyBOP (409 mg, 7.86 mmol) were subsequently added. The mixture was stirred at room temperature under nitrogen atmosphere overnight. Afterwards, the mixture was washed with sodium bicarbonate and the organic phase was dried over magnesium sulfate. Solvent was removed and the residue was

chromatographed on silica gel using EtOAc as eluent. Bromo derivative (*S*,*S*)-**176** (165 mg, 0.27 mmol, 68% yield) was obtained as a white solid that can be crystallized in dichloromethane

Spectroscopic data and physical constants for compound (*S*,*S*)-176:

[α] $^{20}_{D}$ - 15 (*c* 1, MeOH)

M. p.: 180-184 °C (CH_2Cl_2)

IR (ATR) = 3296, 2919, 2851, 1641, 1542 cm^{-1}

^{1}H NMR (250 MHz, $CDCl_3$) δ 1.30 (broad s., CH_2, 14H), 1.39-1.48 (c.a., 2H), 1.54-1.68 (c. a., 2H), 1.73-1.92 (c.a., 2H), 2.10-2.32 (c.a., 2H), 3.45 (t, *J*=7.39 MHz, $2H_1$), 4.04 (broad s., 1H, H_{14}), 6.08 (broad s., 2H, NH_{13}).

^{13}C NMR (62.5 MHz, $CDCl_3$) δ 23.8, 25.6, 28.2, 28.8, 29.2, 29.3, 29.4, 29.5 (CH_2), 32.8 (C_2), 34.1 (C_1), 36.9 (C_6), 52.1 (C_{14}), 173.4 (C_{12})

MS calculated for $C_{28}H_{52}Br_2N_2O_2$ $[M + Na]^+$: 631. 27. Found: 631.23.

Bolaamphiphile *trans*-177

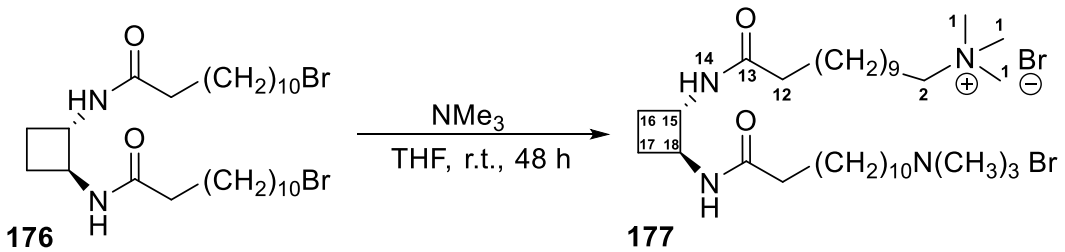

A solution of (*S*,*S*)-**176** (0.030 g, 0.05 mmol) in anhydrous THF (3 mL) was saturated with trimethylamine and the reaction was stirred at room temperature for 48 hours. Then, the solvent was evaporated under vacuo to afford *trans*-**177** (25 mg, 0.03 mmol, 60% yield) as a white solid that can be crystallized in a mixture of MeOH-diethyl ether.

Spectroscopic data and physical constants for compound *trans*-177:

[α] $^{20}_{D}$ - 20.7 (*c* 1.3, MeOH)

M. p.: 115-117 ^{o}C (MeOH)

IR (ATR) = 3296, 2919, 2851, 1641, 1542 cm^{-1}

^{1}H NMR (360 MHz, MeOD) δ 1.32 (broad s., CH_2, 18H), 1.52-1.87 (c.a., 2H), 2.05-2.20 (c.a., 2H), 3.14 (broad s., 9H, H_1), 3.32 (c.a., 2H, H_{12}), 4.20 (broad s, 2H, $H_{15,}$ NH_4).

^{13}C NMR (90 MHz, MeOD) δ 22.5, 22.6, 25.6, 25.9, 28.8, 28.8, 29.0, 29.1, 29.2 (C_3-C_{11}), 35.7 (C_{12}), 51.1 (C_2), 52.1 (C_1), 66.5 (C_{15}), 174.2 (C_{13})

HRMS Calculated for $C_{35}H_{73}N_4O_2$ $[M]^+$: 741.4080. Found: 741.4080.

tert-butyl(_tert_-butoxycarbonyl)((1_S_,2_R_)-2-(_tert_-butoxycarbonylamino)cyclobutane) carbamate, 183

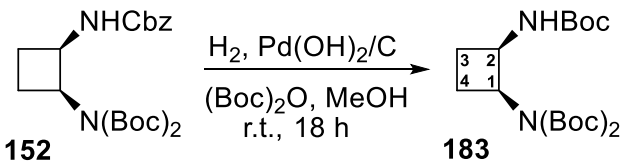

Diamine (*S*,*R*)-**152** (0.2 g, 0.48 mmol) was dissolved in the minimum amount of methanol. Then, di*tert*-butyl dicarbonate (200 mg, 0.92 mmol) and $Pd(OH)_2/C$ (100 mg, 50 % weight) were added. The mixture was hydrogenated under 7 atm of pressure during 12 h. Then, the crude was filtered through Celite™ and washed with methanol. The solvent was evaporated under vacuum. The crude was purified by column chromatography with silica gel (hexane-ethyl acetate; 9:1) to afford (*S*,*R*)-**183** (0.1 mg, 0.26 mmol, 54% of yield) as white solid.

Spectroscopic data and physical constants for compound (*S*,*R*)-183:

[α] $^{20}_{D}$ + 69.6 (*c* 2.17, CH_2Cl_2)

M. p.: 160-165 °C (CH_2Cl_2)

IR (ATR) = 3345.1, 2983.4, 1701.3, 1522.5, 1256.1, 1168.9 cm^{-1}

^{1}H NMR (360 MHz, $CDCl_3$) δ 1.43 (s., 9H, *t*Bu), 1.51 (s., 18H, 2*t*Bu), 1.86-2.00 (c.a., 1H), 2.12-2.40 (c.a., 3H), 4.40 (broad s., 1H, H_1), 4.71 (q, *J*=12.6 Hz, 1H, H_2), 5.71 (broad s., 1H, N*H*)

^{13}C NMR (90 MHz, $CDCl_3$) δ 23.8, 25.98 (C_3-C_4), 28.0 ($C(CH_3)_3$), 28.5 ($C(CH_3)_3$), 50.6 (C_2), 53.9 (C_1), 83.1 ($C(CH_3)_3$), 153.4 (CO_c), 155.6 (CO_c)

HRMS Calculated for $C_{19}H_{34}N_2O_6Na$ $[M + Na]^+$: 409.2309. Found: 409.2313.

((14*R*,17*S*)-cyclobutane-14,1-diyl)bis(1,1'-bromododecanamide), 188

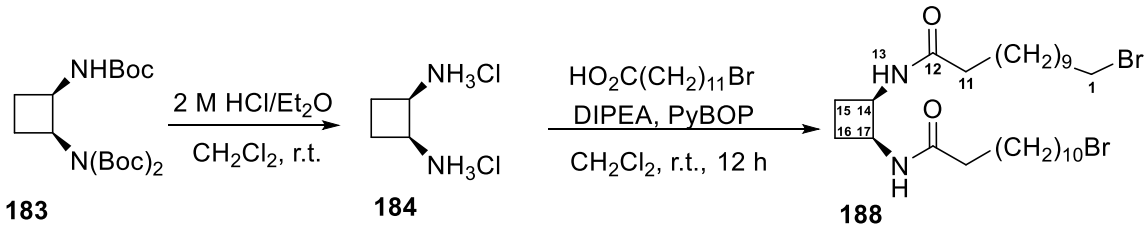

(*R*,*S*)-**183** (0.090 g, 0.23 mmol) was dissolved in CH_2Cl_2 (5 mL). Then, a 2 M HCl solution in diethyl ether (3 mL, 8 mmol) was added. The reaction was stirred at room temperature overnight. After that, the solvent was evaporated under vacuum. (*R*,*S*)-**184** (35 mg, 0.23 mmol, quantitative yield) was obtained as a white solid. This compound was used in next step without further purification. Diamine (*R*,*S*)-**184** (20 mg, 0.13 mmol) was dissolved in anhydrous CH_2Cl_2 (10 mL). Then, bromododecanoic acid (100 mg, 0.36 mmol), DIPEA (0.4 mL, 2.30 mmol) and PyBOP (120 mg, 0.31 mmol) were subsequently added. The mixture was stirred at room temperature under nitrogen atmosphere overnight. Afterwards, the mixture was washed with sodium bicarbonate and the organic phase was dried over magnesium sulfate. Solvent was removed, and the residue was chromatographed on silica gel (EtOAc) to achieve compound (*R*,*S*)-**188** (0.060 g, 0.095 mmol, 73 % yield) as a white solid.

Spectroscopic data and physical constants for compound (*R*,*S*)-188:

M. p.: 94 - 95 °C (MeOH)

IR (ATR) 3290, 2918, 2850, 1641, 1546 cm^{-1}

^{1}H NMR (250 MHz, $CDCl_3$) δ 1.30 (broad s., 14H), 1.38-1.51 (c.a., 2H), 1.58-1.70 (c.a., 2H), 1.80-1.98 (c.a., 2H), 2.15-2.24 (c.a., 2H, H_{11}), 3.43 (t, *J*=7.5 Hz, 2H, H_1), 4.38 (broad s., 1H, H_{14}), 6.28 (broad s., 1H, N*H*).

^{13}C NMR (62.5 MHz, $CDCl_3$) δ 25.8 (C_{16}), 26.2, 28.6, 29.2, 29.7, 29.8, 29.8, 29.9, 29.9 (C_{10}-C_3), 33.2 (C_2), 34.5 (C_1), 37.2 (C_{11}), 50.1 (C_{14}), 174.8 (C_{12}).

HRMS Calculated for $C_{28}H_{52}Br_2N_2O_2Na$ $[M + Na]^+$: 631.2269. Found: 631.2268.

Bolaamphiphile *cis*-177

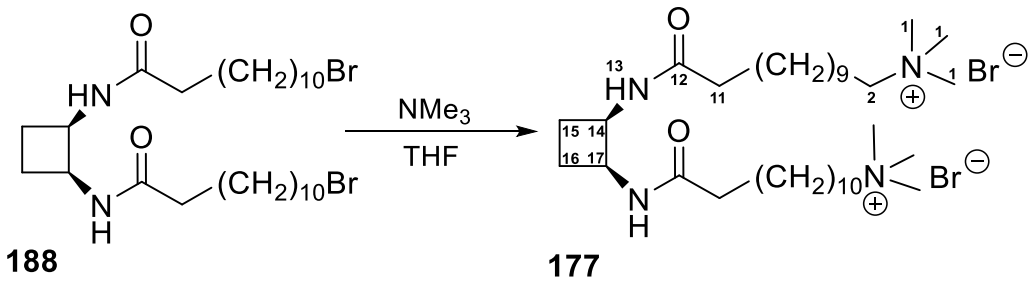

Amide (*R*,*S*)-**188** (0.080 g, 0.13 mmol) was dissolved in anhydrous THF (5 mL). Then, the solution was satured with trimethylamine and the reaction was stirred at room temperature for 48 hours. Compound *cis*-**177** (65 mg, 0.09 mmol, 70% yield) was obtained as a white solid which can be crystallized in methanol.

Spectroscopic data and physical constants for compound *cis*-177:

M. p.: 104 – 105 °C (MeOH)

IR (ATR) = 3295.3, 2917.0, 2850.1, 1648.6, 1537.2 cm^{-1}

^{1}H NMR (250 MHz, MeOD) δ 1.35 (broad s., 16H), 1.58-1.72 (c.a., 2H), 1.94-2.06 (c.a., 2H), 2.16-2.34 (c.a., 2H, H_{11}), 3.15 (s, 9H, H_1), 3.40 (c.a., 2H, H_2), 4.52 (broad s., 1H, H_{14})

^{13}C NMR (62.5 MHz, MeOD) δ 21.1 (C_{15}), 22.7, 24.1, 24.4, 27.2, 27.4, 27.6 (C_4-C_{10}), 34.1 (C_3), 49.8 (C_{11}), 51.1 (C_{14}), 65.4 (C_2), 173.1 (C_{12})

HRMS: Calculated for $C_{34}H_{70}BrN_4O_2$ $[M]^+$: 645.4677. Found: 645.4680.

Benzyl ((15*R*,14*S*)-14-(13'-bromododecanamido)cyclobutane)carbamate, 181

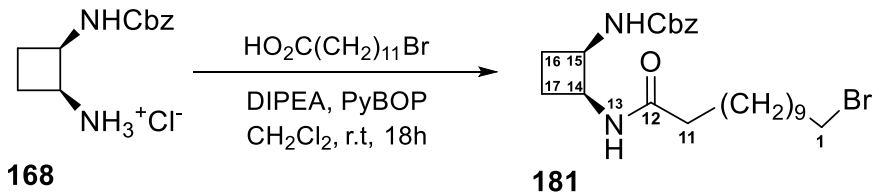

Into a solution containing the bromododecanoic acid (0.13 mg, 0.47 mmol, 2 eq), DIPEA (0.5 mL, 1.87 mmol, 8 eq), PyBOP (300 mg, 0.57 mmol, 2.5 eq) in anhydrous dichloromethane (10 mL) was added diamine (*R*,*S*)-**168** (60 mg, 0.23 mmol) and the mixture was stirred at room temperature under nitrogen atmosphere overnight. Afterwards, the mixture was washed with sodium bicarbonate and the organic phase was dried over magnesium sulfate. Solvent was removed, and the residue was chromatographed on silica gel using EtOAc as eluent obtaining the desired compound (*R*,*S*)-**181** (40 mg, 0.08 mmols, 35% yield) as white solid.

Spectroscopic data and physical constants for compound (*R*,*S*)-181:

[α] $^{20}_{D}$ - 4.3 (*c* 1, MeOH)

M. p.: 65-70 ^{o}C (MeOH)

IR (ATR) = 3319, 2919, 2850, 1691, 1643, 1540 cm^{-1}

^{1}H NMR (250 MHz, $CDCl_3$) δ 1.30 (s., 16H), 1.48-1.69 (c.a., 2H), 2.20-1.69 (c.a., 4H), 2.37-2.24 (c.a., 2H), 3.45 (t, *J*=7.2 Hz, 2H, H_1), 4.24 (broad s., 1H, H_2), 4.51 (broad s., 1H, H_{15}), 5.13 (s., 2H, CH_2-Ph), 5.29 (broad s, N*H*), 6.11 (broad s, N*H*), 4.99 (broad s., 5H, H_{ar})

^{13}C NMR (62.5 MHz, $CDCl_3$) δ 25.9, 26.2 (C_{16}-C_{17}), 28.6 (CH_2), 29.2 (CH_2), 29.7(CH_2), 29.7 (CH_2), 29.8 (CH_2), 29.9 (CH_2), 30.1 (CH_2), 33.3 (CH_2), 34.4 (C_1), 37.1 ($C_{3'}$), 50.9 (C_{14}, C_{15}), 67.34 (CH_2-Ph), 128.6, 128.9 (C_{ar}), 136.9 (C_{ipso}), 156.9 (CO_c), 174.2 (CO_a)

(1*R*,2*S*)-cyclobutane-1,2-dicarboxylic acid, 154

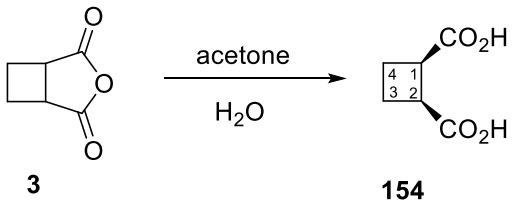

A solution of cycloadduct **3** (3.9 g, 31 mmol) and H_20 (6 mL, 10 eq) in acetone (100 mL) was stirred at room temperature. The progress of the reaction was monitored by ^{1}H NMR following the disappearance of the cycloadduct signals. After three days the reaction was not completed so further H_20 (9 mL) and HCl (2 mL) were added and the reaction was left other three days under stirring. After that, acetone was evaporated under reduced pressure and the residual water was lyophilized to give 4.6 g of (*R*,*S*)-**154** (quantitative yield) as a white solid.

Spectroscopic data for compound (*R*,*S*)-154:

^{1}H NMR (360 MHz, MeOD) δ 2.08 (s., 2H, H_3, H_4), 3.45 (s., 2H, H_1, H_2).

^{13}C NMR (90 MHz, MeOD) δ 20.9 (C_1, C_2), 40.21 (C_3, C_4), 158.31 (CO).

12-bromododecan-1-aminium bromide, 185

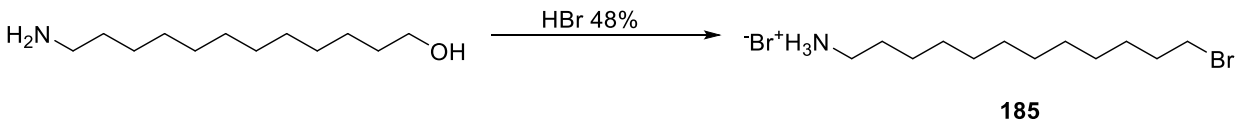

A solution of 12-aminododecanol (0.200 g, 1.0 mmol) was dissolved in aqueous HBr 48% (2 mL) and the solution refluxed overnight. Then, this solution was evaporated and the orange solid residue was dissolved in water (5 mL) and extracted with CH_2Cl_2 (4 x 15 mL). The combined organic extracts were washed with brine dried

over $MgSO_4$ and rotary evaporated to give **185** (0.327g, 94% yield) as a white crystalline solid.

Spectroscopic data for compound 185:

^{1}H NMR (250 MHz, $CDCl_3$): 1.15-1.54 (m, 16H, H_3, H_{10}, 1.71-1.94 (m, 4H, H_{11}, H_2), 3.02 (broad s, s, 2H, H_1), 3.43 (t, 2H, H_{12}), 8.19 (broad s, 3H, NH_3^+).

(15*R*,18*S*)-*N*^{1},*N*^{2}-bis(1-bromododecyl)cyclobutane-15,18-dicarboxamide, 188

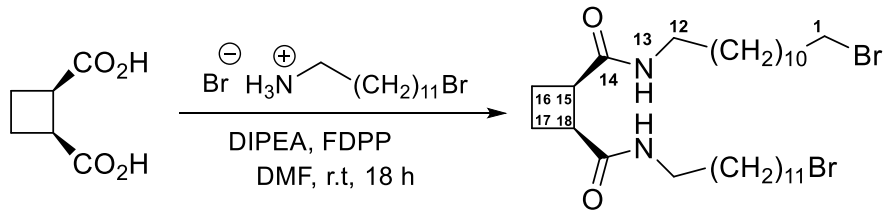

154 **188**

To a stirred solution of (*R*,*S*)-**154** (0.100 g, 0.69 mmol) in a mixture of dry CH_2Cl_2 (10 mL) and DMF (0.7 mL), DIPEA (0.9 mL, 5.32 mmol) and FDPP (0.583 mg, 1.52 mmol) were added. After 10 minutes 12-bromododecan-1-aminium bromide was added as a solid and the mixture was left under stirring overnight. After that, more CH_2Cl_2 was added and the organic phase was washed with $NaHCO_3$ and brine, dried on $MgSO_4$ and concentrated to give a yellow solid. Purification by flash chromatography (EtOAc/MeOH; from 10:0 to 9:1) afforded (*R*,*S*)-**188** (0.340 g, 0.53 mmol, 76% yield) as a pale yellow solid that can be crystallized with CH_3CN.

Spectroscopic data and physical constants for compound (*R*,*S*)-188:

M. p.: 75 -76 °C (CH_3CN)

IR (ATR): 3297.2 (NH), 2915.9, 2848.9 (CH), 1649.4 (C=O); 1547.8 (C=O) cm^{-1}

^{1}H NMR (360 MHz, $CDCl_3$): δ 1.27 (broad s., 28H), 1.37-1.52 (c.a., 8H), 1.86 (q, 4H, H_1, H_2), 2.15 (c.a., 2H), 2.34 (c.a., 2H), 3.21 (dd, 4H, H_{12}), 3.32 (broad s., 2H, H_{15}, H_{18}), 3.42 (t, 4H), 6.11 (broad s., 2H, NH)

^{13}C NMR (90 MHz, $CDCl_3$): δ 22.4 (C_{15}, C_{16}), 26.9 (CH_2), 28.1 (CH_2), 28.8, 29.3, 29.5 (CH_2), 32.8 (CH_2), 34.1 (CH_2Br), 39.7 (CH_2N), 43.2 (C_{15}, C_{18}) 172.5 (CO).

HRMS Calculated for $C_{30}H_{56}Br_2N_2NaO_2$ $[M + Na]^+$: 659.2583. Found: 659.2596.

Bolaamphiphile, *cis*-187

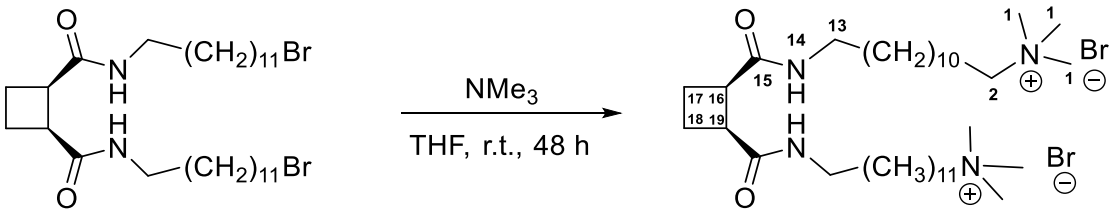

188 **187**

Compound (*R*,*S*)-**188** (0.215 g, 0.337 mmol) was dissolved in 4 mL of THF. Then 15 mL of DMF were added (the solid is insoluble in pure DMF) and the solution was bubbled 10 min with gaseous trimethylamine. The mixture was left one week under stirring, afterwards it was freeze dried to give a glass like solid, which was dissolved in the minimum amount of MeOH and reprecipitated from Et_2O, affording *cis*-**187** as a white solid (0.190 g, 85% yield).

Spectroscopic data and physical constants for compound (*R*,*S*)-187:

^{1}H NMR (360 MHz, MeOD): δ 1.28 (broad s., 28H), 1.76-1.90 (c.a., 3H), 2.10-2.20 (c.a., 2H), 2.29-2.37 (c.a., 2H), 3.17 (broad s., 18H, H_1), 3.31-3.42 (a.c., 4H).

^{13}C NMR (90 MHz, MeOD): δ 21.8, 23.0, 26.4, 27.1, 29.2, 29.5, 29.5, 29.6, 29.6, 29.7, 39.5, 42.6 (C_{16}), 52.6 (C_{13}), 66.9 (C_2), 174.3 (CO).

HRMS Calculated for $[M+Na]^+$: 675.4972. Experimental: 675.4963.

(1*S*,2*S*)-cyclobutane-1,2-dicarboxylic acid, 155

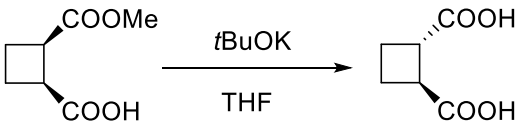

9 **155**

To a stirred solution of *t*-BuOK (0.85 g, 7.5 mmol) in 25 mL of THF at 0°C, hemiester (*S*,*R*)-**9** (0.596 g, 3.77 mmol) dissolved in 5 mL THF was added. The solution was stirred 1h at 0°C after that it was acidified by HCl 1M and more water was added to dissolve the formed salts. The resultant pale yellow solution was dried to give a yellowish solid. The solid was dissolved in water and the resultant solution extracted with EtOAc (x 4). The organic phase was dried on $MgSO_4$ and concentrated to give (*S*,*S*)-**155** as a white solid (0.440 g, 81% yield).

Spectroscopic data for compound (*S*,*S*)-155:

^{1}H NMR (250 MHz, $CDCl_3$): δ 2.11 (broad s., 2H), 3.40 (m., 1H).

(15*S*,18*S*)-*N*^{1},*N*^{2}-bis(1-bromododecyl)cyclobutane-15,18-dicarboxamide, 186

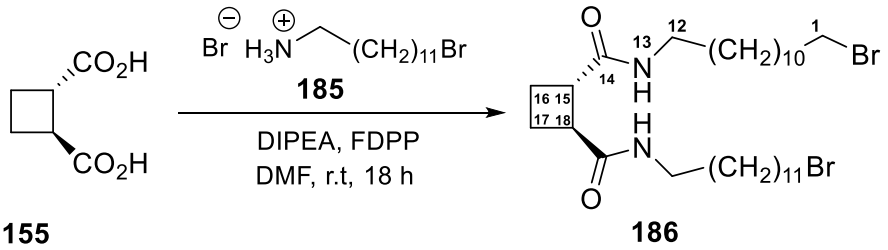

To a stirred solution of enantiopure (*S*,*S*)-**155** (0.100 g, 0.69 mmol) in dry CH_2Cl_2 (12 mL), DIPEA (0.72 mL, 5.32 mmol) and FDPP (0.580 mg, 1.5 mmol) were added. After 10 min the ammonium salt **185** was added as a solid and the mixture left stirring overnight. After that, more CH_2Cl_2 was added and the organic phase was washed with $NaHCO_3$, brine, dried on $MgSO_4$ and concentrated to give an yellow solid. Purification by flash chromatography using CH_2Cl_2/MeOH as eluent (gradient from 10:0 to 9:1), followed by crystallization from EtOAc, afforded (*S*,*S*)-**186** (0.395g, 89% yield) as a white solid.

Spectroscopic data and physical constants for compound (*S*,*S*)-186:

^{1}H NMR (360 MHz, $CDCl_3$): δ 1.26 (broad s., 17H), 1.37-1.44 (c.a., 4H), 1.84-1.94 (c.a., 2H), 2.06-2.14 (c.a., 2H), 3.07-3.15 (c.a., 1H), 3.27-3.40 (c.a., 2H), 6.44 (broad s., 1H).

^{13}C NMR (90 MHz, $CDCl_3$): δ 20.51, 26.90, 28.20, 28.76, 29.24, 29.50, 29.60, 32.88, 34.10, 39.45, 43.22, 174.00.

HRMS: Calculated for $[M+Na]^+$ 659.2583. Experimental 659.2598.

Bolaamphiphile, *trans*-187

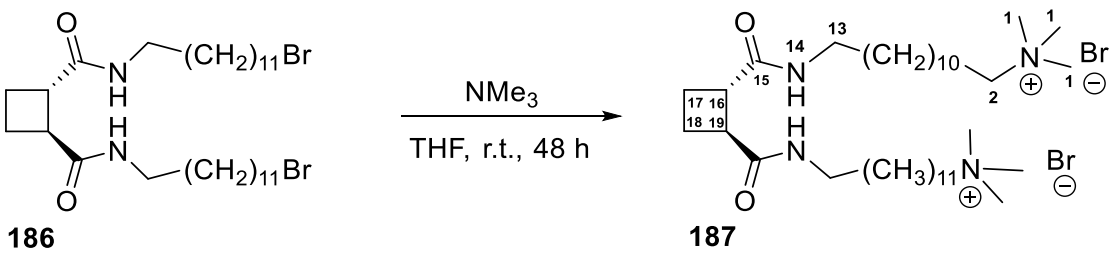

Compound (*S*,*S*)-**186** (0.100 g, 0.337 mmol) was dissolved in 2 ml of THF (2 mL) and then DMF (8 mL) was added. The solution was bubbled 10 min with gaseous trimethylamine and left under stirring three days. Afterwards, it was freeze dried to give a solid, which was crystallized from MeOH/Et_2O affording bolaamphiphiles *trans*-**187** (0.082 g, 83% yield).

Spectroscopic data and physical constants for compound *trans*-187:

^{1}H NMR (360 MHz, MeOD): δ 1.28 (broad s., 28H), 1.76-1.90 (c.a., 3H), 2.10-2.20 (c.a., 2H), 2.29-2.37 (c.a., 2H), 3.17 (broad s., 18H, H_1), 3.31-3.42 (a.c., 4H).

^{13}C NMR (90 MHz, MeOD): δ 21.8, 23.0, 26.4, 27.1, 29.2, 29.5, 29.5, 29.6, 29.6, 29.7, 39.5, 42.6 (C_{15}), 52.6 (C_{13}), 66.9 (C_2), 174.3 (CO).

HRMS Calculated for $[M+Na]^+$ 675.4972. Experimental 675.4963.

Triethoxysilane derivative, *trans*-189

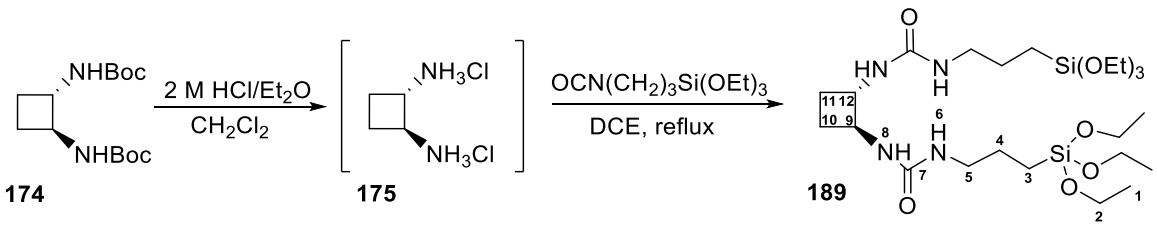

Diamine (*S*,*S*)-**174** (0.11 g, 0.38 mmol) was dissolved in CH_2Cl_2 (5 mL). Then, a 2 M HCl solution in diethyl ether (5 mL, 13.2 mmol) was added. The reaction was stirred

at room temperature overnight. After that, the solvent was evaporated under vacuum. This compound was used in next step without further purification.

Then, a mixture containing compound (*S*,*S*)-**175** (60 mg, 0.38 mmol), 3-isocyanatopropyltriethoxysilane (0.25 mL, 0.10 mmol) and triethylamine (0.2 mL, 1.43 mmol) in anhydrous dichloromethane (5 mL) was stirred at reflux for 18 h. After that, solvent was evaporated and the crude was chromatographed on silica gel using hexane to hexane:EtOAc(8:2) as eluent to afford compound *trans*-**189** (120 mg, 0.21 mmol, 52% yield) as a colorless oil.

Spectroscopic data and physical constants for compound *trans*-189:

[α] $^{20}_{D}$ + 56.7 (*c* 1.54, CH_2Cl_2)

IR (ATR): 3336.1, 2900.0, 1740.3, 1368.2, 1031.0 cm^{-1}

^{1}H NMR (360 MHz, $CDCl_3$) δ 0.61-0.69 (c.a., 2H, H_3), 1.26 (t, *J*=7.0 Hz, 9H, H_2), 1.58-1.77 (c.a., 2H, H_4), 3.18 (c.a., 2H, H_5), 3.84 (q, *J*=10.0 Hz, 6H, H_1), 4.16 (c.a., 2H, H_9, NH_6), 4.89 (broad s., 1H, NH_8)

^{13}C NMR (90 MHz, $CDCl_3$) δ 7.6 (C_3), 14.4 (C_4), 18.4 (C_1), 23.3 (C_{10}), 43.1 (C_5), 58.6 (C_2), 60.8 (C_9), 156.5 (C_7)

Silanol *trans*-231

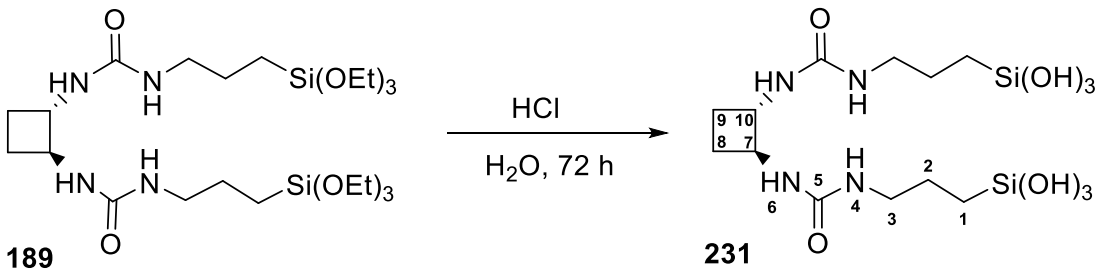

Triethoxysilane *trans*-**189** (0.1 g, 0.17 mmol) was dissolved in a mixture containing miliQ water and HCl in a molar ratio of 0.2 HCl : 600 H_2O (5 mL). The mixture was stirred in an oil bath (80 ^oC) for 3 h and it was left under static conditions at the same temperature for 2 days. After this period no precipitate was observed so it was left at 4 ^oC for 3 days. After that, no solid appeared and the sample was freeze-dried leading to a colorless oil which was identified as *trans*-**231** (0.045 g, 0.11 mmol, 65% yield).

Spectroscopic data and physical constants for compound *trans*-231:

[α] $^{20}_{D}$ = + 25 (*c* 1, MeOH)

IR (ATR) 3336.1, 2900.0, 1740.3, 1368.2, 1031.0 cm^{-1}

^{1}H NMR (360 MHz, MeOD) δ 0.54-0.73 (c.a., 2H, H_1), 1.15-1.32 (c.a., 2H, H_2), 1.48-1.71 (c.a., 2H, H_8), 3.11 (broad s, 2H, H_3), 4.08 (broad s., 2H, H_7, N*H*)

^{13}C NMR (90 MHz, MeOD) δ 13.7 (C_1), 23.4 (C_8), 29.4 (C_2), 42.9 (C_3), 60.2 (C_7), 157.7 (C_5)

HRMS calculated for $C_{12}H_{28}N_4O_8Si_2$ $[M]^+$: 580.86, Found: 279.1 (M-Si(OH)$_3$)

Hybrid silica *trans*-229

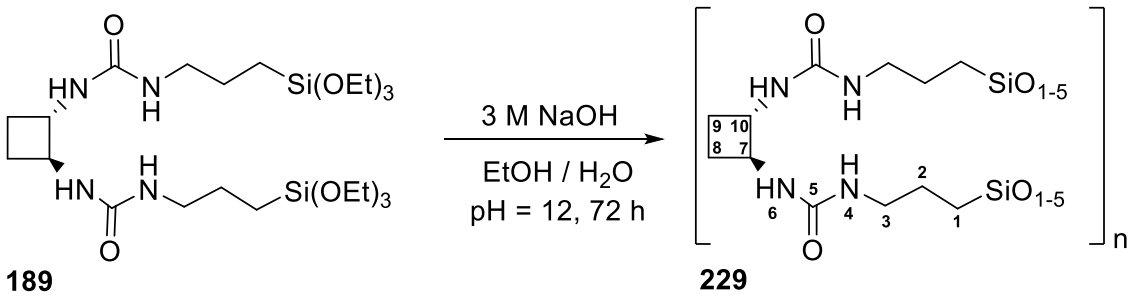

trans-**189** (0.06 g, 0.12 mmol) was first dissolved in ethanol (0.4 mL). Water (0.9 mL) was added leading to a white microcrystalline suspension. An aqueous solution of NaOH (3 M) was added until pH 12 was mantained and the mixture was heated at 80

°C for 3 days under static condition. The resulting yellowish solid *trans*-**229** (20 mg) was filtered, washed with water, ethanol and acetone and then dried in vacuo.

Spectroscopic data for compound *trans*-229:

IR (ATR): 3321.0, 2933.5, 1689.1, 694.6 cm^{-1}

CP-MAS ^{29}Si NMR: δ - 69.34 (T^3).

CP-MAS ^{13}C NMR: δ 11.03 (C_1), 15.23 (C_8), 25.46 (C_2), 45.96 (C_3), 60.41 (C_7), 159.42 (C_5).

Triethoxysilane derivative, *cis*-189

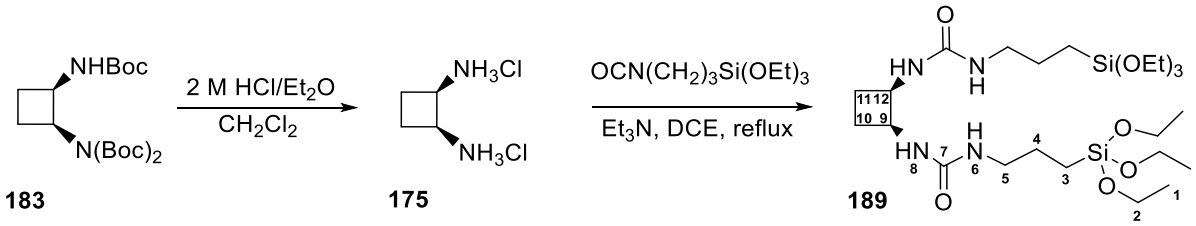

Diamine (*R*,*S*)-**183** (0.49 g, 0.13 mmol) was dissolved in CH_2Cl_2 (5 mL). Then, a 2 M HCl solution in diethyl ether (1.7 mL, 4.5 mmol) was added. The reaction was stirred at room temperature overnight. After that, the solvent was evaporated under vacuum. This compound was used in next step without further purification. A mixture of (*R*,*S*)-**175** (130 mg, 0.82 mmol), 3-isocyanatopropyltriethoxysilane (0.45 mL, 1.82 mmol) and triethylamine (0.34 mL, 2.43 mmol) in anhydrous dichloroethane (12 mL) was stirred under reflux for 18 h. After that, solvent was evaporated and the crude was chromatographed on silica gel using as eluent hexane to hexane:EtOAc (7:2) to afford compound *cis*-**189** as a colorless oil (80 mg, 0.14 mmol, 17 % yield).

Spectroscopic data and physical constants for compound *cis*-189:

IR (ATR): 3336.7, 2976.0, 1700.0, 634.6 cm^{-1}

^{1}H NMR (250 MHz, $CDCl_3$) δ 0.65 (dd, *J*=8.4 Hz, *J'*=7.9 Hz, 2H, H_3), 1.25 (t, *J*=7.1 Hz, 9H, H_1), 1.56-1.69 (c.a., 4H, H_4, H_{10}), 3.19 (c.a., 2H, H_5), 3.84 (q, *J*=10.7 Hz, 6H, H_2), 4.12 (q, *J*= 10.5 Hz, H_9, NH_8), 4.79 (broad s., NH_6).

^{13}C NMR (62.5 MHz, $CDCl_3$) δ 7.97 (C_3), 14.52 (C_1), 18.51 (C_4, C_{10}), 23.35 (C_5), 58.66 (C_2), 60.94 (C_9), 157.15 (C_7).

Hybrid silica *cis*-229

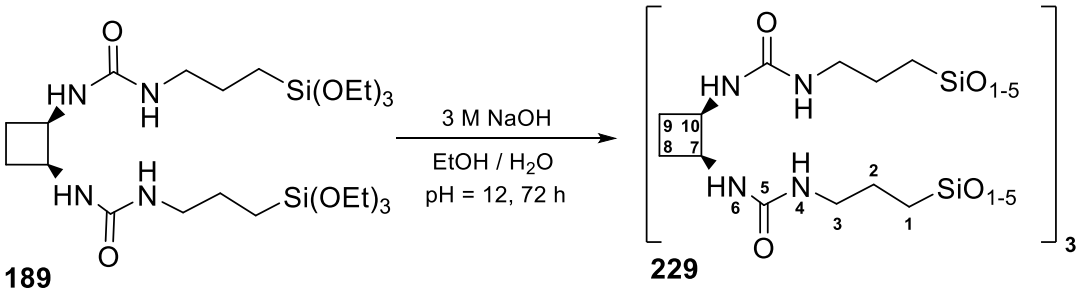

Triethoxysilane *cis*-**189** (0.03 g, 0.06 mmol) was first dissolved in ethanol (0.4 mL). Water (0.9 mL) was added leading to a white microcrystalline suspension. An aqueous solution of NaOH (3 M) was added until pH 12 was mantained and the mixture was heated at 80 ^{o}C for 3 days under static condition. The resulting solid *cis*-**229** (10 mg) was filtered, washed with water, ethanol and acetone and then dried in vacuo.

Spectroscopic data for compound *cis*-229:

IR (ATR): 3321.0, 2933.5, 1689.1, 694.6 cm^{-1}

CP-MAS ^{29}Si NMR: δ –74.74 (T^3).

CP-MAS ^{13}C NMR: δ 10.80 (C_1), 14.97 (C_8), 24.25 (C_2), 44.15 (C_3), 60.63 (C_7), 157.83 (C_5).

Triethoxysilane derivative *trans*-230

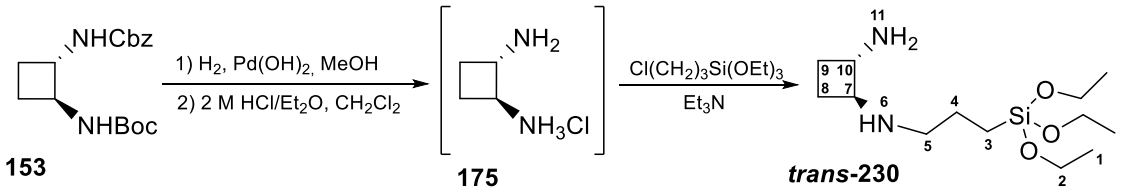

Diamine (*S*,*S*)-**153** (0.15 g, 0.47 mmol) was dissolved in the minimum amount of methanol. Then, $Pd(OH)_2/C$ (45 mg, 30 % weight) was added. The mixture was hydrogenated under 7 atm of pressure during 12 h. Then, the crude was filtered through Celite and washed with methanol. The solvent was evaporated under vacuum. An intermediate amine (70.3 mg, 0.37 mmol, 80% yield) was obtained as colorless oil. This intermediate was dissolved in CH_2Cl_2 (5 mL). Then, a 2 M HCl solution in diethyl ether (1.5 mL, 4 mmol) was added. The reaction was stirred at room temperature overnight. After that, the solvent was evaporated under vacuum. Diamine (*S*,*S*)-**175** (45 mg, 0.37 mmol) was afforded in 78% yield and it was used in the following step without further purification.

(*S*,*S*)-**175** (40 mg, 0.33 mmol), (3-chloropropyl)triethoxysilane (0.04 mL, 0.17 mmol) and freshly distilled triethylamine (0.05 mL) were introduced in a glass tube. The tube was sealed and placed in an oil bath at 87 ^{o}C. A brown precipitate appeared after 1 h. The reaction mixture was left at that temperature overnight (18 h). The sealed tube was opened and the solid was rinsed with pentane (3 x 1 mL). The solvent was evaporated and colorless oil was afforded. *trans*-**230** was obtained (30 mg, 0.10 mmol, 30% yield) and it was used in the next step without further purification.

Spectroscopic data for compound *trans*-230:

[α] $^{20}_{D}$ - 22 (*c* 1, methanol).

^{1}H NMR (250 MHz, $CDCl_3$) δ 0.72-0.82 (a.c., 2H, H_3), 1.25 (t, *J*=13Hz, 9H, H_1), 1.83-1.97 (a.c., 4H, H_8, H_4), 2.84-3.02 (a.c., 2H, H_5), 3.48-3.59 (a.c., 3H, H_6, NH_6), 3.85 (q, *J*=12.5 Hz, 6H, H_2)

Hybrid base catalyzed complex of Rhodium, *trans*-230-Rh

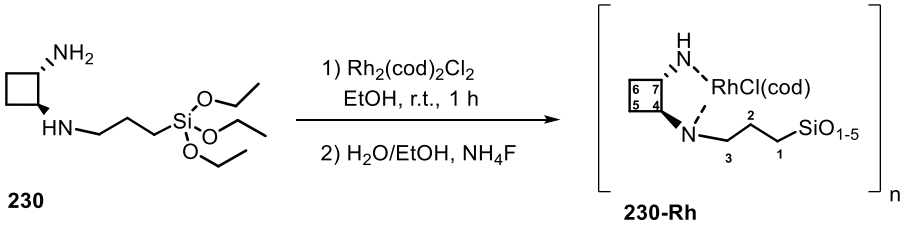

In a Schlenk tub under nitrogen atmosphere, a solution containing *trans*-**230** (0.025 g, 0.09 mmol) and $[Rh(cod)Cl]_2$ (6.5 mg, 0.013 mmol) in dry ethanol (1 mL) was stirred at 20 ^{o}C for 1 h. Then, ethanol (50 µl), distilled water (5 µl) and 0.1 M solution of NH_4F (5 µl) were added. The reaction mixture was then kept at 50 ^{o}C for 12 h and then cooled at room temperature. An orange gel formed after 24 h, which was allowed to stand in a closed vessel for 5 days. The solvent was removed and the yellow powder was washed with ethanol, acetone and water to afford *trans*-**230-Rh** (12 mg).

Spectroscopic data for compound *trans*-230-Rh:

IR (ATR): 3321.0, 2933.5, 1689.1, 694.6 cm^{-1}

CP-MAS ^{29}Si NMR: δ - 69.79 (T^3).

CP-MAS ^{13}C NMR: δ 9.93 (C_1), 25.15 (C_6,C_5), 33.09 (C_2), 57.57 (C_4,C_7), 78.74 (C_3).

(4*S*,1'*R*,3'*R*)-4-[2',2'-dimethyl-3'-(2''-methyl-[1'',3'']-dioxolan-2''-yl)cyclobutane]-*N*-isopropylpyrrolidin-2-one, 240:

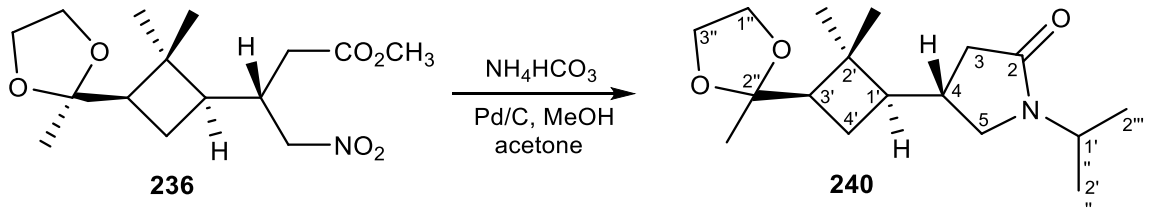

A mixture containing nitro ester **236** (330 mg, 1.1 mmol), acetone (200 µL, 4 eq.), ammonium formate (240 mg, 7 eq) and 10% Pd/C (160 mg) in anhydrous methanol (100 mL) was heated to reflux for 1 hour under nitrogen atmosphere. The reaction mixture was filtered through Celite®, and the solvent was evaporated. The crude was purified by chromatography over silica gel (Et_2O) to afford **240** as a white powder (310 mg, quantitative yield).

Spectroscopic data and physical constants for 240:

^{1}H NMR (250 MHz, $CDCl_3$) δ 1.07 (s, 3H, *trans*-CH_3), 1.1 (d, *J* = 6.25 Hz, 6H, $CH_{3\ isopropyl}$), 1.15 (s, 3H, *cis*-CH_3), 1.23 (s, 3H, $CH_{3\ ketal}$), 1.52 (c.a., 2H, $H_{4'a}$, H_4), 1.73-2.16 (c.a., 3H, $H_{4'b}$, $H_{1'}$, $H_{3'}$), 2.26 (m, 1H, H_{3a}), 2.43 (dd, *J* = 16.2 Hz, *J*= 8.2 Hz, 1H, $H_{3b)}$, 2.85 (dd, *J* = 9.5 Hz, *J*= 6.5 Hz, 1H, H_{5a}), 3.33 (dd, *J* = 9.5 Hz, *J*= 7.25 Hz, 1H, H_{5b}), 3.83-4.09 (c.a., 4H, -OCH_2CH_2O), 4.35 (hept, *J* = *J* = 7.25 Hz, 1H, $CH_{isopropyl}$).

<u>Spectroscopic data are consistent with those reported in reference:</u>

Aguilera, J. *PhD Thesis*, UAB 2010.

(4S,1'*R*,3'*R*)-3'-acetyl-[2',2'-dimethylcyclobutane]-*N*-isopropylpyrrolidin-2-one, 241:

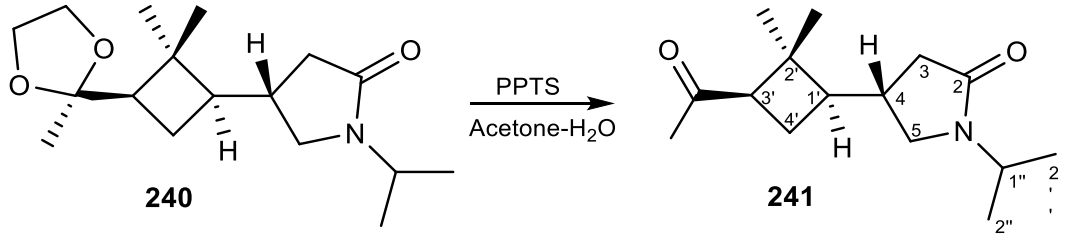

A mixture of ketal **240** (750 mg, 2.54 mmol) and PPTS (270 mg, 2.2 mmol) in wet acetone (60 mL) was heated under reflux for 2 h. The reaction mixture was cooled and solvent was removed at reduced pressure. The residue was poured into EtOAc (30 mL) and the resultant solution was washed with saturated aqueous $NaHCO_3$ and dried ($MgSO_4$). The solvent was evaporated under vacuum to dryness to afford **241** as a white powder which was crystallized in dichloromethane to afford pure ketone (613 mg, quantitative yield).

Spectroscopic data and physical constants for 241:

^{1}H NMR (360 MHz, $CDCl_3$) δ 0.90 (s, 3H, *trans-CH$_3$*), 1.10 (d, J = 2 Hz, 3H, $CH_{3\ isopropyl}$), 1.12 (d, J= 2 Hz, 3H, $CH_{3\ isopropyl}$), 1.35 (s, 3H, *cis-CH$_3$*), 1.73-2.11 (c.a., 3H, $H_{4'a}$, $H_{4'b}$, $H_{1'}$, H_4), 2.07 (s, 3H, *CH$_3$*CO), 2.26 (m, 1H, H_{3a}), 2.44 (dd, J = 15 Hz, J = 9.7 Hz, 1H, H_{3b}), 2.85 (c.a., 2H, H_5, $H_{3'}$), 3.36 (dd, J = 10.5 Hz, J = 7.2 Hz, 1H, H_{5b}), 4.36 (hept, J = J = 6.5 Hz, 1H, $CH_{isopropyl}$).

<u>Spectroscopic data are consistent with those reported in reference:</u>

Aguilera, J. *PhD thesis*, UAB 2010.

(1*R*,3*R*,3'*S*)-Methyl-3'-(1'-isopropyl-5-oxopyrrolidin-3-yl))-2,2-dimethylcyclo-butanecarboxylate, 242:

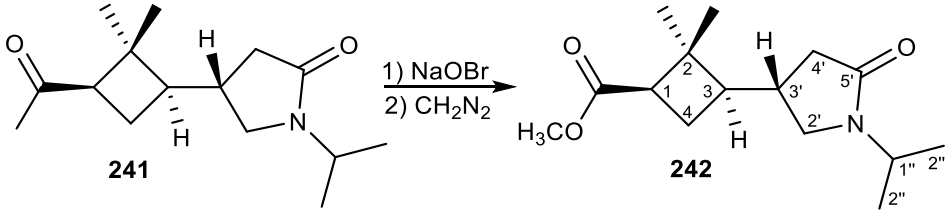

An ice-cooled solution of sodium hypobromite [prepared from bromine (0.55 mL, 7 mmol, 3.5 eq) and sodium hydroxide (1.6 g, 14 mmol, 7 eq)] in water (40 mL) was added to a solution of ketone **241** (500 mg, 1.99 mmol) in 3:1 dioxane-water (28 mL), previously cooled at -5 °C. The mixture was diluted with more dioxane (15 mL) and stirred at -5 °C for 5 h. Then, the reaction mixture was washed with dichloromethane (3x20 mL), treated with sodium bisulfite and, finally, 5% HCl aqueous solutionwas added to reach pH 2-3. The acid solution was extracted with dichloromethane (3x20 mL) and the organic extracts were dried over magnesium sulfate. Solvent was removed to afford the corresponding carboxylic acid.

This acid was directly methylated with an excess of diazomethane (3 eq) as a dichloromethane solution. The residue was purified by flash chromatography in silica gel (EtOAc) to provide **242** as a colourless oil (380 mg, 71% yield over the 2 steps).

Spectroscopic data and physical constants for 242:

^{1}H NMR (250 MHz, $CDCl_3$) δ 0.84 (s, 3H, *trans-CH$_3$*), 0.98 and 1.00 (2d, *J* = 3.5 Hz, 6H, $CH_{3\ isopropyl}$), 1.12 (s, 3H, *cis-CH$_3$*), 1.73-2.12 (complex absorption, 6H, H_{4a}, H_{4b}, H_3, $H_{3'}$), 2.19 (m, 1H, $H_{4'a}$), 2.31 (m, 1H, $H_{4'b}$), 2.58 (dd, *J* = 10.0 Hz, *J* = 7.2 Hz, 1H, H_1), 2.71 (dd, *J* = 12.0 Hz, *J* = 7 Hz, 1H, $H_{2'a}$), 3.26 (dd, *J* = 9.0 Hz, *J* = 7.5 Hz, 1H, $H_{2'b}$), 3.56 (s, 3H, CO_2CH_3), 4.25 (hept, *J*= *J*= 7.5 Hz, 1H, $CH_{isopropyl}$).

<u>Spectroscopic data are consistent with those reported in reference:</u>

Aguilera, J. *PhD thesis*, UAB 2010.

(1'*R*,3'*R*,3''*S*)-3'-[2',2'-dimetil-3'-(1''-isopropylpyrrolidin-3''-yl)cyclobutane] methanol, 237.

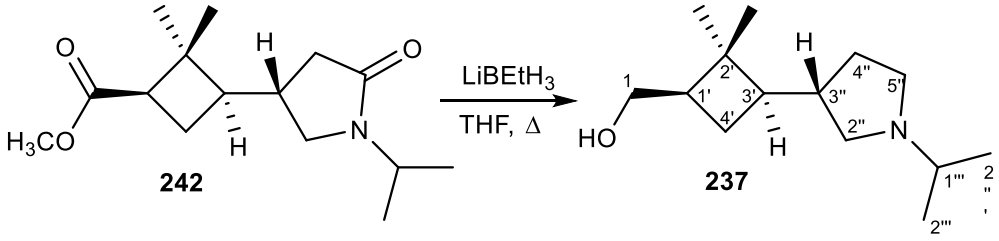

A 1 M solution of $LiBEt_3H$ in THF (10.5 mL, 10.5 mmol, 7 eq) was added to a solution of ester **242** (380 mg, 1.42 mmol) in anhydrous THF (50 mL). The mixture was heated to reflux under nitrogen atmosphere for 18 h. Excess hydride was eliminated by slow addition of methanol (5 mL), and then water (30 mL) was added. The resultant solution was extracted with dichloromethane (3x30 mL), and the combined extracts were dried over $MgSO_4$. Solvents were removed under reduced pressure, and the residue was chromatographed (CH_2Cl_2 – MeOH 20:1) to provide alcohol **237** as a colourless oil (250 mg, 78 % yield).

Spectroscopic data and physical constants for 237:

^{1}H NMR (360 MHz, $CDCl_3$) δ 0.95 (s, 3H, *trans-CH$_3$*), 1.06 (d, *J* = 4 Hz, 3H, $CH_{3\ isopropyl}$), 1.06 (d, *J* = 4 Hz, 3H, $CH_{3\ isopropyl}$), 1.11 (s, 3H, *cis-CH$_3$*), 1.10-1.44 (c.a., 2H, $H_{4'a}$, $H_{3'}$),1.71 (m, 1H, $H_{4'b}$), 1.94 (c.a., 3H, H_{4a}, H_{4b}, H_3), 2.07 (m, 1H, $H_{1'}$), 2.26 (m, 1H, $H_{2''a}$), 2.40 (m, 2H, $H_{5''a}$, $CH_{isopropyl}$), 2.75 (m, 2H, $H_{2''b}$, $H_{5''b}$), 3.51 (m, 2H, *CH$_2$*OH).

<u>Spectroscopic data are consistent with those reported in reference:</u>

Aguilera, J. *PhD thesis*, UAB 2010.

(1'*R*,3'*R*,3''*S*)-4-Benzyl-1-[3'-(1''-isopropylpyrrolidin-3''-yl)-2',2'-dimethyl-cyclobutane)metyl]-piperidine, 238:

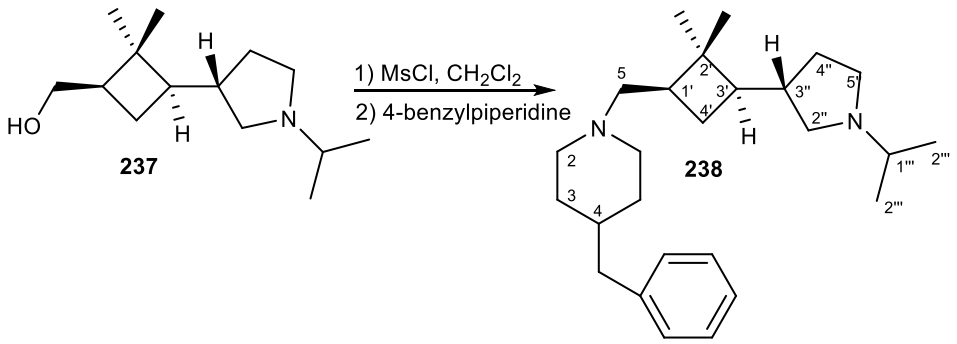

To a mixture containing alcohol **237** (150 mg, 0.66 mmol) in anhydrous CH_2Cl_2 (10 mL), triethylamine (0.12 mL, 0.86 mmol, 1.3 eq), DMAP (8 mg, 0.06 mmol, 0.1 eq) and mesyl chloride (60 µL, 0.8 mmol, 1.2 eq) were added at 0°C. The mixture was stirred for 1h at 0°C. Volatiles were then evaporated under vacuum.

The mesylate was poured into anhydrous acetonitrile (10 mL) and 4-benzylpiperidine was added (1.9 mL, 6.6 mmol, 10 eq). The mixture was stirred overnight. Solvent was then evaporated under reduced pressure. The residue was purified by column chromatography over silica gel (CH_2Cl_2 to MeOH) to afford **238** as a colourless oil (210 mg, 82% over 2 steps).

Spectroscopic data and physical constants for 238:

^{1}H NMR (250 MHz, $CDCl_3$) δ 0.92 (s, 3H, *trans-CH$_3$*), 1.07 (ca, 10H, $C_{2'}$-*CH$_3$*, 2*CH$_3$* $_{isopropyl}$, $H_{3''}$), 1.25 (c.a., 4H, H_3), 1.30 (c.a., 2H, $H_{4''}$), 1.67 (c.a. 2H, H_4, $H_{4'a}$), 1.79 (complex absorption, 6H, H_5, $H_{4'b}$, $H_{1'}$, $H_{3'}$, CH $_{isopropyl}$), 2.27 (c.a., 4H, $H_{2''}$, $H_{5''}$), 2.53 (d, *J*= 7Hz, 2H, *CH$_2$*Bn), 2.81 (m, 4H, H_2), 7.21 (c.a. 5H, Ph).

<u>Spectroscopic data are consistent with those reported in reference:</u>

Aguilera, J. *PhD thesis*, UAB 2010.

(3*S*,1'*R*,3'*R*)-3-[2',2'-dimethyl-3'-(2''-methyl-[1'',3'']-dioxolan-2''-yl)cyclobutane]-4-nitrobutan-1-ol, 243:

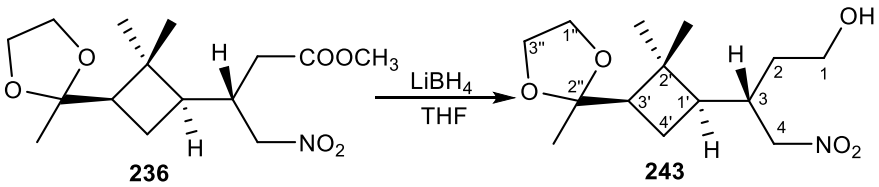

A 2 M solution of $LiBH_4$ in THF (9.5 mL, 19 mmol, 2 eq) was added to a solution of ester **236** (3.0 g, 9.5 mmol) in anhydrous THF (50 mL). The mixture was heated to reflux under nitrogen atmosphere for 2 h. Excess hydride was eliminated by slow addition of methanol (5 mL), and then water (30 mL) was added. The resultant solution was extracted with dichloromethane (5x30 mL), and the combined extracts were dried over $MgSO_4$. Solvents were removed under reduced pressure, and the residue was chromatographed (CH_2Cl_2 to EtOAc) to provide alcohol **243** as a colourless oil (1.9 g, 71% yield).

Spectroscopic data and physical constants for compound 243:

^{1}H NMR (250 MHz,$CDCl_3$) δ 1.12 (s, 3H, *trans*-CH_3), 1.19 (s, 3H, *cis*-CH_3), 1.23 (s, 3H, $CH_{3\,ketal}$), 1.43-1.79 (complex absorption, 5H, $H_{1'}$, $H_{4a'}$, $H_{4b'}$, H_{4a}, H_{4b}), 2.10 (dd, *J*= 7.75, *J* = 11 Hz, 1H, $H_{3'}$), 2.35 (m, 1H, H_3), 3.75 (dd, *J* = 5.75, *J* = 6.25 Hz, 2H, CH_2OH), 3.78-4.02 (complex absorption, 4H, -OCH_2CH_2O-), 4.39 (dd, *J* = 1.75, *J* = 5.5 Hz, 2H, -CH_2NO_2).

<u>Spectroscopic data are consistent with those reported in reference:</u>

Aguilera, J. *PhD thesis*, UAB 2010.

(3*S*,1'*R*,3'*R*)-4-amino-3-[2',2'-dimethyl-3'-(2''-methyl-[1'',3'']-dioxolan-2''-yl) cyclobutane]-butan-1-ol, 244:

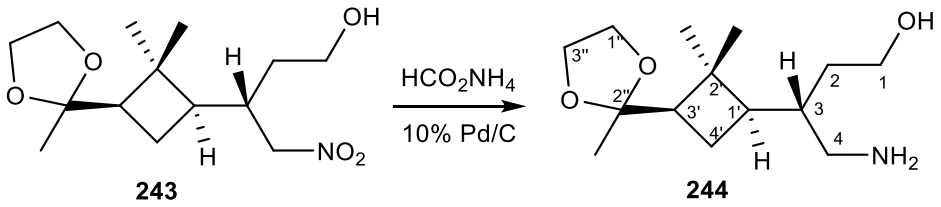

A mixture containing aminoalcohol **243** (400 g 1.4 mmol), ammonium formate (682 mg, 11 mmol, 7 eq), and 10% Pd/C (40 mg) in 25 mL anhydrous methanol was heated at reflux for 1 hour under nitrogen atmosphere. The reaction mixture was filtered through Celite®, and the solvent was evaporated to dryness to obtain **244** as a colourless oil (360 mg, quantitative yield).

Spectroscopic data and physical constants for compound 244:

^{1}H NMR (250 MHz, $CDCl_3$) δ 0.98 (s, 3H, *trans-CH$_3$*), 1.11 (s, 3H, c*is-CH$_3$*), 1.16 (s, 3H, $CH_{3\ ketal}$), 1.17-2.02 (complex absorption, 6H, $H_{1'}$, $H_{4a'}$, $H_{4b'}$, H_{2a}, $H_{2b,}$ $H_{3'}$), 2.35 (m, 1H, H_{4a}), 2.78 (complex absorption, 1H, H_{4b}), 3.44 (m, 1H, *CH$_2$*OH), 3.64 (m, 1H, *CH$_2$*OH) 3.70-4.02 (complex absorption, 4H, -O*CH$_2$CH$_2$*O-), 4.58 (broad singlet, 2H, N*H$_2$*).

<u>Spectroscopic data are consistent with those reported in reference:</u>

Aguilera, J. *PhD thesis*, UAB 2010.

(3*S*,1'*R*,3'*R*)-4-tosylamino-3-[2',2'-dimethyl-3'-(2''-methyl[1'',3'']dioxolan-2''-yl)cyclobutane]-butan-1-ol, 245:

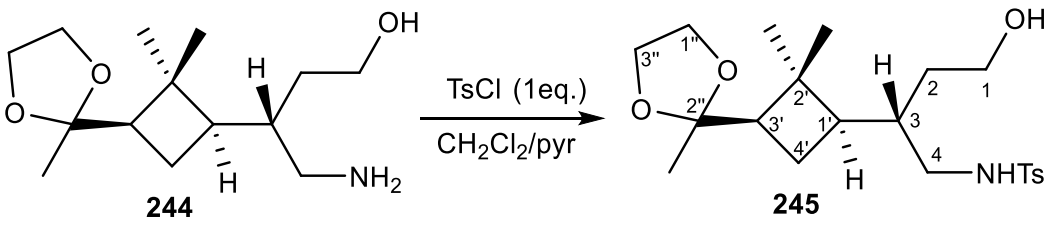

A mixture containing aminoalcohol **244** (1.48 mmol) and 4-toluenesulfonyl chloride (286 mg, 1.48 mmol, 1 eq) in distilled pyridine (40 mL) was stirred at room temperature under nitrogen atmosphere for 18 hours.

The solvent was evaporated under vacuum. The crude was then solved in EtOAc (30 mL) and washed with a saturated aqueous solution of $NaHCO_3$ (3x15 mL), dried over $MgSO_4$ and evaporated at reduced pressure. The residue was chromatographed (EtOAc-hexane 2:1) to provide tosylamide **245** as colourless oil (432 mg, 71% yield).

Spectroscopic data and physical constants for compound 245:

^{1}H NMR (250 MHz, $CDCl_3$) δ 0.94 (s, 3H, *trans-CH$_3$*), 1.08 (s, 3H, *cis-CH$_3$*), 1.17 (s, 3H, $CH_{3\ ketal}$), 1.2-1.62 (c.a., 5H, $H_{1'}$, $H_{4a'}$, $H_{4b'}$, H_{2a}, H_{2b}), 1.74 (m, 1H, H_3), 1.95 (dd, *J*= 18.75 Hz, *J*= 7.75 Hz, 1H, $H_{3'}$), 2.39 (s, 3H, Bn*CH$_3$*), 2.59 (m, 1H, H_{4a}), 2.90 (m, 1H, H_{4b}), 3.60 (m, 2H, *CH$_2$*OH), 3.78-4.02 (c.a., 4H, -O*CH$_2$CH$_2$*O-), 6.15 (dd, *J* = 7.75 Hz, *J*= 4.75 Hz, 1H, N*H*), 7.45 (d, *J*= 9.5 Hz, 2H, H_{meta}), 7.51 (d, *J* = 9.5 Hz, 2H, H_{orto}).

<u>Spectroscopic data are consistent with those reported in reference:</u>

Aguilera, J. *PhD thesis*, UAB 2010.

(3*S*,1'*R*,3'*R*)-3-[2',2'-dimethyl-3'-(2''-methyl[1'',3'']dioxolan-2''-yl)cyclobutane]-*N*-tosylpyrrolidine, 246:

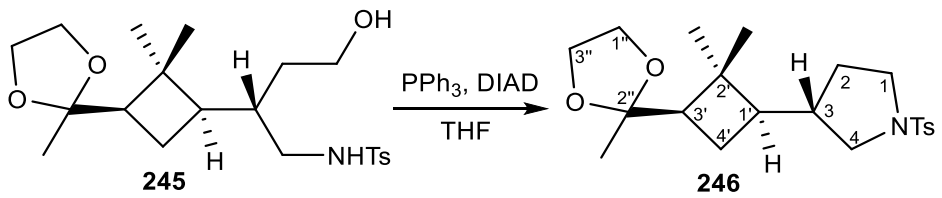

Triphenylphosphine (144 mg, 0.55 mmol, 1.5 eq) was added to a stirred solution of tosylamide **245** (150 mg, 0.36 mmol) in anhydrous THF (12 mL) under nitrogen atmosphere. The mixture was cooled to 0°C and diisopropylazodicarboxylate (0.11 mL, 0.55 mmol, 1.5 eq) was added dropwise. After the addition, the ice bath was removed and reaction was warmed to room temperature and stirred overnight. The mixture was concentrated and poored in cold ether to precipitate most of the $OPPh_3$. After filtration, the ether solution was evaporated to dryness and the crude was chromatographed (CH_2Cl_2) to afford pyrrolidine **246** as a white powder which was crystallized in ether/pentane (136 mg, 97% yield).

Spectroscopic data and physical constants for compound 246:

^{1}H NMR (250 MHz, $CDCl_3$) δ 1.02 (s, 3H, *trans-CH$_3$*), 1.06 (s, 3H, c*is-CH$_3$*), 1.22 (s, 3H, $CH_{3\ ketal}$), 1.38-1.51 (complex absorption, 3H, H_{4a}, $H_{4a'}$, H_2), 1.82 (complex absorption, 2H, H_{4b}, $H_{4'b}$), 2.1 (m, 2H, $H_{3'}$, $H_{1'}$), 2.47 (s, 3H, Bn*CH$_3$*), 2.75 (dd, 1H, *J* = 10 Hz, *J*= 7.5 Hz H_{2a}), 3.18-3.39 (complex absorption, 3H, H_{2b}, $2H_5$), 3.78-4.05 (complex absorption, 4H, -O*CH$_2$CH$_2$*O-), 7.53 (d, *J*= 14.7 Hz, 2H, H_{meta}), 7.56 (d, *J*= 14.7 Hz, 2H, H_{orto}).

<u>Spectroscopic data are consistent with those reported in reference:</u>

Aguilera, J. *PhD thesis*, UAB 2010.

(1'*R*,3'*R*,3''*S*)-1-[2',2'-dimethyl-3'-(*N*-tosylpyrrolidin-3''-yl)-cyclobutane]ethan-one, 247:

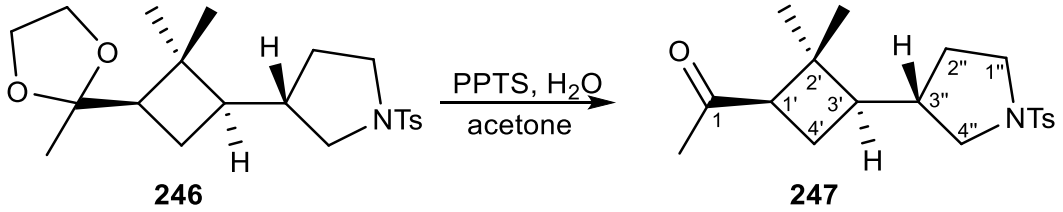

A mixture of ketal **246** (360 mg, 0.92 mmol) and PPTS (115 mg, 0.92 mmol, 1 eq) in wet acetone (15 mL) was heated under reflux for 5 h. The reaction mixture was cooled and solvent was removed under reduced pressure. The residue was poured into EtOAc (30 mL) and the resultant solution was washed with saturated aqueous $NaHCO_3$ and then dried with $MgSO_4$. The solvent was evaporated under vacuum to afford a white powder which is recrystallized in hexane to afford pure ketone **247** (310 mg, 96% yield).

Spectroscopic data and physical constants for compound 247:

^{1}H NMR (250 MHz, $CDCl_3$): 0.77 (s, 3H, *trans*-CH_3), 1.19 (s, 3H, *cis*-CH_3), 1.29 (m, 1H, $H_{3'}$), 1.49-1.93 (complex absorption, 5H, $H_{1''}$, $H_{2'a}$, $H_{2'b}$, $H_{4''a}$, $H_{4''b}$), 1.96 (s, 3H, CH_3CO), 2.40 (s, 3H, BnCH_3), 2.70 (dd, *J*= 18 Hz, *J*= 8 Hz, 2H, $H_{1''}$, $H_{4'a}$), 3.10 (m, 1H, $H_{4'b}$), 3.25 (m, 2H, $H_{1'a}$, $H_{1'b}$), 7.29 (d, *J*= 15 Hz, 2H, H_{meta}), 7.64 (d, *J*= 11 Hz, 2H, H_{orto}).

<u>Spectroscopic data are consistent with those reported in reference:</u>

Aguilera, J. *PhD thesis*, UAB 2010.

(1*S*,1'*R*,3'*R*,3''*S*)-1-[2'',2'-dimethyl-3'-[N-tosylpyrrolidin-3''-yl)cyclobutane] ethanol, 239:

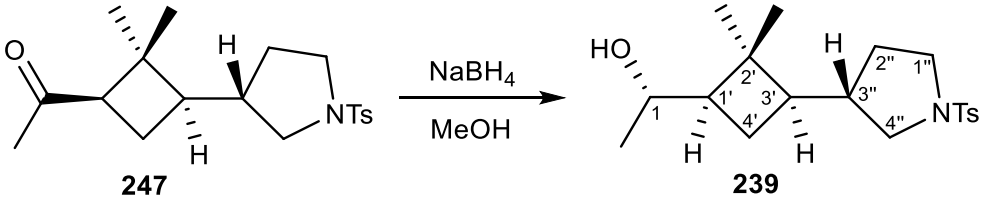

$NaBH_4$ (125 mg, 1.43 mmol, 4 eq) was added to a solution of ester **247** (125 mg, 0.36 mmol) in anhydrous MeOH (15 mL) at 0°C under nitrogen atmosphere. The mixture was warmed up to room temperature and stirred for 5 h. Excess hydride was eliminated by slow addition of water (5 mL). The resultant solution was extracted with ethyl acetate (3x20 mL), and the combined extracts were dried over $MgSO_4$. Solvents were removed at reduced pressure, and the residue was chromatographed (CH_2Cl_2 to EtOAc) to provide a mixture of alcohols **239a** and its epimer **239b** (110 mg, ratio 10:1, d.e. = 82%, 87% yield). Major diastereoisomer **239** was obtained by crystallization (^{i}PrOH).

Spectroscopic data and physical constants for compound 239:

^{1}H NMR (250 MHz, $CDCl_3$) δ 0.97 (s, 3H, t*rans*-CH_3), 1.10 (d, 3H, J = 7 Hz, CH_3-CHOH), 1.12 (s, 3H, *cis*-CH_3), 1.29-1.49 (c.a., 3H, $H_{3'}$), 1.6 (m, 1H, $H_{2'a}$), 1.69-2.03 (c.a., 3H, $H_{1''}$, $H_{2'b}$, $H_{3''}$, $H_{4''a}$, $H_{4''b}$), 2.45 (s, 3H, BnCH_3), 2.68 (dd, 1H, J = 9.6 Hz, J= 7.3 Hz, $H_{4'a}$), 3.26 (c.a., 3H, $H_{1'a}$, $H_{1'b}$, $H_{4'b}$), 3.63 (m, 1H, C*H*OH), 7.37 (d, J= 8.3 Hz, 2H, H_{meta}), 7.71 (d, J= 8.3 Hz, 2H, H_{orto}).

<u>Spectroscopic data are consistent with those reported in reference:</u>

Aguilera, J. *PhD thesis*, UAB 2010.

Synthesis of Ru237, Ru238 and Ru239

[Ru(cod)(cot)] (30 mg, 0.1 mmol) and 0.02 mmol of the corresponding ligand (for **237**, 4 mg; for **238**, 7.5 mg; for **239**, 7 mg) were dissolved in 80 mL of THF and introduced under argon atmosphere in a Fischer-Porter bottle. The system was then pressurized with 3 bar of dihydrogen and stirred at room temperature overnight. The hydrogen was then replaced by argon and the solvent was evaporated under *vacuum*. The isolated particles were further washed with pentane (3 x 10 mL). Organic phases were concentrated and analysed by ^{1}H NMR proving the absence of ligand. The black solid was dried under reduced pressure.

General procedure for Ru-catalyzed hydrogenation reactions

1 mmol of substrate, 0.01 mmol of RuNP and 25 mL of neat and deoxygenated heptane were introduced to a Top Industrie autoclave. The system was purged under argon before being pressurising. The autoclave was pressurized at 40 bar of H_2, stirred and heated at 50 °C overnight. After cooling to room temperature, the autoclave was depressurized and the reaction mixture was then filtered through a celite column and, finally, the organic phase was analysed by gas chromatography and by NMR spectroscopy.